MODE OF ACTION, CONCENTRATIONS AND EFFECTS OF TRIBUTYLTIN IN COMMON SHRIMP *CRANGON CRANGON*

Yves Verhaegen

UNIVERSITEIT GENT

FACULTY OF **BIOSCIENCE ENGINEERING**

"But man is a part of nature, and his war against nature is inevitably a war against himself"

In 1962, marine biologist Rachel Carson published “Silent Spring”, describing the unintentional effects of the pesticide dichlorodiphenyltrichloroethane (DDT) on wildlife, in particular birds. It was the first popular publication questioning the release of large amounts of chemicals in the environment without fully understanding their environmental and health effects. Its publication is often considered as the birth of modern environmentalism, and it indirectly led to the many legislative actions regulating the production, use and disposal of harmful substances. Nevertheless, thanks to human ingenuity and for the sake of progress, many more hazardous chemicals have been marketed since then.

Promoters: Prof. dr. ir. Guy Smagghe
Department of Crop Protection
Faculty of Bioscience Engineering
Ghent University

Dr. Kris Cooreman
Fisheries Department
Flemish Institute for Agricultural and Fisheries Research (ILVO)

Chair of the examination committee:

Prof. dr. ir. Filip Tack
Department of Applied Analytical and Physical Chemistry
Faculty of Bioscience Engineering
Ghent University

Members of the examination committee:

Prof. dr. ir. Peter Bossier
Department of Animal Production
Faculty of Bioscience Engineering
Ghent University

Prof. dr. ir. Karel de Schamphelaere
Department of Applied Ecology and Environmental Biology
Faculty of Bioscience Engineering
Ghent University

Dr. Koen Parmentier
Fisheries Department
Flemish Institute for Agricultural and Fisheries Research (ILVO)

Dr. Patrick Roose
Management Unit of the North Sea Mathematical Models (MUMM)
Royal Belgian Institute of Natural Sciences

Prof. dr. Luc Swevers
Institute of Biology
National Centre for Scientific Research "Demokritos", Athens, Greece

Prof. dr. Els J.M. Van Damme
Department of Molecular Biotechnology
Faculty of Bioscience Engineering
Ghent University

Dean : Prof. dr. ir. Guido Van Huylenbroeck
Rector: Prof. dr. Paul Van Cauwenberge

Lic. Yves Verhaegen

MODE OF ACTION, CONCENTRATIONS AND EFFECTS OF TRIBUTYLTIN IN COMMON SHRIMP *CRANGON CRANGON*

Thesis submitted in fulfilment of the requirements for the degree of
Doctor (Ph.D.) in Applied Biological Sciences

Dutch title: Werkingsmechanisme, concentraties en effecten van tributyltin in grijze garnaal *Crangon crangon*

Cite as: Verhaegen, Y. 2012. Mode of action, concentrations and effects of tributyltin in common shrimp *Crangon crangon*. PhD dissertation, Faculty of Bioscience Engineering, Ghent University, Ghent.

Cover: Richard Lord, Sealord Photography

Printing: University Press

ISBN: 978-90-5989-535-5

This work was supported by a fellowship of the Flemish Institute for Agricultural and Fisheries Research (ILVO)

Dankwoord

Donderdag 15 maart 2012, 3u38 's ochtends. Ik word gewekt door gepraat. Enkele mensen hebben blijkbaar een leuke avond gehad en staan voor ons slaapkamerraam langdurig afscheid te nemen. Mijn vriendin bonkt eens deftig op het raam en kruipt terug onder de wol. Ze vat bijna onmiddellijk terug de slaap, ik niet. Ik denk na over de afgelopen avond die volgde op een prachtige lentedag. Ik had deze mooie dag grotendeels binnenshuis gespendeerd aan het schrijven van het doctoraat, terwijl ik liefst van al was gaan fietsen met enkele vrienden. Paul (A.A.G.) Van Daele, waarmee ik na mijn licentiaatsthesis enkele maanden de bureau heb mogen delen, heeft net zijn doctoraat afgelegd. 9 jaar had hij er over gedaan. Losstaand van zijn langdurige inspanning (en zijn affectie voor paars-wit) was hij voor mij hét romantische voorbeeld van een rasechte wetenschapper, losgerukt uit de nobele tijd der ontdekkingsreizigers en misplaatst in de moderne tijd van 'welvaart' en opportunisme. Ik zie hem na zijn verdediging bezig met zijn twee prachtige zoontjes op de steile trappen van het auditorium. Op één of andere manier heb ik me altijd gespiegeld aan Paul. Een bizar biologisch fenomeen werd voor hem een levensvraag. De verspreiding en fylogenie van ondergrondse Afrikaanse molratten, bij god hoe kom je erbij, dat móet een bioloog zijn. Maar nu heeft hij besloten dit hoofdstuk af te sluiten. Het romantische beeld dat ik altijd van wetenschappelijk onderzoek heb gehad en voor mij een belangrijke drijfveer was, is met Paul nu helemaal verdwenen. De wetenschap is gemoderniseerd, een beschaafde vechtpartij om geld en prestige. Kan je het eigenlijk nog wel wetenschap noemen, als op korte termijn resultaatgericht gepresteerd moet worden? Telkens weer op enkele maanden tijd een 'sexy' project schrijven, fondsen vergaren, uitvoeren en publiceren, tot het einde der dagen. Tantalus en Sisyphus zijn mietjes. In moderne tijden hadden Einstein en Darwin wegens onproductiviteit al na enkele maanden de bons gekregen. Gedaan met 25 jaar broeden op de relativiteits- of evolutietheorie. Ze hadden dan maar romanschrijver moeten worden. Nee, voor mij hoeft het even niet meer. Afhandelen die boel! Op naar de finish en op naar een ander avontuur.

Ik wil mijn promotoren, Prof. dr. Ir. Guy Smagghe en Dr. Kris Cooreman bedanken voor deze leerrijke periode, en niet in zijn minst het ILVO om mij financieel te ondersteunen. Guy, zoals je vaak terecht hebt gezegd, ben ik een koppige steenezel, en lagen we nagenoeg constant in de clinch. Maar op het einde van de rit moeten we tot de conclusie komen dat het gewerkt heeft, en zowel jij als ik fier mogen zijn op wat gepresteerd is. Bedankt, en ik wens je nog veel succes in je verdere carrière.

Alhoewel hij niet als co-promotor vermeld staat, wil ik specifiek Dr. Koen Parmentier bedanken. Koen, ondanks dat je niet meer het labo in Oostende leidt en uiteindelijk niet meer

optrad als co-promotor, heb ik steeds van je onvoorwaardelijke steun, vertrouwen maar vooral ook van je oprechte vriendschap mogen genieten. Bedankt.

Ik heb het geluk gehad om tijdens het doctoraat door veel collega's omringd te worden in Oostende, Gent en Antwerpen. De eerste dag dat ik in Oostende met mijn Oost-Vlaams verbasterd Antwerps accent aanlandde, werd ik door het noeste zeevolk met enige achterdocht aanschouwd. Maar vanuit alle windrichtingen heb ik de laatste jaren appreciatie en affectie mogen ervaren. Alhoewel ik er vaak weinig tijd voor had, was dit van vitaal belang voor mijn goed functioneren.

Ook zonder de oud-collega's van het labo vertebrate morfologie van Prof. Dr. Dominique Adriaens, waar ik het enthousiasme voor wetenschappelijk onderzoek heb opgedaan met een maandwerk en vervolgens thesis, en van het labo zoofysiologie, waar ik als assistent door Nico, Marleen en Dirk geïntroduceerd werd in moleculaire en biochemische analyses, was dit doctoraat er nooit geweest.

Aan mijn broer, ouders, neef, tante, nonkel, oma's, vrienden, vriendin en ex-vriendin vraag ik om vergiffenis. Ik heb jullie de laatste jaren niet de aandacht gegeven die jullie verdienden. Een kleine week geleden werd de vader van een kennis begraven. Zoals op nagenoeg elke afscheidsplechtigheid werd het belang van gezondheid, vriendschap en liefde benadrukt, maar deze keer bleven het voor mij geen holle woorden. Ik kwam kort nadien écht tot het besef dat ik de laatste jaren had achtergesteld wat normaal de prioriteiten van eenieders leven zouden moeten zijn.

Tot slot, terwijl ook jullie druk bezig waren een levensweg langs vele hindernissen te ploeteren, hebben jullie allen bewust of onbewust, rechtstreeks of onrechstreeks bijgedragen aan dit doctoraat. Dit doctoraat is dan ook van jullie, voor jullie.

Op de gezondheid, de vriendschap en de liefde!

En vandaag ga ik gaan fietsen, hopelijk met vrienden.

Table of contents

List of non-standard abbreviations

20E	20-hydroxyecdysone
25dE	25-deoxyecdysone
AA	Amino acids
ADHD	Attention deficit hyperactivity disorder
AFS	Convention on the Control of Harmful Antifouling Systems of IMO
ATP	Adenosine triphosphate
ATPase	Adenosine triphosphatase
BCF	Bioconcentration factor
BMDC	Belgian Marine Data Centre
BPD	Biocidal Products Directive of the EU
BSAF	Biota to sediment accumulation factor
cAMP	Cyclic adenosine monophosphate
cDNA	Copy- or complement-DNA
CEMP	Coordinated Environmental Monitoring Programme of OSPAR
CHO	Chinese hamster ovary
CTE	Carboxy-terminal extension
cvff	Consistent-valence force field
Cy3	Cyanine 3 fluorescent dye
Cy5	Cyanine 5 fluorescent dye
DBD	DNA-binding domain
DBT	Dibutyltin
DFS	Demersal fish survey
DMSO	Dimethylsulfoxide
DNA	Deoxyribonucleic acid
DNase	Deoxyribonuclease
dNTP	Deoxyribonucleotide triphosphate
DOT	Dioctyltin
DPhT	Diphenyltin
DW	Dry weight
DYFS	Demersal young fish survey
EC_{50}	Median effect concentration
ECHA	European Chemicals Agency
EcR	Ecdysteroid receptor

EcRE	Ecdysteroid responsive element
ED_{50}	Median effect dose
EDC	Endocrine disruptive compound
EFSA	European Food Safety Authority
EPS	Extracellular polymeric substances
EST	Expressed sequence tag
FAO	Food and Agriculture Organization of the UN
FI	Fold induction
FXR	Farnesoid-X receptor
FW	Fresh weight
GABA	γ-amino butyric acid
GAPDH	Glyceraldehyde-3-phosphate dehydrogenase
GC	Gas chromatography
GIH	Gonad-inhibiting hormone
GSH	Gonad-stimulating hormone
GSP	Gene-specific primer
HRE	Hormone response element
ICES	International Council for the Exploration of the Sea
ID	Internal diameter
ILVO	Institute for Agricultural and Fisheries Research
IMARES	Institute for Marine Resources and Ecosystem Studies
IMO	International Maritime Organization
IPCS	International Programme on Chemical Safety of the WHO
JH	Juvenile hormone
K_{ow}	Octanol-water partition coefficient
LBD	Ligand-binding domain
LBP	Ligand-binding pocket
LC_{50}	Median lethal concentration
LD_{50}	Median lethal dose
LOEC	Lowest observed effect concentration
LOEL	Lowest observed effect level
LoQ	Limit of quantification
LPUE	Landings per unit effort

L_T	Total length
LXR	Liver-X receptor
MBT	Monobutyltin
MEPC	Marine Environment Protection Committee of IMO
MF	Methylfarnesoate
MIH	Moult-inhibiting hormone
MOA	Mode of action
MOIH	Mandibular organ-inhibiting hormone
MPhT	Monophenyltin
mRNA	Messenger RNA
MSFD	Marine Strategy Framework Directive of the EU
MTS	3-(4,5-dimethylthiazol-2-yl)-5-(3-carboxymethoxyphenyl)-2-(4-sulfophenyl)-2H-tetrazolium, inner salt
MUMM	Management Unit of the North Sea Mathematical Models and the Scheldt estuary
NAO	North-Atlantic oscillation
NOEC	No observed effect concentration
NOEL	No observed effect level
NR	Nuclear receptor
OECD	Organization for Economic Cooperation and Development
ORF	Open reading frame
ORTEP	Organotin Environmental Programme
OSPAR	Convention for the Protection of the Marine Environment of the North-East Atlantic
OT	Organotin
PBT	Persistent, bio-accumulative, and toxic chemicals
PCB	Polychlorinated biphenyl
PCR	Polymerase chain reaction
PDB	Protein data bank of the Research Collaboratory for Structural Bioinformatics
PIA	Phenylisopropyladenosine
PonA	Ponasterone A
POP	Persistent organic pollutants
PPAR γ	Peroxisome-Proliferator-Activated Receptor γ

PPIase	peptidyl-prolyl cis-trans isomerase
PPPD	Plant Protection Products Directive of the EU
PVC	Polyvinyl chloride
QA/QC	Quality assurance/quality control
QUASIMEME	Quality Assurance of Information in Marine Environmental Monitoring in Europe
RA	Retinoic acid
RACE-PCR	Rapid amplification of cDNA ends PCR
REACH	EU regulation on the Registration, Evaluation, Authorisation and Restriction of Chemicals
RLU	Relative luminescence unit
RNA	Ribonucleic acid
ROS	Radical oxygen species
RPA	Risk & Policy Analysts Limited
RPLP1	Ribosomal protein LP1
rRNA	Ribosomal RNA
RT-PCR	Reverse transcriptase PCR
RXR	Retinoid -X-receptor
SEM	Standard error of the mean
SPC	Self-polishing copolymer coating
SSC	Saline-sodium citrate buffer
SSH-PCR	Suppressive subtraction hybridisation PCR
TBT	Tributyltin
TBTO	Bis(tributyltin)oxide
TCTH	Tricyclotin hydroxide
TCTT	Tricyclotin triazole
TDI	Tolerable daily intake
TNTO	Trineophenyltin oxide
TPhT	Triphenyltin
TPTA	Triphenyltin acetate
TPTH	Triphenyltin hydroxide
UNEP	UN's Environment Programme
USP	Ultraspiracle

UTR	Untranslated region
Vtg	Vitellogenin
vTI-SF	Institute of Sea Fisheries from the Johann Heinrich von Thünen Institute
WFD	Water Framework Directive of the EU
WHO	World Health Organization
WW	Wet weight
WWF	World Wildlife Fund

Preface

Goals and outline of this study

Background

Common shrimp (*Crangon crangon* L.) has a wide geographical distribution, ranging from the Icelandic coast and the White Sea (North-West of Russia) to the Moroccan coast and the Black Sea. In the southern North Sea (from Northern France up to Denmark) it dominates the coastal and estuarine areas. In the culinary atmosphere, *Crangon* is a delicacy, sometimes called 'North Sea caviar', as it has a strong and unique taste. With an annual catch of 35,000 to 50,000 tons and a commercial value of the whole North Sea landings of roughly €100 million, common shrimp is one of the top 5 most valuable European fisheries and aquaculture commodities.

Problem definition

Since the early 1970s until the early 2000s, the Belgian landings per unit effort (LPUE), a proxy for local (i.e. the Southern Bight) annual shrimp abundance based on fisheries statistics, shows a gradual, but severe decrease. Since 2007, the local shrimp stock has suddenly recovered, resulting in record landings in 2010. Prior to 2007, several potential causes have been proposed for the long term decline (Redant & Polet 2002):

- **Overfishing**. common shrimp are one of the few commercial species which are believed not to be overfishable, as fishing mortality is much lower than natural mortality, i.e. 5-10% of the total mortality caused by gadoid (cod and whiting) predation (Welleman & Daan 2001).
- **Increased predator pressure**. Cod and whiting are the most important shrimp predators. Increased fishing pressure on these and other species has only led to a decreased predator pressure. The cod stock even collapsed in 1992 and is only slowly recovering.
- **Decreased nursing grounds**. Marshes and creeks are important nursing grounds for juvenile shrimp and many other species. Sand extraction, harbour expansion, impoldering and damming have indeed reduced the surface area of brackish marshes and creeks within the Southern Bight.
- **Increased pollution load**. The production and use of hazardous chemicals exploded after the Second World War. While the release and environmental concentrations of many of such chemicals have strongly decreased due to increasing legislatory restrictions, other 'emerging' chemicals pose a constant threat. Shrimp and other crustaceans are believed to be sensitive towards endocrine disruptive pollutants (Rodríguez et al. 2007).

A similar, yet unexplained situation (i.e. a long-term decline since the 1970s and recent record landings) also occurred in the other commercially exploited North Sea common shrimp stocks. However, international landing data indicated that several other shrimp stocks (e.g. the Wadden Sea), already started recovering in 1991 (ICES 2011). Furthermore, Siegel et al. (2008) observed an associated long term decline in the percentage of gravid shrimp in the Wadden Sea since the 1970s until 1989. Correlation analyses with common parameters, such as water temperature, river runoff, North Atlantic Oscillation (NAO) climate index, fish predator density or fishing pressure, showed no obvious plausible proximate cause. During the same period, the prevalence of 'black spot disease' in shrimp had been growing throughout the whole North Sea (Watermann & Dethlefsen 1983; Knust 1990; Dyrynda 1998). 'Black spots' are bacterial infected nodules accompanied by tumour-like cells from apparently gonadal origin. Watermann & Dethlefsen (1983) postulated that pollution-induced "dissolutions" of the shell and subsequent bacterial and fungal infection could facilitate the occurrence of black spot disease.

Hypothesis

We pose the hypothesis that environmental concentrations of the potent broad spectrum biocide tributyltin (TBT) affects NR functioning in common shrimp, leading to downstream alterations in the expression of genes involved in moulting and reproductive processes. Since the late 1950s, TBT had been used on a massive scale as antifouling agent to decrease drag or surface damage on ship hulls, fish nets and cages due to biofouling. At the end of the 1970s, excessive use of TBT on local recreational vessels led to severe reproductive failures in commercially exploited oyster populations (Alzieu et al. 1982). Consequently, the use of TBT on vessels smaller than 25 m was banned throughout the EU by 1989. Due to its efficacy and lack of performing alternatives, a global ban on vessels longer than 25 m was only achieved, starting in 2003 and totally banned from 2008 onwards. Meanwhile, several marine gastropod populations had nearly completely collapsed due to TBT-related reproductive disorders (i.e. 'imposex' and 'intersex'). It has recently been shown that TBT blocks the mammalian Retinoid-X-Receptor (RXR), a nuclear receptor (NR) which is strongly conserved throughout the animal kingdom (Nishikawa et al. 2005). RXR plays a vital role in endocrinology, as it directly modulates the activity of many other NRs. NRs are the major targets of lipophilic hormones (e.g. steroids), and directly induce tissue specific expression of genes involved in

development, reproduction, immune response, etc. The ligand-dependent nature makes NRs susceptible for exogenous ligands such as pharmaceuticals, pesticides and many other chemicals.

Objectives

Within this PhD-thesis, two main research questions will be addressed. (1) Does TBT affect the functionality of the shrimp RXR receptor?, and, if so, (2) do the TBT concentrations observed in the North Sea disrupt shrimp endocrine functioning?

Research Question 1: Does TBT affect the functionality of the shrimp RXR receptor?

Invertebrate RXR is believed to act as a 'silent' but 'obligate' partner for many other NRs, *i.e.* invertebrate RXR does not bind a hormone (such as 9-*cis* retinoic acid (9-*cis*-RA)) but its presence is necessary to attain a high activity of the partner NR. Thus, investigation of TBT interference in invertebrate RXR activity must be performed indirectly, by measuring the activity of a partner NR. In chapter 2, the open reading frame (ORF) sequences from *C. crangon* RXR (CrcRXR) and its well-known partner protein, ecdysteroid receptor (CrcEcR), will be fully retrieved through a combination of several molecular techniques. Intra- and extraspecies variant regions will be identified within the cloned CrcRXR and CrcEcR isoforms. A phylogenetic analysis based on the obtained receptor sequences will be a first genetic phylogenetic analysis for this species. *In silico* 3D protein structures can then be reconstructed using existing (insect) EcR and (human) RXR templates. In chapter 3, (1) the *in silico* reconstructed receptors will be used to predict the interaction of TBT within the ligand binding pocket (LBP) of CrcRXR and CrcEcR; (2) the effect of TBT on signalling activity of the shrimp CrcEcR-RXR complex will be studied *in vitro* through a mutant *Drosophila* cell line; (3) the gene expression levels of both receptors will be studied *in vivo* after acute exposure of shrimp to TBT.

Research Question 2: Do the TBT concentrations observed in the North Sea disrupt shrimp endocrine functioning?

In chapter 4, common shrimp samples collected during a short time frame in Belgian, Dutch, German and Danish waters will be analysed to give a spatial overview of the organotin (OT) content in shrimp at the major fishing grounds. A focus on the highly polluted Westerschelde estuary will demonstrate the behaviour of OT concentrations in shrimp along a salinity

gradient. Historical TBT concentrations in shrimp will be estimated by applying a Biota-to-Sediment-Accumulation-Factor (BSAF) on available sediment concentrations. Endocrine disruptive effects of the observed concentrations are hard to prove, however. Classically, long-term multi-generation exposures (> 1 month in case of shrimp) are needed to observe subtoxic end-point effects, but such tests are practically unfeasible due to long exposure times and poor survival of shrimp under laboratory conditions. Instead, the subtoxic effects on endocrine sensitive gene expression, which physiologically precede the classic micro- or macroscopically observable responses, are readily quantifiable through modern molecular techniques. In chapter 5, sex specific shrimp genes will be isolated through suppression subtractive hybridization PCR (SSH-PCR), sequenced, and spotted on microarray slides. With the home-made shrimp microarrays, the expression levels of these genes after subchronic (i.e. 7 days) exposure to subtoxic TBT levels will be quantified and will be linked to the affected physiological end-points (*e.g.* moulting, sexual maturation, fat storage).

Chapter 1

General introduction

1.1 Common shrimp (*Crangon crangon*)

1.1.1 Taxonomy and phylogeny

Protostomia, unranked	G. *protos*, first + G. *stomos*, mouth	Grobben 1908
Superphylum **Ecdysozoa**	G. *ecdysis*, moult + G. *zoa*, animal	Aguinaldo et al. 1997
Phylum **Arthropoda**	G. *arthron*, joint + *podos*, foot	von Siebold & Stannius 1845
Subphylum **Crustacea**	L. *crusta*, shell	Pennant 1777
Class **Malacostraca**	G. *malakós*, soft + G. *óstrakon*, shell	Latreille 1802
Subclass **Eumalacostraca**		Martin & Davies, 2001
Superorder **Eucarida**	G. *eu*, true + L. *caris*, shrimp	Calman 1904
Order **Decapoda**	G. *deca*, ten + G. *podos*, foot	Latreille 1803
Suborder **Pleocyemata**	G. *pleon*, abdomen + G. *kýmata*, foetal	Burkenroad, 1963
Infraorder **Caridea**	G. *caris*, shrimp	Dana, 1852
Superfamily **Crangonoidea**		Haworth 1825
Family **Crangonidae**		Haworth 1825
Genus ***Crangon***		Fabricius 1795
Species ***Crangon crangon***		Fabricius 1795

1.1.2 Morphology

The morphology of shrimp is reviewed in detail by Bauer (2004), of which I will give a brief overview. Common shrimp exhibits the typical Malacostracan body plan called the cardioid facies (L., *carid*, shrimp + L. *facies*, appearance; fig 1.1), in which the somites are grouped into tagmata, specialized body regions (i.e. head, thorax or pereon, abdomen or pleon, and telson). The exoskeleton of each somite consists of four sclerotized chitinous plates called sclerites (a dorsal tergite, two lateral pleurites and a ventral sternite). In general, each somite bears a pair of biramous appendages, of which the standard architecture is represented in fig. 1.2. The head (cephalon) consists of five fused cephalic segments, which bear five pairs of specialized appendages. The presence of two pairs of antennae (i.e. antenullae and antennae) is a distinguishing feature of the Crustacea. The exopods of the second pair of antennae are enlarged and flattened to scaphocerites, which mainly serve as an anterior stabilizing fin. The other cephalic appendages form the feeding apparatus (i.e. mandibles, maxillules and maxillae). The rostrum is short and fused to the head. The thorax consists of eight segments, of which the first three are fused with the head, and this is referred to as a cephalothorax.

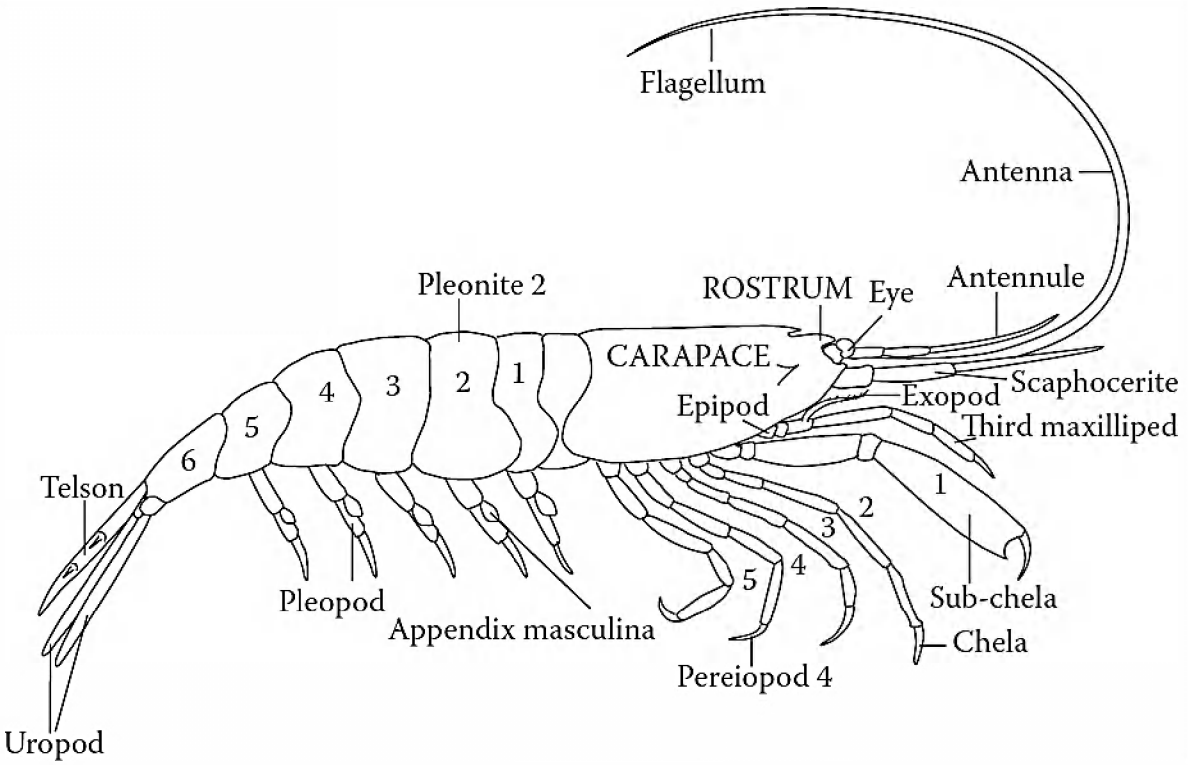

Fig. 1.1. Schematic drawing of common shrimp *C. crangon* (reproduced from Campos & Van der Veer 2008).

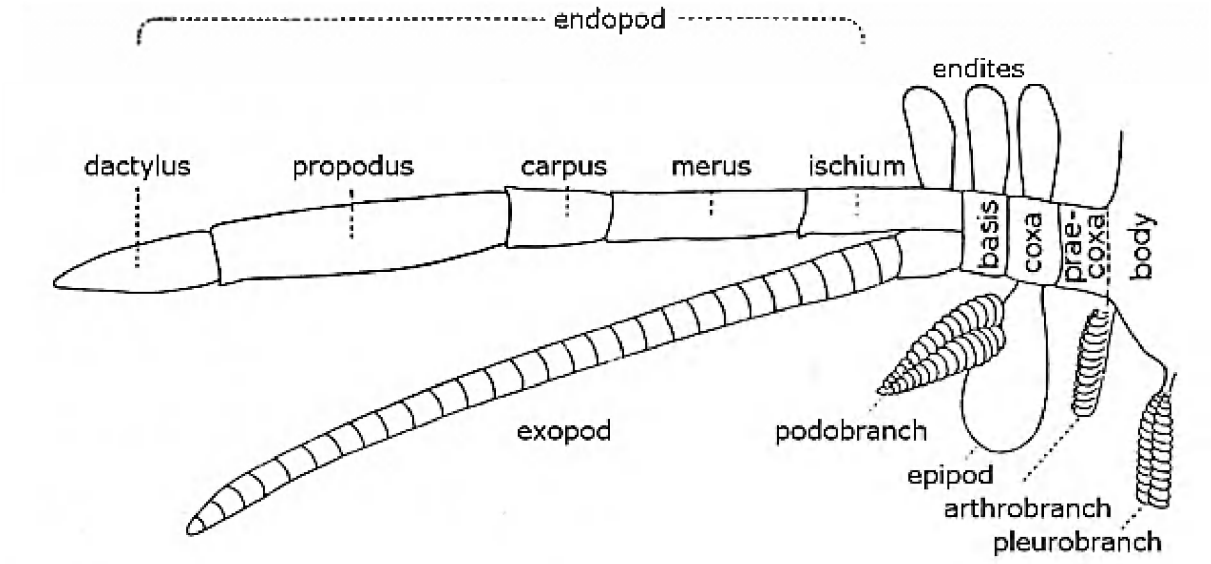

Fig. 1.2. Schematic drawing of a generalized crustacean appendage (adapted from Holthuis 1993).

The first three pairs of appendages of these fused thoracic segments are included in the mouthparts as maxillipeds, and assist in food processing. The other five thoracic appendages slender walking legs, called pereiopods. The first pair of pereiopods, the chelipeds, is enlarged and subchelate (the dactyl folds back against the propodus, which lacks an extension).and

serves both a predatory and defensive function. The second pair of pereiopods is long and slender and possesses a true, 'scissor'-like chela for cutting food items. The tergite of the cephalothorax is enlarged to a dorso-ventrally compressed, cylindrical carapax, which is fused with all thoracic segments and encloses paired, lateral gill chambers. The abdomen consists of six segments (pleonites), with a typical bend in the third pleonite. Typically for the genus *Crangon*, the pleurites of the second pleonite overlap their neighbours. The sixth pleonite is smooth dorsally, without groove(s) or carina(e), in contrast to *C. allmani*. Each pleonite carries a pair of pleopods (swimming legs), except the last segment which carries a pair of uropods. In females, the endopodites of the pleopods keep the fertilized eggs until the nauplius stage (see later), a distinguishing character for members of the Pleocyemata. In common shrimp, the morphology of the first two pairs of pleopods is a key feature for distinguishing sex. In males, the first pair of endopodites is much smaller and twisted around the base of the exopodit, while the second pair of endopodites exhibit a small appendage called the appendix masculine (Tiews 1970). Together with the final body segment, the telson, the uropods form a 'tail fan', which is involved in the typical tail-flip type of escape mechanism.

1.1.3 Anatomy

The following overview of the major organ systems is based on the extensive review made by Felgenhauer (1992) on the internal anatomy of Decapoda.

Digestive system

The digestive system consists of an oesophagus, foregut, the midgut, and the hindgut (fig. 1.3). The foregut consists of two chambers, which possess multiple chitinous plates (ossicles) and extensive musculature, i.e. the cardiac and pyloric chamber, and is surrounded by a large digestive gland, the hepatopancreas. The midgut gives rise to blindly ending anterior (at the foregut juncture) and posterior (at the hindgut juncture) caeca. Osmoregulation, nutrient absorption, and the production of the peritrophic membrane that wraps the faecal material have been attributed to this gut region. The hindgut is characterized by chitinous scales or spines, which direct the faecal mass towards the anus, which is situated at the base of the telson. The hepatopancreas is a large trilobed organ, which releases digestive enzymes in the midgut where it takes up the released nutrients. It is also the main organ of reserve and detoxification of xenobiotics, and is highly sensitive to physiological and environmental conditions (Johnston et al. 1998).

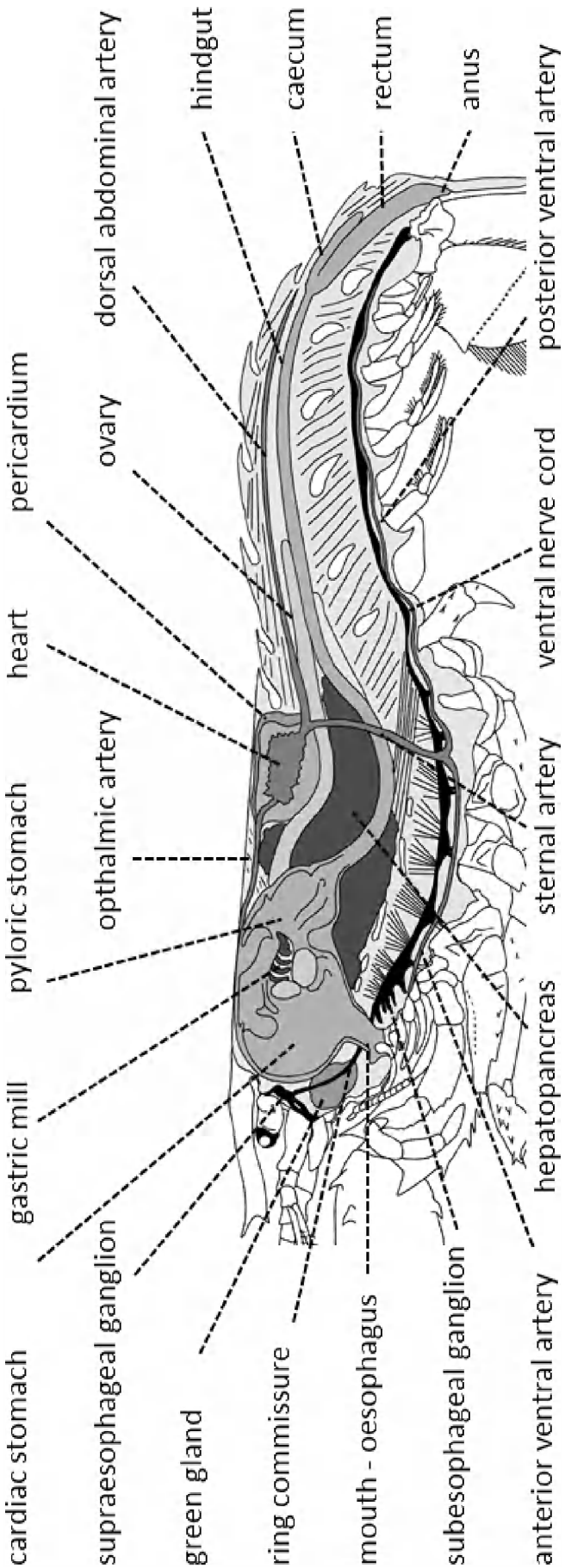

Fig. 1.3. Anatomy of a representative pleocyemate decapod, *Homarus americanus* (based on Herrick 1911).

Circulatory system

The circulatory system of decapods is centred around a bulbous, dorsal heart, which receives blood through three pairs of ostia. It is surrounded by a pericardial sac that is penetrated by passageways where oxygen-rich, venous blood returns to the pericardial chamber. The hemolymph is pumped into the hemocoel through several major arteries, which possess valves to prevent backflow.

Respiratory system

C. crangon possesses phyllobranchiate gills at the base of the pereiopods, i.e. pleurobranch, arthrobranch, podobranch and exopod gills (see fig. 1.1). The gills are the primary sites for respiration, but especially the posterior gills also play a role in ion-regulation, and acid-balance. The exopodites of the second maxillae form a flattened "bailer" termed scaphognathites that draws water over the gills through the gill chambers and out at the anterior end.

Excretory system

The antennal, urinary or green glands are paired excretory organs located at the base of the second pair of antennae and extract nitrogenous waste from the hemolymph and maintains ionic and water balance. The large bladder of the green gland exits on the coxa of the second pair of antennae.

Reproductive system

In male *C. crangon*, the testes are simple tubes connected to each other anteriorly, which lie dorsally on the hepatopancreas and extend diverticula into the first abdominal somites. The round, aflagellate and nonmotile spermatocytes mature as they transit the vas deferens to the gonophore at the base of the fifth walking legs. In addition, the vas deferens packages the spermatozoa into simple cordlike spermatophores. Males do not have ovulatory organs but deposit spermatophores near the female genital opening (Lloyd & Yonge, 1947).

In female *C. crangon*, the paired ovaries are located in the same relative position as the testis in males, extending into the posterior abdominal somites. The size highly depends on the age and reproductive condition of the female. The eggs pass from each ovary through the oviducts and exit via the gonophores on the third pair of pereiopods. The eggs are fertilized as they are

attached to the carrying setae on the endopodites of the female pleopods with secretions from a cement gland (Abbott & Perkins 1977; Lloyd & Yonge 1947).

Exoskeleton

In contrast with insects, the crustacean exoskeleton lacks a waxy, watertight cuticle, but instead it is reinforced with calcium carbonate (Passano 1960). The integument consists of an outer epicuticle, an exocuticle, an endocuticle and an inner membranous layer supported by the hypodermis. In the epicuticle, spherulitic calcite islands are surrounded by a lipid-protein matrix. In the exo- and endocuticles, the calcite crystals aggregates are interspersed with chitin-protein fibres organized in lamellae. The inner membranous layer is not calcified and consists of proteins and chitin.

Nervous system

The central nervous system is composed of a pair of supraoesophageal ganglia, which are connected with the eyes and the antennae, and the suboesophageal ganglion, which is connected with the mouth, oesophagus, antennal glands, and the 'ladder like' ventral nerve cord, which is connected to the appendages, muscles, etc. The main sense organs include a pair of compound eyes, tactile hairs (on the second pair of antennae and distributed on the whole body), chemoreceptors (on the antennules and distributed on the whole body) and statocysts (at the base of the antennules).

Endocrine system

The crustacean endocrine axis comprises two major neuroendocrine glands situated in the eyestalks: the X-organ-sinus gland complex, and the Y-organ (Laufer et al. 1993; Chang & Mykles 2011; fig. 1.4). The sinus gland is the storage and release site for several peptide hormones, i.e. moult-inhibiting hormone (MIH), gonad-inhibiting hormone (GIH), mandibular organ inhibiting hormone (MOIH) and several other hormones regulating the blood glucose levels (crustacean hyperglycaemic hormone), chromatophore activity (chromatophorotropic hormones), eye adaptation (light-adapting and dark-adapting hormones) and neurodepression. GIH interacts with GSH (gonad-stimulating hormone), which is released by the brain and the thoracic ganglia, to orchestrate the reproductive cycle. In females, these hormones regulate the synthesis and release of vitellogenin by the ovaries and hepatopancreas.

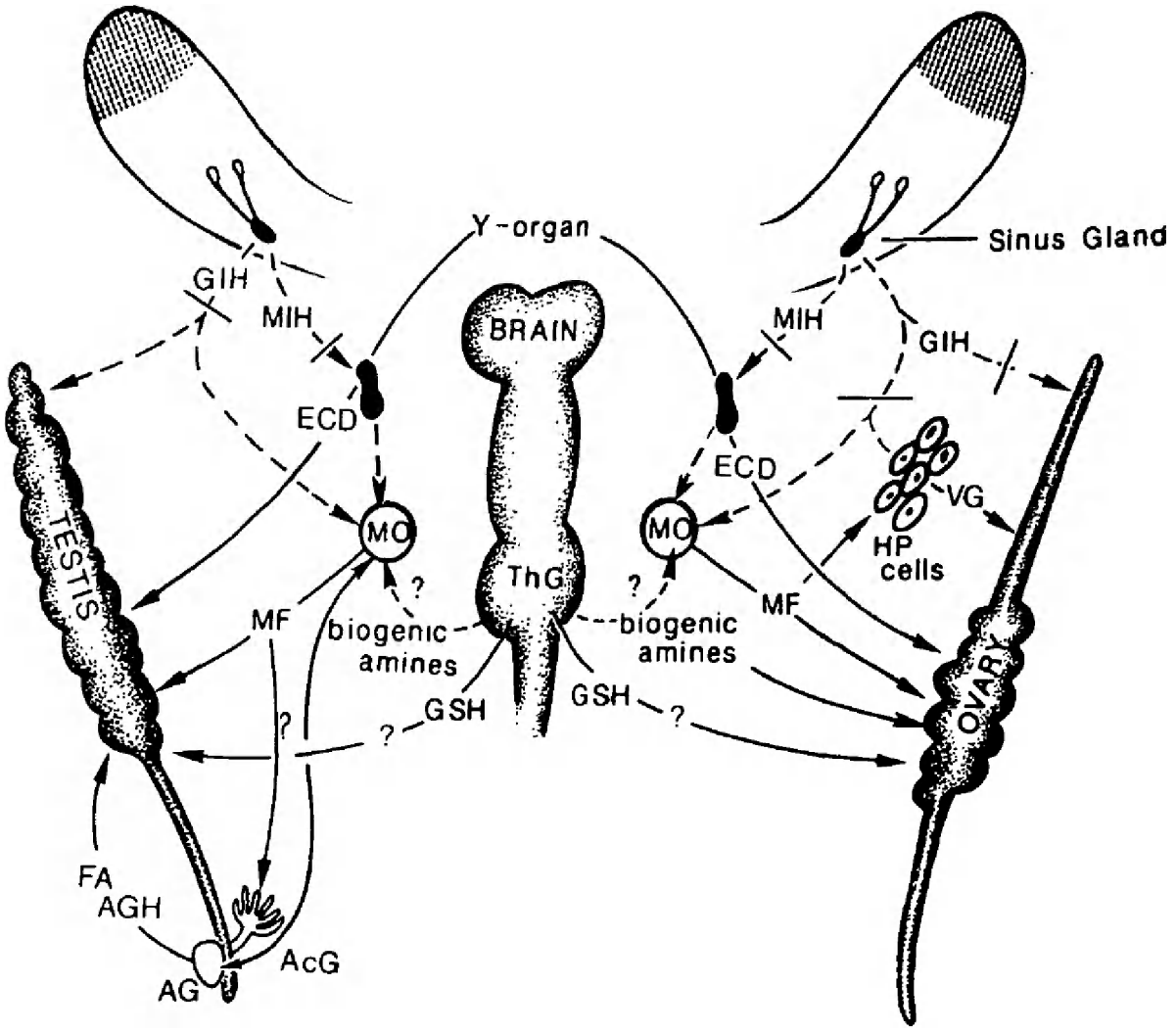

Fig. 1.4. The major endocrine glands of higher crustaceans (Malacostraca) and their target tissues involved in reproduction (reproduced from Laufer et al. 1993). Stimulatory effects are indicated with solid lines, inhibitory effects with dashed lines. AcG, accessory gland; AG, androgenic gland; AGH, androgenic gland hormone; ECD, ecdysteroids; FA, farnesylacetone; GIH, gonad-inhibiting hormone; GSH, gonad-stimulating hormone; HP, hepatopancreas; MF, methylfarnesoate; MIH, moult-inhibiting hormone; MO, mandibular organ; ThG, thoracic ganglion; VG, vitellogenin.

Vitellogenin is then transported to the developing oocytes, where it is modified to the yolk protein vitellin, which will be the major nutrient source for the developing embryo. In males, GIH-GSH act on the androgenic glands, which are attached to the vas deferens. The hormone released from the androgenic gland (androgenic gland hormone) is responsible for male differentiation and secondary sex characteristics. MOIH inhibits the release of methylfarnesoate (MF, fig. 1.5) by the paired mandibular organs, which are situated close to the Y-organs. The precise role of the terpenoid methylfarnesoate, the crustacean analogue of juvenile hormone (JH), is yet unclear.

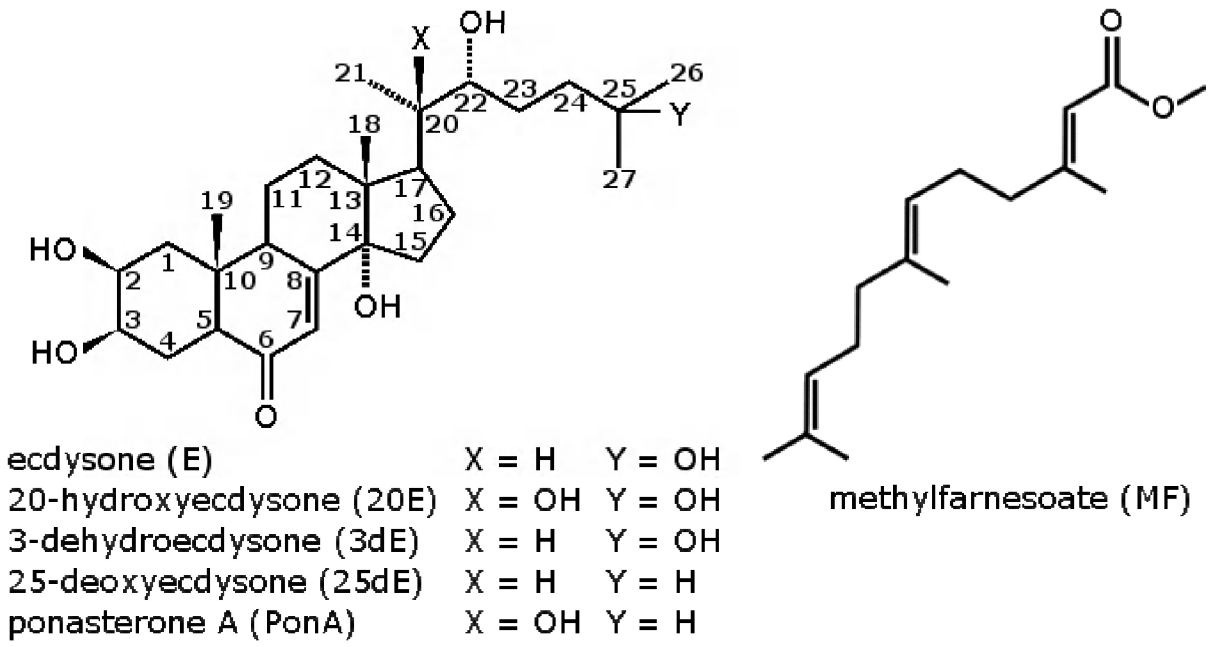

Fig. 1.5. Structure of the major ecdysteroids and the terpenoid methylfarnesoate.

Laufer et al. (1987) suggested that MF acts in a similar manner as JH, i.e. maintaining juvenile morphology and enhancing adult. MIH controls the time of onset of moulting activity by preventing the output of ecdysone by the Y-organs. The paired Y-organs are located in the anterior branchial chamber and releases the moulting prohormone ecdysone (fig 1.5), which is converted by a 20-hydroxylase activity in certain peripheral tissues (e.g. ovaries, testes, epidermis) to 20-hydroxyecydysone (20E). 20E is the main biologically active ecdysteroid, which mediates several aspects of crustacean growth and reproduction. The Y organ also secretes two other ecdysteroids, i.e. 3-dehydroecdysone and 25-deoxyecdysone (25dE). 25dE is the precursor of the active ponasterone A (PonA), the primary circulating ecdysteroid in the premoult stage. The ecdysteroids are the main regulators of moulting and morphogenesis (see later). In several crustaceans, ecdysteroids also stimulates vitellogenesis in the ovaries (Gohar & Souty-Grosset 1984; Gunamalai et al. 2004; Okumura et al. 1992; Steel & Vafopoulou 1998).

1.1.4 Moulting

C. crangon moults every 13-30 days at 12°C (Lloyd & Yonge, 1947) and every 8-9 days at 16-18°C (Price & Uglow, 1979). With each moult, the body size increases by 1-3 mm (Lloyd & Yonge, 1947). The moult cycle is generally divided in 4 basic phases (Drach 1939), which are initiated by alterations in circulating ecdysteroid levels (fig. 1.6): intermoult ($C_{0\text{-}4}$), premoult ($D_{0\text{-}4}$), ecdysis (E), and postmoult (A_0-B_2) (Skinner 1962). During intermoult

(metecdysis), food reserves (i.e. lipids, glycogen, and proteins) are stored in the hepatopancreas and reproduction occurs, ecdysteroid levels remain low. During premoult (proecdysis), as the old exoskeleton is being prepared for moulting, ecdysteroid levels increase, peak, and then drastically decrease. The drastic decrease triggers ecdysis.

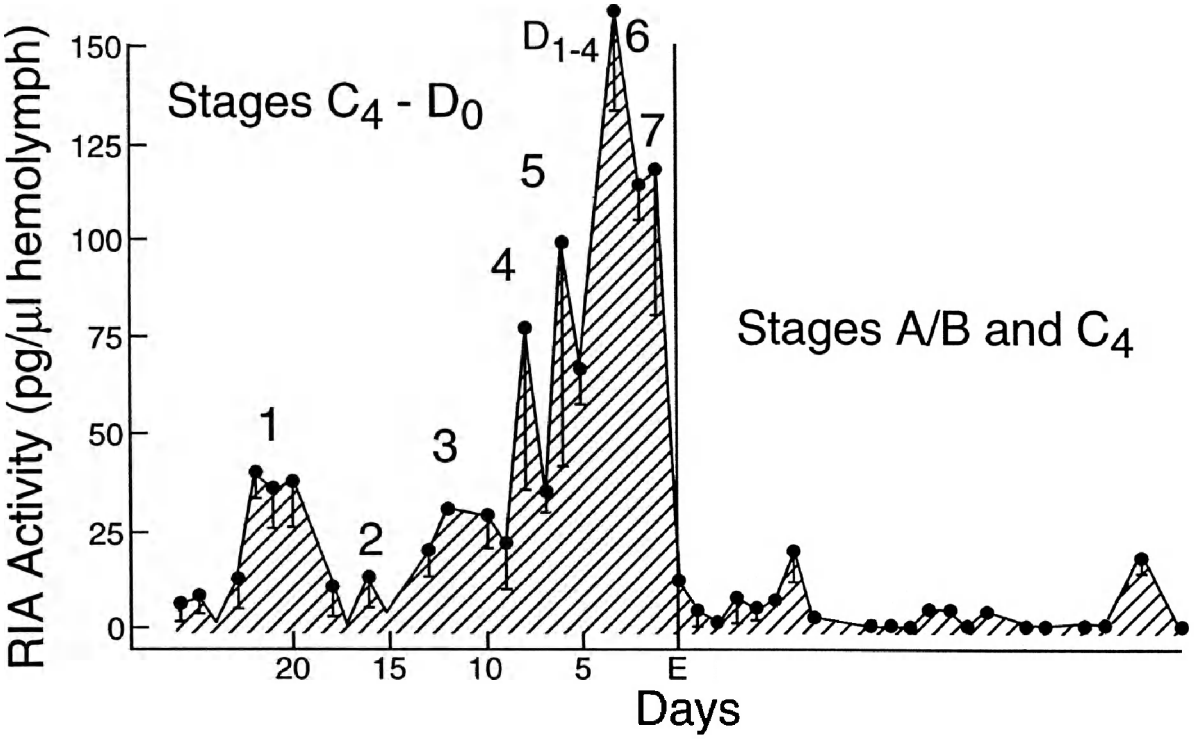

Fig. 1.6. Radioimmunoassay active ecdysteroid hemolymph levels during the moult cycle in fiddler crab *Celuca pugilator*. The major ecdysteroid titre peaks are represented by 1-7 (redrawn from Hopkins 1983).

Shortly before ecdysis, the animal stops feeding, while the epidermal cells separate from the old cuticle (apolysis) and secrete a new epicuticle and exocuticle. Enzymes are released above the new epicuticle to dissolve the old endocuticle and soluble products (mainly calcium) are reabsorbed and stored in the body (mainly in the hepatopancreas). As the animal swallows water its blood volume increases and internal pressure splits the cuticle between the cephalothorax and abdomen and the animal pulls itself out of its old exoskeleton. During postmoult (postecdysis), ecdysteroid levels in the hemolymph are low, as the animal continues to take up water and new soft cuticle is stretched. During the latter half of postmoult the exoskeleton is completed, feeding recommences and the absorbed water is gradually replaced by tissue.

1.1.5 Life cycle

C. crangon can reach 3.3 years of age, with the largest majority (70-90%) of the population in the 1st year class, 10-20% in the 2nd year class and the rest in their 3rd year (Oh *et al.* 1999). About 50% of the smallest adult stages are males, but this ratio decreases in the 30-45 mm classes, and at 60 mm the population is almost 100% female (Siegel et al. 2008). Previously, Boddeke (1962) suggested that *C. crangon* is an obligate protandric hermaphrodite, where all young individuals are male and change sex after reaching a certain size. However, *C. crangon* is a facultative rather than an obligate protandric hermaphrodite, as a maximum of 9.2% oocyte developing males is observed during September (Martens & Redant 1986). The observed changes in sex ratio in relation to size are mainly caused by a slower growth and higher mortality in male shrimp. *C. crangon* exhibits two reproductive peaks, i.e. summer and winter breeding, which are absent at lower and higher latitudes, respectively (Kuipers & Dapper 1984). Although a significant breeding activity occurs during summer, winter is regarded as the main breeding season in the Southern North Sea. During winter, females carry up to 2,800 eggs of 430 µm in size (Boddeke 1982, 1989). Hatching takes place offshore, together with the moulting of the female, roughly 1.5 months after spawning (Redant 1978). Larvae that hatch from winter eggs are bigger (Boddeke 1982) and show a higher starvation resistance (Paschke et al. 2004) than summer eggs (see later). The pelagic larvae slowly (due to lower temperatures and food availability) develop through the instar stages (zoea 1-6) into benthic postlarvae. During this period, the pelagic larvae passively migrate to coastal waters (van Donk & De Wilde 1981), where they metamorphose and settle down as post-larvae. Through selective tidal migration, they invade shallow tidal flats, estuaries and creeks and marshes as juveniles (7-15mm) (Beukema 1992; Cattrijsse et al. 1997). These areas serve an important 'nursery' function, as water temperatures and food availability are high and predator pressure low. Settlement peaks are observed in May-July, where the settled juveniles can exploit the annual calanoid copepod bloom (Boddeke et al. 1986). After about one month, the juveniles have grown rapidly up to 20-25 mm (Beukema 1992) and gradually migrate from the nursery areas into deeper sublittoral areas. Fast growing females hatched from winter eggs can reach a marketable size (55 mm) in October and maturity in December to produce a new cohort of winter larvae. In contrast to winter eggs, summer eggs are smaller (370 µm) but more numerous because of larger brood size (up to 4,500 eggs) and shorter spawning intervals. During summer, hatching takes place about 18 days after spawning (Redant 1978). While these larvae grow fast due to higher temperatures and prey availability, they face a

higher mortality. The summer larvae settle down in August-October but are likely to reach maturity after winter. From December onwards, shrimp migrate to deeper waters, up to 90 km offshore (Boddeke 1976). Until March, lower temperatures and food availability lead to a higher mortality and halted growth. In spring, the surviving shrimp return to the more shallow areas where they will grow quickly due to higher temperatures and higher prey abundance. Surviving adult females can reach maximum total lengths (L_T, from the tip of the scaphocerites to the tip of the telson) of nearly 80 mm and can spawn up to 10 times more eggs than smaller females (Redant 1978) as soon as May.

1.1.6 Behaviour and niche

C. crangon is a hyperbenthic species, burrowing itself in sand to avoid predators and to ambush prey. It prefers sediment of 125-710 µm grain size (Pinn & Ansell 1993). Burrowing takes 9-10 seconds and is achieved by rapid beating of the abdominal limbs (pleopods) followed by violent shuffling and completed by the antennae sweeping sand over the back to leave only the eyes and antennae above the sediment surface (Pinn & Ansell 1993). Swimming activity (by peristaltic trusting of the pleopods) is mostly confined to the nepheloid layer (i.e. the water layer just above the sediment, which contains a high amount of suspended material). *C. crangon*'s main escape mechanism is to rapidly flipping the tail, using the uropods-telson as a 'tail fan'. Onset of foraging activity of *C. crangon* is light-controlled, and mainly occurs at nights with peaks at dawn and dusk (Addison et al. 2003). *C. crangon* can be considered as opportunistic omnivores (Wilcox & Jeffries 1974), as the distal composition greatly varies with the available food items. Juveniles mainly prey on meiofaunal species such as ostracods and harpactoids, while adult shrimps prefer macrofaunal species such as sand clam (*Mya arenaria)*, cockle (*Cardium edule)*, mud worm (*Nereis spp.*), mud shrimp (*Corophium volutator),* newly recruited plaice (*Pleuronectes platessa*) (Phil and Rosenberg 1984). Depending on locality and season, the major food items may include newly recruited shore crab (*Carcinus maenas*) (Reise 1977), mysids (*Mysis* sp.) and amphipods (*Gammarus* sp.) (Oh et al. 2001), algae (*Ulva lactuca* and *U. intestinalis*) (Oh et al. 2001) and detritus (Plagmann 1939). Large *C. crangon* also exhibit substantial cannibalistic behaviour on newly recruited *C. crangon*, especially when the abundance of other food items is low. In turn, *C. crangon* is an important prey for many juvenile and adult fish species, especially for Gadiformae, Pleuronectidae, Triglidae (gurnards), *Pomatoschistus sp.*(gobies), *Agonus cataphracus* (armed bullhead), *Liparis liparis* (sea snail) and juvenile *Dicentrarchus labrax*

(sea bass) (Cattrijsse et al. 1997; ICES 1996). *C. crangon* occupies a key trophic position by transferring energy from the lower trophic (benthic) levels to the (semipelagic) top predators (Pihl and Rosenberg 1982, 1984; Evans 1984). *C. crangon* is also an important dietal component for seabirds, especially gulls (*Larus* sp.), terns (*Sterna* sp.) (Walter & Becker 1997) and redshanks *Tringa sp.* (Holthuijzen 1979; Goss-Custard et al. 1977).

1.1.7 Geographical distribution and habitat

C. crangon has a wide geographical distribution, ranging from the White Sea (North-West of Russia), Iceland (Gunnarson et al. 2007) and from the British coasts (Henderson & Holmes 1987) into the Baltic (Dornheim 1969), to the Moroccan coast and through the Mediterranean (Labat 1977) into the Black Sea (Luttikhuizen et al. 2008) (fig. 1.7).

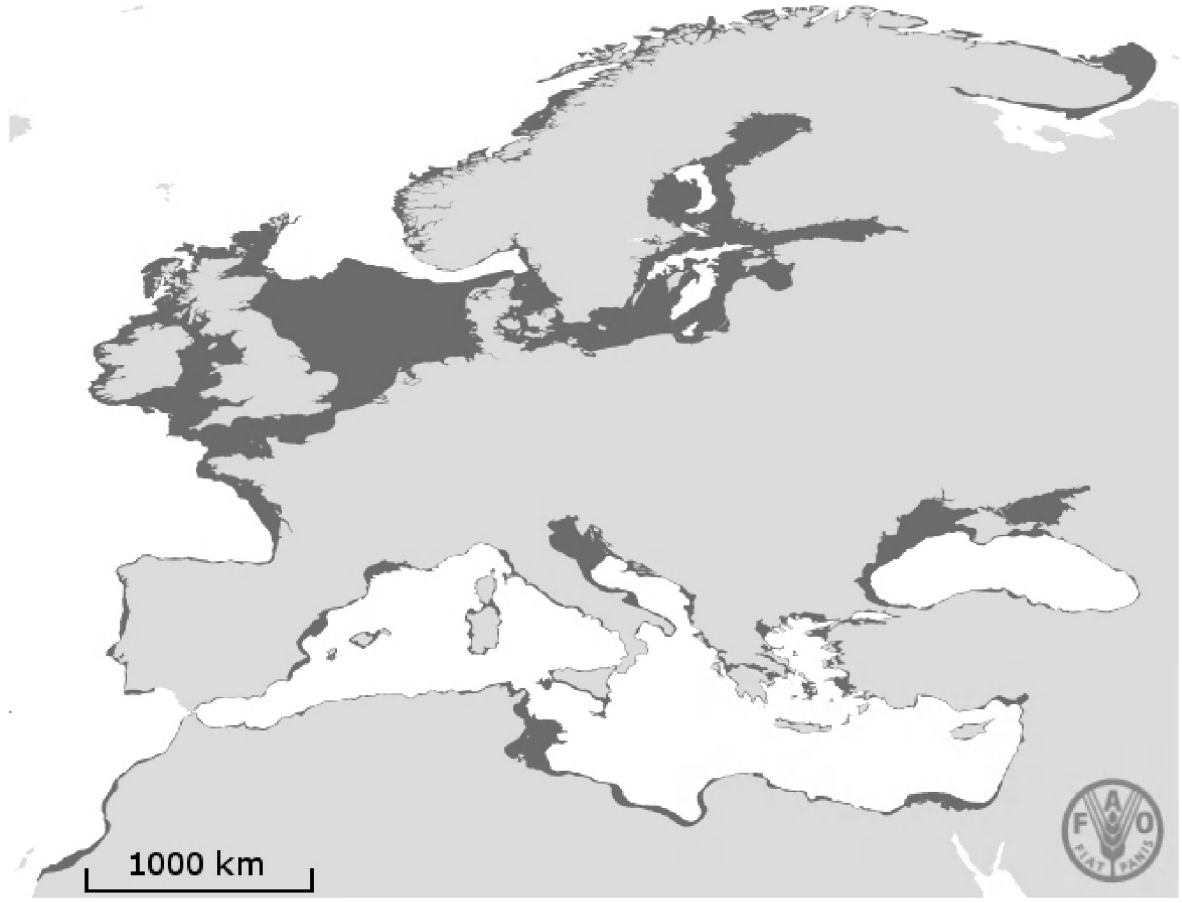

Fig 1.7. Geographical distribution of common shrimp (according to FAO 2012a).

Gene flow between the different populations is only restricted by oceanographic barriers, as drift of the offshore spawned larvae can cover a large area. *C. crangon* can tolerate salinities as low as 5 g l^{-1} (Cieluch et al. 2005; Gelin et al. 2001; Hageman 1970) and temperatures as high as 25-30°C (Caudri 1937; Weber & Spaargaren 1970; van Donk & de Wilde 1981;

Berghahn 1983) Apart from the low salinities and high temperatures, hydrographical restrictions only exist due to low oxygen contents (Haefner Jr. 1971; Hagerman & Vismann 1995). Although *C. crangon* can be found up to 40 m of depth, they typically dwell the shallow (<15 m, eulittoral and sublittoral) muddy or sandy tidal flats, creeks, marshes and estuaries, whereas *C. allmanni* inhabits the more offshore sandy areas of the North Sea. *C. crangon* is considered to be the dominant mobile epibenthic species in northern Europe (e.g. Pihl & Rosenberg 1982; Beyst et al. 2001; Amara & Paul 2003). During summer peaks, *C.crangon* can reach densities of 60 m^{-2} (Beukema 1992) or 80% of the estuarine biomass (Cattrijsse et al. 1997).

1.1.8 Fisheries

With an annual catch of 35,000 tons or more (fig. 1.8), a retail price of peeled shrimp of more than €30 kg^{-1} and a commercial value of the whole North Sea landings of roughly €100 million, common shrimp is one of the most valuable European fisheries and aquaculture commodities.

C. crangon is considered one of the few commercial species that cannot be overfished, as fishing mortality is much lower than natural mortality, i.e. 5-10% of the total mortality caused by gadoid (cod and whiting) predation (Welleman & Daan 2001).

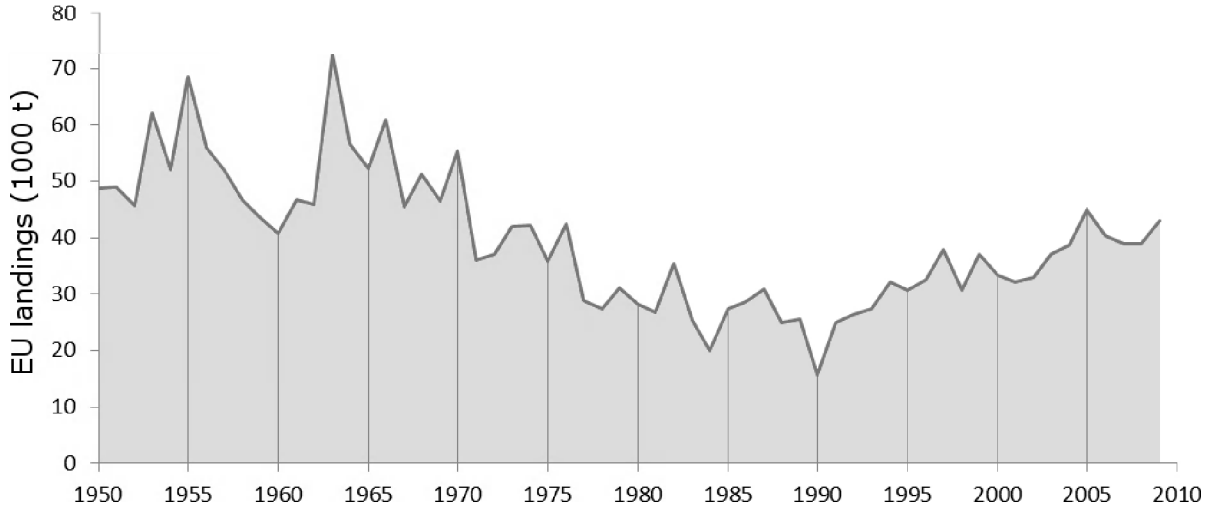

Fig 1.8. Total annual *C. crangon* EU landings (according to FAO 2012b).

Commercial fishery on *C. crangon* is carried out on a large scale along the entire North Sea coasts of Denmark, Germany, the Netherlands, Belgium and Northern France. Shrimp fisheries in other regions are limited to or nearby estuaries; England, France, Portugal, and Italy. It is also locally fished and sold in small quantities in several North African countries.

EU marketed shrimp are caught mostly in the Wadden Sea by the Dutch, German and Danish shrimp fisheries (45%, 40% and 10% of the total annual catch, respectively). Historically, fodder shrimp fishery (i.e. <50 mm shrimps used for feed production) was a major fishery and exceeded the food consumption fishery. However, Boddeke's (1962) hypothesis on sex reversal implied that exploitation of smaller shrimp may severely affect the population's fitness. The campaign which followed Boddekes statement resulted in the wide scale introduction of rotating shrimp sorting machines and in the termination of the fodder shrimp fishery in 1971. From the late 1960s, a strong, unexplained decrease in stock size and in the fraction of ovigerous females was observed in the Wadden Sea (Siegel et al. 2008). After an extremely bad year in 1990, the trend reversed and stock size and the fraction of ovigerous females have been rising, resulting in recent record landings. Due to oversupply, fishermen are currently considering to reduce their catch effort in order to counteract a further auction price drop. In contrast to the Wadden Sea, shrimp abundance in the Southern Bight did not recover until recently (based on Belgian fisheries data, Fig. 1.9). Currently, the local Belgian shrimp fleet exists of about 30 small vessels (engine power 104–221 kW), mainly built in the early 60s or mid-80s, which perform daily trips to provide fresh un-peeled cooked shrimp each morning. The Belgian shrimp fishery accounts for merely 1.2% of the annual EU catch. In contrast to the Wadden Sea, the shrimp abundance in the Southern Bight during winter is too low to support an intensive winter fishery. As a result, most Belgian shrimp fishermen focus on flatfish during winter, and investment in ship and gear modernization is rare due to lower profit compared to the Wadden Sea fishery. Furthermore, because auction price is based on total EU landings, the auction price dropped since 1991 due to increased landings in the Wadden Sea fishery, further decreasing the profit made by Belgian shrimp fishermen.

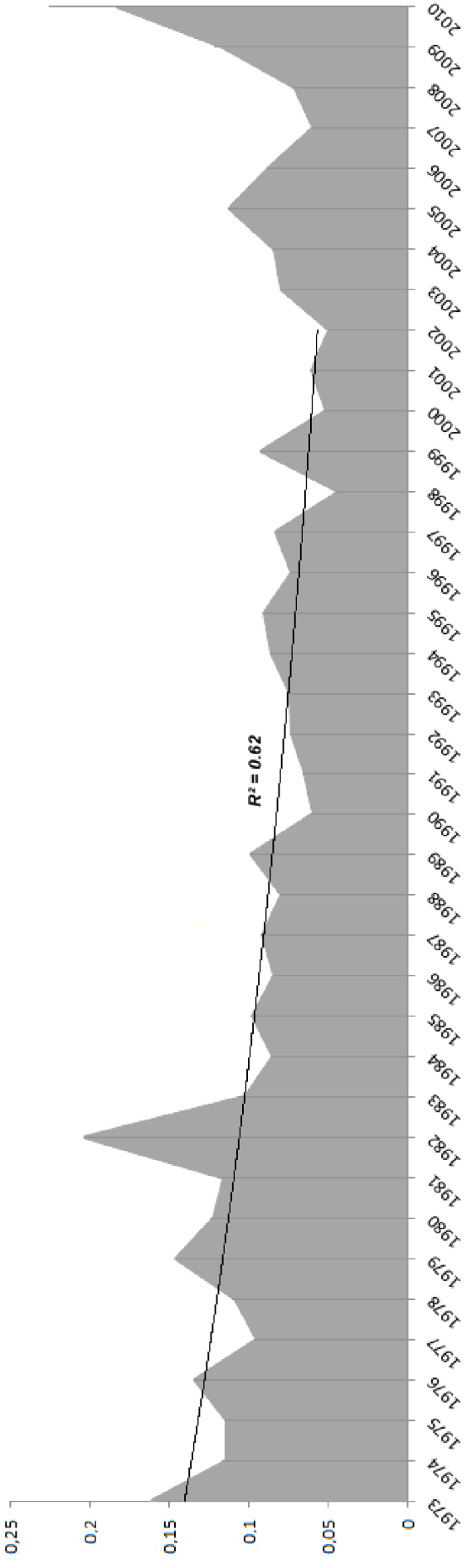

Fig 1.9. Long-term annual time series of landings per unit effort (LPUEs) for the local Belgian fleet (Y-axis, average monthly LPUEs in kg fresh weight (FW) horsepower^{-1} fishing hours^{-1}) during 1973–2010.

1.2 Nuclear receptors (NRs)

1.2.1 Types and functions

Many hormones act by binding to specific membrane-associated receptors, activating intracellular signalling cascades and triggering rapid nongenomic changes in cell functioning. Some lipophilic hormones however, passively diffuse through the plasma membrane (e.g. steroids such as testosterone) or are translocated by transmembrane carriers (e.g. thyroid hormone and calcitriol, the hormonally active form of vitamin D) into the cytoplasm and bind to NRs to trigger specific changes in gene expression. These NRs are ligand-activated transcription factors with a strongly conserved domain structure, and can directly induce target gene expression through interaction with specific hormone response elements (HREs) present within the target gene promoters. It is this ligand-dependent nature that makes EcR and other NRs susceptible for exogenous ligands such as, pharmaceuticals, pesticides and many other chemicals. NRs are classified into four functional types (Mangelsdorf et al. 1995; Novac & Heinzel 2004). Inactivated type I NRs are located in the cytosol, while type II NRs are located in the nucleus. Ligand binding induces conformational changes in the NR (see later), triggering a number of downstream events which are specific for each NR type. Ligand activation of type I NR leads to dissociation of heat shock proteins, homodimerization and translocation into the cell nucleus, where both NRs bind to the HRE, consisting of an inverted repeat. The NR – DNA complex in turn recruits additional proteins that are responsible for the transcription of the downstream gene(s) into RNA and eventually into protein(s). Type II NRs typically form a heterodimeric receptor, usually with RXR (see later) which is bound to a direct repeat HRE. Depending on the NR, the unliganded NR-DNA complex may exhibit a basal transactivation activity, or a corepressor protein complex may be associated with the NR, completely blocking its activity. When the ligand is present, a coactivator complex is recruited (replacing the corepressor complex), and downstream gene transcription is stimulated. Type III NRs are similar to type I NRs, but bind to direct repeat HREs. Type IV NRs can form monomers or dimers, but only a single NR binds to a half site HRE.

1.2.2 Structure

NRs are characterized by a modular structure comprising five distinct structural and functional protein domains (Evans 1988; Billas et al. 2009; fig. 1.10 and 1.11). The *N*-terminal A/B-domain is highly variable in length and amino acid composition and normally has a weak constitutive transactivation activity. As this domain is generally highly variable

between receptor isoforms and contains multiple phosphorylation sites, it is believed to be responsible for tissue and target gene-specific effects. In the C-domain or DNA-binding domain (DBD), two strongly conserved zinc finger motifs are present. Each motif contains four cysteine residues chelating a single zinc ion to form a tight loop structure. The first finger contains the proximal P-box, an α-helix that binds to HRE. The second finger contains the distal D-box, an α-helix perpendicular to the P-box and responsible for receptor dimerization.

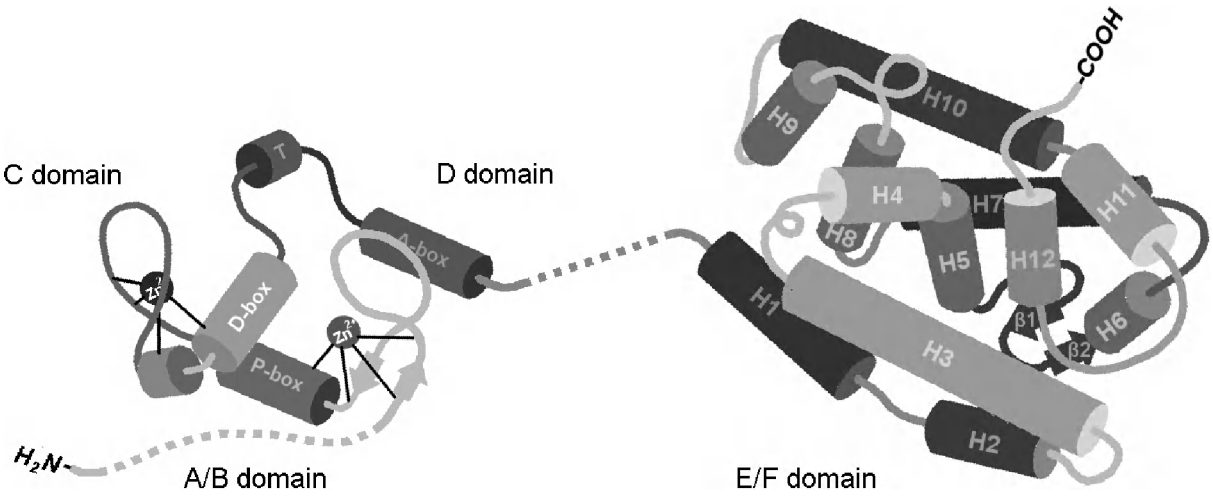

Fig.1.10. Simplified protein structure of a theoretical nuclear hormone receptor in an active holo-conformation (H12 closes the LBP). The variant A/B- and D-domain are represented by dotted lines; α-helices and β-sheets by cylinders and arrows, respectively.

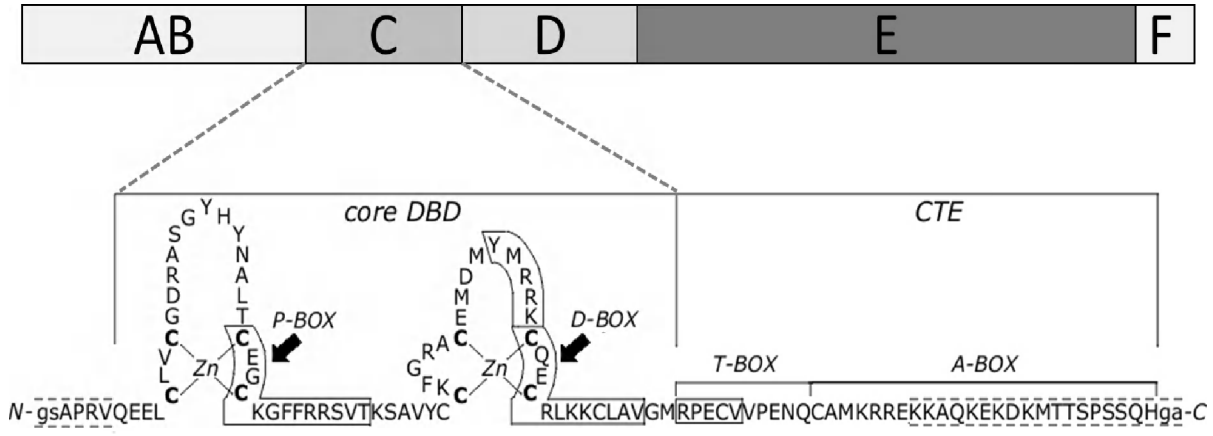

Fig. 1.11. Schematic drawing of nuclear receptor domain structure and of the core DBD and C-terminal extension (CTE) of *D. melanogaster* EcR (based on Devarakonda et al. 2003). α-Helices are boxed and β-sheets are shaded.

The poorly conserved D-domain has an ill-defined function, but behaves as a flexible hinge between the DBD and ligand-binding domain (see later). It contains the carboxy-terminal extension (CTE) of the DBD that generally consists of two conserved T- and A-boxes and

stabilizes the ternary heterodimer-DNA complex. The first residues of the T-box form a strongly conserved short α-helix and are believed to be important for dimerization and DNA-binding. The A-box is a long α-helix and contributes to DNA-binding. The moderately conserved E/F-domain or ligand-binding domain (LBD) has a complex tertiary structure of generally 12 α-helices referred to as a three-layered α-helical sandwich fold: helices H4/H5, H8 and H9 are flanked on one side by H1 and H3, and on the other side by H7 and H10/H11. The ligand-binding pocket (LBP) is situated within this structure and is closed on one side by an anti-parallel β-sheet and on the other side by H12. Ligand binding leads to a conformational shift from the inactive (apo) to the active (holo) state, where H12 closes the LBP, that in turn promotes the release of co-repressors and the binding of co- activators on the transactivation function in H12. The size and shape of the LBP and the presence of polar residues within the predominantly hydrophobic LBP determine the ligand selectivity and thus the receptor susceptibility to exogenous agonists.

NRs are characterized by having several variant deletion/insertion sites within their protein structure, leading to different isoforms of the same NR. These isoforms can be created evolutionary by gene duplication, alternative promotor usage or by alternative RNA splicing from a single gene. Splicing sites are most frequently observed within the variable A/B and D domain and are rarely found within the strongly conserved C and especially E/F domain. NR isoforms are often tissue and developmental stage specific and exhibit different dimerization and transactivation activity and specificity. Each NR isoform might control a diverse set of end-point effects in distinct tissues and life stages.

1.2.3 Nomenclature and phylogeny

All NR genes are believed to be derived from a single ancestral NR gene in an early metazoan. According to a phylogenetic study using nine complete NR sets of different animals (Bertrand et al. 2004), the bilaterian ancestor assumedly had about 25 NR genes. Gene loss and gene duplication have led to diverse sets of NRs (fig. 1.12). For example, 21 NR genes have been detected in *D. melanogaster* (Adams et al. 2000), 48 in humans (Robinson-Rechavi et al. 2001) and 270 in the nematode *Caenorhabditis elegans* (Sluder et al. 1999). NRs are categorized into seven (0 to 6) subfamilies, based on sequence homology (NR Nomenclature Committee (NRNC) 1999) (Fig. 1.8). Each NR is represented by a code in the form of NRxyz, where x is the sub-family, y the group and z the gene. Subfamily NR0 contains NRs that lack a DBD or LBD.

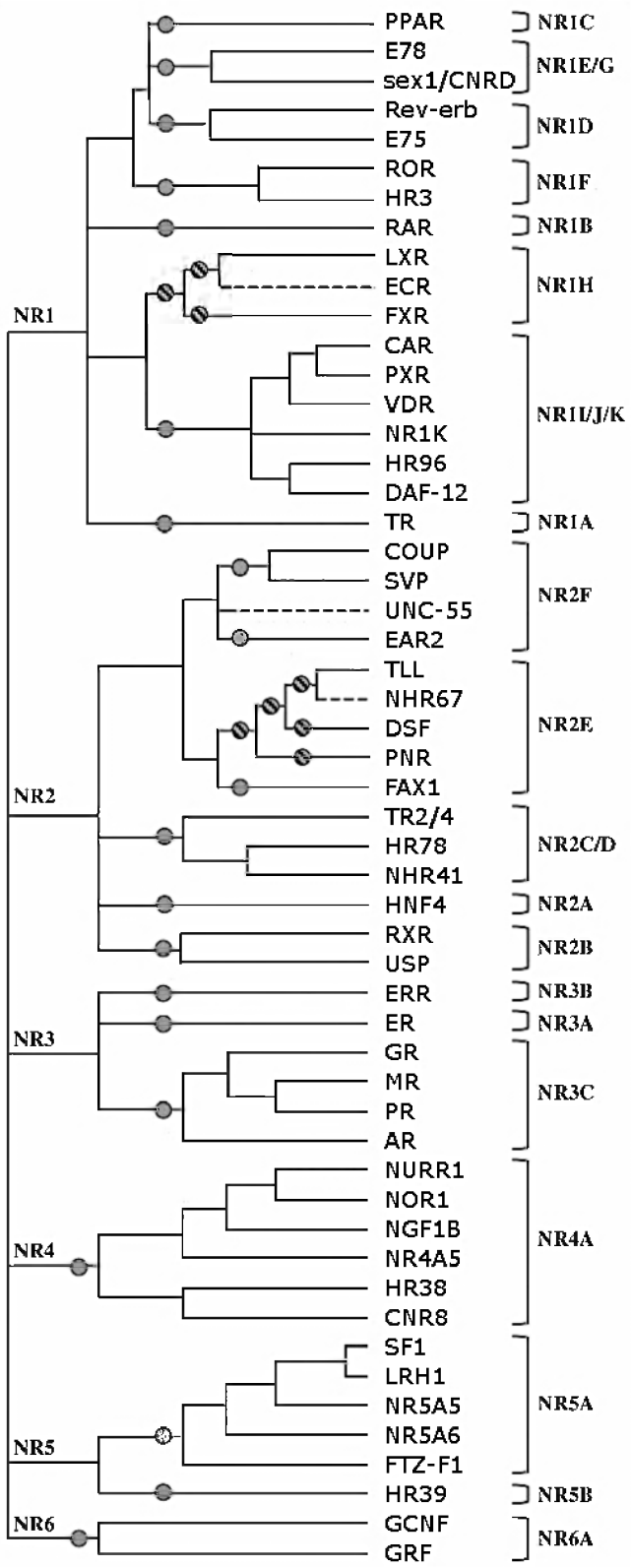

Fig 1.12. Phylogenetic tree of the NR superfamily (adapted from Bertrand et al. 2004). Gene groups are identified with the official gene nomenclature (NRNC 1999) on the right. Open circles indicate genes that are inferred to have existed in the common ancestor of insects, nematodes, and chordates. Hatched circles represent alternative ancestral genes. The broken lines leading to EcR, UNC-55, Rev-erbg, NHR67, and to the coral TLL/DSF indicate the lack of significant resolution of phylogenetic methods to position these genes.

1.2.4 The retinoid-X-receptor (RXR)

RXR, the fourth member of group B of the NR subfamily 2, is highly conserved throughout the animal kingdom. RXR serves as a heterodimerization partner for many other NRs, and as such is involved in the control of multiple endocrine pathways. The name RXR refers to 9-*cis*-RA, the putative ligand of vertebrate RXRs (Wolf 2006), whereas the natural ligand(s) for invertebrate RXRs is still under debate. The putative endogenous ligand for crustacean RXR is the terpenoid methylfarnesoate, which has been confirmed in the crab *C. pugilator* (Wu et al. 2004), but not in the water flea *Daphnia magna* (Wang & LeBlanc 2009). For decapod RXR, splicing sites have been observed in the T-box, between H1 and H3 and between H7 and H8 of the LBD (Kim et al. 2005).

1.2.5 The invertebrate ecdysteroid-receptor (EcR)

EcR, the first member of group H of the NR subfamily 1, is related to Liver X receptor (LXR) and Farnesoid-X-receptor (FXR), two vertebrate steroid hormone receptors. In order to achieve a high transactivation activity, EcR is believed to heterodimerize with RXR. While EcR structure and functioning in insects (especially Diptera and Lepidoptera) are well documented, our understanding of EcR structure and functioning in crustaceans remains limited. In decapod EcR, splicing sites in the A/B-domain, in the *C*-terminus of the D domain and between H2 and H4 have been observed (Chung et al. 1998; Asazuma et al. 2007).

.

1.3 Endocrine disruption

Since the publication of Rachel Carson's *Silent Spring* (Carson 1962), there has been increasing awareness that chemicals can exert profound and deleterious unintentional effects on wildlife and humans. Scientific and public awareness on chemicals which may interfere in the endocrine system of wildlife and humans arose after a first review on endocrine disruption by Colborn et al. (1993). An endocrine disruptive compound (EDC) is defined by the World Health Organization's (WHO) International Programme on Chemical Safety (IPCS) as:

"An exogenous substance (or mixture) that alters function(s) of the endocrine system and consequently causes adverse health effects in an intact organism, or its progeny, or (sub)populations"

The 'discovery' of endocrine disruption led to a shift from the classical diagnostic (eco)toxicological approach, in which the discovery of adverse effects preceded mechanistic research, to a precautionary toxicological approach, in which potential EDCs are identified based on their chemical structure and biological behaviour. Since 1993, a considerable amount of data has been collected on the early molecular events involved in endocrine disruption. EDCs can act at multiple sites via multiple mechanisms of action (MOAs). They can block the hormone receptors and thereby prevent natural hormone action (antagonism). Other EDCs mimic the biological activity of a hormone, activating the hormone receptor and finally leading to changes in gene expression characteristic for the hormone (agonism) (fig. 1.13).

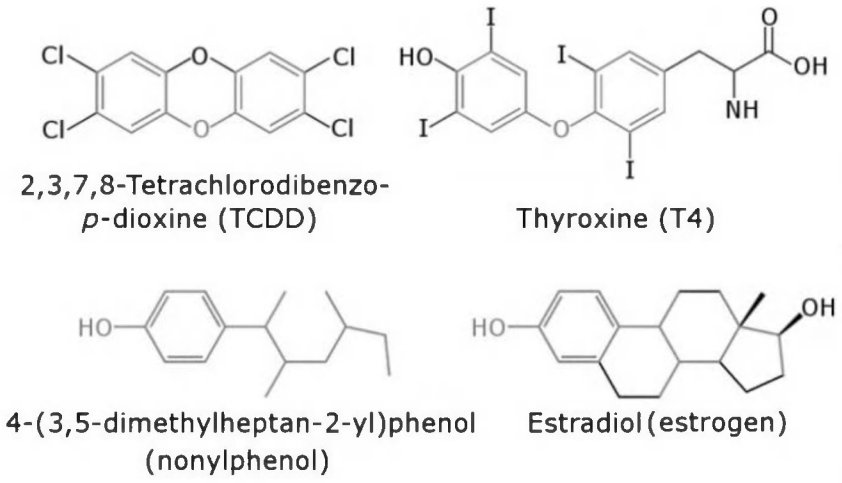

Fig. 1.13. Examples of EDCs (the dioxin tetrachlorodibenzodioxin and nonylphenol) mimicking hormone (thyroxin and oestradiol) structure and activity.

Numerous *in vitro* systems have been developed to evaluate the interactions of exogenous chemicals with hormone receptors, especially vertebrate thyroid, oestrogen and androgen receptors (Charles 2004). Receptor-mediated mechanisms have received the most attention, but other mechanisms have been shown to be equally important (Damstra et al. 2002). These mechanisms include inhibition of hormone synthesis, transport, or metabolism and activation of receptors through processes such as receptor phosphorylation or the release of cellular complexes necessary for hormone action. Endocrine disruption research is prone to many uncertainties and controversy (Damstra et al. 2002). Due to knowledge gaps and the complexity of the endocrine system, the relationship between these molecular events and adverse health effects is poorly understood. Most importantly, proven *in vitro* effects do not necessarily lead to significant *in vivo* effects, due to compensation by normal homeostatic mechanisms. *In vivo* effects may also occur unpredictably in other target tissues, due to cross-talk between different endocrine pathways. The dose–response paradigm is perhaps the most controversial issue. There is a large discrepancy between the high exposures in laboratory experiments and the low levels in the natural environment. Several authors (Calabrese 2004; Conolly & Lutz 2004) suggest the existence of non-traditional (i.e. non-monotonic) dose-response curves (fig. 1.14).

In reality, humans and animals are exposed to complex and variable combinations of chemicals and their derivatives (e.g. by biotransformation or photo-oxidation). While the exposures to each individual compound may be well below harmful levels, mixture effects can be additive (e.g. when substances exhibit similar modes of action), less or greater than additive, or even counteracting (Kjærstad et al. 2010). Timing of exposure is also critical to the understanding of dose–response relationships for EDCs. Identical *in vitro* exposure levels may produce different *in vivo* effects, depending on the life stage. For example, developmental or even maternal exposure may lead to permanent alterations in the endocrine functioning of the (offspring) adult (time lag), while adult exposure could be without effect (Walker & Gore 2011). Sensitivity to endocrine disruption may also vary considerably on the individual level with stress and health status, nutrition, genetic predisposition (e.g. receptor variants), past exposures (e.g. adaptation). In complex ecosystems, the range of risk modulators may be even greater.

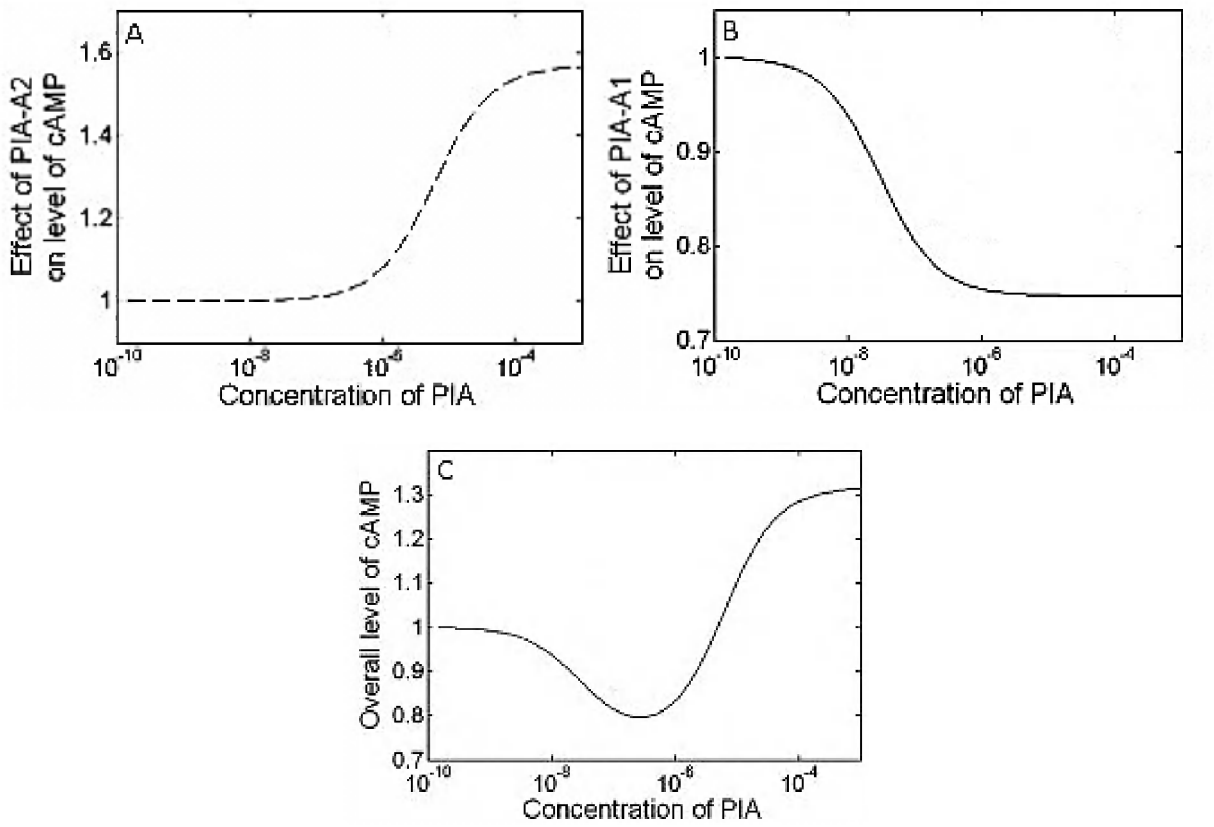

Fig. 1.14. Hypothetical model of a biphasic dose-response curve. Phenylisopropyladenosine (PIA) can bind two adenosine receptors, A1 and A2, which are present in equal amounts. Bound A2 receptor activates cAMP formation at higher PIA concentrations (to max. 157%, Fig.B), while bound A1 receptor decreases cAMP formation at lower PIA concentrations (to min. 75%, Fig C). The resulting biphasic dose-response curve is represented in Fig.D. (modified from Conolly & Lutz 2004)

EDCs encompass a variety of chemicals, including natural and synthetic hormones, plant constituents, pesticides, compounds used in the plastics industry and in consumer products, and other industrial by-products and pollutants (Damstra et al. 2002). While some EDCs are rapidly degraded in the environment, others are persistent and even bio-accumulative, and can be transported over long distances across national borders and can affect the health of humans and wildlife during several generations, even at remote areas (e.g. PCBs, dioxins, pesticides). For the same compound, the threat of endocrine disruption at low doses over vast areas outweighs by far direct toxic effects of point pollution. In humans, observed EDC effects include developmental, reproductive, as well as metabolic effects (e.g. obesity, liver disease, cardiovascular and pulmonary complications), psychological effects (e.g. learning disabilities and ADHD) and certain forms of cancer (Damstra et al. 2002). In wildlife, observed effects vary from subtle changes in the physiology and sexual behaviour of species to permanently altered sexual differentiation. organotins (OTs) provide one of the clearest examples of

environmental endocrine disruption (see 1.4). Observed wildlife effects however are nearly always confined to the individual level under laboratory conditions (Cheek 2006), while ecological risk assessment tends to focus on populations and communities. This may be problematic, because there is a limited understanding of how individual responses affect population and community. In contrast to human health, long-term epidemiological data in wildlife are scarce, hampering the diagnostic discovery of adverse EDC effects (Cheek 2006). Currently, routine ecotoxicological assessments only focus on a few wildlife species. Few studies have considered invertebrates, despite the knowledge that they are key to ecosystem structure and function. Even if potential wildlife EDC effects are observed, it is often impossible to demonstrate a causal link with a certain chemical due to insufficient historical and geographical exposure data and due to potential time lags between exposure and effect. Knowledge of the fate and transport of chemicals is also limited, particularly among the different environmental compartments (i.e. water, sediment, and biota). Interpretation of body burden data are often hampered by rapid metabolization (Elsby et al. 2001), so quantification of metabolites in biological samples is necessary. For these reasons, cause-effect relationships are currently available for only few persistent chemicals in highly contaminated areas.

1.4 Organotin compounds

1.4.1 Organotin chemistry and applications

Organotins (OTs), generally represented by the formula R_XSnL_{4-X}, contain a tetravalent tin atom (Sn) covalently bound to one to four organic substituents (R_X, such as CH_3, C_4H_9, C_5H_{11} and C_8H_{17}) and one to three halogen atoms or oxygen- or sulphur-based organic moieties (L_{4-X}, such as Cl, F, SR' and OR') (fig. 1.15).

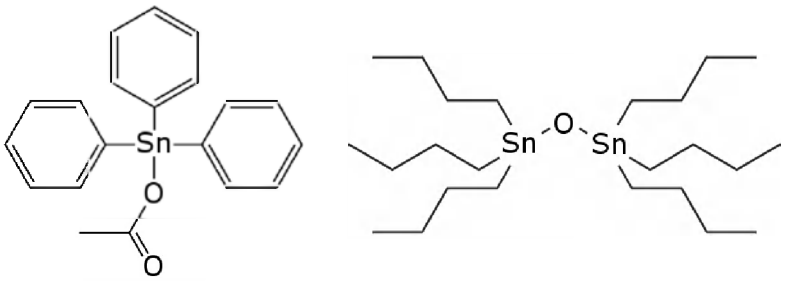

Fig. 1.15. Chemical structures of triphenyltinacetate (left) and bis(tributyltin)oxide (TBTO) (right).

The number and nature of the organic substituents largely determine the electronegativity of the tin atom and thus the physical and chemical properties of the OT. For example, while monobutyltintrichloride (C_4H_9-$SnCl_3$) is readily soluble in water, tetrabutyltin ($(C_4H_9)_4Sn$) is only soluble in non-polar solvents. OTs are quite stable because of the non-polar nature of the carbon-tin bond. Long chain alkyl groups are cleaved less easily from the Sn ion than shorter alkyl groups and aryl, allyl and vinyl groups.

Table. 1.1. Nomenclature and physicochemical properties of TBTO (ECHA 2008).

CAS Bis(tributyltin)oxide	**IUPAC** Hexa-n-butyldistannoxane
Formula $C_{24}H_{54}OSn_2$	**Dissociation constant** 6.25
Appearance Colourless liquid	**Vapour pressure** 1 x 10^{-5} Pa at 20°C
Molecular weight 596.07 g	**Melting point** <-45°C
Density 1.17 g cm^{-1} at 20°C	**Boiling point** 173°C
Water solubility 4 mg l^{-1} at 20°C, pH 7	**Flash point** 190°C
Log K_{ow} 3.2-4.1	**Decomposition** >230°C

While the first OTs were experimentally synthesized in the 1850s by Carl Löwig and Edward Frankland, they only became economically relevant after World War II, especially as heat and light stabilizers in PVC materials, which still is the major use today (15,000 tons in 2002 in the EU; RPA 2007). Mono- and diOTs (i.e. OTs having one and two organic substituents,

respectively), especially dioctyltin, dibutyltin and dimethyltin, reduce PVC degradation by scavenging hydrochloric acid. Some formulations have been approved for food contact applications. Mono- and diOTs are used as catalysts to speed up polymerization reactions during the curing of coatings and the synthesis of plasticizers, silicones, electrodeposition coatings and polyurethanes (~1,500 tons per year in EU). MonoOTs and to a lesser extent diOTs are also used as a precursor for ZnO_2 glass coatings (~780 tons in 2002 in EU; RPA 2007). In the 1950s, the powerful biocidal properties of trialkyltin and triaryltin derivatives were discovered by the research team of Prof. Dr. van der Kerk (Van der Kerk & Luijten 1954). Owing to their relatively poor mammalian toxicity (see 1.4.7), TBT $(C_4H_9)_3Sn$-L) and triphenyltin (TPhT, $(C_5H_{11})_3Sn$-L) were widely used as pesticides and active antifouling ingredients since the late 1950s (1,330 tons in 2002 in the EU; RPA 2007). Other applications include preservation of wood, textile, paper and leather (until 2003) and of water-based paints and adhesives, polyurethane foams and other polymers (until 2006); surface and instrument disinfectants (until 1995 and 1990, respectively; RPA 2007).

1.4.2 TriOTs in crop protection

In the early 1960s, triphenyltin hydroxide and triphenyltin acetate ("fentins" TPTH and TPTA) became popular as broad-spectrum fungicides (e.g. Brestan) to tackle a range of agricultural fungal diseases, particularly potato blight (*Phytophthora infestans*); leaf spot (*Cercospora beticola*, *Ramularia beticola*), and powdery mildew (*Erysiphe betae*) on celery, peanuts, and sugar beet; *Pseudoperonospora humuli* on hop; grey moulds on onions; rice blast; brown rust on beans; and coffee leaf rust (Duft et al. 2002). Other triOT pesticides such as tricyclohexyltin-hydroxide and -triazole (TCTH and TCTT) and trineophenyltin oxide (TNTO) were used as acaricides on citrus, top fruit, vines, vegetables, and hops (RPA 2005). In the early 1960s (Murbach & Corbaz 1963), fentins were used as effective anti-feedants, sterilising crop feeding insects such as the Colorado potato beetle. The use of TPhT as a pesticide has been prohibited by amendments 2002/478/EC and 2002/479/EC to the 91/414/EEC Plant Protection Products Directive (PPPD). Estimates of historical annual TPhT use in agriculture are unavailable. The use of the acaricides TCTH, TCTT and TNTO are permitted under the PPPD. In 2003, it has been estimated (by industry) that a total of 100 tons per year of tri-substituted OTs (excluding TPhT) were used in pesticides (RPA 2003).

1.4.3 TriOTs in antifouling applications

Biofouling is the settlement and growth of marine organisms on submerged man-made structures such as ship hulls, buoys and fish cages. The bio-fouling process basically consists of three steps (Cao et al. 2011). First, dissolved organic material (proteins, polysaccharides, proteoglycans) are attracted to the surface by physico-chemical interactions (Brownian motion, electrostatic interaction, Van der Waals forces,…), forming a conditioning film. Secondly, microorganisms (bacteria and diatoms) passively adsorb or actively adhere through excretion of extracellular polymeric substances (EPS) to the sticky surface, forming a biofilm. This 'microfouling' on ship hulls can already increase fuel consumption with 18% (Lewin 1984). Finally, larvae and spores of 'macrofoulers' (e.g. barnacles, mussels, tubeworms, sponges, seaweeds) settle down on the biofilm and evolve to a complex biological community 2-3 weeks later. Biofouling can increase fuel consumption with 40% after six months (Champ 2000). Other impacts include increased hull corrosion and more frequent and time consuming hull maintenance (dry-docking). More than 2,000 years ago, wooden ship hulls were already covered with copper and lead plating to prevent biofouling (Omae 2003). Until the 1960s, copper and arsenic compounds in wax, tar and resin formulations were used. Since the 1960s, TPhT and especially TBT compounds were used as antifouling agent. At first, free association coatings were applied. These coatings consisted of an insoluble (e.g. vinyl or epoxy) or soluble (resin) matrix which will slowly leach the OT. In 1974, the first self-polishing copolymer coating (SPC) revolutionized the entire shipping industry (Cao et al. 2011). In SPC coatings, TBT is slowly hydrolysed from an acrylic polymer, which is washed away by passing seawater to reveal a fresh coating surface. In SPC coatings, the polishing rate was easily controllable by manipulating the polymer chemistry, while TBT leached at a rate independent of sailing speed. TBT use peaked in 1996, when 85% of the ships were equipped with a TBT-based coating (OSPAR 2011). Around 4,000 tons of TBT were used that year in antifouling agents, 3,000 and 1,330 tons of TBT were produced and sold in the EU, respectively (Klingmüller & Waterman 2003). Estimates of global annual fuel savings ranged from $500 million to one billion (Champ 2000).

1.4.4 Environmental fate

In aqueous solution, TBTO dissociates to two hydrated TBT cations. At pH 6.25, half of the TBT occurs as cation (Arnold et al. 1997). As the pH increases more of these free ions will form complexes with chloride, hydroxide and carbonate. The main inputs of OT compounds into the marine environment are direct releases from antifouling on ships, discharges to water

from industry, waste water treatment plants and waste treatment through riverine inputs (Hoch 2001; fig. 1.16). Besides, there is continuous re-location and re-suspension through dredged spoil disposal. Environmental levels of TBT range from undetectable in the open ocean to 17 ng l^{-1} in estuaries and 100 ng l^{-1} in harbours (Fent 1996).

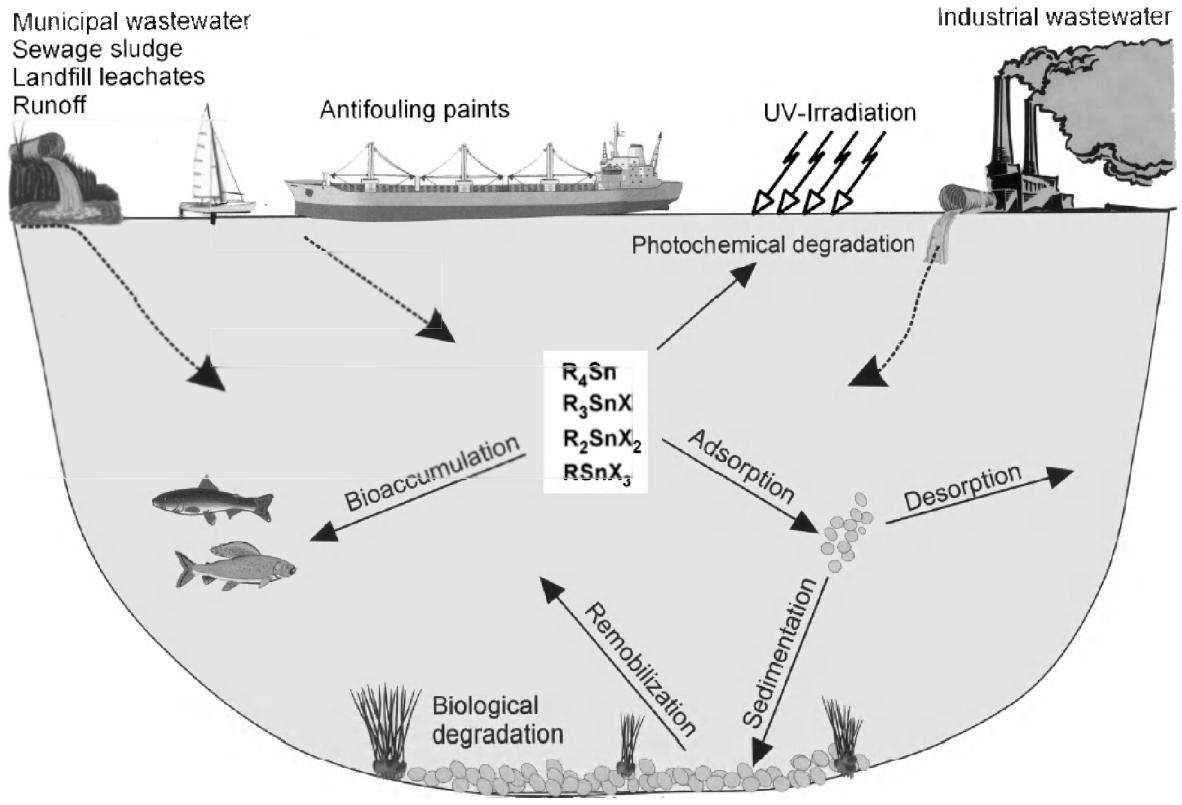

Fig. 1.16. Distribution and fate of OTs and their general routes into the aquatic environment (reproduced from Hoch 2001).

The Henry's Law coefficient for TBTs is estimated around 2 x 10^{-5} kPa mol^{-1}, indicating that the volatility from aqueous surfaces is too low for long-range air transport. The high octanol/water partition coefficient (K_{ow}, around $5x10^4$) for TBTs in 25‰ seawater (Laughlin et al. 1986) indicates that TBT will preferentially associate with sediment, biota, dissolved organic matter, and suspended particulate matter. OT compounds interact with metal oxides in the sediment and proteins in biota by forming five- or six coordination complexes with electronegative oxygen and nitrogen atoms (Omae 1989). The association of TBT with particulate material results in sedimentary sinks with concentrations reaching several orders of magnitude higher than those in the overlying water column. Reported levels of TBT in sediments reached up to 2,000 µg kg^{-1} dry weight (DW). TBT sorption is characterized by a rapid, reversible stage, where 80% of the final sediment concentration is sorbed within 10 minutes (Langston & Pope 1995), and a slow, non-reversible stage, where TBT diffuses into

the porous microstructure of the organic material (Pignatello & Xing 1996; Ma et al. 2000). Several studies have shown that the toxicity of polluted sediment may be more closely related to the pollutant concentration in pore water than in the bulk sediment (Kemp & Swartz 1988; Landrum 1989). Monitoring data, however, are often limited to concentrations in surface water and sediment.

1.4.5 Bioaccumulation, bioconcentration, and depuration

Bioaccumulation refers to the degree of contaminant uptake by an organism. Total accumulation will depend upon intake rate through multiple exposure routes (dietary, dermal, respiratory) and depuration rate (excretion and breakdown). Bioconcentration refers to the accumulation as a result of direct exposure to the surrounding medium. The bioconcentration factor (BCF) is commonly applied to aquatic species and is defined as the ratio of the concentration in the water column to the concentration in the organism. According to EU regulations on the registration, evaluation, authorization and restriction of chemicals (REACH), a substance is considered to be bioaccumulative (B) when the BCF is higher than 2,000 l kg^{-1}, and very bioaccumulative (vB) when its BCF is higher than 5,000 l kg^{-1}.

In contrast to many other persistent EDCs, OTs have a very low lipid solubility, do not accumulate in fatty tissues and subsequently show limited biomagnification. Instead, they bind to electronegative atoms (e.g. N, P, S, and O) in proteins. Among invertebrates, annelids and crustaceans exhibit BCFs around 10^3, while molluscs and particularly predatory prosobranchs exhibit concentration factors up to 10^5 (ECHA 2008). In marine species, an inverse relationship of BCF with concentration is observed (the lower the concentration, the higher the BCF value; Salazar & Salazar 1996). In biota, OT compounds are actively depurated from the detoxifying organs. In the gills and digestive gland of the blue mussel (*Mytilus edulis*), the depuration of TBT is a biphasic process involving a rapid and a slow TBT depuration process, with half-lifes of 2.2-5.3 and 28-69 days, respectively (Page et al. 1995). The depuration in other tissues only followed the slower process. In marine fish, depuration half-lives between 7 and 29 days are reported (Yamada & Takayanagi 1992).

1.4.6 Persistence

Persistence reflects the resistance of the substance towards degradation, which can be of a chemical (e.g. hydrolysis, photolysis) or biological (i.e. enzymatic breakdown or transformation) nature. It is quantified by the degradation half-life, i.e. the time needed to degrade or transform half of the substance. A substance with a half-life of more than 60 days

in marine water or more than 180 days in marine sediment is considered to be persistent (P) according to REACH regulations.

TBT degradation consists of a progressive dealkylation down to less toxic inorganic tin:

$$(C_4H_9)_3SnX \rightarrow (C_4H_9)_2SnX_2 \rightarrow (C_4H_9)SnX_3 \rightarrow SnX_4$$

Dissolved in sterile water and in the dark, the C-Sn bonds are stable against hydrolysis. In sunlight however, a slow iron (III) photo-induced degradation (half-life > 89 days) is observed (Maguire et al 1983). Dissolved in non-sterile estuarine water, the half-life drastically decreases to 7 to 13 days and 3 to 6 days in the dark and in sunlight, respectively (Lee et al. 1989), suggesting the importance of bacteria and microalgae (diatoms and dinoflagellates). OT compounds are however rapidly adsorbed to suspended solids and subsequently deposited (see 1.3.4), where degradation is much slower. Sarradin et al. (1995) estimated the half-life of TBT from the vertical distribution of butyltin compounds in marine sediments to be 2.1 years, while other scientists reported half-lives of 1 up to 15 years (Sarradin et al. 1995; ECHA 2008). Bacteria as well as Eukaryota have an active cytochrome P450 dependent monooxygenase system that oxidizes TBT to a series of hydroxylated derivatives. These hydroxylated derivatives spontaneously dealkylate to less toxic DBT or MBT or are transformed to water soluble sulphate or carbohydrate conjugates by phase-two enzyme systems, which facilitates the depuration of TBT (Lee 1996).

1.4.7 Toxicity

Toxicity is the degree to which a certain chemical can cause harm on a certain target organism. Generally, a distinction is made between acute toxicity and chronic toxicity. Acute toxicity focuses on lethal effects of high exposure during a short time period (e.g. 96 hours). Mortality values such as the median lethal concentration (LC_{50}) and median lethal dose (LD_{50}) refer to the concentration (e.g. in $\mu g\ l^{-1}$) and dose (e.g. in mg kg^{-1} body weight (BW) day^{-1}), respectively, that kill half of the organisms during the exposed time period. Regarding chronic toxicity, the focus is on sublethal effects of lower, often environmentally relevant concentrations during an extended time period (weeks up to years). Sublethal effects include alterations in growth, immune response, reproductive success, and even offspring effects. Sublethal effect values include the median effect concentration (EC_{50}) and median effect dose (ED_{50}). The lowest observed effect concentration (LOEC) and lowest observed effect level (LOEL) refer to the lowest concentration or dose, respectively, at which an effect is observed.

The no observed effect concentration (NOEC) and no observed effect level (NOEL) refer to the highest concentration or dose, respectively, at which no statistically significant effect is observed. Although the use of NOEC and NOEL values is disputed as they are in conflict with the scientific fundament of hypothesis testing, they are still common practice (Yanagawa 2001). According to REACH regulations, a substance is toxic when the NOEC for marine organisms is less than 0.01 mg l^{-1}, or when the substance is classified as carcinogenic, mutagenic, or toxic for reproduction, or when there is other evidence of chronic toxicity.

The impairment of the mitochondrial ATPase-ATPsynthase complex at micromolar levels is since long known as the main lethal effect of OTs (Aldridge 1958; Stockdale et al. 1970). TBT blocks the proton channel of ATPase (Stockdale et al. 1970) and ATPsynthase (von Ballmoos et al. 2004), thereby completely blocking the electron transport chain and thus the cellular energy metabolism. Non-mitochondrial biochemical effects include haemolysis (Kleszcynska et al. 1997), release of Ca^{2+} from the sarcoplasmatic reticulum (Kang et al. 1998), inhibition of phosphatidylserine-induced histamine release (Iwai et al. 1992), and the induction of apoptosis in lymphocytes (Stridh et al. 1999). In general, acute OT toxicity strongly decreases with decreasing number of alkyl substituents:

$$R_3SnL \gg R_2SnL_2 > RSnL_3 > SnL_4$$

While inorganic tin and monoOTs are considered non-toxic, diOTs are considered mildly toxic and triOTs are extremely toxic to all types of living species. The sensitivity of the various zoological groups depends on the length of the alkyl chains. Higher organisms are most sensitive to trimethyl- and triethyltins, fungi and bacteria are most sensitive to tripropyl- and tributyltins (Evans & Smith 1975). The acute toxicity strongly decreases with further lengthening of the alkyl chains. Trioctyltins are practically considered non-toxic. The inorganic substituent (L) does not have a significant effect on toxicity, but influences volatility and solubility, and thus the bio-availability.

The sublethal effects of TBT on marine invertebrates, especially molluscs, have been well-documented since the 1980s, when TBT was linked to shell deformations and effects on the reproduction of the Pacific oyster (*Crassostrea gigas)* (Alzieu et al.1982) and to the incidence of imposex in dog whelk (*Nucella lapillus*) populations (Bryan et al. 1986). Imposex is characterized by the formation of male sexual organs, i.e. penis and vas deferens, the latter blocking the oviduct, and by ovarian spermatogenesis, ultimately resulting in sterile females. Imposex has been reported in over 150 mollusc species from field observations (Matthiessen

et al. 1999). *N. lapillus* is the most sensitive species and also the most widely used in TBT-specific environmental monitoring programs. A LOEC of 2 ng l^{-1} was reported for *N. lapillus* (Gibbs et al. 1987). TBT also induces a second masculinization phenomenon in the periwinkle *Littorina littorea*, referred to as intersex (Oehlmann 1998). It is a change in the female pallial organs towards a male morphological structure. Intersex occurs at 100-fold higher concentrations than imposex, and is used as biomarker in areas of high TBT exposure.

1.4.8 Mode of action

Prior to 2001, several hypotheses have been proposed concerning the mechanism of TBT induced imposex, but experimental evidence is weak:

- increased levels of APGWamide (Ala-Pro-Gly-Trp), a neuropeptide hormone that controls the production of male accessory sex organs in gastropods (Féral & LeGall 1983; Oberdörster & McLellan-Greene 2000).
- increased androgen levels, such as testosterone, due to inhibition of P450 aromatase (Bettin et al. 1996), or due to inhibition of testosterone excretion (Ronis et al. 1996).

In 2001, it became clear that expression of the aromatase gene was down-regulated by TBT and TPhT in human ovarian granulosa cells, similar to the effects of treatment with ligands for either Peroxisome-Proliferator-Activated Receptor γ (PPARγ) or RXRs (Mu et al. 2001). In 2004, Nishikawa et al. (2004) showed that TBT and TPhT are high affinity agonists for human RXRα. As RXR is a strongly conserved NR within the animal kingdom, a similar pathway may lead to imposex in molluscs. Furthermore, Nishikawa et al proved that 9-*cis*-RA, the (putative) natural RXR ligand, also induced imposex in rock shell *Thais clavigera*, which implies that RXR plays an important role in the differentiation and growth of male genital tracts in female gastropods.

1.4.9 EU policy regarding the use of TBT

The harmful effects of TBT on the coastal environment were first observed in the Bay of Arcachon, located along the French Atlantic coast halfway between the Gironde estuary and the Spanish border (Alzieu et al. 1982). Here, shellfish farming, primarily oyster farming (10,000-15,000 tons per year), and watersport tourism (a total mooring capacity of 7,800 pleasure boats) are the major activities. TBT contamination of the bay waters coincided with a major crisis, starting in 1975, in the oyster farming sector. Oyster production within the bay suffered from a progressive decline of reproduction and juvenile recruitment ('spatfall') and from a general outbreak of shell calcification anomalies. Oyster production dropped back to 3,000 tons in 1981. In January 1982, following the recommendations of an *ad hoc* committee, France enforced a 2-year ban on the application of paints containing more than 3% by weight of TBT on boats less than 25 m long, in areas of extensive oyster cultures along the English channel and the Atlantic coast (Champ 2000). In September of the same year, the ban was expanded to cover all the coastal areas of France and all TBT-containing paints. Other EU countries enforced similar national restrictions starting in 1985. In 1989, The EU adopted a ban on the use of TBT and TPhT antifouling paints on boats < 25 m (Directive 89/677/EEC). The following year, the members of the International maritime organisation (IMO) agreed resolution 29 of the IMO marine environment protection committee (MEPC), banning TBT on vessels < 25 m and limiting the vessel release rate at 4 µg TBT cm^{-2} day^{-1}. The legislation was adopted internationally with governments imposing national regulations. At that time, TBT use on larger vessels was not targeted, as it was assumed that offshore levels would be too low to cause effects. At the 42th MEPC meeting in 1998, several EU countries called for a world-wide ban on TBT paint on all ships. At the following meeting in 1999, the international convention on the control of harmful antifouling systems (AFS convention) was proposed. The convention stated that reapplication of TBT-containing paints would be prohibited after the 1st January 2003, and no ships or structures (e.g. aquaculture cages) should bear TBT as of the 1st January 2008. The 159 IMO member states adopted the Convention in October 2001. The treaty could only enter into force once a minimum of 25 member states representing 25 % of the world's shipping tonnage had signed. The treaty was controversial, as adequate alternative antifouling agents were lacking (Champ 2000). Several IMO parties and shipping companies strongly opposed the forthcoming ban, while the TBT industry organized into a pressure group called organotin environmental programme (ORTEP). Consequentially, many countries became reluctant to sign the treaty. In 2000 and 2001, respectively, Germany and Belgium attempted to enforce their own legislation, but were ruled out by the Commission. In

November 2002, the EU adopted the IMO-proposal and interdicted the application of TBT based formulations on EU flagged vessels after 1st of July 2003 and the presence of those paints on all ships visiting EU ports from 1st of January 2008 (EC 782/2003). Meanwhile in the IMO, the deadline of 1st January 2003 had passed. On 17th September 2007, the AFS convention was finally ratified and entered into force on 17th September 2008.

At EU level, several Directives are also of importance in OT regulation, besides the AFS-related EU measures discussed earlier. Regarding other uses of TBT, the biocidal products directive (BPD, directive 98/8/EC) led to an official cessation of non-notified use in September 2006. Non-notified use of other OTs already ceased in December 2003.

1.4.10 EU policy regarding the environmental impact of TBT

The convention for the protection of the marine environment of the North-East Atlantic (OSPAR) was set up in 1992 and entered into force in 1998. OSPAR is the current legal instrument guiding international cooperation on the protection of the marine environment of the North-East Atlantic. The OSPAR commission currently has 16 contracting parties (*i.e.* 15 EU states and the EU itself) and observers which are an active part of the commission. The observers include 18 intergovernmental organizations (*e.g.* ICES, IMO, OECD, and UNEP) and 34 international non-governmental organizations, representing both environmental groups (*e.g.* Greenpeace, WWF) and industry. OSPAR's hazardous substances strategy aims at reducing the discharge of persistent, bio-accumulative and toxic (PBT) substances to achieve (close to) zero concentrations for man-made synthetic PBT substances and near background values for naturally occurring PBT substances by 2020 ('the generation goal'). OSPAR's work on hazardous substances comprises the identification of such contaminants, the monitoring and assessment of their sources and pathways and their concentrations and effects in the marine environment, and the identification and promotion of control measures required to achieve the objectives.

TBT is currently on the OSPAR list of chemicals for priority action, and monitoring of the concentrations in sediment and of the biological effects (imposex/intersex in marine gastropods) are mandatory elements of OSPAR's coordinated environmental monitoring programme (CEMP) since 2003. Target compounds include TBT, dibutyltin (DBT) and monobutyltin (MBT) and TPhT, diphenyltin (DPhT), and monophenyltin (MPhT). Monitoring of TBT concentrations in marine biota is currently included in pre-CEMP, which contains components for which the contracting parties are preparing a co-ordinated monitoring. As filter feeders accumulate high OT concentrations, target species are the

bivalves *Mytilus edulis* and *M. galloprovincialis*, or *Crassostrea gigas* where *Mytilus* species are absent. In the EU water framework directive (WFD, directive 2000/60/EC) and the new EU marine strategy framework directive (MSFD, directive *2008*/56/EC), TBT is also included on lists of priority hazardous substances for monitoring.

1.4.11 Alternatives to TBT

After 1996, shipping companies slowly started to proactively switch back to copper-based coatings, which were regarded as the best intermediate alternative (Cao et al. 2011). Meanwhile, the paint manufacturing sector started developing alternatives. In 2003, while the IMO ban was not ratified yet, production of TBT-based antifouling paints almost completely ceased. In some alternative coatings, TBT had been replaced by other biocides (e.g. irgarol, zinc pyrithione, ziram and thiram). Since 2005, non-toxic and non-stick coatings (e.g. hempasil) were developed, which render the ship's hull too smooth for organisms to attach. Although they are more expensive than copper-based coatings, their efficacy and longer shelf life make them a success story.

Chapter 2

Retinoid-X and ecdysteroid receptors in common shrimp

Parts of this chapter have been published as:

Y. Verhaegen, K. Parmentier, L. Swevers, P. Rougé, T. Soin, W. De Coen, K. Cooreman and G. Smagghe, 2010. The brown shrimp (*Crangon crangon* L.) ecdysone receptor complex: cloning and functional expression in an EcR-deficient Drosophila cell line. General and Comparative Endocrinology, 168, 415-423.

Y. Verhaegen, K. Parmentier, L. Swevers, E. Renders, P. Rougé, W. De Coen, K. Cooreman and G. Smagghe, 2011. The heterodimeric ecdysteroid receptor complex in the brown shrimp *Crangon crangon*: EcR and RXR isoform characteristics and sensitivity towards the marine pollutant tributyltin. General and Comparative Endocrinology, 172, 158-169.

2.1 Introduction

In 2004, Nishikawa et al. (2004) showed that TBT binds and activates the human RXRα, and that 9-*cis*-RA, the natural ligand for RXRα, induced imposex in the rock shell *Thais clavigera*. In contrast with vertebrate RXR, invertebrate RXRs do not form active homodimers, but are believed to act as a 'silent' but 'obligate' partner for many other NRs. In other words, invertebrate RXR is believed not to bind a hormone ligand, but its presence within the heterodimer is necessary to attain a high activity of the partner receptor. Thus, while RXR does not have a transactivational capacity on itself, it is of major importance in modulating the activity of other NRs. As a consequence, RXR activity can only be measured indirectly by measuring the altered activity of the partner protein. EcR is the most well-known invertebrate partner protein for RXR. Through EcR, circulating levels of ecdysteroid hormones, such as 20E and ponA, determine developmental (e.g. moulting) and reproductive (e.g. spawning) timing in many invertebrates. In this chapter the molecular cloning of RXR and EcR from common shrimp is described. The obtained genetic sequences are analysed phylogenetically and their 3D protein structure is reconstructed *in silico*. In chapter 3, this information will then be used to develop and apply an ecdysteroid-responsive cell line containing shrimp EcR and RXR.

2.2 Material and Methods

2.2.1 Collection of *C. crangon* and isolation of RNA

Ovaries were dissected out of a large (>75 mm L_T) female *C. crangon* which was sampled during low tide at Bredene beach (Belgium). Total RNA was isolated through acid guanidinium-phenol-chloroform extraction (Chomczynski and Sacchi, 1987) using TriReagent® (Sigma-Aldrich, Bornem, Belgium), according to the manufacturer's protocol. The quality and quantity of the extracted RNA was examined by gel electrophoresis and spectrophotometry using a Nanodrop™ ND-1000 (Thermo Fisher Scientific, Asse, Belgium).

2.2.2 Molecular cloning of conserved partial sequences of CrcEcR and CrcRXR

First strand cDNA synthesis was performed using SuperScript™ II reverse transcriptase (Invitrogen, Merelbeke, Belgium) with the oligo$(dT)_{12\text{-}18}$ primers according to the manufacturer's protocol. The cDNA sequences of CrcRXR and CrcEcR were derived using several successive PCR techniques. First, partial sequences for the strongly conserved DBDs were obtained through degenerate PCR consisting of 35 cycles of 50 µl reactions (3 mM

$MgCl_2$ and annealing temperature 59°C). Degenerate primers were designed based on the known coding sequences from four other Decapoda species: *C. maenas*, *Gecarcinus lateralis*, *C. pugilator* and *Marsupenaeus japonicus* (see table 2.1 for the primer sequences). The PCR products were purified after gel electrophoresis using the QIAEX II gel extraction kit (Qiagen Hilden, Germany), were ligated in pGEM®-T easy vector (Promega Benelux, Leiden, The Netherlands) and transformed in *Escherichia coli* TOP10F' cells (Invitrogen). After a standard colony PCR (using a primer pair targeting the T7 and SP6 promoter), the plasmids from several positive colonies were purified using the Qiaprep Spin Miniprep kit (Qiagen) and sequenced by AGOWA (Berlin, Germany). Based on the partial DBD sequences obtained, forward non-degenerate primers in the DBD were designed and combined with a reverse degenerate primer situated in LBD. The same cloning routine was performed as described above.

2.2.3 Molecular cloning of the 5' and 3' ends of CrcRXR and CrcEcR

5' and 3' Rapid Amplification of cDNA Ends PCR (RACE PCR) were performed using gene specific primers (GSPs) designed in the T-box and H3-H4 of the obtained DBD-LBD sequences, respectively (see Table 2.1 for primer sequences). Initially, the SMART™ RACE cDNA amplification kit (Clontech Laboratories, Palo Alto, CA) was used with some slight alterations to the manufacturer's proposed reaction mix. Reactions included 1% (v/v) RACE-Ready cDNA, 1.5 mM $MgCl_2$, 0.2 mM dNTP mix, 0.025 U/µl Platinum® Taq DNA Polymerase (Invitrogen) and 0.25 µM GSP in a total volume of 10 µl. Further nested PCR with inner primers on the undiluted primary RACE PCR products was needed to obtain a satisfactory yield, except for the 3' cDNA ends of CrcRXR. The RACE PCR for the 3' cDNA ends of CrcEcR had to be performed with the FirstChoice RLM RACE kit (Applied Biosystems, Lennik, Belgium) and included an extra nested PCR, using 2 mM $MgCl_2$, 0.2 mM dNTP mix and 0.025 U/µl Platinum® Taq Polymerase in 50 µl reactions. After purification using the E.Z.N.A.® Cycle Pure kit (OMEGA Bio-Tek, Norcross, GA), the RACE PCR products were ligated with T4 DNA ligase (Promega Benelux, Leiden, The Netherlands) in the pGEM®-T easy vector (Promega), and transformed in *E. coli* TOP10F' cells (Invitrogen). For each ligation reaction (i.e. 5'CrcRXR and 3'CrcRXR, 5'CrcEcR, and 3'CrcEcR) the inserts of 16 colonies were amplified through a standard colony PCR and visualised through agarose gel electrophoresis.

Table 2.1. Overview of primers used. Key to degenerate nucleotides: Y = C+T; R = A+G; I = Inosine; V = G+A+C; N = A+C+G+T; K = G+T. Restriction sites for ligation in the Ract-Hadh expression vector are underlined, Kozak sequences are represented in italics.

		CrcRXR	CrcEcR
DBD	**Fw**	5'-TGT GAR GGI TGC AAR GGG TTC-3'	5'-TGY GAR GGA TGC AAA GGI T-3'
	Rev	5'-YTG GTA ICG GCA RTA YTG GCA-3'	5'-CGR CAY TCC TGA CAC TTI C-3'
DBD-LBD	**Fw**	5'-GCA CTG TGC GAA AAG ACC TCA-3'	5'-CGG AAA TAA CTG CGA AAT GGA-3'
	Rev	5'-GCR TAI ACY TTY TCN CKY A-3'	5'-TCI GCR TTR TCV ACY TTC AT-3'
3' RACE	**Out**	5'-CCT GTT GAC CAA GGG GAC GCT GT-3'	5'-TCA CGA GCA GCA AGA ACT GAT CCA CA-3'
	In	-	5'-GCC AGG CTT CGA CAC ACT ACA ACG AGA-3'
5' RACE	**Out**	5'-TGG TGC CAA CTC CTG CCT GAT GTG-3'	5'-AGT GTG TCG AAG CCT GGC AGT TGC TT-3'
	In	5'-GAT GAT TCT GGG TCG CCA TCT CCT TTG-3'	5'-CAC TGA GAC TCC GGT ACC ACA CAT TCG-3'
ORF	**Fw**	5'- ATA GTC GAC *AAA* ATG TCA GGG TCA CTG GAT CG-3'	5'- ATA GGA TCC *AAC* ATG TCA CCG CCA TCT TC-3'
	Rev	5'- CAG CTG CAG TTA GCT AGT CGG TGA GGA GTT GT-3' -3'	5'- A AGT GTC GAC TTA ACG TTG CTC ATA ACC GTG A-3'
	Rev	-	5'-AC GTC GAC ATT AAG TAT TGG TTT TCT GTC CAG ATG- 3'

Based on differences in electrophoretic mobility of the amplified inserts, a total of twelve colonies were selected for plasmid purification (E.Z.N.A.® Plasmid Mini Kit I, OMEGA Bio-Tek) and insert sequencing by AGOWA.

2.2.4 Molecular cloning of the complete open reading frames of CrcEcR and CrcRXR

Based on the obtained 5' and 3' sequences, 5' and 3' end primers were designed to amplify and ligate the complete ORFs into the Ract-Hadh expression vector. The purpose of cloning the complete ORFs of the RXR and EcR isoforms into an expression vector (Swevers et al. 1996) is to analyse the functionality of the corresponding proteins in chapter 3. The Kozak sequences were slightly adapted to a *Drosophila* Kozak consensus sequence (Cavener 1987), while restriction sites were added to facilitate cloning in the RAct-HAdh expression vector, and extra nucleotides at the 5'-end of the primers were added to make sure that cloned PCR fragments contained undisrupted restriction sites for subcloning (see table 2.1 for primer sequences). It should be noted here that an alternative ORF reverse primer was constructed for CrcEcR as an alternative 3' end was observed after the 3'RACE PCR reactions. The PCR of the full ORFs was performed with the Expand Long Range dNTPack (Roche Applied Science, Mannheim, Germany) at an annealing temperature of 48°C. PCR products were purified, cloned in PGEM-T vector and transformed in TOP10F' cells as described above. Colony PCR was performed on twelve and 42 colonies for CrcRXR and CrcEcR, respectively, and plasmid inserts were visualised through gel electrophoresis. Based on differences in gel mobility of the amplified inserts, four and eight colonies for CrcRXR and CrcEcR, respectively, were selected for plasmid purification and sequencing.

2.2.5 Sequence comparison and phylogenetic analysis

Secondary structure predictions of the LBDs were performed with the freely available neural network algorithms NNPredict (McClelland & Rumelhart 1988; Kneller et al. 1990), Porter (Pollastri & McLysaght 2005) and Prof (Ouali & King 2000; Meiler et al. 2001; Meiler & Baker 2003). The available RXR (including Diptera and Lepidoptera Ultraspiracle receptor, USP) and EcR (and related deuterostome LXR and FXR) sequences were obtained through a similarity search using the BLAST tool (http://blast.ncbi.nlm.nih.gov/blast.cgi) and reduced to 52 RXR/USP and 45 EcR/LXR sequences (table 2.2), which subsequently were aligned using ClustalW2 (Larkin et al. 2007). The phylogenetic trees of receptor LBDs were constructed with MEGA 4.1 (Tamura et al. 2007) using the neighbour-joining method (Saitou & Nei

1987). Gaps in the alignment were handled with the complete deletion method and a bootstrap test with 1,000 replications (Efron 1979) was performed. The evolutionary distances were computed using the Poisson correction for amino acids (Zuckerland & Pauling 1965).

Table 2.2. Overview of the RXR/USP and EcR/LXR amino acid sequences used for the phylogenetic analysis. GenBank accession numbers are given in the last two columns (continued on the next page).

Species		RXR/USP	EcR/LXR
Crustacea > Malacostraca > Eucarida > Decapoda			
C. crangon	Pleocyemata – Caridea	ACO44668	ACO44665
Celuca pugilator	Pleocyemata – Brachyura	AAC32789	AAC33432
Gecarcinus lateralis	Pleocyemata – Brachyura	AAZ20368	AAT77808
Carcinus maenas	Pleocyemata – Brachyura	ACG63787	AAR89628
Marsupenaeus japonicus	Dendrobranchiata	BAF75376	BAF75375
Other Crustacea			
Neomysis integer	Malacostraca - Peracarida	unpublished	ACJ68423
Daphnia magna	Branchiopoda	ABF74729	BAF49029
Calanus finmarchicus	Maxillopoda	ACP19739	-
Insecta			
Aedes aegypti	Diptera	AAG24886	AAA87394
Chironomus tentans	Diptera	AAC03056	P49882
Culex quinquefasciatus	Diptera	XP_001866328	XP_001844581
Drosophila melanogaster	Diptera	NP_476781	NP_724456
Lucilia cuprina	Diptera	AAG01569	AAB81130
Bombyx mori	Lepidoptera	NP_001037470	NP_001037331
Chilo suppressalis	Lepidoptera	BAC53670	BAC11713
Helicoverpa armigera	Lepidoptera	ACD74808	ABN11286
Spodoptera exigua	Lepidoptera	ACD39740	ACA30302
Plodia interpunctella	Lepidoptera	AAT44330	AAR84611
Apis mellifera	Hymenoptera	NP_001011634	BAF46356
Camponotus japonicus	Hymenoptera	-	BAF79665
Melipona scutellaris	Hymenoptera	AAW02952	-
Nasonia vitripennis	Hymenoptera	-	NP_001152828
Pheidole megacephala	Hymenoptera	-	BAE47509
Polistes fuscatus	Hymenoptera	AAX37292	-
Scaptotrigona depilis	Hymenoptera	ABB00308	-
Leptinotarsa decemlineata	Coleoptera	BAD99298	BAD99296
Tenebrio molitor	Coleoptera	CAB75361	CAA72296
Tribolium castaneum	Coleoptera	NP_001107766	NP_001107650
Blattella germanica	Blattodea	CAH69897	CAJ01677
Locusta migratoria	Orthoptera	AAF00981	AAD19828
Acyrthosiphon pisum	Hemiptera	ACR45970	NP_001152832
Bemisia tabaci	Hemiptera	ABN11285	ABN11284
Myzus persicae	Hemiptera	ABN11290	ABN11289
Pediculus humanus	Phthiraptera	XP_002424949	XP_002430228
Xenos pecki	Strepsiptera	AAX37291	-
Chelicerata > Arachnida			
Liocheles australasiae	Scorpiones	BAF85823	BAF85822
Ornithodoros moubata	Ixodida	BAF91724	BAE45855
Amblyomma americanum	Ixodida	AAC15588	AAB94566.1
Ixodes scapularis	Ixodida	XP_002435070	XP_002405625
Myriapoda			
Lithobius forficatus	Chilopoda	AAO18151	-
Mollusca > Gastropoda			
Biomphalaria glabrata	Pulmonata	AAL86461	-

Lymnaea stagnalis	Pulmonata	AAW34268	-
Nucella lapillus	Prosobranchia	ABS70715	-
Thais clavigera	Prosobranchia	AAU12572	-
Deuterostomia > Chordata > Vertebrata			
Danio rerio	Osteichthyes	AAC59720	NP_001017545
Gallus gallus	Aves	NP_990625	NP_989873
Xenopus tropicalis	Amphibia	NP_001015937	NP_001072853
Bos taurus	Mammalia	NP_001068876.1	AAX31375
Sus scrofa	Mammalia	NP_001123685	ABP88970
Rattus norvegicus	Mammalia	NP_036937	NP_113814
Homo sapiens	Mammalia	AAH63827	EAW71850
Other Deuterostomia			
Strongylocentrotus purpuratus	Echinodermata	XP_001201896	NP_001123279
Saccoglossus kowalevskii	Opisthobranchia	-	NP_001161579
Ciona intestinalis	Chordata – Tunicata	NP_001071809	BAE06541
Branchiostoma floridae	Chordata – Cephalochordata	AAM46151	EEN45473
Radiata			
Tripedalia cystophora	Cnidaria	AAC80008	-

2.2.6 *In silico* three-dimensional modelling of the LBPs of CrcRXR and CrcEcR

The availability of the crystal structure of the PPARγ/RXRα complex bound to 9-*cis*-RA (RCSB Protein Data Bank (PDB) code 3DZU) (Chandra et al. 2008) allows us to model the 3D structure of full length CrcRXR (ACO44668). Modeling of truncated CrcRXR$_{\Delta EF}$ (ACO44671) was not achieved, as too many of the amino acids of the LBP were missing to build an accurate model. Modeling of the LBD of CrcEcR and truncated CrcEcR$_{\Delta EF}$ (ACO44671) was based on the crystal structure of the TcEcR LBD of *Tribolium castaneum* in complex with ponA (PonA; PDB code 2NXX) (Iwema et al. 2007). Multiple amino acid sequence alignments were initially carried out with CLUSTAL- X (Thompson et al. 1997) using the Risler's structural matrix for homologous amino acid residues (Risler et al. 1998). Molecular modelling was performed on a Silicon Graphics O2 R10000 workstation with the programs InsightII, Homology and Discover3 (Accelrys, San Diego, CA). Steric conflicts were corrected during the model building procedure using the rotamer library (Ponder & Richards 1987) and the search algorithm implemented in the Homology program (Mas et al. 1992) to maintain proper side-chain orientation. An energy minimization of the final models was carried out with InsightII by 300 cycles of steepest descent using the consistent valence forcefield (cvff) of Discover2. PROCHECK (Laskowski et al. 1993) was used to assess the geometric quality of the 3D-models. Molecular cartoons were drawn with PyMol (W.L. DeLano, http://pymol.sourceforge.net). 3DZU and 2NXX and structurally-related proteins were also used as templates for CrcRXR and CrcEcR$_{\Delta EF}$, respectively, in the fold recognition program Phyre (http://www.sbg.bio.ic.ac.uk/phyre/html/index.html) (Bennett-Lovsey et al. 2008) to yield readily superposable 3D-models. Electrostatic potentials were calculated and

displayed with GRASP using the parse3 parameters (Nicholls et al. 2005). The solvent probe radius used for molecular surfaces was 1.4 Å and a standard 2.0 Å-Stern layer was used to exclude ions from the molecular surface (Gilson & Honing 1987). The inner and outer dielectric constants applied to the protein and the solvent were fixed at 4.0 and 80.0, respectively, and the calculations were performed keeping a salt concentration of 0.145 M.

2.3 Results

2.3.1 CrcRXR structure and isoforms

Initially, a single clone of a partial DBD (84 bp) sequence was obtained through degenerate PCR. A 663 bp clone from DBD to LBD was sequenced using a degenerate reverse primer situated in the LBD. Two 591 bp and 653 bp cloned 5' RACE PCR products exhibited different 5' untranslated regions (UTRs) 63 bp upstream of the start codon, the three 3' RACE PCR products (844 bp, 863 bp and 929 bp) were identical in the overlapping sequences. While in frame stop codons were detected in all clones, none of the sequenced 3' UTRs contained a poly-A tail. Sequencing of the full ORF of 1218 bp shows 78 and 80% sequence identity to the RXR of *C. pugilator* and *M. japonicus*, respectively (Table 2.3). The A/B domain of CrcRXR is short but well conserved compared to the related species, particularly the 5' sequence MSGSLDRQSPL and 3' sequence LSTSP(S/T)QYPP(N/S).

Minor differences can be observed in the DBD of CrcRXR compared to *C. pugilator*: Glu145 is replaced by Asp116, Ser147 is substituted by Ala118, and Thr168 by Gly139 (Fig. 2.1). The 32 AA long hinge region is almost identical to CpRXR, only differing in two AAs. Based on secondary structure predictions the LBD appears to lack the second α-helix, a phenomenon also observed in RXR of other crustacean (Asazuma et al. 2007) and non-crustacean species (Hayward et al. 1999). Three ORF variants for CrcRXR of 406 AA (FJ231415), 400 AA (FJ231414) and 225 AA (FJ231416) in size were cloned (Fig. 2.4). The 400 AA variant, named as $CrcRXR_{D\text{-}5}$, has a 5 AA deletion in the T-box in the hinge-region compared with the full length variant of 406 AA (CrcRXR). The 225 AA variant, named as $CrcRXR_{\Delta EF}$, has an out of frame deletion of 91 AA starting in H3 of the LBD, leading to a premature stop codon. Interestingly, the deleted sequence is immediately flanked by two ACAGA sequences in non-truncated CrcRXR, rendering a single ACAGA sequence in $CrcRXR_{\Delta EF}$. The *in vivo* expression of CrcRXR, $CrcRXR_{D\text{-}5}$, and $CrcRXR_{\Delta EF}$ was confirmed in multiple tissues through semiquantitative RT-PCR, using combinations of two forward and two reverse primers situated in the two variant sites (fig. 2.5, see also fig. 2.2 for variant sites and primer

situation). The existence of a CrcRXR$_{D\text{-}5,\ \Delta EF}$ could not be confirmed due to the presence of multiple bands.

2.3.2 CrcEcR structure and isoforms

Initially, degenerate PCR yielded two short partial sequences of the strongly conserved DBD (79 bp) and LBD (168 bp). The use of a non-degenerate primer pair, targeting the DBD and LBD, allowed determination of four longer identical sequences (from DBD to LBD) of 778 bp, allowing the development of gene specific primers for RACE PCR. A 442 bp and two 403 bp identical 5' RACE cDNA clones and two identical 501 bp 3' RACE cDNAs were isolated. The full ORF cDNA sequence of 1323 bp were generated using primers designed at the start and stop codon. CrcEcR showed high similarity to EcR of other crustacean species *C. pugilator* and *M. japonicus* with 77% and 67% sequence identity over the entire length, respectively (Table 2.3).

Compared to similar EcRs, CrcEcR contains a short A/B-domain of merely 25 amino acids (AAs), which appear to be strongly conserved within Decapoda (Fig. 2.3). The DBD domain AA sequence of CrcEcR is identical to that of the crab *C. pugilator*. The poorly conserved hinge region of CrcEcR is long compared to other Decapoda species and contains a predicted short α-helix (EEEGRQL).

Three CrcEcR variants were cloned, consisting of 441 (FJ23410), 376 (FJ231411) and 358 amino acids (AA) (FJ231412) in length (Fig. 2.4). The 376 AA variant, named as CrcEcR$_{\Delta EF}$, is characterized by an alternative 3' sequence starting at 355 AA, compared with the full length variant of 441 AA (CrcEcR). This alteration is situated between H9 and H10 of the LBD, leading to the lack of H10 to H12 of the LBD and thus possibly leading to an impaired ligand binding and heterodimerization.

Interestingly, all secondary structure predictions applied indicate a *C*-terminal helix (SISYKSSGQKTNT) in the alternative CrcEcR C-tail. The 358 AA variant, named as CrcEcR$_{D\text{-}18,\ \Delta EF}$, is also characterized by this alternative *C*-tail, but in addition it exhibits an 18 AA deletion in the hinge-region. These results suggest that a 422 AA variant, named as CrcEcR$_{D\text{-}18}$, a variant containing a normal LBD and the 18 AA deletion, is likely to exist.

The *in vivo* expression of CrcEcR, CrcRXR$_{D\text{-}18}$, CrcRXR$_{\Delta EF}$, and CrcEcR$_{D\text{-}18,\ \Delta EF}$ was confirmed in multiple tissues through semiquantitative RT-PCR, using combinations of two forward and two reverse primers situated in the two variant sites (fig. 2.5, see fig. 2.4 for variant sites and primer situation).

Table 2.3. Comparison of predicted amino acid sequences of RXR and EcR receptor homologues with CrcRXR and CrcEcR. Amino acid length and sequence identity (between brackets) with CrcRXR and CrcEcR are given for *C. pugilator*, *M. japonicus*, *D. magna*, *Blatella germanica*, *Amblyomma americanum*, *D. melanogaster*, *Neomysis integer*, *Calanus finmarchicus* and *Homo sapiens* homologues. See table S2 in supplementary material for the accession numbers of the used sequences. CfiRXR was used as the available NiRXR sequence lacks the C-terminal 11 residues of the E/F-domain. Domain structures were defined based on conserved motif structure after alignment using ClustalW. Pairwise identities were calculated using the Blast 2 sequences interface with standard settings (www.ncbi.nlm.nih.gov/blast/bl2seq/wblast2.cgi).

Region	Length, in amino acids (% identity)								
	CrcRXR	CpRXR	MjRXR	DamRXR	BgRXR	AamRXR	DmUSP	CfiRXR	HsRXRα
A/B	76	105 (65%)	114 (73%)	81 (38%)	94 (42%)	81 (31%)	103 (28%)	80 (26%)	134 (22%)
C	66	66 (95%)	66 (95%)	66 (95%)	66 (92%)	66 (90%)	66 (92%)	66 (86%)	66 (86%)
D	31	26 (73%)	30 (63%)	25 (20%)	25 (28%)	36 (25%)	64 (29%)	29 (27%)	25 (24%)
E/F	232	268 (86%)	232 (83%)	228 (71%)	228 (73%)	231 (64%)	275 (43%)	230 (56%)	237 (68%)
Total	405	465 (83%)	442 (82%)	400 (66%)	413 (65%)	414 (60%)	508 (49%)	405 (53%)	462 (60%)
	CrcEcR	CpEcR	MjEcR	DamEcR	BgEcR	AamEcR	DmEcR	NiEcR	HsLXR
A/B	32	156 (81%)	104 (71%)	326 (78%)	207 (68%)	188 (62%)	234 (65%)	209 (46%)	97 (18%)
C	66	66 (100%)	66 (98%)	66 (93%)	66 (96%)	66 (95%)	66 (89%)	66 (83%)	66 (69%)
D	117	74 (67%)	104 (54%)	109 (37%)	75 (49%)	94 (37%)	101 (29%)	77 (40%)	57 (19%)
E	218	218 (86%)	221 (69%)	217 (74%)	219 (73%)	219 (67%)	221 (59%)	217 (48%)	224 (40%)
F	7	4 (50%)	4 (-)	3 (33%)	3 (-)	3 (33%)	227 (14%)	1 (-)	3 (33%)
Total	440	518 (75%)	499 (67%)	721 (65%)	570 (64%)	570 (60%)	849 (54%)	570 (45%)	447 (37%)

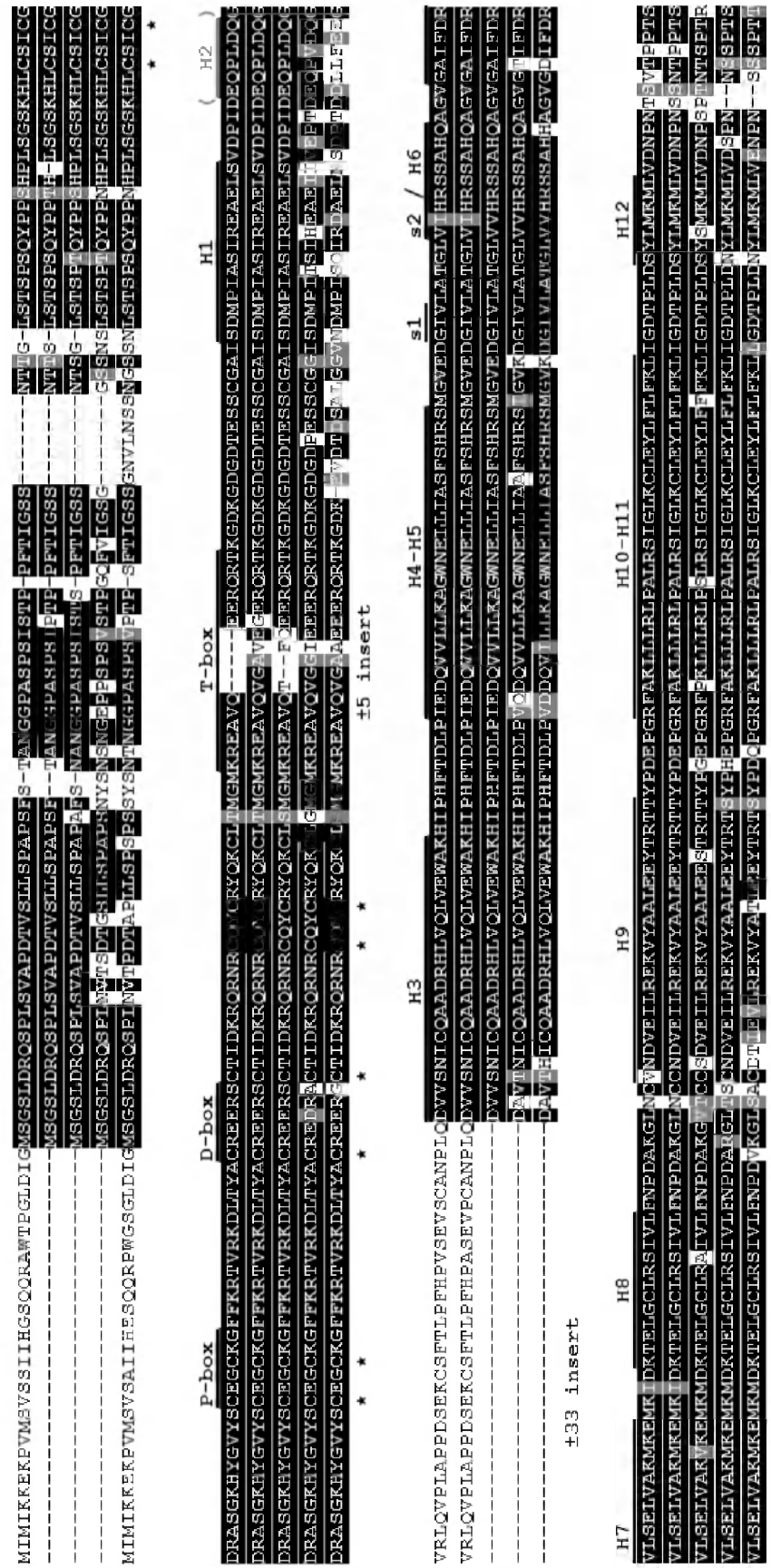

Fig. 2.1. Alignment of CrcRXR with the available RXR sequences of related Decapoda species; *C. pugilator*, *G. lateralis*, *C. maenas* and *M. japonicus*. Conserved α-helices (H1–H12), β-sheets (s1-s2) and domains are indicated above the sequences; conserved cysteine residues (indicated with an *) in the DBD and LBD and variant insert sites are indicated below the sequences. The multiple aligned sequences were shaded using BOXshade 3.2 (http://www.ch.embnet.org/software/box_form.html): black shading indicates identical amino acids, grey shading indicates similar amino acids and white background indicates unrelated amino acids.

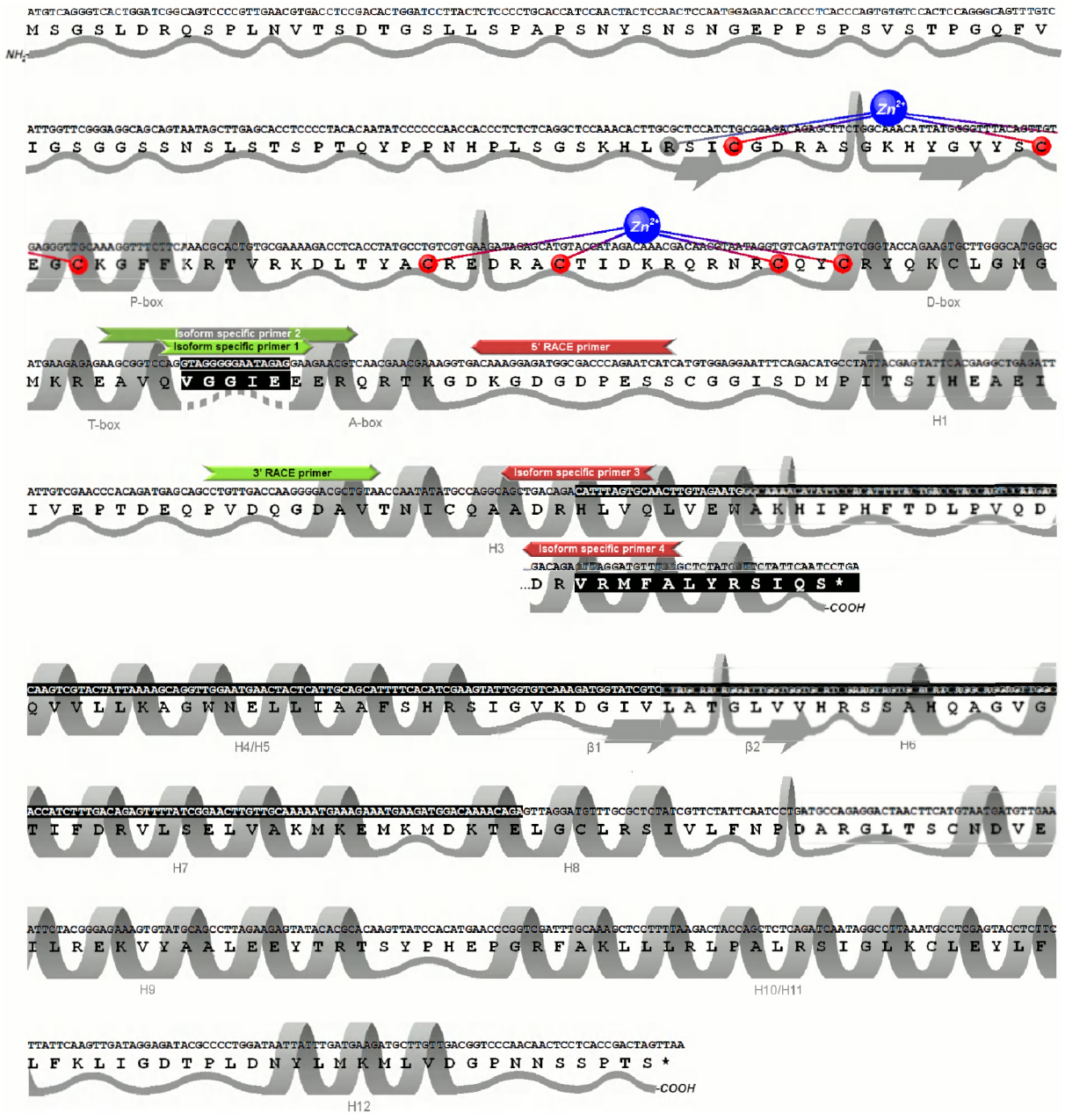

Fig. 2.2. Nucleotide sequences and deduced AA sequences for CrcRXR. Variant sites are marked in black. The forward and reverse primers used are represented by green and red arrows, respectively (full ORF primers are not shown). The predicted secondary structures are shown in a graphical manner in grey scale in the background. The cysteine residues forming the zinc finger with the bivalent zinc ion (in blue) are marked red.

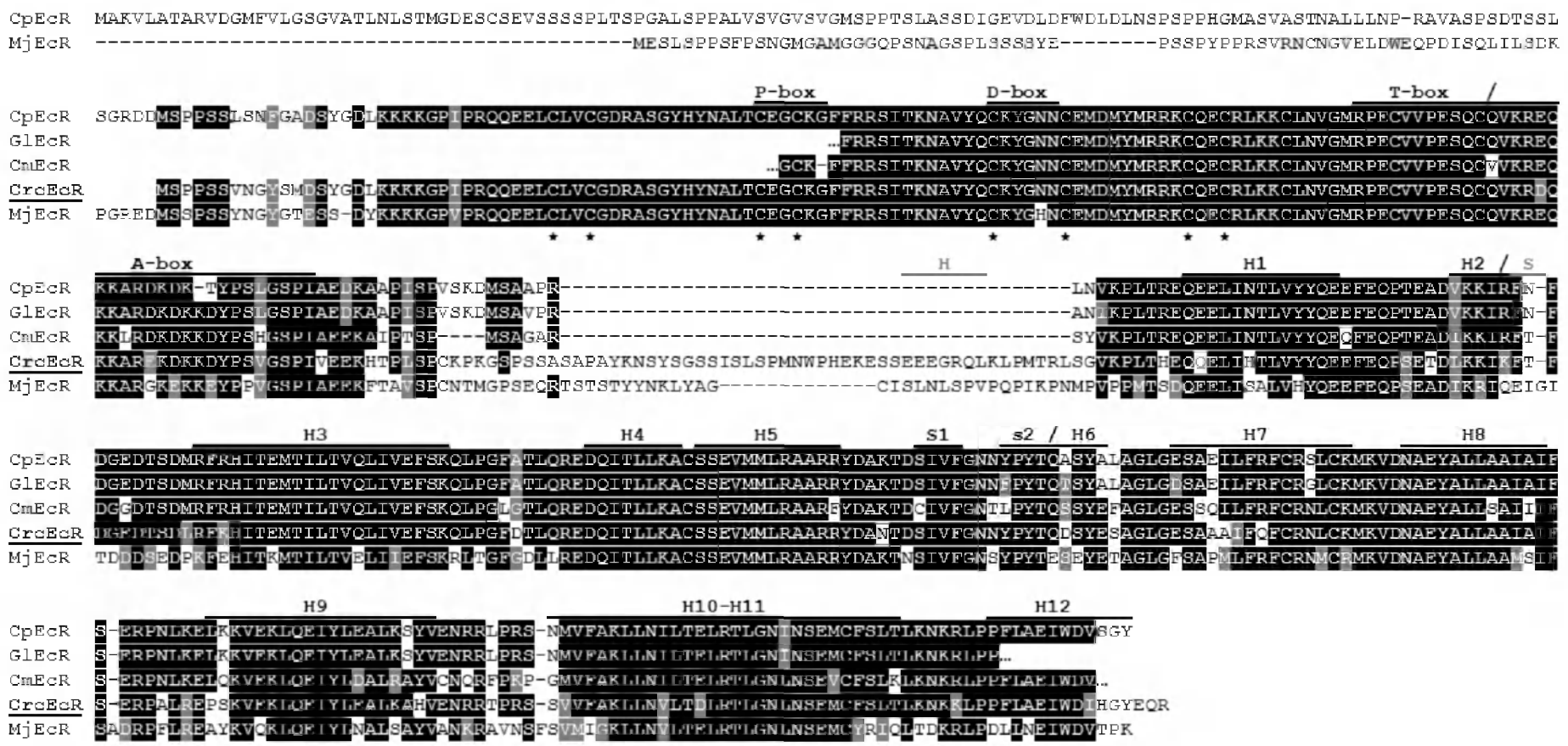

Fig. 2.3. Alignment of CrcEcR with the available EcR sequences of related Decapoda species; *C. pugilator*, *G. lateralis*, *C. maenas* and *M. japonicus*. Conserved α-helices (H1–H12), β-sheets (s1-s2) and domains are indicated above the sequences; conserved cysteine residues(indicated with an *) in the DBD and LBD and variant insert sites are indicated below the sequences. The multiple aligned sequences were shaded using BOXshade 3.2 (http://www.ch.embnet.org/software/box_form.html): black shading indicates identical amino acids, grey shading indicates similar amino acids and white background indicates unrelated amino acids.

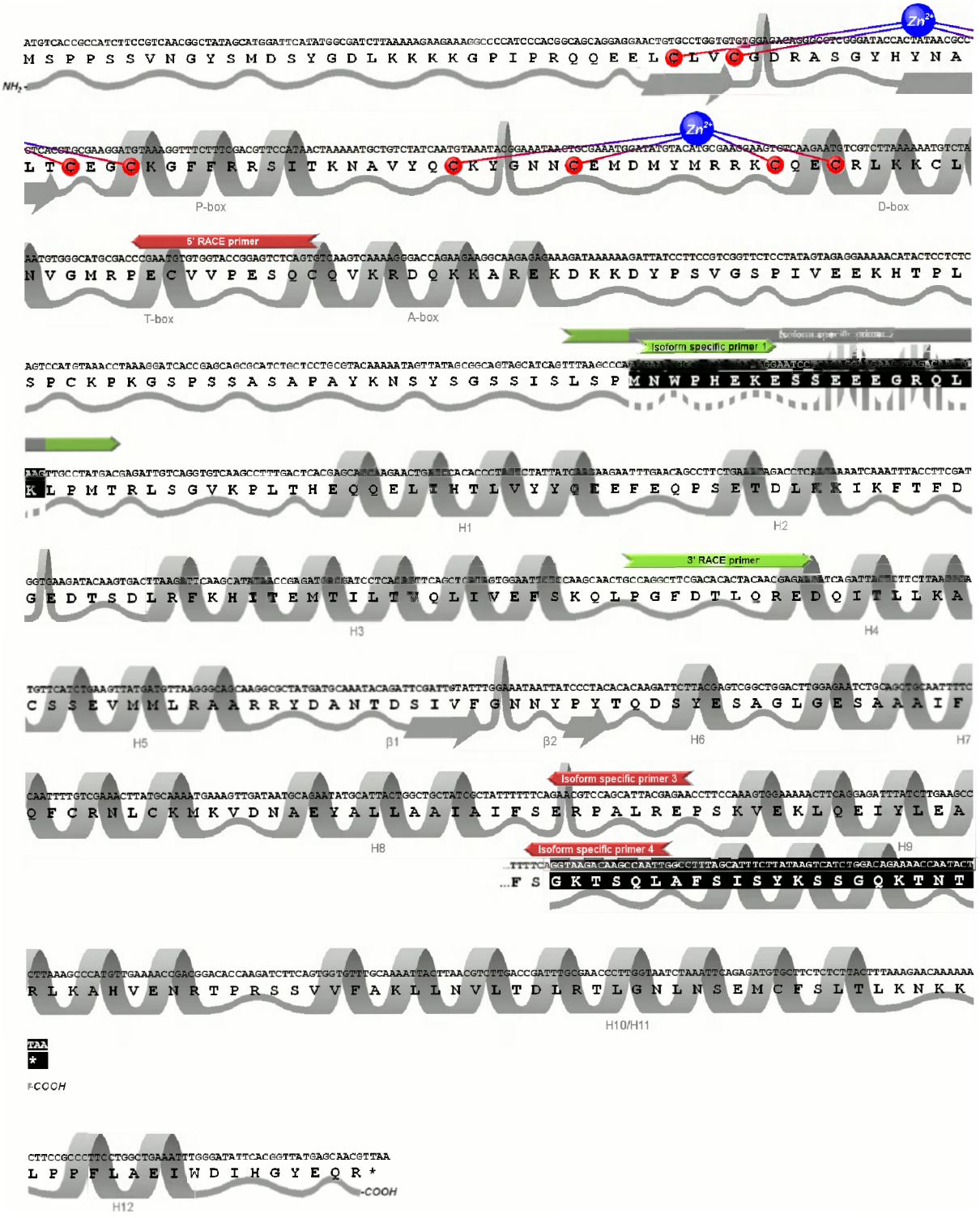

Fig. 2.4. Nucleotide sequences and deduced AA sequences for CrcEcR. Variant sites are marked in black. The forward and reverse primers used are represented by green and red arrows, respectively (full ORF primers are not shown). The predicted secondary structures (a-helices, β-sheets and β-turns) are shown in a graphical manner in grey scale in the background. The cysteine residues forming the zinc finger with the bivalent zinc ion (in blue) are marked red.

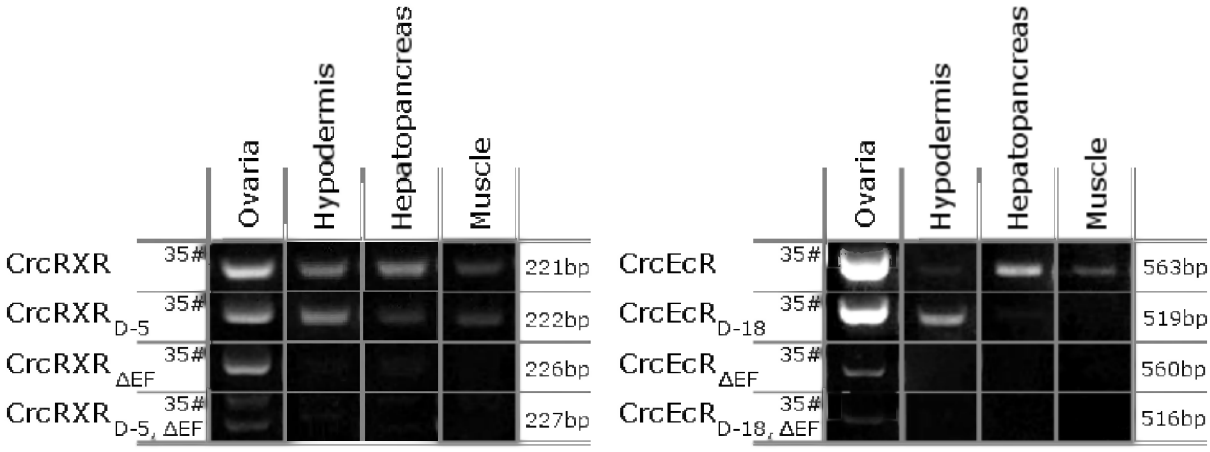

Fig.2.5. Semiquantitative RT-PCR confirmation of *in vivo* expression of the putative CrcRXR and CrcEcR isoforms in several tissues. Amplified gene names and cycle number are given on the left, template tissue is given at the top, amplicon size is given at the right. The *in vivo* expression of $CrcRXR_{D\text{-}5,\ \Delta EF}$ could not be confirmed due to the presence of non-specific bands.

2.3.3 Phylogenetic analysis based on RXR and EcR LBDs

The phylogenetic trees obtained through a neighbour-joining analysis using the LBD of USP/RXR and EcR are shown in Fig. 2.6. As these phylogenetic trees are based on amino acid substitutions within the LBD, sequence divergence may reflect changes in ligand binding preferences. Phylogenetic relationships within the crustacean order of Decapoda are clearly visible in both trees exhibiting strong bootstrap values: the infraorder sister groups Brachyura (crabs; *Carcinus, Gecarcinus, Celuca*) and Caridea (shrimps; *Crangon*) are representatives of the suborder Pleocyemata, which in turn is the sister group of the suborder Dendrobranchiata (prawns; *Litopeneaus*). These two belong to the order Decapoda (superorder Eucarida) which together with the order Mysida (superorder Peracarida) are representatives of the class Malacostraca. In our analysis, RXR and EcR of *Daphnia* (order Cladocera; class Branchiopoda) clusters with the subphylum Hexapoda, which, in case of the RXR tree, encompasses the divergent USP Lepidoptera and Diptera homologues. Both RXR and EcR phylogenetic relationships confirm earlier observations (Budd & Telford 2009) that insects can be considered as a terrestrial (Pan)crustacean clade. Arthropod RXR/USP clearly separate from the other Protostomia clade of Mollusca RXR, which clusters closely with Deuterostomia RXRs. This has been observed before (Wang et al. 2007) and may be related to a common high affinity of 9-*cis*-RA to Mollusca and Deuterostomia RXR (Mark & Chambon 2003; Nishikawa 2003). The remarkable divergence of the *N. integer* (Peracarida) EcR sequence used probably reflects a strongly divergent ligand binding specificity. As no

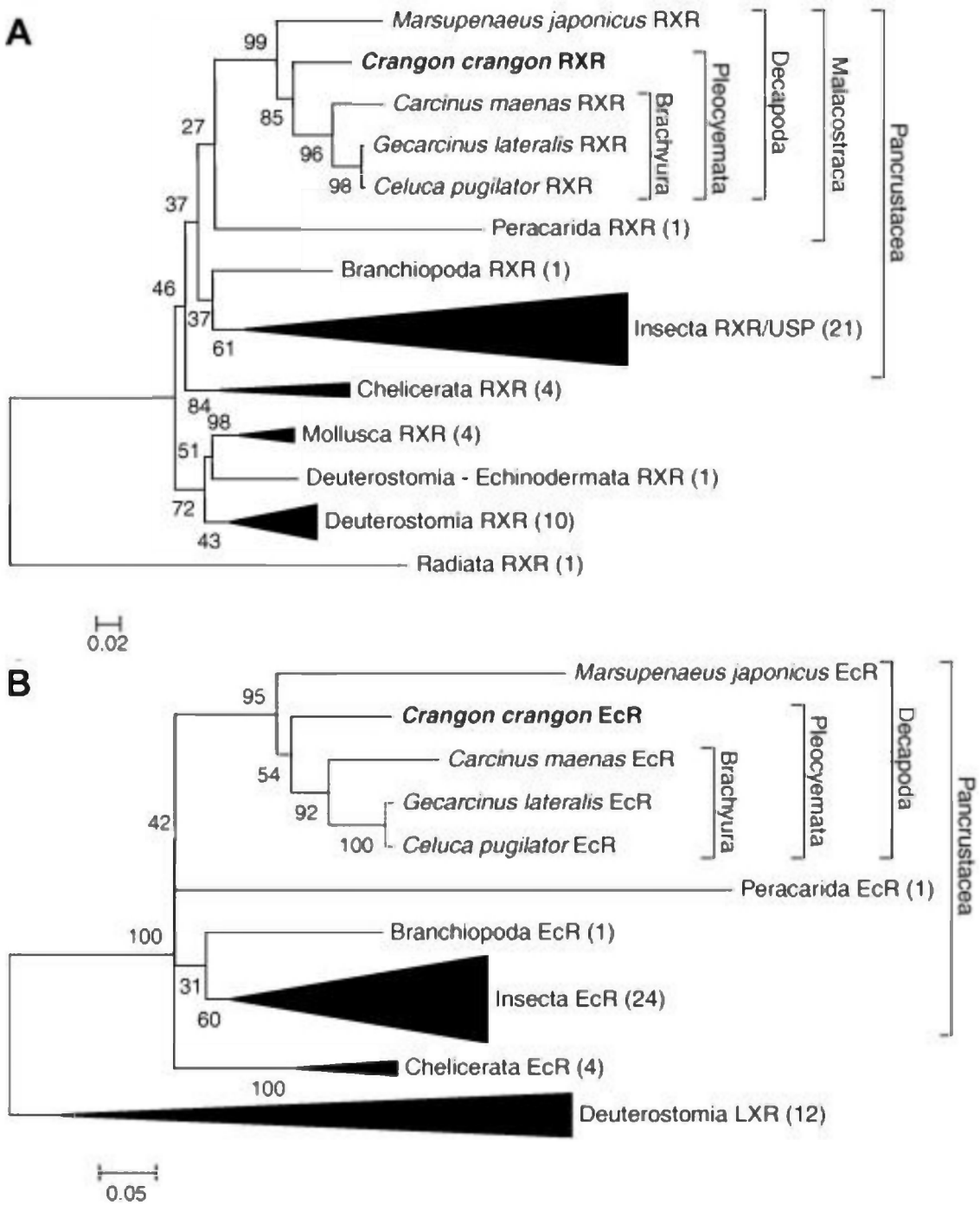

Fig. 2.6. Phylogenetic trees of the LBD domains of RXR/USP (A) and EcR/LXR (B). Trees were constructed using the neighbour-joining algorithm (complete deletion and Poisson correction). The RXR tree was rooted with jellyfish *Tripedalia cystophora*, the EcR tree with the cluster of 11 Deuterostomia LXR(-like) receptors. The figures at the nodes represent bootstrap proportions out of 1000 bootstrap replicates. Branch lengths are proportional to sequence divergence, the bars below each figure represent the number of differences per site. It should be noted that Hemiptera (*Acyrthosiphon, Bemisia* and *Myzus*), Myriapoda (*Lithobius*), Echinodermata (*Strongylocentrotus*) and the crustacean clade Maxillopoda (*Calanus*) were deliberately excluded from the RXR phylogenetic analysis to promote tree reliability; otherwise Maxillopoda and Hemiptera would cluster with the Hexapoda clade; Myriapoda with Branchiopoda and Chelicerata; and Echinodermata with Mollusca, rendering overall poor bootstrap values. Detailed sequence information can be found in table 2.2.

other Peracarida EcR and RXR sequences are currently available, it is unclear at what phylogenetic level this differentiation occurs.

2.3.4 *In silico* 3D-modeling of CrcRXR

The high percentages of identity (~73%) and similarity (~92.5%) that full CrcRXR shares with the RXRα template allowed us to build a rather accurate 3D-model for CrcRXR. About 80% of the residues of the CrcRXR model were correctly assigned on the best allowed regions of the Ramachandran plot, the remaining residues being located in the generously allowed regions of the plot except for the four residues Arg44, Asp129, Ala193 and Thr311 which occur in the non-allowed region (data not shown). The fold-recognition program Phyre yielded a readily superposable 3D-model for CrcRXR with, however, some discrepancies that mainly concerned the loop regions.

The modelled full CrcRXR consists of a small *N*-terminal DBD linked to a larger *C*-terminal LBD by a long α-helix-containing hinge linker (Fig. 2.7.A, B). Both domain structures superimpose with a few discrepancies mainly located in the more flexible loop regions (Fig. 2.7.C). Mapping of electrostatic potentials on the molecular surface of CrcRXR reveals the prominent electropositive character of the DBD which specifically binds to DNA-elements for regulating gene expression (Fig. 2.7.D). The LBD of full CrcRXR contains a differently shaped and sized LBP, which is narrower and rather less extended than that occurring in the human RXRα template receptor (Fig. 2.7.E). In addition, the LBD of full CrcRXR differs from that of RXRα with respect to a more pronounced hydrophilic character. Docking experiments suggest that 9-*cis*-RA should accommodate the LBP of CrcRXR *via* essentially hydrophobic interactions like in RXRα (Fig. 2.7.G, H).

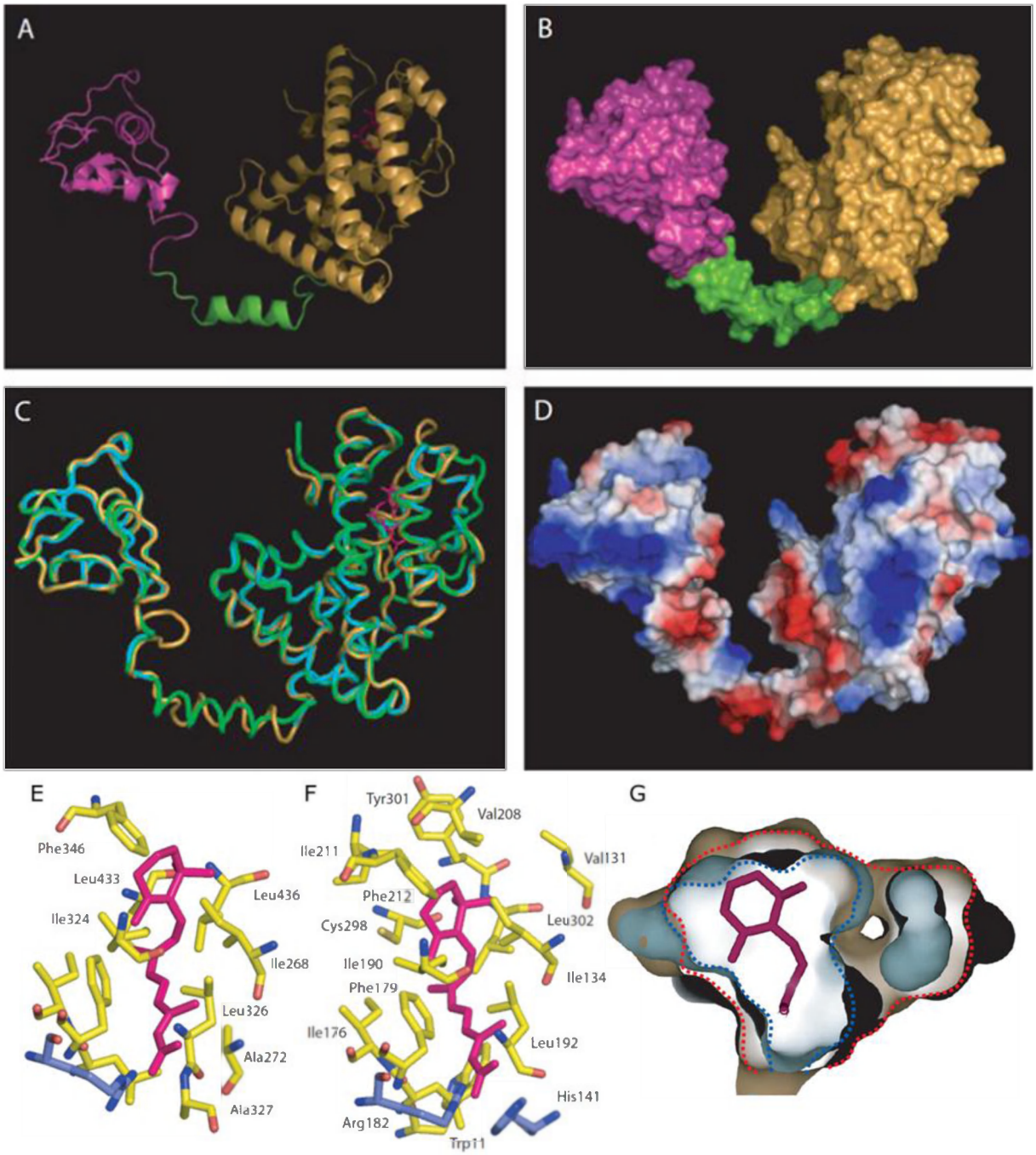

Fig. 2.7. *In silico* modeling of CrcRXR (**A**) and (**B**) Ribbon diagram (A) and molecular surface (B) of full-length CrcRXR showing the overall organization of the modelled full-length CrcRXR in two distinct DBD (colored magenta) and LBD (colored orange) domains, connected by an a-helix-containing hinge linker (colored green). 9-*cis*-RA docked into the LBP is represented in pink stick. (**C**) Superposition of CrcRXR (colored orange) to the human RXRa (colored blue) harbouring 9-*cis*-RA (pink stick) into the LBP and DamRXR from *D. magna* (colored green). (**D**) Mapping of electrostatic potentials on the molecular surface of CrcRXR. Electropositive and electronegative areas are colored blue and red, respectively, and neutral areas are white. Residues at the LBP of RXRα (**E**) and CrcRXR (**F**) interacting with 9-*cis*-RA (pink stick) by hydrophobic (residues colored yellow) and hydrophilic (residues colored blue) interactions. (**G**) Clipping planes of the superimposed LBPs of CrcRXR (red dotted line) and RXRα (blue dotted line) showing the docking of 9-*cis*-RA, represented in pink. Note the different size and shape between the human and the shrimp LBP.

2.3.5 *In silico* 3D modeling of the LBPs of CrcEcR and docking of PonA

The high percentages of both identity (~69%) and similarity (~91%) that CrcEcR LBD shares with the template TcEcR LBD (Mouillet et al. 1997) allowed us to build a rather accurate 3D model. About 87% of the residues of the modelled CrcEcR LBD were correctly assigned on the best allowed regions of the Ramachandran plot, the remaining residues being located in the generously allowed regions of the plot except for Asp35 which occurs in the non-allowed region (result not shown). Some discrepancies that were observed with our lab-made modelled structures essentially deal with the shape of the loops connecting the α-helical stretches of CrcEcR LBD. These discrepancies occur outside the groove responsible for the binding of ecdysteroid hormone. The modelled CrcEcR LBD consists of a canonical EcR LBD structure built up by twelve α-helices tightly packed around a ligand binding groove that specifically anchors ecdysteroids (Fig. 2.8.A). In addition, Fig. 2.8.C demonstrates that the amino acid residues Glu224, Met254, Thr255, Gly310 and Tyr320 of the ecdysteroid binding cavity create a network of 9 H-bonds participating in the binding of PonA in association with stacking interactions of residues Phe309, Tyr315 and Trp436. Upon docking to the ecdysteroid binding cavity of CrcEcR LBD, the alkyl chain of PonA becomes inserted in one of the two pockets located at the bottom of the binding cavity (Fig. 2.8.E). Compared with coleopteran EcR (Iwema et al. 2007), differences in steric interactions of PonA within the LBD appear to be limited to the stacking interaction of Tyr315 and the lack of a water-mediated binding of Asn410 at the end of the PonA hydrocarbon tail. The shorter alternative 3' tail in $CrcEcR_{\Delta EF}$ leads to a lack of H10, H12 and most of H11 (Fig. 2.8.B). H10 and H11 are the major constituents of one side of the sandwich fold observed in the normal CrcEcR-LBD, while H12 normally closes the LBP in the ligand-activated receptor.

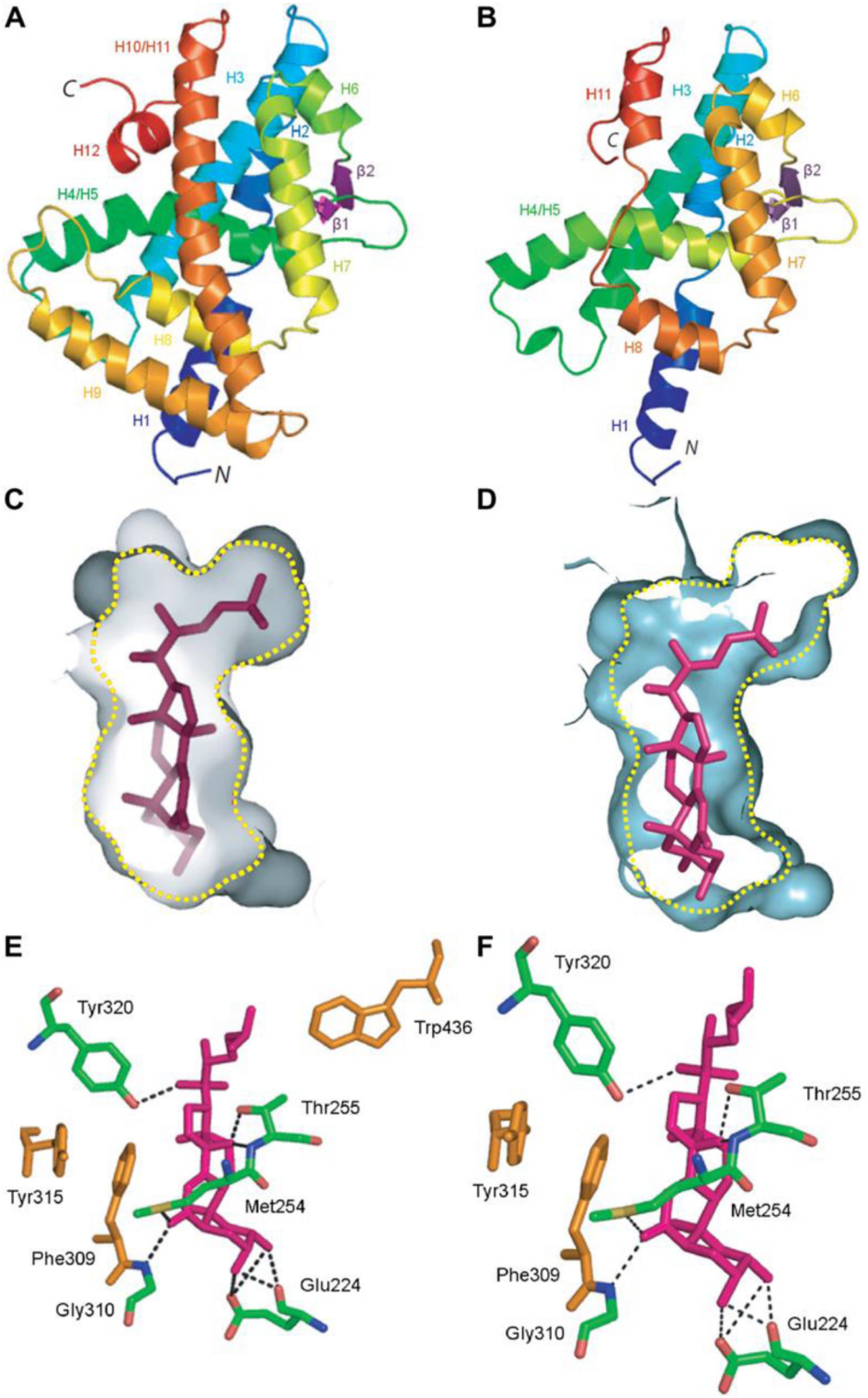

Fig. 2.8. *In silico* modeling of the LBD of CrcEcR isoforms. (**A**) and (**B**) Ribbon diagram of the LBD of full-length CrcEcR and truncated CrcEcR$_{\Delta EF}$, respectively, showing the α-helices building the 3D-fold of the receptor. Helices are differently colored and numbered H1–H12, the two short strands of β-sheet are colored purple and numbered b1 and b2. (**C**) and (**D**) Clip (yellow dotted line) showing the anchoring of PonA to the LBP of full-length CrcEcR and truncated CrcEcR$_{\Delta EF}$, respectively. (**E**) and (**F**) PonA complexed to residues forming the LBP of full-length CrcEcR and truncated CrcEcR$_{\Delta EF}$, respectively. PonA is represented in pink stick and H-bonds anchoring PonA to hydrophilic residues are in black dotted lines. Hydrophobic residues making stacking interactions with PonA are colored orange.

Interestingly, the α-helix observed at the end of the alternative 3' tail (H11 in Fig. 2.7.B) replaces the 3' end of H10 and as such conserves the LBP (Fig. 2.8.D), that only exhibits a confined distal expansion. Despite the lack of Trp436 and the related stacking interaction in the deleted isoforms, docking experiments reveal that the PonA-binding scheme in CrcEcR$_{\Delta EF}$ remains very similar to that observed earlier in non-truncated CrcEcR (Fig. 2.8.E and 2.8.F): a network of nine hydrogen bonds with residues Glu20, Met50, Thr51 and Tyr116 anchors PonA to the LBP (Fig. 2.8.F). Two additional stacking interactions with Phe105 and Tyr111 complete the binding.

2.4 Discussion and conclusions

2.4.1 CrcRXR and CrcRXR structure and isoforms

We cloned and characterized cDNAs encoding RXR and EcR from *C. crangon*. CrRXR and CrcEcR exhibit the strongly conserved domain structure which is typical for NRs: a poorly conserved A/B transactivating domain, a strongly conserved DNA binding C-domain, a variable hinge D-region, a well conserved ligand binding E-domain and an extremely short F-tail, which is even lacking in crustacean RXR (Chung et al. 1998; Durica et al. 2002; Wu et al. 2004; Kim et al. 2005; Asazuma et al. 2007; Wang et al. 2007; Hopkins et al. 2008). Based on the high sequence similarities with CpRXR (83%) and CpEcR (75%) of the closely related land crab *C. pugilator,* we can assume the successful cloning of common shrimp CrcRXR and CrcEcR.

In CrcRXR, a 5 AA insert exists in the T-box, a C-terminal extension of the DBD-region critical for dimerization. In concordance with Kim et al. (2004), we refer to the shrimp isoform lacking the insert as CrcRXR$_{D\text{-}5}$. This insert has previously been observed in RXR from the crabs *C. pugilator* and *G. lateralis* (Kim et al. 2005; Wu et al. 2004). In *G. lateralis*, Kim et al. (2004) even observed three variants at this splicing site (T+7, T+8 and T+12) and another splicing insert site between H1 and H3 of the LBD (LBD+33) and one between H7 and H8 (LBD+35) of the LBD. The latter two splicing sites, which were not observed in the *C. crangon* LBD, could also have a large impact on the dimerization interface normally observed at H7-H10 (Iwema et al. 2009). In *C. crangon*, truncated CrcRXR isoforms were found: a 275 bp deletion between H3 and H7 leads to a frame shift and a premature stop-codon. Kim et al. (2004) also observed truncated forms in *G. lateralis*, exhibiting an alternative sequence starting at helix 3 and leading to a premature stop-codon. In concordance, we refer to the truncated shrimp isoform as CrcRXR$_{\Delta EF}$.

The most striking sequential differences are found in CrcEcR, where the A/B-domain is limited to a strongly conserved stretch of 25 AAs and the hinge region has a C-terminal extent of 42 AA compared to the closely related Brachyura EcRs. A truncated CrcEcR isoform, $CrcEcR_{\Delta EF}$, was cloned, exhibiting an alternative C-terminal sequence starting between H9 and H10, leading to the lack of H10-H12 and a premature stop codon. Interestingly, secondary structure prediction algorithms indicate a C-terminal helix in this alternative C-tail. A second variant was found, $CrcEcR_{D\text{-}18,\ \Delta EF}$, exhibiting an 18 AA deletion at the C-terminal end of the D-domain. In *C. pugilator* EcR, a splicing site has also been identified in the C-terminus of the D-domain, rendering three isoforms (+6 AA, +10AA and +36AA) (Chung et al. 1998), however, sharing no homology with the $CrcEcR_{D\text{-}18}$ variant.

2.4.2 *In silico* three dimensional modeling of CrcRXR and CrcEcR

We used the obtained sequence data to *in silico* reconstruct the LBD of CrcEcR and predict the steric interactions involved in PonA docking. The accurate 3D model indicates that the steric interactions involved in PonA docking are similar to that of coleopteran EcRs, as differences appear to be limited to the stacking interaction of Tyr315 and the lack of a water-mediated binding at the end of the PonA hydrocarbon tail. However, a water molecule was also not observed in the structures of the *Heliothis* and *Bemisia* EcRs complexed with PonA (Billas et al. 2003; Carmichael et al. 2005). *In silico* analysis showed that the truncation in $CrcEcR_{\Delta EF}$ does not affect the LBP or the interactions with PonA, albeit a minor elongation of the cavity and the associated lack of the stacking/hydrophobic interaction of PonA with Trp436 were observed (Fig. 2.4). However, the *C*-terminal part of H9 and the complete H10 believed to be important for heterodimerization with RXR, were lacking (Iwema et al. 2009). According to the *in silico* reconstruction, the *C*-terminal α-helix observed in the variant 3' end of $CrcEcR_{\Delta EF}$ replaces the 3' end of H11 and as such preserves the LBP. The modelled CrcRXR is characterized by an α-helix in the hinge region which introduces some restriction in the flexibility between the DBD and LBD. The more pronounced hydrophilic LBP of CrcRXR is narrower and less extended than that of the human RXRα template receptor. On the other hand, CrcRXR resembles RXRα in the fact that 9-*cis*-RA should accommodate the LBP (Fig. 2.2 E-G). In water flea *D. magna* (unpublished data Smagghe, Rougé, LeBlanc), DamRXR is also characterized by a long α-helix in the hinge region, but 9-*cis*-RA accommodation in DamRXR is subject to some steric hindrance. In $CrcRXR_{\Delta EF}$, the truncation eliminates the LBP, assumedly rendering a ligand-independent CrcRXR isoform.

In *T. castaneum*, ligand-independence of the RXR receptor has been shown, and this was caused by the filling of the LBP with hydrophobic side chains of the loops L6 and L11 (Iwema et al. 2007). Furthermore, due to the truncation in CrcRXR$_{\Delta EF}$, the complete heterodimerization interface situated at H7-H10 is lacking, suggesting affected dimerization with CrcEcR. The availability of the *Crangon* EcR and RXR *in silico* models can have practical applications to predict endocrine disrupting activities of exogenous compounds. *In silico* generated 3D receptor models are interesting templates for 3D quantitative structure-activity relationship studies (3D QSAR), where correlations between the binding affinity of the ligand molecules and structural features of the common target (*i.e.* in our case the receptor LBD) are sought. This approach is popular for predicting drug toxicity in vertebrate receptors (Vedani et al. 2006), more recently for vertebrate endocrine disruption (Lill et al. 2005; Iguchi and Katsu, 2008; Cui et al. 2009) or to a lesser extent for insecticide activity in target insect species (Hormann et al. 2008; Nakagawa et al. 2009). However, no such model has been used to our knowledge to investigate the endocrine disrupting potential of drugs and chemicals to important non-target invertebrate species such as *C. crangon*. The described accurate model of the LBDs of shrimp EcR and RXR should allow predictive *in silico* docking of potential ligands, thus establishing a shrimp specific high throughput virtual screening system to identify candidate EDCs.

Chapter 3

Disruption of the hormone-nuclear receptor interaction by organotin

Parts of this chapter have been published as:

Y. Verhaegen, K. Parmentier, L. Swevers, P. Rougé, T. Soin, W. De Coen, K. Cooreman and G. Smagghe, 2010. The brown shrimp (*Crangon crangon* L.) ecdysone receptor complex: cloning and functional expression in an EcR-deficient Drosophila cell line. General and Comparative Endocrinology, 168, 415-423.

Y. Verhaegen, K. Parmentier, L. Swevers, E. Renders, P. Rougé, W. De Coen, K. Cooreman and G. Smagghe, 2011. The heterodimeric ecdysteroid receptor complex in the brown shrimp *Crangon crangon*: EcR and RXR isoform characteristics and sensitivity towards the marine pollutant tributyltin. General and Comparative Endocrinology, 172, 158-169.

3.1 Introduction

In the previous chapter, the molecular cloning of RXR and EcR from common shrimp is described. In this chapter, we report the transfection of expression plasmids of these receptors in a *Drosophila* cell line, and the use of this transfected cell line in an assay with an ecdysteroid responsive reporter construct to screen for ecdysteroid responsiveness of the different shrimp EcR-RXR receptor complexes. The mutant *Drosophila* Kc cell line L57-3-11 (Swevers et al. 1996; Cherbas and Cherbas 1997; Hu et al. 2003) used, is characterized by inactivated DmEcRB1 and DmEcRB2 isoforms, which results in a 90% loss of endogenous 20E response and represents a continuous arthropod cell line which can be used to study ligand binding to exogenous (*e.g.* crustacean) EcRs. The EcRE-b.act.luc reporter construct used, is composed of seven copies of the ecdysteroid responsive element (EcRE), derived from the *Drosophila* hsp27 promoter, a *Bombyx mori* derived basal actin promoter (b.act), the reporter gene for firefly luciferase (luc), and a termination signal. The ecdysteroid activated shrimp EcR-RXR complexes will transactivate luciferase expression through the EcREs, which in turn will break down the enzymatic substrate luciferin (in excess in the cell medium), thereby producing a quantifiable luminescent signal.

Regarding the potential RXR agonism of TBT, a 3D *in silico* model of TBT docked in the LBP of shrimp RXR is reconstructed. X-ray diffraction derived crystal structures of TBT bound to human RXRα LBD previously revealed that TBT lacks the typical carboxylate group which buries other RXR ligands, such as 9-*cis*-RA, in the hydrophobic ligand binding pocket (Antunes et al. 2010). Instead, TBT occupies the LBP only partially and the tin atom covalently binds with residue C432 of helix H11 (Le Maire et al. 2009). While this interaction is markedly different from other known RXR ligands, it induces identical residue positioning and side-chain orientations and hence full-agonism, as observed by Nahoum et al. (2007).

The putative anti-ecdysteroidal effect of TBT on the CrcEcR:CrcRXR heterodimer is observed by exposing a Kc cell line containing a functional shrimp EcR-RXR receptor complex. Finally, the tissue-specific effects of *in vivo* exposure of shrimp to TBT on EcR and RXR gene expression is determined through semiquantitative RT-PCR.

3.2 Material and Methods

3.2.1 Transfection and growth conditions of EcR deficient Kc L57-3-11 cell line

The variant CrcEcR and CrcRXR ORFs were restriction digested out of the PGEM-T vector (see 2.2.4), purified, ligated in the Ract-Hadh vector (Swevers et al. 1996) and transfected in

TOP 10F' cells as described earlier (see 2.2.2). For each isoform, a colony containing the correct insert (after colony PCR and sequencing) was grown overnight in 200 ml liquid LB cultures and the plasmids were extracted with the E.Z.N.A.® Plasmid Maxi Kit I (Omega Bio-Tek) to obtain a sufficient amount of plasmid necessary for the *in vitro* study (see 3.2.3). Plasmids used in experiments include the EcRE-b.act.luc reporter construct, the expression constructs for cloned EcR and RXR isoform ORFs described above, the expression vector for *D. melanogaster* EcR-B1 ORF (Swevers et al. 1996) and empty Ract-Hadh expression vector. The L57-3-11 cell line was obtained from the *Drosophila* Genomics Research Center (Indiana University, Indianapolis, IN) and maintained in Schneider's medium containing 10% heat inactivated foetal bovine serum (Invitrogen, Merelbeke, Belgium) and 1% antibiotic-antimycotic solution (Sigma--Aldrich) at 25°C under a constant 10 µM 20E selection to keep endogenous DmEcR expression low. Multiple transient transfections were simultaneously performed, each in a 500 µl reaction volume containing $3x10^6$ cells, 1.5 µg of reporter construct and a different combination of 1.5 µg CrcEcR- and CrcRXR isoform-expressing vectors. In parallel, control transfections were performed in a similar manner with 3 µg empty vector (as a negative transfection control) and 1.5 µg empty vector in combination with 1.5 µg of expression vector of DmEcR-B1 (as a positive transfection control), CrcEcR isoform and CrcRXR isoform. Starting at $3x10^6$ cells, the transfected cells were grown for 72 h in a 6-well plate at 25°C.

3.2.2 Confirmation of CrcEcR and CrcRXR expression in the L57-3-11 cell line

In order to confirm the high expression levels of the transfected CrcEcR and CrcRXR plasmids in comparison with the endogenous DmEcR, semiquantitative RT-PCR experiments were performed. RNA was extracted from approximately $6x10^6$ control L57-3-11 cells (negative transfection control) and L57-3-11 cells transfected with CrcEcR and CrcRXR. Prior to the cDNA synthesis, a RQ1 RNase-free DNase (Promega) treatment was applied using 1U μg^{-1} RNA template. cDNA was synthesized as described above using a final concentration of 10 ng/µl random hexamer primers. For the semiquantitative RT-PCR, reactions were performed containing 0.5% (v/v) cDNA, 1.5 mM $MgCl_2$, 0.2 mM dNTP mix, 0.025 U/µl Platinum® Taq DNA Polymerase (Invitrogen) and 0.25 µM GSPs at a final volume of 10 µl. Specific primer pairs were designed for CrcEcR (5'-CGG AAA TAA CTG CGA AAT GGA-3' and 5'-CCT GAC AAT CTC GTC ATA GGC-3'), CrcRXR (5'-GCA CTG TGC GAA AAG ACC TCA-3' and 5'-TTT GCC CAT TCT ACA AGT TGC-3'),

DmEcR (5'-CCT CCG GCT ACC ACT AC AAC-3' and 5'-GGC TCG CAT GTC ATA AGG TC-3') and DmUSP (5'-ATA GAC AAG CGG CAG AGG AA-3' and 5'-GGA CTG TGG AAT AGG GAC CA-3') which yield PCR products of ~360-380 bp for each primer pair. As for the external control, universal 18S rRNA primers were designed (5'-CCC GTC GCT ACT ACC GAT T-3' and 5'-GAT CCT TCC GCA GGT TCA C-3'). Following PCR conditions were used: an initial 30 s denaturation at 94°C, followed by 35 cycles of 30 s denaturation at 94°C, annealing at 55°C and 30 s elongation at 72°C. The semiquantitative RT-PCR experiment consisted of triplicate reactions sampled at the end of the annealing step after 23-26-29 cycles for 18S rRNA, 29-32-35 cycles for CrcEcR and CrcRXR and 35-38-41 cycles for DmEcR and DmUSP. All PCR products were visualized on a single 2% agarose gel by ethidium bromide staining. Relative intensity of each band was determined through ImageJ image processing program (Abramoff et al. 2004).

3.2.3 *In vitro* reporter assay with transfected Kc L57-3-11 cell line

After 72 h in 6-well plates at 25°C, 20,000 cells of each transfection reaction were exposed in quadruplicate to 10 nM PonA or an equal volume of pure ethanol in 100 µl volumes in white, flat-bottomed 96-well plates during 24 h at 25°C. Stock solutions of 1 µM PonA (≥95%; Invitrogen) were prepared in ethanol. Luciferase expression was measured using the Steady-Glo® luciferase assay system kit (Promega, Leiden, the Netherlands) with a Tecan M200 luminometer (Tecan, Mechelen, Belgium). The fold inductions (FIs) were calculated as the quotient of the measured relative luminescence units (RLUs) of the PonA treatment and the RLUs of the ethanol treatment (blanc). Reporter gene transactivation is considered significant when a two-tailed student's *t*-test ($p < 0.05$, $n = 4$) indicates a significant difference between the observed FI and the FI of the negative transfection control.

3.2.4 TBT: *in silico* docking in the modelled CrcRXR-LBP and *in vitro* effect on CrcEcR-CrcRXR-heterodimer functioning

For *in silico* docking of TBT in the CrcRXR LBP, the human RXRα LBD in complex with TBT (PDB code 3E94) (Le Maire et al. 2009) was used as a template. For methodological details on the reconstruction we refer to Section 2.3.4. TBTO was purchased at Greyhound Chromatography, Birkenhead, UK (≥99% pure). Prior to the *in vitro* exposure of the L57-3-11 cell line transfected with the full CrcEcR and CrcRXR receptors to TBTO, cell toxicity of TBTO was determined by the colorimetric 3-*(*4,5-dimethylthiazol-2-yl)-5(3-carboxyme-

thonyphenol)-2-(4-sulfophenyl)-2-tetrazolium, inner salt (MTS) approach (Cory et al. 1991): 150,000 cells were exposed to 1 nM, 10 nM, 100 nM, 1 µM and 10 µM of TBTO in 100 µl volumes in quadruplicate in a flat-bottomed transparent 96-well plate. After incubation at 25°C during 24 h, 20 µl of Celltiter 96® AQ_{ueous} One Solution (Promega Corp., Madison, WI) was added and the plates were incubated at 37°C during 2 h prior to absorbance measurement at 490 nm in a microtiter plate reader (PowerWave X340, Bio-Tek Instruments Inc., Winooski, VT). Subsequently, the cell line was exposed in triplicate during 24 h at 25°C to the highest observed non cytotoxic TBTO concentration (10 nM) in the presence and absence of 10 nM PonA. The luciferase expression was measured as described earlier in Section 3.2.3.

3.2.5 *In vivo* effect of TBTO on tissue-specific expression of CrcEcR and CrcRXR isoforms

Interference of TBT in ecdysteroid signalling may lead to an altered gene expression of EcR and RXR, as NRs are known to autoregulate and cross-regulate their own gene expression. EcR is known to be subject to a positive autoregulatory loop to increase EcR levels and sensitize the animal to ecdysone pulses (Karim & Thummel 1992).

Prior to 96 h-exposure to TBTO, non-gravid female shrimp caught at the Oostende bank of 40-45 mm L_T were acclimatized in 0.47 µm filtered natural seawater (35 ppt) at 14.8 ± 0.6°C under a 16L:8D regime in 50 l glass tanks for approximately two weeks. 50% of the tank volume was replaced each 48 h. The shrimp were fed *ad libitum* with mussels (*Mytilus edulis*), plaice filet (*Pleuronectes platessa*) and brine shrimp nauplii (*Artemia salina*). After acclimatization, 64 shrimp were transferred individually to disposable polypropylene containers and exposed during 96 h to three concentrations (16.78, 67.10, and 268.42 nM, including a solvent control containing 0.05% DMSO; 16 shrimp/treatment) of TBTO (stock solutions were prepared in dimethylsulfoxide (DMSO)) in 0.5 l filtered natural seawater. Shrimp were considered dead when *rigor mortis* and discoloration was observed. LC_{50} was determined through Probit analysis using GraphPad Prism version 4.03 (GraphPad Software, San Diego, CA). After 96 h, live shrimp from the solvent control and from the 67.10 nM TBTO-exposure were collected for immediate dissection in RNAlater® (Ambion Inc, Austin, TX) and processed for semiquantitative RT-PCR. Ovaries, hepatopancreas, cuticular hypodermis (*i.e.* endocuticle, epidermis and basal membrane) and tail muscle were isolated and pooled for both samples. Subsequently, 10-30 µg of each tissue was homogenized manually using a microcentrifuge tube pestle in 300 µl TRK lysis buffer (Omega Bio-Tek).

RNA extraction and DNase treatment were performed using the E.Z.N.A.™ tissue RNA kit (Omega Bio-Tek) according to the manufacturer's protocol. Good RNA integrity was confirmed visually on a 2% agarose gel, RNA quantity and DNA and protein contamination were quantified using a Nanodrop® ND-1000 spectrophotometer, after which the RNA concentration was adjusted to 100 ng μl^{-1}. cDNA was synthesized using the RevertAid First Strand cDNA synthesis kit (Fermentas, St. Leon-Rot, Germany) using 5 µM of a 10:1 random primer:oligo$(dT)_{18}$ primer mix. The obtained cDNA was purified using the High Pure PCR purification kit (Roche Applied Science, Mannheim, Germany). The second step reactions of the semiquantitative protocol were performed using the 2 x Red Taq 1.5 mM $MgCl_2$ master mix (VWR International, Leuven, Belgium), 0.5% (v/v) cDNA and 0.25 µM of gene specific primers (GSPs) at a final volume of 50 µl. The primer sequences used are given in Table 3.1. The CrcEcR and CrcRXR isoform sequences obtained in chapter 2 indicate two variant sites in both receptor sequences. For both receptors, the combination of two forward primers, which can discriminate between isoforms in the 5' variant site, and of two reverse primers, that can discriminate between isoforms in the 3' variant site, leads to four possible primer pairs and thus potentially four CrcEcR and CrcRXR isoforms (Fig.2.2 and 2.4). External control reactions (detecting glyceraldehyde-3-phosphate (GADPH) mRNA, β-actin mRNA and 18S rRNA; primer sequences are given in table 3.1) were performed at the same reaction conditions. The following PCR conditions were used: an initial 2 min-denaturation at 94°C, followed by 35 cycles of 20 s-denaturation at 94°C, annealing at 54°C during 30 s and 30 s-elongation at 72°C, finished by a final elongation step at 72°C for 5 min. PCR products were visualized on a single 2% agarose gel by GelRed™ (Biotium, VWR International) staining.

Table 3.1. Overview of primers used for the semiquantitative RT-PCR.

		CrcEcR	CrcRXR
Isoform specific primers	**1**	5'-TGA ATT GGC CTC ATG AAA AG-3'	5'-CAG GTA GGG GGA ATA GAG GA-3'
	2	5'-TTT AAG CCC ATT GCC TAT GA-3'	5'-AAG CGG TCC AGG AAG AAC-3'
	3	5'-TTC TCG TAA TGC TGG ACG TT-3'	5'-GTT GCA CTA AAT GTC TGT CAG C-3'
	4	5'-CAA TTG GCT TGT CTT ACC TGA-3'	5'-CGC AAA CAT CCT AAC TCT GTC-3'

Control gene	Forward primer	Reverse primer
β-actin	5'- ACT-TCG-AGC-AGG-AAA-TGA-CC -3'	5'- CGT-GGA-TAC-CGC-AGG-ATT -3'
GADPH	5'-AAC-ATT-CCA-TGG-AGC-AAG-G-3'	5'-GTG-GTG-CAG-GAA-GCA-TTG-3'
18S rRNA	5'- CCC-GTC-GCT-ACT-ACC-GAT-T -3'	5'-GAT-CCT-TCC-GCA-GGT-TCA-C-3'

3.3 Results

3.3.1 *In vitro* transactivational activity of CrcEcR and CrcRXR isoforms

Semi-quantitative RT-PCR on the transfected L57-3-11 cell line clearly confirms that co-transfected CrcEcR and CrcRXR are overexpressed, compared to the endogenous DmEcR and DmUSP mRNAs (Fig. 3.1). The FIs generated by 10 nM PonA in the cell lines after transfection with the possible combinations of CrcEcR and CrcRXR isoforms are given in Fig. 3.2. The cell line transfected with *D. melanogaster* DmEcR-B1 isoform was considered as a positive transfection control and exhibited a 3.6-fold higher induction after treatment with 10 nM PonA compared with the negative transfection control (i.e. cell line transfected with empty expression plasmid).

Overall, these results indicate that transactivation of the EcRE depends on the constitution of the heterodimer. The full CrcEcR receptor was able to activate reporter gene expression without the need for CrcRXR, which would suggest functional CrcEcR homodimerization and/or dimerization with endogenous DmUSP. Co-transfection of CrcRXR with CrcEcR did not have any enhancing effect, while co-transfection of the two variant CrcRXRs apparently neutralized CrcEcR-related transactivation. The truncated CrcEcR isoforms, $CrcEcR_{\Delta EF}$ and $CrcEcR_{\Delta EF,\ D\text{-}18}$, behave differently: $CrcEcR_{\Delta EF,\ D\text{-}18}$ was only active in combination with $CrcRXR_{\ D\text{-}5}$, while $CrcEcR_{\Delta EF}$ was active in combination with every CrcRXR isoform. Interestingly, CrcRXR and $CrcRXR_{\Delta EF}$ transfection significantly increases luciferase expression without the need of CrcEcR. This suggests that these RXRs transactivate the ecdysteroid-responsive element as heterodimer with endogenous DmEcR isoforms.

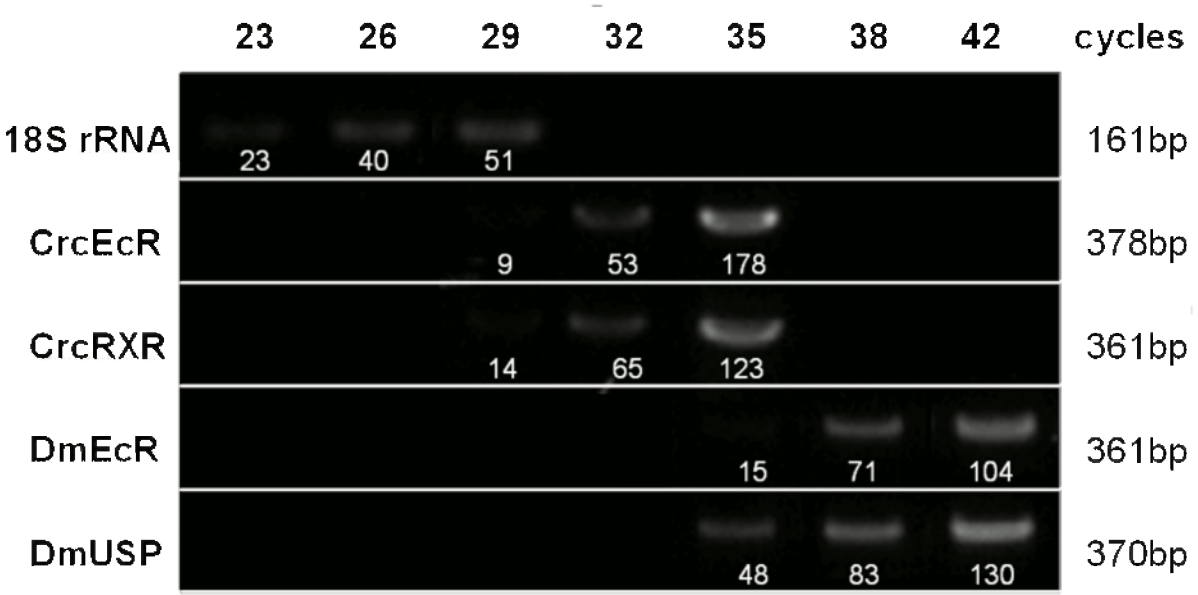

Fig. 3.1. Quantification of mRNA levels of exogenous CrcEcR/RXR and endogenous DmEcR/USP in transfected L57-3-11 cells by semiquantitative RT-PCR. Intensities (after background subtraction) are given under each band. Fragment lengths are presented at the right in base pairs, and PCR cycle numbers are given above the figure.

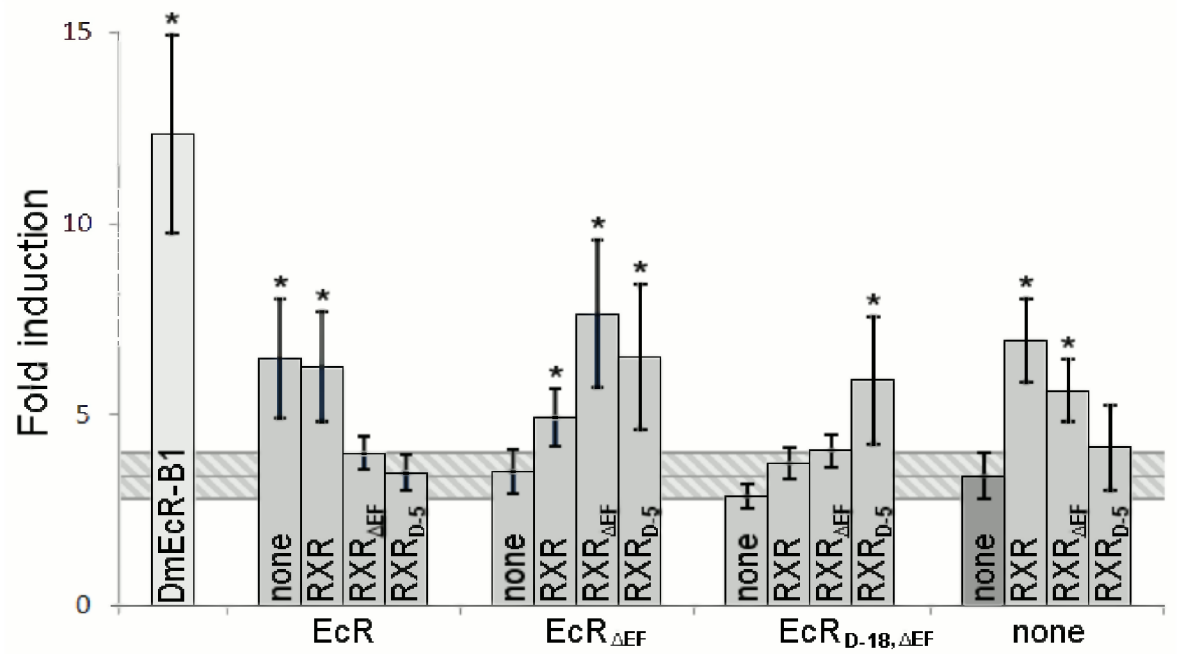

Fig. 3.2. Overview of luciferase induction by 10 nM PonA through different combinations of CrcEcR and CrcRXR isoforms. FI is calculated as the RLUs after 10 nM PonA treatment divided by the RLUs after ethanol treatment (blank). The arced background band represents the mean of the negative control FI with its associated SEMs (n = 4). Asterisks above bars indicate FIs significantly different from that of the negative control after a Student's *t*-test (two-tailed, $p < 0.05$).

3.3.2 TBT: *in silico* docking in the CrcRXR LBP

The *in silico* analysis predicts that the CrcRXR LBP can accommodate the smaller TBT biocide molecule (Fig. 3.3) in a similar manner as in RXRα (LeMaire et al. 2009). The three butyl substituents of TBT establish enough van der Waals interactions with most of the residues belonging to the 9-*cis*-RA binding pocket to position the tin atom against H11and stabilize CrcRXR in its active conformation.

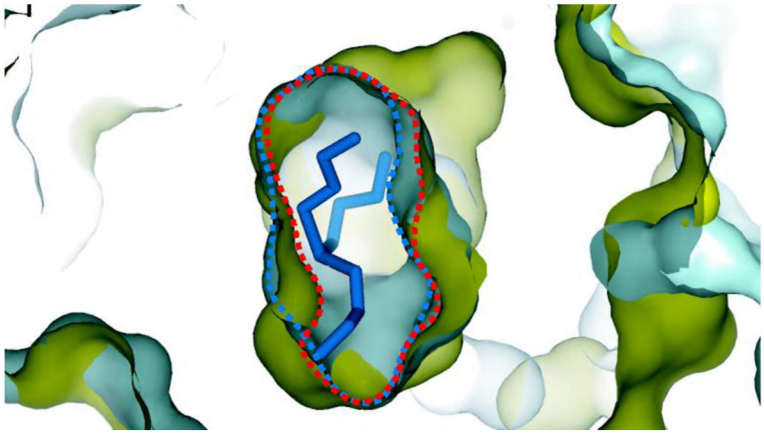

Fig. 3.3. Clipping planes of the superimposed LBPs of CrcRXR (red dotted line) and RXRα (blue dotted line) showing the docking of TBT into the LBP of CrcRXR (green) and RXRα (blue).

3.3.3 TBT: *in vitro* effect on CrcEcR-CrcRXR transactivational activity

In the *in vitro* assay with *D. melanogaster* cells, the cell viability (expressed as EC_{50}) of TBTO after 24 h was estimated at 96.5 nM (95% confidence interval 76.5-121.5 nM, R^2 = 0.992; Fig. 3.4).

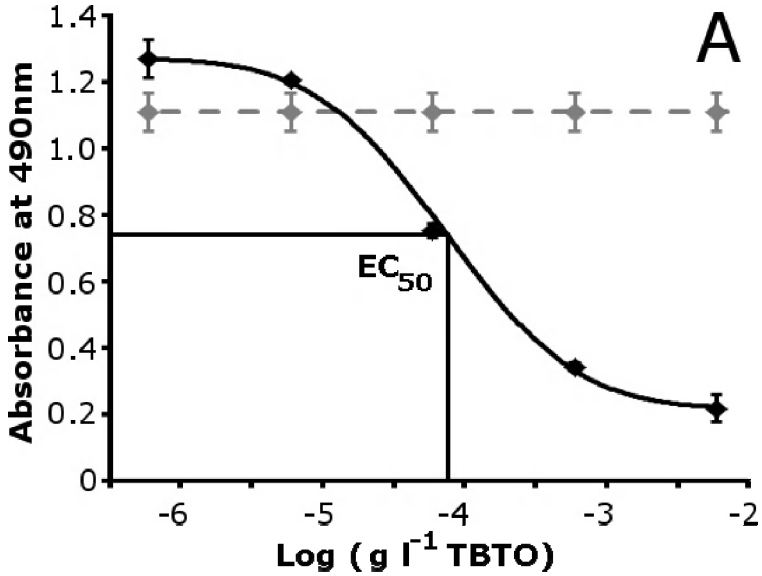

Fig. 3.4. L57-3-11 cell toxicity (Y-axis) after 24 hrs *in vitro* exposure to different TBTO concentrations (X-axis), measured through the MTS approach.

10 nM TBTO did not affect cell viability but significantly reduced reporter gene activation by 10 nM PonA with 64% (Student's *t*-test, two tailed, $p < 0.05$) (Fig. 3.5).

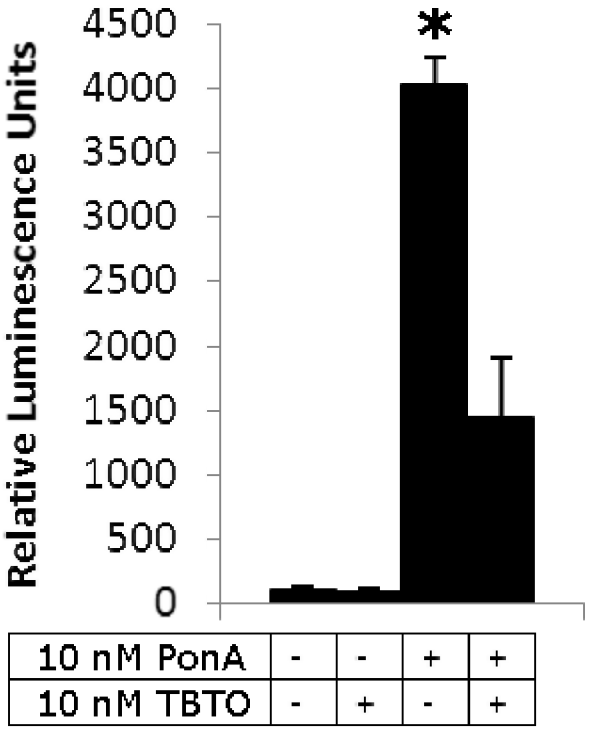

Fig. 3.5. Influence of 10 nM TBTO on reporter gene trans-activation by 10 nM PonA through CrcEcR–CrcRXR (receptor isoforms were not tested). Four different treatments were performed in quadruplicate (from left to right): a negative control, exposure to 10 nM TBTO, a positive control (10 nM PonA) and exposure to 10 nM TBTO in the presence of 10 nM PonA. Data are presented as the mean ± SEM ($n = 4$). An asterisk denotes a significant difference with the respective control (Student's *t*-test, two tailed, $p < 0.05$).

3.3.4 TBT: tissue specific effect on CrcEcR and CrcRXR expression

The LC_{50} after 96 h of *in vivo* exposure of shrimp to TBTO was determined at 67.10 nM (95% confidence interval 29.0-155.2 nM, $R^2 = 0.937$; Fig. 3.6). The semi-quantitative RT-PCR revealed that acute TBTO exposure evoked tissue- and isoform-specific effects on CrcEcR and CrcRXR expression (Fig. 3.7): The high expression levels of CrcEcR, $CrcEcR_{D-18}$ and CrcRXR observed in ovaries were strongly reduced.

The semiquantitative approach also indicated that the low expression levels of CrcEcR in dermis and of $CrcEcR_{D-18}$ and $CrcRXR_{D-5}$ in hepatopancreas were up regulated. Control gene expression remained stable after TBTO exposure, although a small decrease in β-actin expression can be observed in tail muscle.

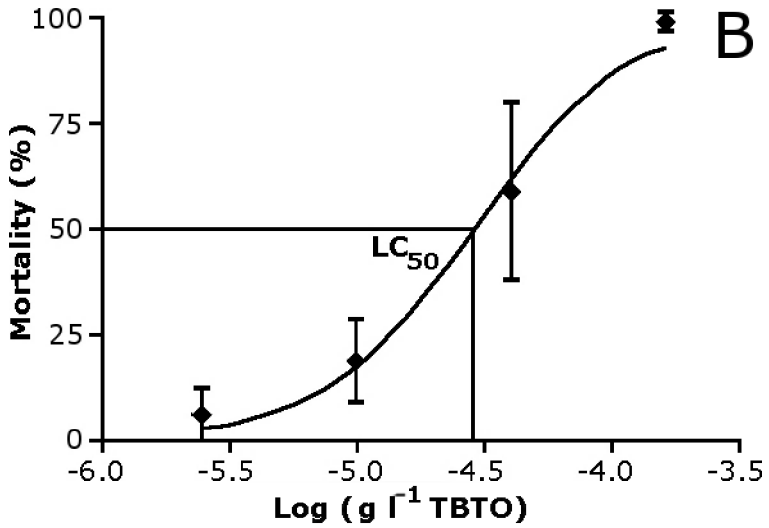

Fig. 3.6 *In vivo* toxicity (Y-axis) after 96 hr exposure of adult female shrimp to different TBTO concentrations (X-axis).

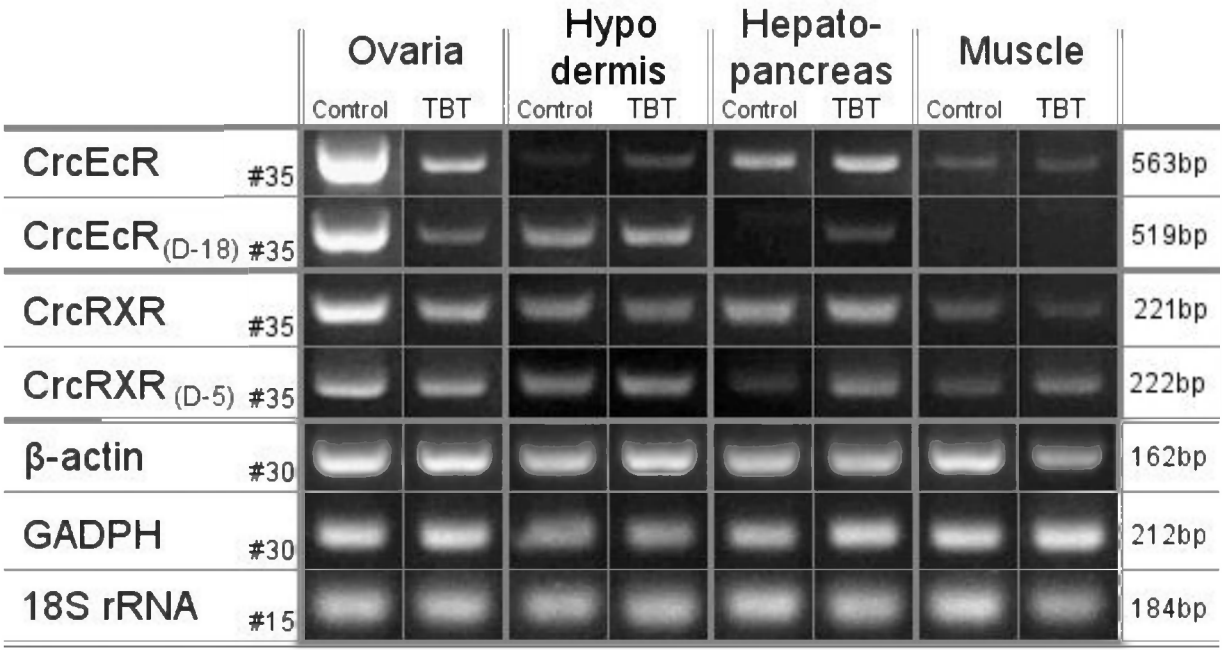

Fig. 3.7. mRNA levels in ovaries, hypodermis, hepatopancreas and muscle of *C. crangon* after exposure to TBT. Semiquantitative RT-PCR results of *C. crangon* exposed to 67 nM TBTO (40 µg l^{-1}) for 96 h compared with mRNA expression in the control group for the non-truncated CrcEcR and CrcRXR isoforms. mRNA levels of the control genes b-actin, glyceraldehyde-3-phosphate (GADPH) and 18S rRNA are also represented. Amplified gene names and cycle number are given on the left, template tissue and experimental group are given at the top, amplicon size is given at the right. Truncated CrcEcR and CrcRXR isoforms are not shown as they were detected at higher PCR cycle numbers.

3.4 Discussion and conclusions

3.4.1 Applications of the L57-3-11 cell line

The *in vitro* EcR reporter assay clearly indicated the activity of the CrcEcR receptor in the mutant *Drosophila* L57-3-11 cell line: binding of 10 nM PonA to expressed shrimp CrcEcR/RXR led to a six-fold increase in EcR-dependent reporter activation. The FI after 'rescue' transfection with fly DmEcRB1 was twice as high. In similar experiments with the L57-3-11 cell line with exogenous lepidopteran EcR (Swevers et al. 1996), induction in the BmEcR expressing cell line was much lower than in the DmEcR rescued cell line. These researchers proposed that higher exogenous EcR concentrations are required because of quantitative differences in protein interaction with either USP or the transcriptional apparatus in the *Drosophila* host cell line. The transfected L57-3-11 cell line can be used as *in vitro* bioassay to confirm candidate EDC activity in crustaceans. While a crustacean cell line would be ideal for a cell based bioassay, but are not available, primary cell cultures obtained from crustaceans are practically unsuited for bioassays due to their limited lifespan. Immortal cell lines require less labour and represent a continuous and reliable bioassay instrument. However, so far no reports on an established crustacean cell line exist (Claydon & Owens 2008; Lee et al. 2011). To achieve a cell line for investigating the functioning of a crustacean EcR, non-crustacean cell lines can be transfected with crustacean EcR and RXR. Mammalian cell lines have the major advantage that endogenous EcR is naturally absent. Kato et al. (2007) used a complex two-hybrid system with transfected chimeric genes containing the LBDs of *D. magna* EcR and RXR in vertebrate CHO cells. An arthropod cell line is closer to crustacean cells (*e.g.*, posttranslational modifications, co-factors). Based on our results, we believe that using the transfected *Drosophila* Kc L57-3-11 cells can be used to efficiently evaluate different compounds for possible endocrine disrupting effects in crustaceans. Good examples are compounds that influence crustacean moulting (Zou 2005) such as certain pesticides (Schimmel et al. 1979; Baer & Owens 1999; Snyder & Mulder 2001; Meng & Zou 2009a; Palma et al. 2009), PCBs (Fingerman & Fingerman 1977; Zou and Fingerman, 1999), aromatic hydrocarbons (Cantelmo et al. 1981, 1982), estrogenic agents (Zou & Fingerman 1997; Montagna & Collins 2007), phtalates (Zou & Fingerman 1999) and non-steroidal ecdysteroid agonists used in insect pest control (Weis & Mantel 1976; Clare et al. 1999; Dhadialla et al. 1998; Waddy et al. 2002; Soin et al. 2010). Moreover, the cell line could also present a more fundamental scientific vehicle to compare the functionality and interactions of intra- and interspecies EcR-RXR/USP isoform heterodimers. For example, it would enable to

screen potential RXR ligands for their effect on ecdysteroid signalling, which is expected to be different between insects and crustaceans (Fang et al. 2005; Hayward et al. 2003; Iwema et al. 2009; Wang & LeBlanc 2009).

The results however indicate the sensitivity and robustness of the used *Drosophila* reporter system can be enhanced. The observed luciferase induction levels by the exogenous shrimp receptors were only slightly (but yet significantly) higher than that of the negative control (non-transfected L57-3-11 cells). The cell line exhibits a noticeable FI, as endogenous DmEcR receptor isoforms other than B1 and B2 are still active. The endogenous expression of DmEcR isoforms and DmUSP may be specifically inactivated through modern *in situ* genome editing techniques such as zinc-finger nucleases and transcription activator-like effector nucleases (TALENs). Minor differences in the cellular machinery involved in ecdysteroidal transactivation (e.g. substituents of the coactivator complex) between dipterans and crustaceans may also be an important factor, as the positive control (transfection with DmEcR-B1) gave much higher FIs than the CrcEcR transfections. The use of a crustacean EcRE in the reporter construct instead of a *Drosophila* EcRE can be a relatively easy adaptation to increase the sensitivity of the system towards exogenous crustacean EcR receptors. Furthermore, in transient transfected cells, variability in cell number and especially transfection efficiency can have an unwanted effect on the magnitude of receptor and reporter expression and hence in measured FIs. After the expression of the exogenous CrcEcRs and CrcRXRs has been successfully performed through transient transfections, stable transfections (using a vector containing a selectable marker gene) can be performed to isolate and propagate clones which have incorporated the transfected CrcEcR and CrcRXR genes in the cellular genome. The use of robust stable cell lines would greatly reduce the variability which is inherent to transient cell lines.

3.4.2 The antagonistic ecdysteroidal effect of the RXR agonist TBT

While the physiological presence and functionality of natural RXR ligands is still under debate, the ubiquitous environmental pollutant TBT has been shown to be a potent RXR agonist in many species, especially in gastropods. In the current experiment, a reduction of 64% in gene transactivation was demonstrated caused by 10 nM PonA, when our insect cell reporter system containing CrcEcR and CrcRXR was exposed to 10 nM TBTO. Along this line, 3D docking confirmed that TBT indeed fits in the modelled LBP of CrcRXR. Earlier, Mu & LeBlanc (2004) reported that TBT and other RXR agonists such as MF and

pyriproxyfen also have an antagonistic effect on the ecdysteroid signalling in water flea *D. magna*. Recently, Wang & LeBlanc (2009) reported that TBT directly activates *D. magna* RXR, in contrast to the other RXR agonists tested. Furthermore, they found a potentiating effect of TBT at 100 nM on the signalling by 1 µM of 20E in human HepG2 cells transfected with *D. magna* EcR and RXR. The differences in activity of TBT(O) between our and the latter study (inhibition versus stimulation) likely are the result from the type of *in vitro* reporter system used. In Wang & LeBlanc (2009), luciferase expression is induced by the Gal4-RXR construct. Heterodimerization of this construct with the daphnid EcR renders the construct ecdysteroid responsive, and thus creates a situation opposite of natural EcR:RXR heterodimer functioning. Our system better reflects the natural situation, as luciferase expression is induced by interaction of the CrcEcR DBD with an ecdysteroid responsive element, while TBT negatively modulates CrcEcR activity through its heterodimerization partner RXR.

Furthermore, using a semiquantitative RT-PCR approach, we showed that TBTO leads to tissue- and isoform-specific alterations of EcR and RXR expression. EcR and RXR are ecdysteroid responsive genes as proven in adult female *D. magna* (Wang et al. 2007) and *Americamysis bahia* (Hopkins e al. 2008). Wang et al. (2007) showed that the RXR agonist pyriproxifen down regulates RXR mRNA expression in female *D. magna*, while 20E up regulated RXR mRNA expression. In contrast, exposure of *C. pugilator* to the RXR ligand all-*trans*-RA increased UpRXR mRNA expression, while no immediate change in UpEcR mRNA expression was observed (Chung et al. 1998). In *C. crangon*, we observed a strong down regulation of CrcEcR, $CrcEcR_{D\text{-}18}$ and CrcRXR in the ovaries and up regulations of $CrcEcR_{D\text{-}18}$ and $CrcRXR_{D\text{-}5}$ in the hepatopancreas and of CrcEcR in the hypodermis. To our knowlegde, this is the first report that a TBT compound is inducing tissue- and isoform-specific alterations of EcR and RXR mRNA expression in Crustacea.

Chapter 4

Organotin contents in common shrimp

Parts of this chapter have been published as:

Y. Verhaegen, E. Monteyne, T. Neudecker, I. Tulp, G. Smagghe, K. Cooreman, P. Roose and K. Parmentier, 2012. Organotins in North Sea brown shrimp (*Crangon crangon* L.) after implementation of the TBT ban. Chemosphere, 86, 979-984.

The research performed in this chapter was achieved in cooperation with Dr. Patrick Roose and Drs. Els Monteyne of the marine chemistry lab of the Management Unit of the North Sea Mathematical Models and the Scheldt estuary (MUMM) in Oostende.

4.1 Introduction

Spatial and recent data on OT concentrations in common shrimp are too scarce to investigate the potential hazardous effects of OTs in wildlife *C. crangon* populations. A limited amount of data on OT concentrations in *C. crangon* is available for the Westerschelde and the Southern Bight only (Table 4.1).

Table 4.1. Earlier reported OT concentrations (in µg kg^{-1} DW shrimp meat) in *C. crangon*.

OT	Location	Concentration	Date	Reference
TBT	BCS3	368	June 2003	Willemsen et al. 2004
TBT	BCS3	259	June 2003	Willemsen et al. 2004
TBT	W. Schelde	575.2	Spring 2003	Veltman et al. 2006
TPhT	W. Schelde	50.1	Spring 2003	Veltman et al. 2006
TBT	W. Schelde	350-1700	March 2003 – July 2005	Janssen et al. 2007
TPhT	W. Schelde	36-260	March 2003 – July 2005	Janssen et al. 2007

In this chapter, TBT and TPhT concentrations are reported in *C. crangon* caught within a short time frame (1st of September – 10th of November 2009) at multiple sampling stations ranging from De Panne (Belgium) to Esbjerg (Denmark), covering the major commercial fishing grounds. Furthermore, we focus on the Westerschelde as a heavily polluted European estuary, associated with one of the most densely populated areas (Flanders) and largest ports (Antwerp) in the world, while it encompasses a large *C. crangon* population and an important nursery ground, the estuarine tidal marsh "Verdronken Land Van Saeftinghe" (Cattrijsse et al. 1997). The trend in *C. crangon* TBT and TPhT content along the salinity gradient is related to the sediment concentrations. Associated biota-sediment accumulation factors (BSAFs) are derived.

4.2 Material and methods

4.2.1 Sample collection

Samples were collected between the 1st of September 2009 and the 10th of November 2009 during the Dutch, German and Belgian Demersal (Young) Fish Surveys (DFS in the Netherlands, DYFS in Germany and Belgium), performed by the Institute for Marine Resources and Ecosystem Studies (IMARES, The Netherlands), Johann Heinrich von Thünen-Institute, Institute of Sea Fisheries (vTI-SF, Germany) and the Institute for Agricultural and Fisheries Research (ILVO, Belgium; all sample information is given in Table 4.2).

Samples were immediately frozen aboard and stored at -20 °C at the related institutes prior to dispatching in polystyrene foam insulated containers to ILVO in Oostende. Further sample preparation, extraction, clean-up, gas chromatographic (GC) analyses and quality control were done in accordance with the guidance for monitoring OTs in marine biota (Monteyne et al. 2010) and were performed at the marine chemistry lab of the Management Unit of the North Sea Mathematical Models and the Scheldt estuary (MUMM) in Oostende, an accredited laboratory in accordance with the recognized International Standard ISO/IEC 17025:2005.

4.2.2 Sample preparation

Shrimp were allowed to thaw overnight, peeled and briefly rinsed with ultrapure water to obtain approximately 100 g of tail muscle for each sampling station. Samples were mixed in borosilicate petri-dishes using a rotor/stator type homogenizer (Ultraturrax T25 basic, IKA-Labortechnik, Staufen, Germany), freeze-dried with a Christ LMC-2 (Martin Christ Gefriertrocknungsanlagen, Osterode am Harz, Germany) lyophilizer and pulverized manually using a porcelain mortar and pestle. The powder was weighed for calculation of dry weight (DW) – wet weight (WW) ratio, and stored in a desiccator cabinet for days until analysis.

4.2.3 Sample extraction and clean-up

The procedure for OT extraction was based on the use of acid reagents in methanol and stirring in hexane. About 1 g of shrimp powder was transferred into an amber 40 ml screw cap vial, 15 ml methanol and 7 ml hexane were added. Samples were buffered to pH 5 by adding 3 ml 4 M sodium acetate. An aliquot of 25 µl of tripropyltin solution (10 µg Sn g^{-1} in methanol) was added as recovery standard prior to derivatization for QA/QC purposes to control the ethylation efficacy of TBT. Ethylation is combined with a continuous desorption process by adding 4 ml of sodium tetraethyl borate (Sigma-Aldrich,) prepared with deionized water (5%, *v/v*) drop by drop to vigorously stirred samples. For degradation of boroxin, formed due to the intensive derivatization (Smedes et al. 2000), an aliquot of 5 ml of 10 M sodium hydroxide was added to the samples. Finally, internal standards tetrapropyltin (used for quantification) and pentyltriphenyltin (additional standard for QA/QC purpose) of a concentration of 4 µg Sn g^{-1} in hexane were added to the samples, and the phases were separated by centrifugation. All solvents used were of purity for organic residue analysis. Chlorinated and ethylated OTs were obtained from QUASIMEME (Wageningen, The Netherlands). Internal standard and recovery standard tetrapropyltin and tripropyltin chloride were purchased from Schmidt (Amsterdam,

The Netherlands). Glassware was washed with 10% hydrochloric acid and rinsed six times with ultrapure water. Custom-made chromatography columns (200 mm x 9 mm internal diameter (ID)) filled with 2 g of florisil (Merck, Darmstadt, Germany) and 25 ml of hexane was used for clean-up elution. The extracts were stored at 4 °C until GC-analysis.

4.2.4 Gas chromatographic analysis

A large-volume injection technique was developed (Monteyne *et al.* in prep.). 50 µl of sample was injected by an autosampler (Combipal, CTC Analytics, Italy) at a rate of 1.7 µl s^{-1} through a Programmed Temperature Vaporizing (PTV) injector (Thermo Electron Corporation, Austin, Texas), using a glass sintered liner. The analytic system consisted of a Trace GC (ThermoQuest, Milan, Italy), a 20 m Rtx®-5 SILMS analytical column (0.25 mm ID) with a 5% phenyl polysilphenylene-siloxane stationary phase (0.25 µm film thickness; Restek, Bellefonte, USA). The oven was kept at 35 °C for 4 min and temperature was risen at a rate of 20 °C min^{-1} to 120 °C (ramp 1), at a rate of 7 °C min^{-1} to 150 °C (ramp 2) and finally at a rate of 20 °C min^{-1} to 300 °C (ramp 3) (5 min hold). A carrier flow of helium of 1.5 ml min^{-1} was used. The compounds were detected by a Finnigan Trace MS in electron-impact ionisation mode operating in selected ion monitoring.

4.2.5 Quality control

Multi-level calibration curves (r^2 > 0.995) in the linear response interval of the detector were created for quantification. The identification was based on retention times and intensity ratios of three monitored ions for quantification. The quality control was performed by regular analysis of procedural blancs, a procedural spike of 100 ng Sn g^{-1}, duplo measurements, internal reference material (mussel tissue) and certified reference material (mussel tissue ERM®-CE477). Recovery of MBT, DBT and TBT in ERM®-CE477 was respectively 117 ± 14%, 97 ± 15% and 99 ± 11% (n=12, 4 year period). Recovery of TPhT in the procedural spike is 90 ± 15%. Also half yearly an international proficiency test was successfully participated (QUASIMEME). Limits of quantification (LoQ) for TBT and TPhT were 1 µg kg^{-1} DW. LoQs of monobutyltin (MBT), dibutyltin (DBT), monophenyltin (MPhT) and diphenyltin (DPhT) were 10, 10, 3 and 1 µg kg^{-1} DW, respectively.

All concentration results further used in this article are expressed as µg of OT ion kg^{-1}, expressed on a DW basis.

4.2.6 Sediment data and the biota-sediment accumulation factor

Concentrations of OTs and other pollutants and organic carbon content in the <63 µm sediment fraction and median grain size and $CaCO_3$ content of unsieved sediment at the sampling stations in the Westerschelde estuary during 1999-2009 were obtained through online databases of the Belgian Marine Data Centre (BMDC, http://www.mumm.ac.be/datacentre/) and the Dutch Rijkswaterstaat (www.waterbase.nl). Sediment OT concentrations were used to calculate the biota-sediment accumulation factor (BSAF), a parameter describing bioaccumulation of sediment-associated non-polar organic contaminants into organisms or their tissues (Burkhard 2009). BSAFs are useful for ecological risk assessments because concentration data are usually available for sediment, in contrast to biota. BSAFs are applied to TBT as the organic portion of the molecule provides properties conducive to yielding meaningful BSAFs. As TBT does not accumulate in fatty tissues as organic contaminants but accumulates in body tissues in a similar manner as metals (i.e.through selective binding to proteins; Kannan et al. 1996; Kim et al. 1996; Tanabe 1999), tissue concentrations were not lipid normalized and expressed on a DW basis. Thus, the BSAF for TBT is calculated from three measured variables: concentration of TBT in the organism on a dry weight basis (C_o, in µg kg^{-1} DW), concentration of TBT in the <63 µm sediment fraction on a dry weight basis (C_s, in µg kg^{-1} DW),), and the organic carbon content of the dry <63 µm sediment fraction (f_{soc}, in g organic carbon g^{-1} DW):

$$BSAF = \frac{C_0}{C_s/f_{soc}}, \text{ in µg kg}^{-1} \text{ tissue DW / µg organic carbon kg}^{-1} \text{ DW}$$

4.2.7 Tolerable human daily intake (TDI)

Based on the no observed adverse effect level of TBT for immunotoxicity in rats, multiplied with a safety factor 1/100, a TDI of 0.25 µg kg^{-1} body weight has been proposed (Penninks, 1993). The European Food Safety Authority (EFSA) established a group TDI for the sum of DBT, TBT, TPhT and dioctyltin (DOT) to 0.25 µg kg^{-1} body weight, due to the similarity of their immunotoxic properties. Hence, for each sampling station, summed OT concentrations were used to calculate the allowed daily consumption (in kg FW shrimp meat).

4.3 Results and discussion

4.3.1 Spatial distribution of OT accumulation in common shrimp

In the autumn of 2009, TBT and TPhT levels in shrimp ranged from 4-124 and from 1-24 µg kg^{-1} DW, respectively (Fig.4.1; Table 4.2). Levels of MBT, DBT, MPhT and DPhT were all below the LoQs (10, 10, 3 and 1 µg kg^{-1} DW, respectively) and are not further discussed. In general, offshore OT concentrations are low, but increase towards major estuaries (Westerschelde, Rhine-Meuse Delta, Ems-Dollard, Weser and Elbe). In this respect, shrimp OT concentrations in the German Bight (GW2-GW10, Fig.4.1; Table 4.2) are relatively high, increasing towards the Elbe estuary. The German Bight is characterized by a high direct inflow of riverine water from the Weser and Elbe and advection from the rivers Rhine, Meuse and Ems-Dollard through the continental coastal current. In the German Bight, intensive shipping activity and strong tidal shear currents lead to a continuous disturbance of the sediment bed and resuspension of particulate matter, which affects the biological availability of pollutants (Becker et al. 1992).

TPhT concentrations relative to TBT were highest (>50%) in the stations near the Schelde and Ems-Dollard estuaries and within the Oosterschelde estuary (BCS1, BCS2, ES1, NW8, NCS5, GW1), reflecting the large (historic) use of fentin fungicides in (potato) agriculture in the related catchment areas. Lowest OT concentrations were observed inshore in the Southern Wadden Sea near Texel, near-shore at the Northern Wadden islands Sylt and Rømø and offshore at the Southern sandbanks near De Panne.

Fig. 4.1. (pages 82-83). Spatial distribution of TBT (light grey bars) and TPhT (dark grey bars) concentrations in shrimp meat (Y-axis, in µg kg^{-1} DW) from the stations along the South-Eastern coast of the North Sea.

Table 4.2. (page 84). Sample station details, measured OT concentrations (in µg kg^{-1} dry weight (DW) shrimp meat) and the allowed daily consumption of shrimp meat (in kg fresh weight (FW)) according to the TDI of OTs for a 60 kg person.

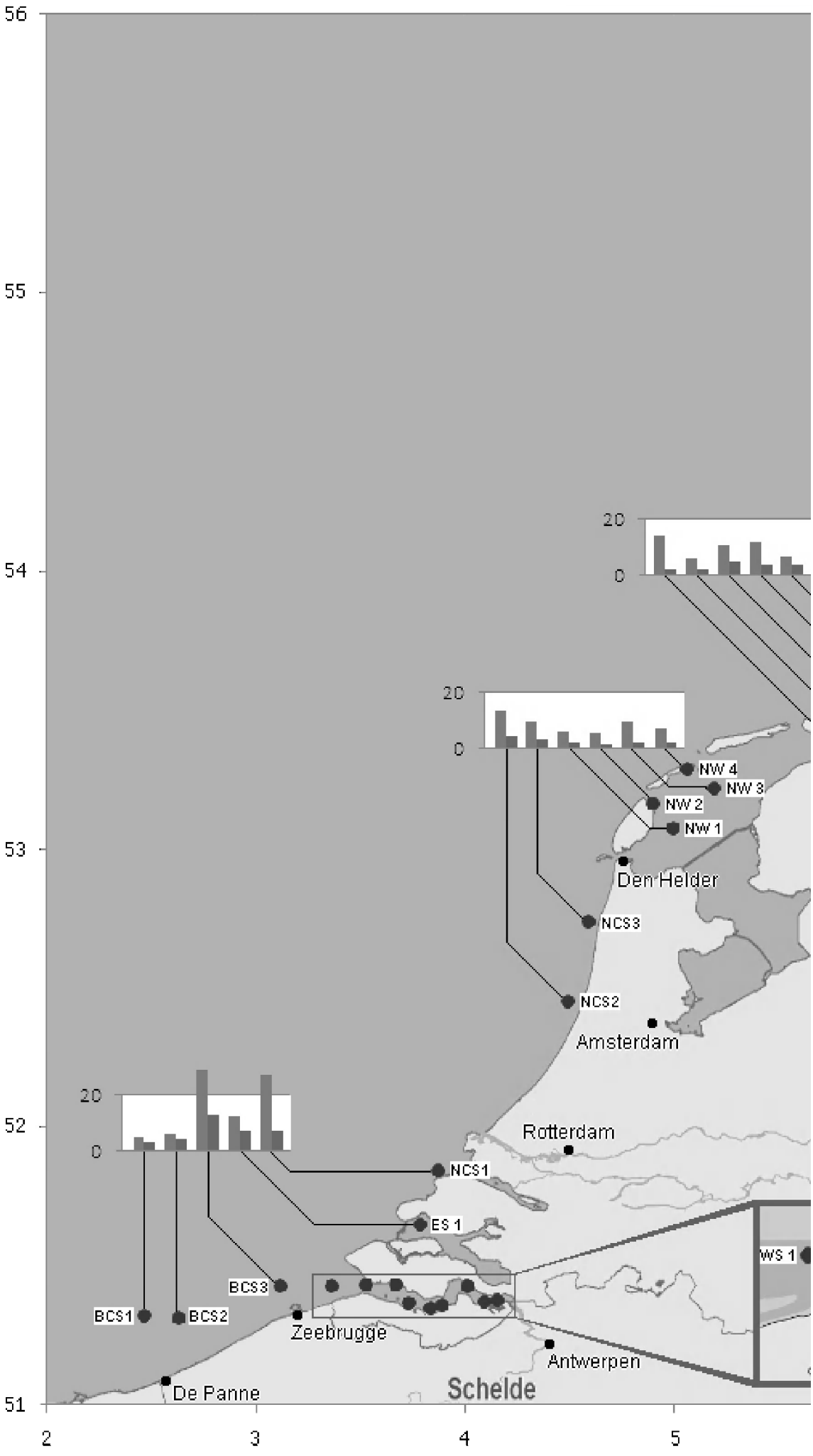
56
55
54
53
52
51
2
3
4
5
20
0
NW 4
NW 3
NW 2
NW 1
Den Helder
NCS3
NCS2
Amsterdam
Rotterdam
NCS1
ES 1
WS 1
BCS3
BCS1
BCS2
Zeebrugge
Antwerpen
De Panne
Schelde

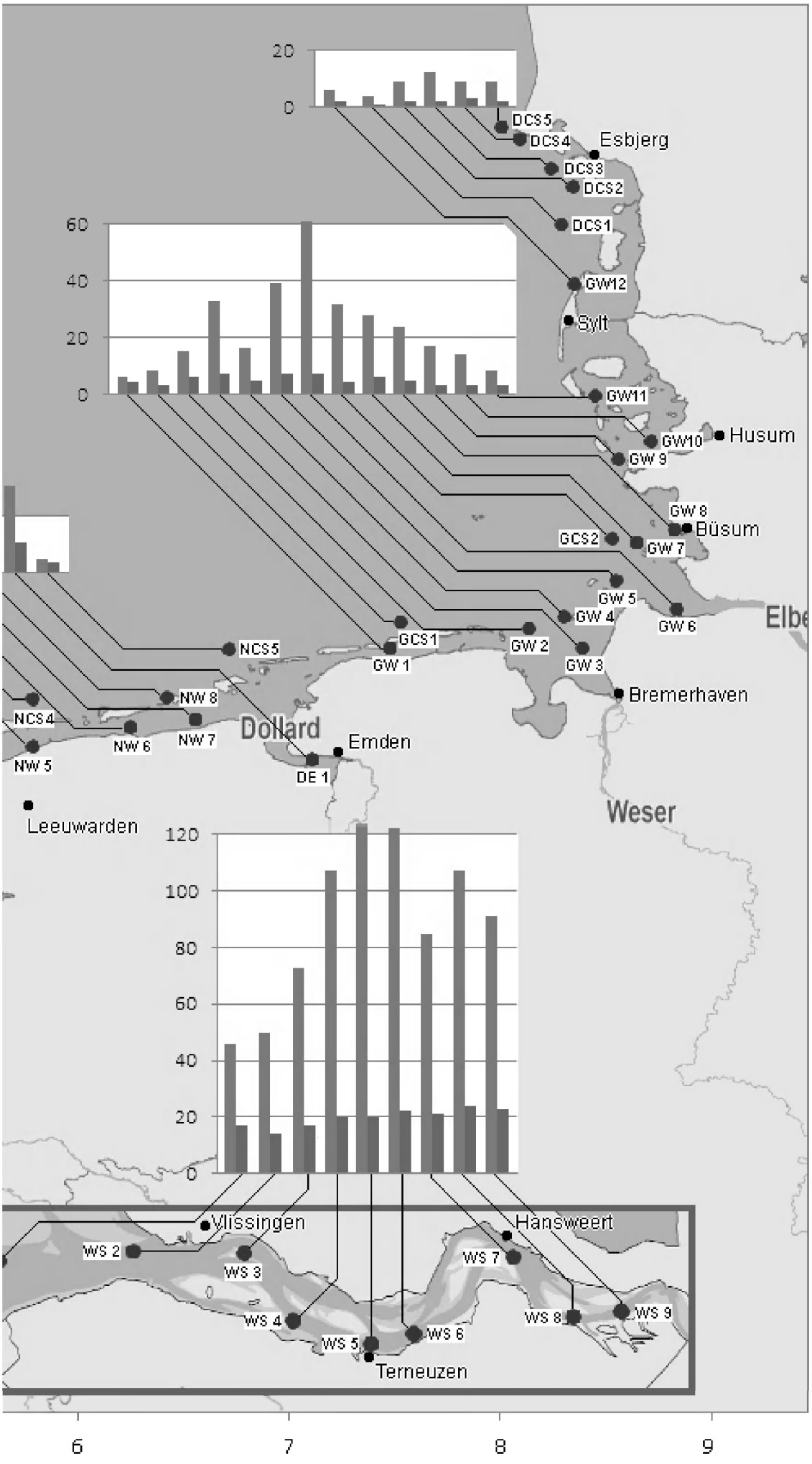
20
0
DCS5
DCS4
Esbjerg
DCS3
DCS2
DCS1
60
40
20
0
GW12
Sylt
GW11
GW10
Husum
GW 9
GW 8
Büsum
GCS2
GW 7
GW 5
GW 4
GW 6
Elbe
GCS1
GW 2
GW 3
NCS5
GW 1
Bremerhaven
NW 8
NCS4
NW 6
NW 7
Dollard
Emden
NW 5
DE 1
Leeuwarden
Weser
120
100
80
60
40
20
0
Vlissingen
Hansweert
WS 2
WS 3
WS 7
WS 4
WS 8
WS 9
WS 5
WS 6
Terneuzen
6
7
8
9

Station	Date	Latitude	Longitude	Vessel	TBT	TPhT	TDI
BCS1	1/10/09	51°19.35'N	2°27.80'E	Belgica	5	3	8.37
BCS2	2/10/09	51°18.55'N	2°38.06'E	Belgica	6	4	4.70
BCS3	29/09/09	51°25.50'N	3°7.00'E	Belgica	29	13	1.59
ES 1	22/09/09	51°38.90'N	3°44.98'E	Schollevaar	12	7	3.52
NCS1	2/11/09	51°50.62'N	3°52.37'E	Isis	27	7	1.97
NCS2	1/10/09	52°27.05'N	4°29.27'E	Isis	13	4	3.94
NCS3	22/10/09	52°44.30'N	4°35.21'E	Isis	9	3	5.58
NW 1	7/09/09	53°4.52'N	4°59.38'E	Stern	6	2	8.37
NW 2	2/09/09	53°9.87'N	4°53.56'E	Stern	5	1	11.16
NW 3	20/09/09	53°13.08'N	5°11.23'E	Stern	9	2	4.09
NW 4	1/09/09	53°17.13'N	5°3.58'E	Stern	7	2	7.44
NW 5	16/09/09	53°22.03'N	5°47.72'E	Stern	14	2	4.19
NCS4	7/10/09	53°32.32'N	5°47.56'E	Isis	6	2	8.37
NW 6	17/09/09	53°24.04'N	6°15.22'E	Stern	11	5	4.19
NW 7	21/09/09	53°32.43'N	6°25.58'E	Stern	12	4	4.19
NW 8	23/09/09	53°27.82'N	6°33.68'E	Stern	7	4	4.09
DE 1	30/09/09	53°19.04'N	7°4.70'E	Isis	31	11	1.59
NCS5	7/10/09	53°42.64'N	6°43.18'E	Isis	5	4	7.44
GW 1	15/09/09	53°43.12'N	7°28.63'E	Chartered	6	4	4.70
GCS1	16/09/09	53°48.47'N	7°31.85'E	Chartered	8	3	4.09
GW 2	9/09/09	53°47.13'N	8°8.25'E	Chartered	15	6	3.19
GW 3	10/09/09	53°43.08'N	8°23.12'E	Chartered	33	7	1.67
GW 4	10/09/09	53°49.72'N	8°18.03'E	Chartered	16	5	3.19
GW 5	30/09/09	53°57.45'N	8°32.85'E	Chartered	39	7	1.46
GW 6	29/09/09	53°51.43'N	8°49.97'E	Chartered	61	7	0.98
GCS2	15/09/09	54°4.27'N	8°31.60'E	Chartered	32	4	1.86
GW 7	16/09/09	54°5.45'N	8°38.70'E	Chartered	28	6	1.97
GW 8	14/09/09	54°8.32'N	8°49.27'E	Chartered	24	5	2.31
GW 9	24/09/09	54°23.22'N	8°33.43'E	Chartered	17	3	3.35
GW10	24/09/09	54°27.12'N	8°42.58'E	Chartered	14	3	3.94
GW11	23/09/09	54°34.60'N	8°24.78'E	Chartered	8	3	4.09
GW12	8/10/09	55°0.50'N	8°21.00'E	Isis	6	2	8.37
DCS1	28/09/09	55°13.33'N	8°17.25'E	Chartered	4	1	13.39
DCS2	10/11/09	55°21.33'N	8°20.58'E	Chartered	9	2	4.09
DCS3	28/09/09	55°25.10'N	8°14.35'E	Chartered	12	2	4.78
DCS4	28/09/09	55°31.53'N	8°5.65'E	Chartered	9	3	5.58
DCS5	28/09/09	55°34.00'N	8°0.50'E	Chartered	9	2	4.09
WS 1	29/09/09	51°25.46'N	3°21.50'E	Belgica	46	17	1.06
WS 2	14/10/09	51°24.00'N	3°31.75'E	Zeeleeuw	50	14	1.05
WS 3	14/10/09	51°25.87'N	3°40.21'E	Zeeleeuw	73	17	0.74
WS 4	14/10/09	51°22.11'N	3°43.92'E	Zeeleeuw	107	20	0.53
WS 5	15/10/09	51°20.85'N	3°49.86'E	Zeeleeuw	124	20	0.47
WS 6	15/10/09	51°21.42'N	3°53.13'E	Zeeleeuw	122	22	0.47
WS 7	14/10/09	51°25.67'N	4°0.71'E	Zeeleeuw	85	21	0.63
WS 8	15/10/09	51°22.32'N	4°5.33'E	Zeeleeuw	107	24	0.51
WS 9	14/10/09	51°22.62'N	4°8.99'E	Zeeleeuw	91	23	0.59

4.3.2 Detailed spatial distribution of OT accumulation in common shrimp in the Westerschelde estuary

In Westerschelde estuary shrimp, TBT concentration increases gradually from 50 µg kg^{-1} DW near Vlissingen (WS2) to 124 µg kg^{-1} DW upstream of Terneuzen (WS5) (Fig. 4.1). Further upstream near Hansweert (WS7) the concentration drops to 85 µg kg^{-1} DW, and tends to rise again further upstream (107 µg kg-^{1} at WS8). A similar spatial pattern in OT concentration in sediment is observed (Fig. 4.3.2A) (Monteyne & Roose, data courtesy of BMDC). The lower OT concentrations in shrimp and sediment at WS7 is related to the strong currents associated with the narrow cross-section of the estuary near Hansweert, which prevent the local deposition of finer, $CaCO_3$ rich sediments (Fig. 4.2B). Sediment data also reveal TBT does not tend to accumulate like the organic pollutant benzo-[a]-pyrene (fig 4.2.E) but rather like mercury (Fig. 4.2C), which is in line with the metal-type accumulation of TBT observed in biota (Tanabe 1999). For TPhT, a similar trend was clear in the sediment but less clear in shrimp. TPhT concentrations in shrimp increase gradually from 14 to 24 µg kg^{-1} DW between Vlissingen and Saeftinghe. In sediment, TPhT concentration increases from 2 to 7.5 µg kg^{-1} DW, with an intermediary minimum at WS7.

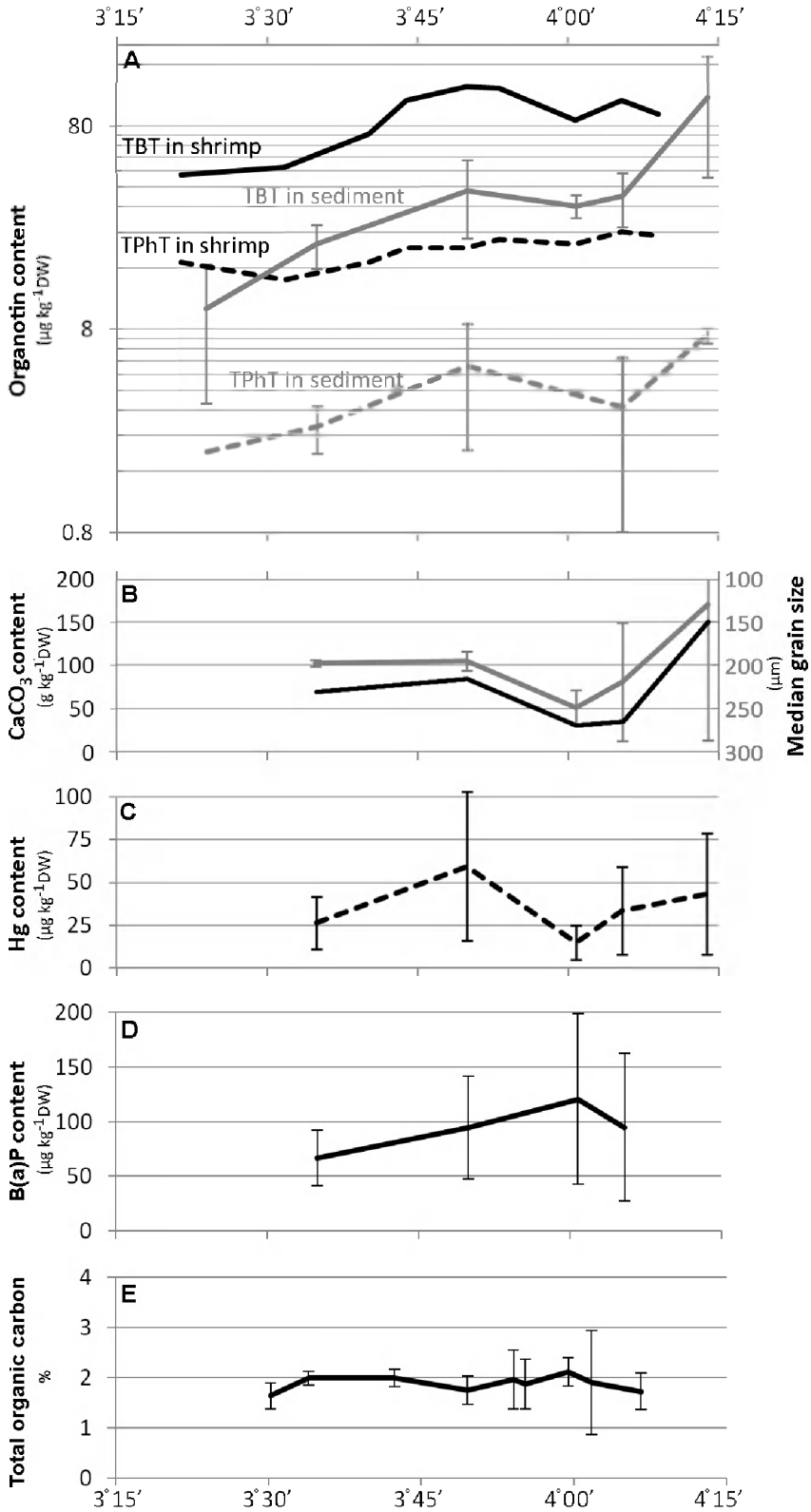

Fig. 4.2. (**A**) TBT and TPhT concentrations (Y-axis, in µg kg^{-1} DW) in shrimp meat and in the <63 µm sediment fraction along the longitudinal gradient in the Westerschelde estuary (X-axis).(**B**) $CaCO_3$ content (Y-axis, in g kg^{-1} DW) and the inverse median grain size (Y'-axis, inverted, in µm) of the sediment. (**C**) and (**D**) <63 µm sediment mercury and benzo-[a]-pyrene content (Y-axis, in µg kg^{-1} DW), respectively. (**E**) Total organic carbon content of the <63 µm sediment fraction.

4.3.3 Temporal variation of TBT in shrimp and sediment and BSAF in the Westerschelde estuary

Based on our measurements at sampling station BCS3 (29 µg kg^{-1} DW) and the findings of Willemsen et al. (2004) near BCS3 (368 and 259 µg kg^{-1} DW), the TBT concentration in shrimp has decreased 8-fold in 10 years. Several observations indicate that the associated BSAFs should be based on the TBT concentrations measured in sediment instead of in suspended solids. TBT content in shrimp exhibits a comparable spatial trend as in sediment (Fig. 4.2.A). The sediment in the Westerschelde exhibits a clear spatial (Fig. 4.2.A) and temporal trend in TBT content (Fig. 4.3).

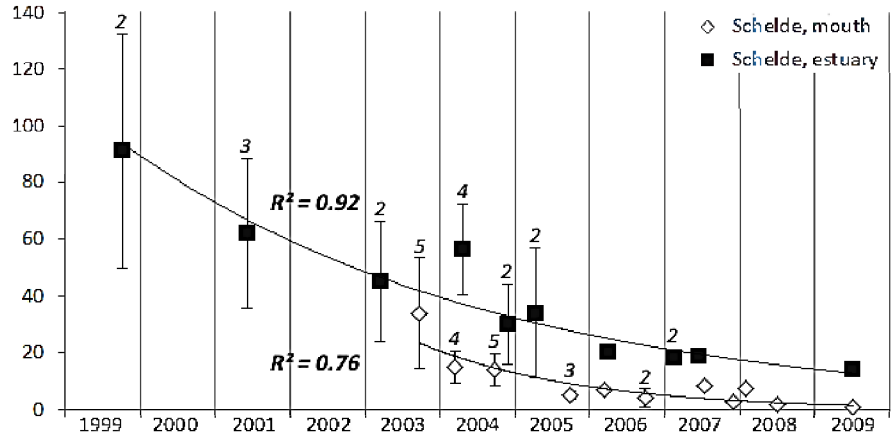

Fig. 4.3. Temporal trend of <63 µm sediment TBT concentrations (Y-axis, in µg kg^{-1} DW) in the Westerschelde lower estuary (Terneuzen–Vlissingen, between WS2-WS6) and mouth (Southern Vlakte van de Raan, roughly near BCS3-WS1) during 1999-2009 (X-axis). Concentrations from different sampling locations (see Fig.4) were pooled for the lower estuary and mouth. Means, standard deviations and sample sizes are presented for each sampling date. The single measurement (<LoQ) in the Westerschelde mouth in the summer of 2009 is depicted as 1 µg kg^{-1} DW.

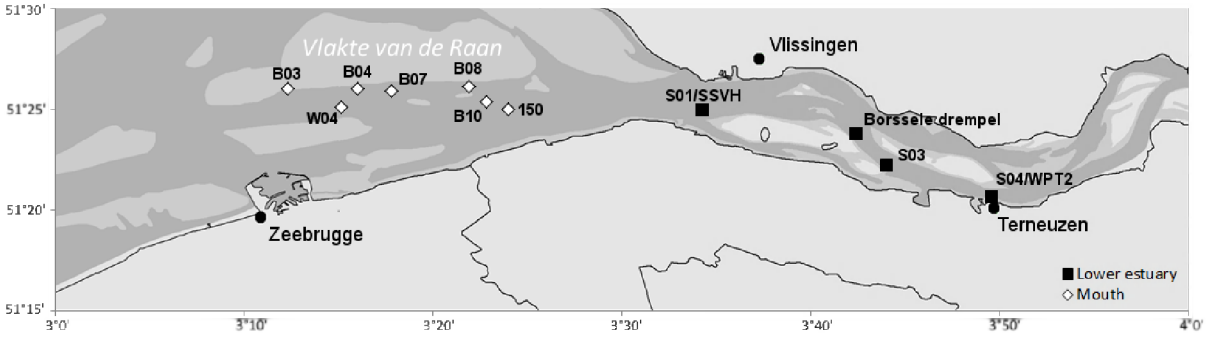

Fig. 4.4. Geographical situation of the sample locations used in Fig.4.3 and equations 4.1 and 4.2. The concentrations at the locations marked with a white diamond and black square were used for the Schelde mouth and estuary, respectively.

The exponential regression associated with the temporal trend (equation 4.1) show a good fit ($R^2 = 0.93$).

Equations 4.1 and 4.2. Exponential regression formula of the temporal trend in TBT sediment (<63 µm fraction) concentration in the Westerschelde lower estuary (4.1) and mouth (4.2).

$$TBT\ conc.\ (in\ \mu g\ kg^{-1}\ DW\ sediment) = 92.9934 \times e^{-0.000556417 \times (\text{date} - 06/10/1999, \text{in days})} \quad \text{(Eq. 4.1)}$$

$$TBT\ conc.\ (in\ \mu g\ kg^{-1}\ DW\ sediment) = 23.4562 \times e^{-0.00127852 \times (\text{date} - 24/09/2003, \text{in days})} \quad \text{(Eq. 4.2)}$$

The regression formula was used to extrapolate the decreasing TBT concentration in the lower Westerschelde estuary to October 2009, the period of shrimp sampling, and to subsequently derive the related BSAFs. Based on the average TBT content in shrimp muscle (101.3 ± 19.1 µg kg^{-1} DW) at stations WS3-WS9, the TBT content in the <63 µm fraction in the lower Schelde estuary in September 2009 deduced from equation 4.1 (12.3 µg kg^{-1} DW), an organic carbon normalized BSAF of 0.15687 ± 0.03029 (in µg kg^{-1} tissue DW / µg kg^{-1} organic carbon DW) is derived for shrimp in the Schelde estuary. An averaged organic carbon content of 1.88 ± 0.15% (n = 49, at 9 sampling stations) was applied, as the spatial variation in organic carbon content in the <63µm sediment fraction of the Westerschelde estuary content was small during 1993-2007 (Fig. 4.2.E). For reasons of comparison with other marine biota, Veltman et al. (2006) derived a *C. crangon* BSAF of 1.4 based on the TBT concentration in DW suspended solids, which was the highest BSAF observed in various marine invertebrates and fish species. These findings were in line with these of Takahashi et al. (1999), who found a limited metabolization capacity of TBT in Caprellidae (Crustacea; Malacostraca) compared to other marine species.

4.3.4 Consumer health risk

DW to FW ratio of peeled shrimp was determined at 22.4 ± 1.1% (n = 46). According to the TDI set by EFSA, a 60 kg person is allowed to consume 5.22 ± 2.86 kg on a daily basis (n = 35; Table 4.2) of FW shrimp meat from commercially exploited shrimp areas (excluding the inner Ems-Dollard estuary, Oosterschelde and Westerschelde). This renders common shrimp a healthy seafood product, in contrast to less than a decade ago. In 2003, the daily consumption of 169 g of peeled shrimp was sufficient to exceed the TDI for TBT alone. According to Avia et al. (2011), the average daily consumption of *C. crangon* meat in

Germany and Belgium is estimated at 0.063 g and 1.4 g per person, respectively. These numbers should be handled with care, as a large part of especially the German population are virtually non-consumers, but it can be concluded that even people consuming common shrimp on a daily basis can do so with no health risks with respect to OT intake.

Chapter 5

Disruption of downstream gene expression by organotin

The research performed in this chapter was achieved in cooperation with Prof. Dr. Wim de Coen, Prof. Dr. Dries Knapen, Dr. An Hagenaars, and Drs. Lucia Vergauwen of the laboratory for System Ecophysiological and Ecotoxicological Research (SPHERE lab) at Antwerp University.

.

5.1 Introduction

Although the *in vitro* assay clearly showed disruption of NR functioning at subtoxic TBT concentrations in chapter 3, it remains tedious to link these molecular observations with the observed population decline and reduced percentage of gravid shrimp (Siegel et al. 2008), due to the intrinsic complex nature of the shrimp endocrine system and the limited fundamental insights in these pathways. Most importantly, disruption of NR functioning does not necessarily translate into observable endocrine disruption in the actual organism. Moreover, there are invariably multiple potential stressors in the natural environment, further hampering the examination into the causative MOA of the observed effects in the natural population. Even under stringent laboratory conditions, end-point effects may be of an obscure, but nocif nature. Subtle changes in endocrine functioning may have delayed, but detrimental consequences that become evident later in adult life, or even in a subsequent generation. Therefore, long-term multi-generation exposures are preferred to verify EDC effects at the organism and population level, but such tests are practically unfeasible due to long exposure times and poor survival of shrimp under laboratory conditions. An alternative approach is to look at the EDC induced changes in normal patterns of gene expression, either as a direct or as a compensatory response. The relatively new research field of ecotoxicogenomics, which combines classical toxicity testing with high-throughput genomic techniques (i.e. microarray) and related bioinformatics, has the potential to unravel the complex gene expression cascades affected by TBT.

In this chapter, the effects of TBT on shrimp gene transcription is assessed by constructing a shrimp specific DNA microarray, which allows us to compare the relative expression of multiple genes in two different samples (e.g. exposed shrimps versus a reference sample) in one analysis. A DNA microarray is a specially treated glass microscope slide on which many small, known DNA ‘spots’ are linked to the surface in a well-organized pattern (i.e. replicate spots, control spots,…). The mRNA from both samples is then extracted, converted into two cDNA samples which each receive a different fluorescent label (cyanine 3 and 5). Then, both samples (exposed and reference) are combined on a single microarray slide, where the differentially labelled cDNAs will compete for hybridization with the available DNA spots of matching sequence. The resulting image of fluorescent spots is visualized in a confocal scanner and digitized for quantitative analysis, and thus indicates the relative abundance of each spotted DNA gene fragment in the mRNA samples.

To date, no full genomic DNA sequence or large scale transcript datasets are available for *C. crangon*. A shrimp EST library enriched with sex-associated gene fragments was constructed through SSH-PCR to be able to build the custom microarray. In SSH-PCR, hybridization and subsequent suppression of common gene fragments within both mRNA samples (i.e. male and female) leads to a 10 to 100 fold enrichment of differentially expressed mRNAs.

5.2 Material and methods

5.2.1 Suppressive subtraction hybridization – PCR (SSH-PCR)

RNA was extracted using TriReagent® (Sigma-Aldrich NV, Bornem, Belgium), according to the manufacturer's protocol, from five large male (56-63 mm L_T) and five female (78-86 mm L_T) shrimp. A DNase treatment was performed with 1U RNAse-free DNase and 1U RNAse inhibitor per 30 µl sample (Fermentas, St. Leon-Rot, Germany). The quality and quantity of the extracted RNA was examined by gel electrophoresis and spectrophotometry using a Nanodrop™ ND-1000 (Thermo Fisher Scientific BVBA, Asse, Belgium). The five male and five female RNA samples were brought to a common concentration of 200 ng μl^{-1} and pooled per sex to two 1 µg RNA samples. cDNA was prepared using a SMART approach (Zhu et al. 2001). SMART Oligo II oligonucleotide and CDS primer (Table 5.1) were used for first-strand cDNA synthesis. In both cases, first-strand cDNA synthesis was started from 0.5 µg RNA in a total reaction volume 10 µl. 1 µl of 5-times diluted first-strand cDNA was then used for PCR amplification with SMART PCR primer. 19 PCR cycles (each cycle included 95°C for 10 s; 66°C for 20 s; 72°C for 3 min) were performed. SMART-amplified cDNA samples were further digested by *Rsa* I endonuclease.

Table 5.1. Oligonucleotides used during SSH-PCR

SMART Oligo II	5'-AAGCAGTGGTATCAACGCAGAGTACGCrGrGrG-3'
CDS primer	5'-AAGCAGTGGTATCAACGCAGAGTAC-d(T)30-3'
SMART PCR primer	5'-AAGCAGTGGTATCAACGCAGAGT-3'
Adapter 1	5'-CTAATACGACTCACTATAGGGCTCGAGCGGCCGCCCGGGCAGGT-3' 3'-GGCCCGTCCA-5'
PCR primer 1	5'-CTAATACGACTCACTATAGGGC-3'
Nested primer 1	5'-TCGAGCGGCCGCCCGGGCAGGT-3'
Adapter 2R	5'-CTAATACGACTCACTATAGGGCAGCGTGGTCGCGGCCGAGGT-3' 3'-GCCGGCTCCA-5'
Nested primer 2R	5'-AGCGTGGTCGCGGCCGAGGT-3'

Subtractive hybridization was performed in both directions (male vs. female and female vs. male) as described in Diatchenko et al. (1996, 1999). A graphical representation of the SSH-PCR method is given in Fig. 5.1.Briefly, the following procedures were performed: for each direction, two tester populations were created by ligation of different suppression adapters (Adapters 1 and 2R). These tester populations were mixed with 30X driver excess (driver cDNA had no adapters) in two separate tubes, denatured and allowed to renature. After first hybridization, these two samples were mixed and hybridized together. Subtracted cDNA was then amplified by primary PCR (25 cycles with PCR primer 1) and secondary PCR (10 cycles with nested primers 1 and 2R).

5.2.2 Sex specific shrimp cDNA library

cDNA fragments of both enriched libraries were ligated into the pGEM-T vector (Promega, Madison, WI) and transformed competent JM 109 *E. coli* cells (Promega, Madison, WI), according to the manufacturer's protocols. Insert containing clones were isolated from the LB-agar plates using blue/white screening (Messing et al. 1977), and grown overnight in 150µl liquid LB medium in 96-well microtiter plates. Lysates, replicates and glycerol stocks were made. Clone inserts were amplified from the lysates with vector-specific primers (SP6 and T7 primer). PCR products were purified enzymatically with exonuclease I and shrimp alkaline phosphatase according to Werle et al. (1994). Specificity of amplification was checked with agarose gel electrophoresis, and PCR yield was quantified using a Nanodrop™ ND-1000 microspectrophotometer. The PCR products were sequenced by the VIB Genetic Service Facility (http://www.vibgeneticservicefacility.be). Expressed sequence tag (EST) sequences were extracted from the raw data by trimming vector and primer sequences from the insert sequences and removing any sequences of poor quality (<50 bp). The Codoncode sequence assembly program was applied on the combined EST data of both cDNA libraries to obtain a maximal of contiguous consensus sequences ('contigs'). The obtained contig and singlet sequences were identified based on their similarity to sequences in the National Center for Biotechnology Information (NCBI) database as determined by the Basic Local Alignment Search Tool (BLAST) (http://www.ncbi.nlm.nih.gov/BLAST). The obtained sequences were compared with DNA and protein databases using BLASTN and BLASTX analysis software, respectively. Functional annotation with Gene ontology (GO) terms was performed using the bioinformatics tool 'BLAST2GO' (www.blast2go.de).

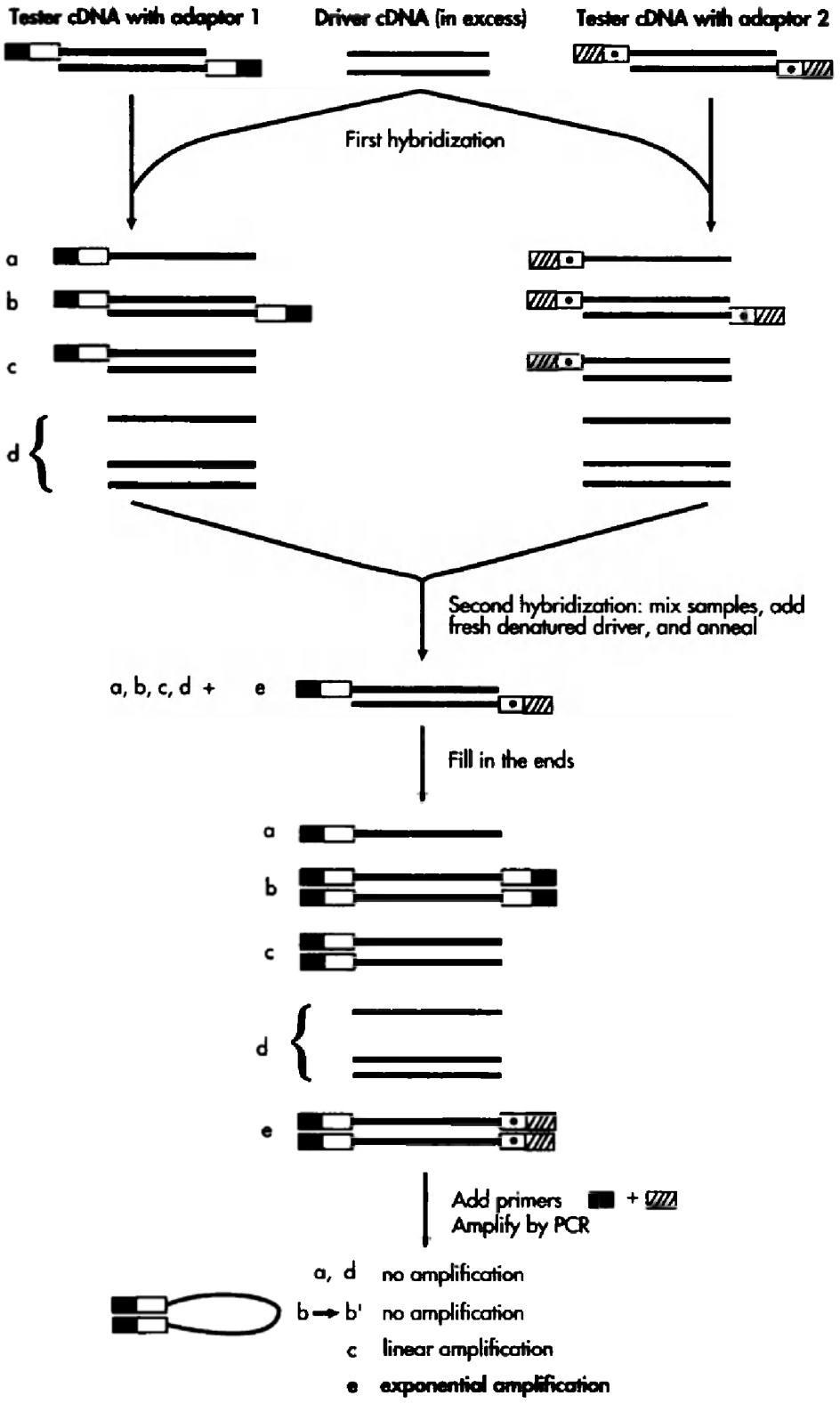

Fig. 5.1. Scheme of the SSH method. Solid lines represent the *Rsa*I digested tester or driver cDNA. Solid boxes represent the outer part of adapter 1 and corresponding PCR primer P1. Shaded boxes represent the outer part of adapter 2 and corresponding PCR primer P2. Clear boxes represent the inner part of the adapters and corresponding nested PCR primers NP1 and NP2. Note that after filling in the recessed 3' ends with DNA polymerase, types a, b, and c molecules having adapter 2 are also present but are not shown (reproduced from Diatchenko et al. 1996)

5.2.3 Microarray construction

A total of 604 unique EST fragments were chosen from both cDNA libraries (Fig. 4.1), amended with CrcEcR, CrcRXR, β-actin, GAPDH and 18S rRNA cDNA fragments, for microarray construction. Before spotting, PCR products were purified using Montage PCR96 Plates (Millipore, Billerica, MA, USA) and transferred to 384-well V-bottomed plates (Genetix, Hampshire, UK) in 50% DMSO at a concentration of approximately 67.5 ng l^{-1}. A Qarray Mini Robot (Genetix, Hampshire, UK) with an 8- solid pin-head was used to spot 9 blocks in quadruplicate fields on aminosilane coated Nexterion® microarray slides (Schott AG, Mainz, Germany). Each replicate field also contained artificial control genes 8,9, 10 from the SpotReport Alien cDNA Array Validation System (Stratagene, La Jolla, CA) (labelling and hybridization efficiency, sensitivity, intra-array variability), negative control spots human β actin and salmon sperm DNA (non-specific hybridization); and a SSC buffer spot (pin carryover). After spotting, the arrays were moistened over a hot water bath, snap-dried and the cDNA was covalently cross linked to the slide using 3×10^5 J ultraviolet radiation (UV Stratalinker 2400, Stratagene, La Jolla, CA, USA).

5.2.4 Chemicals, exposure, and RNA preparation

The TBT concentrations in *C. crangon* observed by Janssen et al. (2007) in the period 2002-2006 ranged between 350-1,700 µg kg^{-1} DW. However, no BCF for TBT in *C. crangon* is currently available to estimate the needed exposure level to obtain these tissue concentrations. BCFs for other crustaceans are available, but vary considerably between species. Regarding the close relationship of shrimp with the sediment, one of the main routes of exposure of shrimp to TBT is through sediment pore water. In estuarine sediments, filtered pore water concentrations of TBT up to 2.35 µg l^{-1} have been observed (Burton et al. 2004). As this level more or less corresponds to the LC_1 (1.3 µg l^{-1}) observed in the 96 hr acute exposure of shrimp to TBT in chapter 3 (Fig. 3.4.), the highest exposure concentration for the subtoxic exposure was set at 2 µg l^{-1}. The static-renewal exposure experiment consisted of four exposure concentrations (i.e. 2,000, 200, 20 and 2 ng l^{-1} TBTO) and a control, each in four replicate 40L glass tanks and 10 shrimp per replicate. Adult shrimp were bought from North Sea Life (www.northsealife.be). 200 female shrimp from 55-60 mm L_T were selected and acclimatized in the exposure facility during 24 hours. In each replicate, shrimp were separated by vertical, perforated PET-G plates to avoid social stress (e.g. cannibalism). The shrimp were fed 25 g *Calanus finmarchicus* ("Red plankton", Ocean Nutrition Europe NV, Essen, Belgium) *ad libitum* in the late afternoon on a daily basis. A 18L:6D light regime (28.7 ± 13.7

lux) was applied, including an artificial sunrise and sunset of 30 min each. Seawater was directly pumped from the nearby beach in Oostende, filtered through a 10µm carbon filter, continuously aerated and kept at 15°C. pH, temperature, $\%O_2$ and salinity were monitored in the control replicates on a daily basis and just before and after water renewal. Debris (i.e. unconsumed food, faeces, shedded exoskeletons) was removed and 80% of the tank volumes was renewed each 48 hours through siphoning. Prior to each renewal, a stock solution of 120 µg l^{-1} TBTO was prepared in a disposable polypropylene measuring jug. Effluent water was filtered over a double 10µm carbon filter (>99.8% of OTs were captured) prior to disposal. Because of the poor laboratory survival of shrimp, the exposure experiment was sustained as long as the average survival of the control replicates was higher than 70%.

From each replicate, cephalothoraxes were collected in 7.5 volumes of RNAlater® (Qiagen) and placed at 4°C overnight for RNA extraction. Abdomens were pooled per concentration (including the control) to obtain a sufficient amount of tissue for OT determination. Subsequent homogenization, sample extraction, clean-up and gas chromatographic analysis were described in 4.2.2-4.2.5.

5.2.5 Preparation of cDNA, labelling and microarray hybridization

The pooled cephalothorax samples were homogenized with mortar and pestle in liquid nitrogen and stored at -80 °C. RNA from 100 mg from each pooled replicate was extracted with TriReagent® (Sigma-Aldrich), followed by a DNase treatment with 1U RNAse-free DNase and 1U RNAse inhibitor per 30 µl sample (Fermentas, St. Leon-Rot, Germany). RNA integrity was controlled by denaturing formaldehyde-agarose gel electrophoresis. RNA concentration and purity were analysed on a Nanodrop 2000 spectrophotometer (Thermo-Scientific). From each RNA sample, 5µg of RNA was diluted in 14.5 µl DEPC-treated water. 4µg RNA from each sample was pooled in 80µl DEPC-treated water to obtain the reference sample needed for the reference design microarray experiment. For this design, two replicates from each treatment will be labelled with Cy3 and two with Cy5, which will be competitively hybridized with Cy5 and Cy3 labelled reference sample on a total of 20 spotted slides, respectively. Single strand cDNA from each sample (including references) was prepared in 30 µl volumes with final concentrations of 0.2 µg μl^{-1} random hexamer primers (Invitrogen); 15 µmol dATP, dCTP and cGTP and 9 µmol dTTP from the Fermentas dNTP pack; 6 µmol aminoallyl labelled dUTP (Gentaur BVBA, Kampenhout Belgium); 0.3 µmol DDT and 400U Superscript II Reverse Transcriptase (Invitrogen). cDNA samples destined to be labelled with

Cy3 were spiked with 1 ng mRNA spike 8, 0.5 ng mRNA spike 9 and 0.1 ng mRNA spike 1 from the SpotReport Alien cDNA Array Validation System (Stratagene). cDNA samples destined to be labelled with Cy5 were spiked with 0.1 ng mRNA spike 8, 0.5 ng mRNA spike 9 and 1 ng mRNA spike 10. Remaining RNA was hydrolysed by heating (65°C, 15 min) and adding 20 µl of 0.5 M NaOH and 0.25 M EDTA. These aminoallyl labelled cDNA samples were purified with the QIAquick PCR purification Kit (Qiagen). The columns were washed with potassium phosphate wash buffer (4.75 mM K_2HPO_4, 0.25 mM KH_2PO_4, pH 8.6) in 80% ethanol and eluted with a total of 60 µl potassium phosphate elution buffer (3.8 mM K_2HPO_4, 0.2 mM KH_2PO_4, pH 8.6). The samples were dried in a vacuum centrifuge at 30°C during 1hr and labelled with Amersham CyDye Cy3 or Cy5 mono N-hydroxysuccinimidyl esters (GE Life Sciences) in 9 µl 50 mM Na_2CO_3-50% DMSO (pH 9) during 1.5 hrs in the dark at room temperature. Excess dyes were removed from these probes by purification with the QIAquick PCR Purification Kit and eluted with a total of 60 µl kit elution buffer. Labelling efficiency was determined with a Nanodrop 1000 spectrophotometer (Thermo-Scientific) at 550nm (Cy3) and 650nm (Cy5). The threshold for optimal dye incorporation was 150 pmol, and a frequency of incorporation of 20–50% was considered appropriate for hybridizations. From each labelled sample a subsample of 100 pmol dye was dried to completion in a vacuum centrifuge in the dark at room temperature. Prior to hybridization, the spotted microarray slides were pretreated with hybridisation buffer (50% formamide, 5 times standard sodium citrate buffer (SSC, 8.765 g l^{-1} NaCl and 4.41 g l^{-1} sodium citrate, pH7), 0.1 % SDS and 0.1 mg ml^{-1} BSA) during 1hr at 42 °C, washed with ultrapure water (1 min) and isopropanol (1 min) and finally dried at 1,200 rpm during 5 min. Per hybridization, the Cy3 and Cy5 labelled probes were each resuspended in 24 µl hybridization buffer including 0.1 mg ml^{-1} sheared salmon sperm DNA (Invitrogen). The resuspended probes were combined, mixed and denatured at 95°C during 5 min prior to application on the spotted array. Arrays were covered with cleaned 25 × 75 × 0.1mm coverslips (Schott AG) and incubated in a hybridization chamber (Genetix, Hampshire, UK) in a hybridization oven at 42°C overnight (16 hours). Hybridized arrays were washed in Coplin jars in a series of wash buffers, while being gently stirred in darkened conditions: 5 min in 2 times SSC, 0.1% SDS at 42°C; 20 min in 0.1 times SSC, 0.1% SDS at room temperature; 5 min in 0.1 times SSC at room temperature; 15 s in 0.01 times SSC at room temperature; 1 min in ultrapure water at room temperature; and finally 1 min in isopropanol at room temperature. Washed arrays were immediately dried at 1,200 rpm during 5 min.

5.2.6 Data acquisition, preprocessing and detection of differential expression

Hybridized and washed slides were scanned at 532 and 635 nm using the Genepix Personal 4100A confocal scanner (Axon Instruments, Union City, CA), which was placed in a Nozone cabinet (SciGene) to avoid ozone depletion of the fluorescent labels. The photomultiplier tube voltage was automatically adjusted for each slide to obtain an overall ratio close to one. Scanned images were analysed using Genepix pro 6.1 software (Axon Instruments) for spot identification and quantification of the fluorescent signal intensities. The raw datasets were imported in R Bioconductor (Gentleman et al. 2004). The Bioconductor package "arrayQualityMetrics" (Kauffmann et al. 2009) was used to assess hybridisation quality (Kauffmann et al. 2009). In the MA-plot of the raw data, outlier detection of microarray replicates was performed by computing Hoeffding's statistic D_a on the joint distribution of the average spot intensity ($A=1/2(\log_2(I_1)+\log_2(I_2))$ and the red/green intensity ratio ($M = \log_2(I_1) - \log_2(I_2)$) for each array. Subsequently, the following method was applied to detect outlier spots on the arrays. If the intensity of a spot is not higher than the local background intensity plus two standard deviations of the local backgrounds on the entire array, the spot receives a weight 0 on that particular array. Only spots receiving weight 0 on all arrays were excluded from the analysis. All remaining spots were included in the analysis. Raw data were background corrected, normalized and analysed through linear modelling in the Bioconductor package Limma (Smyth 2004). Because the quality control showed that there was high inter-array variation, we chose to perform vsn (Huber et al, 2002) which is a between-array normalisation instead of only normalising within-arrays (e.g. loess). Spots were individually background corrected by subtracting background from the foreground signal. From each array, the best three spot replicates (i.e. the best red and green signal intensities after background correction but before normalisation.) were selected based on outlier detection. For each unique reporter identity, the spot which deviated the most from the mean of the spot replicates was deleted and this process was iterated until a maximum of three replicate spots remained. Differential gene expression (log-fold changes) was statistically analysed through moderated *t*-tests. Differentially expressed genes were selected based on both of the following criteria: log2 fold change logFC > 0.75 and uncorrected $p < 0.05$. *P*-values were adjusted for multiple testing with the Benjamini & Hochberg (1995) "fdr" approach for control of the false discovery rate.

5.3 Results

5.3.1 SSH library

A total of 1,536 random cDNA clones were sequenced from both libraries, yielding 500 female and 606 male redundant EST fragments with an average sequence length of 359 ± 187 bp. Female specific gene fragments included fragments from various cuticular proteins (58 fragments, especially from endocuticle structural glycoprotein bd-1), vitellogenins (41), c-type lectins (7), sptzle 2-like protein (4), cysteine dioxygenase (4), and ATP synthase f0 subunit 6 (4). Male specific gene fragments included fragments from cathepsins (30, especially cathepsin l fragments), carcinin (15), a gene similar to a hypothetical protein from the insect *Thermobia domestica* (14), cytochrome c oxidase subunits (8), crustin-p (6), male reproductive related proteins (4), and legumain precursor (4).

The ESTs were assembled using Codoncode Aligner to group the redundant ESTs into overlapping contigs. Clustering and assembly resulted in 161 contigs and 368 singlets, thus yielding 529 nonredundant ESTs. The redundancy of the library was 52.17%. BLASTX searches identified 209 nonredundant ESTs with significant BLAST hits (*E*-value < 1E-04) and 320 novel *C. crangon* ESTs. Gene Ontology (GO) analysis allowed the functional annotation of 188 nonredundant ESTs to a total of 400 GO-terms (934 GO-hits), with an average of five and a maximum of 33 associated GO terms per sequence. In order to visualise the multilevel GO terms represented by the ESTs, they were split over the 3 main categories [Biological Process (BP), Molecular Function (MF), and cellular localization (CC)) (Fig. 5.2). In the BP category the majority of second level GO terms were associated with either metabolic (22%) or cellular processes (18%), in the MF category the majority of third level GO terms were associated with either hydrolase activity (15%), protein binding (13%) or nucleotide binding processes (12%) and in the CC category most fifth level GO terms were associated either with the cytoplasm (27%), intracellular organelle (26%) or cytoplasmic part (20%). Also of note in the BP category were terms associated with biological regulation, developmental process, and reproduction. In the MF category a number of sequences were found to be associated with nucleic acid binding and structural constituents of the cuticle. In the CC category, several sequences were associated with the proton-transporting ATPase and ATPsynthase complexes.

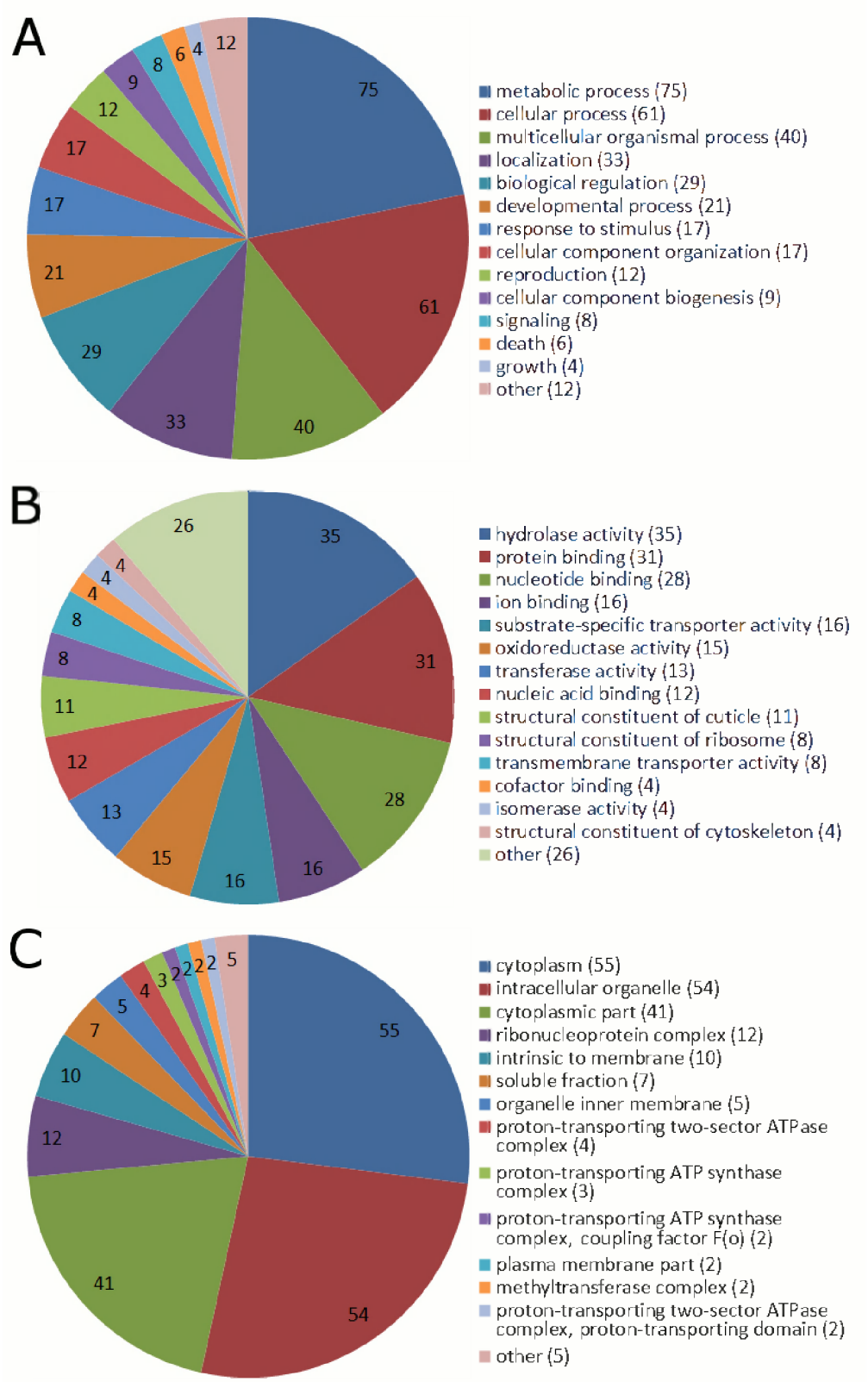

Fig. 5.2. Pie chart representations of the distribution of GO terms associated with the assembled EST library (male and female cDNA libraries combined into 161 contigs and 368 singlets) across the three major GO categories: (**A**) second level biological process GO terms, (**B**) third level molecular function GO terms, and (**C**) fifth level cellular component GO terms. Number in brackets represents the number of ESTs associated with each GO category. Keep in mind that one EST can be assigned to more than one GO terms.

5.3.2 Exposure experiment

The experiment lasted 6 days, as the survival in the control replicates neared 70%. During the experiment, pH was 7.29 ± 0.11, salinity 36.82 ± 0.11 ppt, oxygen saturation 89.60 ± 2.63 %, and water temperature 16.46 ± 0.50 °C (n = 9). Mortality and moulting rates are given in table 5.2. Mortality between all replicate treatments was high, ranging from 0 to 40%. Surprisingly, consistently higher mortality rates were observed in the control replicates, and were significantly lower than the mortalities observed in the 2 ng l^{-1} (p = 0.0255) and 200 ng l^{-1} (p = 0.0036) treatments. Due to the high mortality in the control replicates, the exposure was terminated after 138 hrs. No significant differences were observed in moulting. Contradictory, mortality at ecdysis was only observed in the control treatments (33% of the moulted control shrimp, p = 0.024).

Table 5.2. Mortality and moulting ratings after 138 hrs of TBTO exposure

	Mortality	Moulting
Control	32.5 ± 5.0%	22.5 ± 18.9%
2 ng l^{-1}	12.5 ± 12.6%	22.5 ± 15.0%
20 ng l^{-1}	20.0 ± 14.1%	17.5 ± 9.6%
200 ng l^{-1}	7.5 ± 9.6%	25 ± 10.0%
2 µg l^{-1}	17.5 ± 17.1%	10.0 ± 8.2%

5.3.3 Microarray analysis

Based on the nonredundant EST library, 604 inserts were selected from the male and female specific cDNA libraries to be analysed on altered gene expression after subtoxic exposure to TBT. Raw data of the four control replicates (0A-0D) and the four replicates of the highest exposure (i.e. 2 µg l^{-1}; 4A-4D) were analysed for differential gene expression.

Table 5.3. Overview of the analysed microarray hybridisations. The value of Hoeffding's statistic D_a (last column) is a statistical measure representing the interarray variability in spot intensities and red/green intensity ratios. Arrays with $D_a \leq 0.15$ can be regarded as outliers.

Array	Cy3	Cy5	*Da*
1	0A	Reference	0.13
2	0B	Reference	0.17
3	Reference	0C	0.14
4	Reference	0D	0.08
5	4A	Reference	0.34
6	4B	Reference	0.17
7	Reference	4C	0.37
8	Reference	4D	0.08

Unfiltered pooled correlation between spot replicates across the arrays was estimated at R^2= 0.41, suggesting that replicate spots shared less than a quarter of their variability due to local artefacts on the hybridized microarray slides. A total of 653 out of 3,690 spots were deleted as they did not pass the QC (i.e. they received a weight 0 on all arrays). 600 distinct genes were left in the analysis, all represented by three spot replicates on each microarray. The filtered pooled correlation between spot replicates across the arrays after outlier removal was R^2= 0.76. 43 genes had a p <0.05, meaning a significant difference in gene expression between control and exposure treatments (table 5.4). 10 of these gene fragments also passed the |logFC|>0.75 criterion for differential expression, meaning their transcript level after TBT exposure was more than 0.595 times down regulated or 1.68 times up regulated. Six genes were significantly up regulated, i.e. vitellogenin (Vtg), an endocuticle structural glycoprotein, actin 5c, and three unknown gene fragments. Four gene fragments were significantly down regulated, i.e. fragments from myosin heavy chain, arthrodial cuticle protein, sarcoplasmatic calcium-binding protein and an unidentified gene fragment. The gene fragments exhibiting a significant difference in expression level between exposed and control treatments, but not passing the logFC criterion, encompassed several cuticular proteins (chitinase, cuticle protein cb6, and cuticle proprotein), myosin and actin chains, adhesin wi1-like, hemocyanin, ribosomal protein, sodium and chloride dependent GABA transporter 1, and a peptidyl-prolyl cis-trans isomerase-like protein (PPIase-like).

5.4 Discussion

In order to expand upon the transcriptomic coverage of *C. crangon*, we generated transcript data representing the largest collection of *C. crangon* ESTs to date. As *C. crangon* is not an established model with a deep molecular-based research history, this EST library may contribute to comparative genomics for the discovery of new genes, alleles and polymorphisms. While a great deal of attention has been paid to developing certain insect models, much less attention has been paid on crustacean ESTs. 5,174,553 insect and 879,072 crustacean EST sequences are currently available (http://www.ncbi.nlm.nih.gov). Of the 429,449 Decapod ESTs, 213,063 ESTs belong to Pleocyemate species, of which the majority from Anomuran and Brachyuran crabs (166,389 ESTs from six species). 13,064 ESTs from the non crab Pleocyemate species originate from three Caridean shrimp species: 12,885 ESTs from *Macrobrachium rosenbergii*, 132 ESTs from *Neocaridina denticulata*, and 47 ESTs from *Palaemonetes varians*. The *C. crangon* EST library (529 nonredundant sequences)

obtained during this study are the first ESTs available from representatives of the Caridean superfamily Crangonoidea. While most EST libraries are constructed for creating a large catalogue of genes, we constructed our library for capturing ('gene fishing') a number of potential candidate expressed genes that may be of future importance in ecotoxicological studies. With the creation of a custom *C. crangon* microarray using this EST library, a first screening of gene expression changes in response to environmental TBT levels in crustaceans was performed. Female shrimp were exposed subchronically to subtoxic TBTO concentrations, ranging from 2 ng l^{-1} to 2 µg l^{-1} TBTO. Microarray analysis of exposed versus control shrimp revealed that the expression of 21 identified and 22 unidentified gene fragments was affected. Several myosin and actin gene fragments were down regulated. Muscle and cytoskeletal fibres are known to be one of the first targets of oxidative stress (Urbanciková & Korytár 1999), which may be induced by TBT by blocking the electron transport chain, thereby increasing radical oxygen species (ROS) levels. According to several authors, TBT also interacts with calmodulin, thereby increasing intracellular Ca^{2+} concentration, activating some proteases which in turn lead to an increased depolymerisation of cytoskeletal fibres (Show & Orrenius 1994; Cima & Ballarin 2000; Dalle-Donne et al. 2001 Gómez-Mendikute et al. 2002). The down regulation of sarcoplasmatic calcium-binding protein is likely also related to the known effect of TBT on the release of Ca^{2+} from intracellular stores. Other down regulated genes included arthrodial cuticle protein, chitinase, and cuticle protein cb6.

Table 5.4. (pages 104 and 105). BLAST and Bioconductor results for the significantly differentially expressed genes (moderated t-test $p < 0.05$), ranked according to their logFC. Low LogFC values indicate a strong down regulation, high LogFC values a strong up regulation. Expressed genes passing the |logFC|>0.75 criterion are arced dark grey. For each probe, following parameters are given: identity code (ID), sequence length (Length), sequence description (Seq.Description), expect value (eValue), sequence similarity (Simil.), Log2-fold change of exposed (4A-D) versus control (0A-D) treatments (logFC), the average expression value ('spot intensity') across all arrays and channels (AveExpr), the logFC to its standard error (moderated t-statistic (t)), the associated *p*-value (P-value), and the *p*-value adjusted for multiple testing (adj.P.Value). The adjusted *p*-values indicate a high chance on false positives (~62.9%).

ID	Length	Seq. Description
CrF5_03_A	569	myosin heavy chain
CrF1_03_A	176	---NA---
CrM3_05_A	371	arthrodial cuticle protein
CrF5_06_B	372	sarcoplasmic calcium-binding protein
CrF4_09_B	498	myosin light chain alkali
CrF1_08_A	722	---NA---
CrF8_12_H	465	---NA---
CrF2_10_B	395	hemocyanin
CrM6_06_B	624	skeletal muscle actin 6
CrM3_01_E	693	---NA---
CrF1_04_C	541	predicted: hypothetical protein (*S. purpuratus*)
CrF3_01_C	433	ribosomal protein lp1
CrM7_01_B	90	---NA---
CrM7_05_A	377	---NA---
CrF6_07_H	127	---NA---
CrF6_01_E	624	chitinase
CrF1_08_B	551	cuticle protein cb6
CrF3_08_C	618	myosin light chain
CrF4_09_H	322	actin-like protein
CrF6_01_A	334	skeletal muscle actin 6
CrF6_03_C	85	---NA---
CrF6_01_G	478	---NA---
CrF2_10_C	306	---NA---
CrM4_08_E	76	---NA---
CrM8_04_H	37	---NA---
CrF8_07_C	572	---NA---
CrM7_05_G	582	cuticle proprotein
CrF7_01_B	324	---NA---
CrM4_11_H	600	peptidyl-prolyl cis-trans isomerase-like
CrM1_08_E	267	---NA---
CrM5_06_E	308	---NA---
CrF6_10_H	317	---NA---
CrF7_01_D	249	adhesin wi-1
CrM1_08_C	374	sodium- and chloride-dependent gaba transporter 1
CrM4_11_B	224	---NA---
CrM1_06_B	620	---NA---
CrF6_11_D	306	hypothetical protein (*T. domestica*)
CrM8_09_F	514	endocuticle structural glycoprotein bd-1
CrF7_12_D	447	actin 5c
CrF3_01_B	131	---NA---
CrM1_05_C	326	---NA---
CrF2_11_D	363	---NA---
CrM6_07_B	121	vitellogenin [*Pandalopsis japonica*]

eValue	Simil.	logFC	AveExpr	t	P.Value	adj.P.Val
2.47E-57	90.05%	-0.938	10.243	-2.638	0.014	0.629
		-0.883	9.759	-2.964	0.006	0.629
6.12E-15	59.45%	-0.854	10.764	-2.244	0.033	0.629
2.35E-14	86.20%	-0.787	10.248	-2.090	0.046	0.655
1.96E-11	80.9%	-0.701	12.520	-2.181	0.038	0.629
		-0.682	9.880	-2.361	0.026	0.629
		-0.676	11.134	-3.049	0.005	0.623
1.73E-09	76.3%	-0.611	8.877	-2.884	0.008	0.629
5.49E-49	95.0%	-0.598	10.270	-2.659	0.013	0.629
		-0.562	9.449	-2.687	0.012	0.629
7.30E-01	42.00%	-0.546	9.615	-2.143	0.041	0.629
1.47E-21	82.9%	-0.543	9.792	-2.246	0.033	0.629
		-0.541	11.980	-2.250	0.033	0.629
		-0.513	12.142	-2.757	0.010	0.629
		-0.490	10.804	-2.467	0.020	0.629
1.60E-41	55.6%	-0.488	12.387	-2.485	0.019	0.629
1.40E-06	64.9%	-0.445	8.778	-3.355	0.002	0.482
1.32E-47	83.75%	-0.427	12.794	-2.163	0.040	0.629
1.36E-06	93.0%	-0.418	10.932	-2.096	0.046	0.655
6.08E-42	94.2%	-0.408	12.093	-2.205	0.036	0.629
		-0.395	13.562	-2.172	0.039	0.629
		-0.369	13.506	-2.183	0.038	0.629
		-0.350	9.036	-2.379	0.025	0.629
		-0.285	8.803	-2.578	0.016	0.629
		0.268	8.867	2.362	0.026	0.629
		0.409	15.327	2.261	0.032	0.629
9.59E-39	61.95%	0.425	9.381	2.357	0.026	0.629
		0.428	11.701	2.133	0.042	0.629
1.95E-21	84.4%	0.437	10.296	2.246	0.033	0.629
		0.458	9.570	2.150	0.041	0.629
		0.535	9.193	2.258	0.032	0.629
		0.562	15.636	2.527	0.018	0.629
1.51E-06	41.53%	0.597	9.917	2.465	0.020	0.629
2.55E-29	75.05%	0.603	12.384	3.182	0.004	0.559
		0.618	9.584	2.367	0.025	0.629
		0.618	10.422	2.647	0.013	0.629
4.58E-06	72.50%	0.634	10.437	2.291	0.030	0.629
4.37E-25	70.25%	0.767	10.174	3.389	0.002	0.482
4.53E-04	80.00%	0.781	13.733	2.265	0.032	0.629
		0.802	8.619	2.222	0.035	0.629
		0.814	10.051	3.437	0.002	0.482
		0.825	8.781	2.642	0.014	0.629
1.71E-01	89.0%	0.863	10.472	2.062	0.049	0.681

The expression of vitellogenin (Vtg), actin5c, and endocuticle structural glycoprotein were up regulated. Vtg is the precursor of the major egg-yolk protein vitellin and one of the most commonly employed vertebrate biomarkers of endocrine disruption (Mazurova et al. 2008). In invertebrates, multiple Vtg isoforms exist having different functionalities. For example, they are also involved in calcium or iron metabolism (Abdu et al. 2002; Yokota et al. 2003). In contrast to vertebrates and Lophotrochozoa (e.g. molluscs), arthropod vitellogenesis is regulated by ecdysteroid and juvenile hormones, and not by oestrogens. In arthropods, vitellogenesis is negatively regulated by ecdysteroids (Hannas et al. 2011). An up regulation of vitellogenesis would thus suggest an antiecdysteroidal effect of TBT, which we proved *in vitro* in chapter 3. Gene fragments from adhesin wi1-like, ribosomal protein lp1 (RPLP1) and hemocyanin were also found to be up regulated. Adhesin wi1 is a major fungal antigen. Whether the adhesin wi1-like gene fragment originates from *C. crangon* or rather from a shrimp pathogen is unsure, but its up regulation may indicate a lowered immune response. RPLP1 forms a pentameric complex with other ribosomal proteins that regulates ribosome assembly and plays a role in translation initiation. In arthropods (Pongsomboon et al. 2008; Carpenter et al. 2009), RPLP1 expression is known to be positively affected by viral infections, but TBT effects have not been found. Hemocyanin is the most abundant circulating blood protein, and acts as an oxygen transporting metalloprotein containing copper. Hemocyanin blood levels are known to be sensitive towards hypoxia and increased levels of trace metals (Cd, Cu, Zn) (Engel et al. 1993), but effects of TBT exposure have not been observed. In vertebrates, the circulating levels of the analogue (but not homologue) haemoglobin are known to be affected by OTs. Weakly up regulated gene expression included that of sodium- and chloride-dependent GABA transporter 1 and a peptidyl-prolyl cis-trans isomerase-like protein (PPIase-like). GABA transporter 1 is the major transmembrane transporter responsible for the rapid clearance of the major inhibitory neurotransmitter γ-amino butyric acid (GABA), in order to maintain fast synaptic transmission, and its function depends on the electrochemical gradient across the neuronal membrane. TBT is known to act as a Cl^-/OH^- antiporter, and likely affects the GABAergic system at low doses by disturbing Cl^- homeostasis (Yamada et al. 2010). PPIases are a large superfamily of ubiquitous enzymes involved in protein folding, signal transduction, trafficking, assembly and cell cycle regulation (Göthel & Marahiel 1999). Some of these isomerases bind and activate steroid receptors or act as a modulator of intracellular calcium release channels.

Within the observed TBT induced shifts in gene expression in this study, cytotoxic markers can be discerned related to the disruption of calcium homeostasis. The up regulation of vitellogenin and up as well as down regulation of several cuticular proteins may indicate a second, potentially endocrine-disruptive effect related on the y-organ – ecdysteroidal endocrine axis, which may affect shrimp development and reproduction.

Recently, the group of Prof. dr. LeBlanc (Wang et al. 2011) proved TBT effects on ecdysis and reproduction of the crustacean *D. magna* (TBT LC_{50} = 2.5 µg l^{-1}). In *D. magna*, prolonged exposure of neonatal Daphnids to 3.3 nM (0.95 µg l^{-1}) TBT or less led to more offspring than observed among control organisms. At 3.6-5.0 nM (1.04-1.45µg l^{-1}), *Daphnia* died during moulting at the release of the first brood of offspring. Above 5.0 nM, exposed Daphnids died during juvenile exuviation. According to the authors, these results demonstrate increased TBT toxicity at the time ecdysteroid levels (i.e. during exuviation and especially during reproductive activity) are at their highest, and include impaired ecdysis and suppressed vitellogenesis. Earlier, Iguchi and Katsu (2008) reported that 1 µg l^{-1} TBT reduces reproduction in *Daphnia*, but had no effect on moulting. After 21 days of exposure of neonatal *D. magna* to ≤ 1.25 µg l^{-1} of TBT, Oberdörster et al. (1998) did not find any differences in reproductive success or moulting, but found an increase in steroid metabolization. The contradicting results of especially Wang & LeBlanc (2009) and Wang et al. (2011) in *Daphnia* (i.e. pro-ecdysteroidal effect,) versus our results in common shrimp and those of Mu & LeBlanc (2004) and Iguchi & Katsu (2008) in *Daphnia* (i.e. anti-ecdysteroidal effect) appear paradoxal. However, subtle differences in test concentrations, endocrine systems of the test species, used developmental stages, differences in tested receptor isoforms or even used concentrations or combinations of receptor ligands, may lead to such paradoxal outcomes due to our relatively poor understanding of crustacean endocrine functioning.

This study was the first to investigate subtoxic effects of TBT on the shrimp transcriptome. However, the discussion with respect to differentially expressed genes observed in this study has to be done with caution, because (1) differences in expression levels are rather low, (2) the false positive rates (adjusted *p*-values) are high, and (3) no confirmative studies using qRT-PCR have been performed. The high observed false discovery rates can be drastically reduced by improving shrimp laboratory survival and the quality of the microarray analysis. For future studies with common shrimp, a better laboratory survival is indispensable. Exposure studies require a homogenous testing population, ideally laboratory reared specimens. The low correlation between the expression profiles within the control and

exposure replicates observed in this study (leading to outlier microarrays) may be largely caused by a heterogeneous testing population and moreover poor laboratory survival. The quality of the microarray analysis could be strongly enhanced by tailoring oligonucleotides from the available cDNA sequences into suited microarray probes and commercially spotting of these probes on oligonucleotide arrays. Currently, the *C. crangon* transcriptome is being sequenced, with an estimated 66 times coverage and should provide a large EST database for a more comprehensive common shrimp microarray. With the rapid development and hence cost reduction in pyrosesquencing techniques, direct sequencing of the transcriptome (RNAseq) of TBT exposed and control shrimp could even provide a more sensitive approach. Regardless of the applied technique, characterizing the many unidentified ESTs observed in this and other studies would strongly increase the output value of microarray and RNAseq analyses. In case of ecotoxicological studies, this would greatly help to unravel the affected metabolic pathways.

Chapter 6

General Conclusions and Future Perspectives

6.1 General conclusions

Since the early 1970s until the early 2000s, the Belgian landings per unit effort (LPUE), a proxy for local annual shrimp abundance based on fisheries statistics, shows a gradual, but severe decrease, threatening the sustainability of the Belgian shrimp fishing fleet. Since 2007, the local shrimp stock has suddenly recovered, resulting in record landings in 2010. In the Wadden Sea, which provides 95% of landed shrimp in the EU, a similar decrease in annual landings has been observed since the mid-1960s. The Wadden Sea shrimp stock however already started to recover gradually in 1990, also reaching record landings in 2010. Field observations indicate the potential involvement of (chemically mediated) endocrine disruption. In the Wadden Sea, a severe parallel decrease and subsequent increase in the percentage of gravid shrimp has been observed (Siegel et al. 2008). During the same period, unusual high prevalence of shell infections have been frequently encountered throughout the whole North Sea (Watermann & Dethlefsen 1983; Knust 1990; Dyrynda 1998). In 2004, Nishikawa et al. (2004) showed that TBT is a potent agonist of human RXRα, a NR which is strongly conserved throughout the animal kingdom. This dissertation hypothesized that environmental concentrations of the potent broad spectrum biocide tributyltin (TBT) affect NR functioning in common shrimp, leading to downstream alterations in the expression of genes involved in moulting and reproductive processes. Since the late 1950s, TBT had been used on a massive scale as antifouling agent to decrease drag or surface damage on especially ship hulls due to biofouling. In 1989, the use of TBT on vessels smaller than 25 m was banned at EU level due to severe reproductive failures in commercially exploited oyster populations and declining marine gastropod populations. A EU ban on all ship became effective in 2003, while a complete ban at IMO level entered-into-force in 2008.

Since the 1960s, multiple environmental incidents with toxic chemicals had led to increased scientific, public and governmental awareness regarding the unsound use of chemicals. Endocrine mediated toxicity did not gather any special attention until the 1990s, when several reports associated certain health and environmental issues with the presence of previously thought harmless doses of chemicals. Since then, hundreds of peer-reviewed scientific publications have made associations of background EDC concentrations with health and to a lesser extent environmental effects. In the latter case, the identification of a single cause-effect linkage between a chemical and observed population level effects is severely hampered by the complexity of environmental exposures (e.g. multiple exposure routes, mixture effects). Furthermore, unravelling the underlying mode of action necessitates a profound knowledge of

the biology of the assumed affected species, which is most of the time lacking. Due to these obstacles, a weight-of-evidence approach is generally accepted to assess the cause-effect relationship based on concepts of temporality, strength of association, consistency of observation, biological plausibility, and evidence of recovery (WHO 2002).

EDCs can affect endocrine regulation by blocking (antagonism) or activating (agonism) hormone receptors, or by interfering in hormone or hormone receptor metabolism (i.e. synthesis, transport or breakdown). In either case, the hormone-receptor interaction is directly or indirectly affected, leading to alterations in the downstream complex of cross-talking signalling pathways, which ultimately lead to changes in the behaviour or structure of the target cells. Due to the intensive cross-talk between these pathways, unpredictable effects may occur in other target tissues. Furthermore, these complex pathways are characterized by developmental stage and tissue specific receptor isoforms and cellular machineries (e.g. receptor coactivators), and thus the same extracellular signal may evoke opposite cellular effects, even within the same animal.

While potentially being the largest subphylum of multicellular organisms (in species richness as well as in global biomass), crustaceans have received little attention regarding the potential impacts of EDCs. In crustaceans, ecdysteroid hormones play a pivotal function in development as well as reproduction. Circulating ecdysteroids diffuse into the intracellular compartment where they bind and activate their nuclear receptor EcR, which in turn recruits the nuclear receptor RXR to form an active heterodimeric EcR:RXR receptor. This active heterodimer can then directly interact with DNA to transactivate the expression of early ecdysteroid-responsive genes, thereby initiating multiple signalling cascades.

In common shrimp, this dissertation shows that low, subtoxic concentrations of TBT exert a strong anti-ecdysteroidal effect, leading to alterations in the downstream complex of cross-talking signalling pathways, which ultimately lead to changes in gene expression related to cellular calcium homeostasis cuticular structure and vitellogenin synthesis.

A significant amount of evidence has been gathered during this study regarding the association of TBT with the long term decrease and afterwards recovery of shrimp stock size and reproduction:

1) *In silico* prediction reveals TBT accommodates CrcRXR in a similar manner as human RXRα, locking the receptor in its agonist conformation.

2) *In vitro*, a low, subtoxic TBT concentration (5.8 µg l^{-1}) strongly repressed CrcEcR:CrcRXR activity with 64%.
3) *In vivo* acute exposure of shrimp to TBT (albeit at a toxic concentration of 38.9 µg l^{-1}) leads to a strong downregulation of especially CrcEcR isoforms in the ovaries. EcR is known to be subject to a positive autoregulatory loop to increase EcR levels and sensitize the animal to ecdysone pulses (Karim & Thummel 1992).
4) *In vivo* subchronic exposure of shrimp to an environmental subtoxic TBT concentration (1.9 µg l^{-1}) resulted in significant alterations in expression of genes involved in intracellular calcium homeostasis and of cuticular genes and especially in the up regulation of vitellogenin, the precursor of the major eggyolk protein vitellin which is used as EDC biomarker in mostly fish species.
5) Comparison of field data generated during this study with available monitoring data reveal that TBT concentrations in shrimp have decreased 8-fold since 1999, shortly after the major shipping companies started to switch to alternative antifouling agents.
6) Fisheries data indicate a fast recovery of the shrimp stock at the Belgian coast shortly after the IMO ban on TBT in 2003. On EU scale, fisheries data and field data clearly indicate a recovery in stock size and percentage of gravid shrimp since 1990, shortly after the EU ban on TBT on ship <25 m (i.e. mostly recreational and fishing vessels). The difference in onset of recovery between the Wadden Sea and Belgian Flat can be explained by differences in local shipping activities.

6.2 Future research needs

As long as a crustacean cell line has not been achieved, the transfected L57-3-11 cell line can be used as *in vitro* bioassay to investigate EDC activity in crustaceans. It is recommended that the robustness and sensitivity of the cell line should be enhanced by e.g. stable transfection with CrcEcR and CrcRXR, a more profound inactivation of endogenous DmEcRs and DmUSP through *in situ* genome editing techniques, and the use of crustacean EcRE upstream of the luciferase reporter gene. If successful, this enhanced cell line could represent a sensitive, reliable, rapid, and cost-effective tool for identifying cause-effect relationships of chemicals on crustacean endocrinology. Concerning the putative effect of TBT, reliable dose-response curves of the *in vitro* effect on CrcEcR:CrcRXR signalling may eventually bridge the gap between chemical measurements and population level effects. As the ecological

relevance of *in vitro* data may be arguable, they should ideally be accompanied by observations of higher order effects (e.g. histological, physiological and population effects).

Although the economic and environmental important common shrimp has been studied intensively through field studies, its biology is poorly understood due to its poor laboratory survival. In order to perform reliable laboratory studies with common shrimp, successful laboratory rearing of this species is crucial to provide a more homogenous testing population and to achieve a strongly reduced mortality under artificial conditions. Because of this knowledge gap, reliable experimentally derived ecotoxicological parameters such as BCFs, BSAFs, depuration and degradation rates are not available for any compound in common shrimp. A good laboratory survival would enable the reliable quantification of such parameters as well as long-term exposure experiments, which are necessary to obtain dose-effect data on physiological end-points such as reduced brood size or delayed moulting.

In general, one of the major shortcomings of current ecotoxicity testing is the limited number of available test species, rendering extrapolations to most species impossible. Therefore, the ecotoxicological research community faces a huge challenge in expanding the set of model organisms. Otherwise, the usefulness of costly routine chemical environmental monitoring programmes will remain limited as long as the observed exposure levels cannot be linked to biological effects with certain reliability. It is striking that currently no invertebrate marine model organism is generally accepted or intensively investigated within ecotoxicology and environmental genomics research. The major reason is the poor knowledge on the culture of especially marine species. As such, the evolution of ecotoxicology and environmental risk assessment depends heavily on an accompanying progress made in the field of aquaculture, where the focus should not solely be laid on economic, but also on environmental important species.

Another major drawback in current ecotoxicological research is the limited knowledge of the complex endocrine systems of potential target organisms. The relatively new research field of ecotoxicogenomics, which combines classical toxicity testing with high-throughput genomic techniques (i.e. microarray) and related bioinformatics, has the potential to unravel the complex gene expression cascades involved in endocrine signalling and endocrine disruption. In this dissertation, 'home-built' cDNA microarrays were prepared to screen the expression of a limited number of ESTs obtained through SSH-PCR and subsequent cloning. The sensitivity and specificity as well as transcriptome coverage of this approach was low (it should be noted here that the obligatory use of wild-caught shrimp and their poor laboratory survival lead to a

high variation in expression profiles among the replicate treatments). With the recent developments in pyrosesquencing techniques, huge EST databases can now be rapidly and cost-effectively generated by transcriptome sequencing (RNAseq). In combination with the rapid development and hence cost-reduction of commercially printed oligonucleotide microarrays, the sensitivity, specificity and transcriptome coverage can thus be greatly enhanced.

6.3 Scientific uncertainties should not postpone political action

At the moment, linking laboratory findings with wildlife observations or extrapolations of low-dose chemical effects is prone to many uncertainties (e.g. strictly controlled laboratory environment versus unknown biotic and abiotic variations) and as such, an easy target for well-funded scientific criticism. This problem shall persist, as long as our understanding of invertebrate endocrinology and ecosystem functioning is insufficient. Meanwhile, harsh policy decisions should not be postponed based on the argument of insufficient scientific data. The case of the much contested TBT ban is a textbook example of related brave political action. The TBT ban on ship <25 m was easily accepted, as it was based on a pernicious economic impact on shellfish farming and furthermore as it mostly targeted a recreational activity. In contrast, the ban in 2003 was much disputed, as critics stated that the sole reason was the environmental impact on several irrelevant sensitive gastropod species. Furthermore, the ban would lead to a high economic loss due to the lack of an efficient antifouling alternative to TBT, leading to increased fuel and maintenance costs. However, the ban stimulated the paint-manufacturers to look for decent alternatives. Although other obvious TBT induced effects than in marine molluscs were not detected, IMO and the EU acted on the principle of protecting an ecosystem by protecting the most sensitive species. Indeed, this approach proved to be a success.

The increased shrimp stock size associated with decreasing TBT concentrations could also have profound beneficial effects on human health and economy, and on the environmental impact of shrimp fisheries. First of all, the direct impact on the health related issues regarding consumption of common shrimp and other seafood is evident. The daily consumption of common shrimp is no longer considered a health threat regarding OT intake. A higher catch efficiency of common shrimp may reduce hours at sea, hours of fishing and hence labour, related health risks, and fuel consumption. Reducing the fishing effort also leads to a reduction in fishing mortality, bycatch and sea bed disturbance.

Summary

With an annual catch of 35,000 – 50,000 tons and a commercial value of roughly €100 million, common shrimp is one of the most valuable European fisheries and aquaculture commodities. Since the late 1960s, European landings strongly decreased until 1990, due to a strongly reduced shrimp abundance and percentage of egg-bearing females. In the Wadden Sea, the shrimp stock and hence landed volumes recovered slowly after 1990 to record landings in 2010. In the Southern Bight (i.e. Northern France to Dutch Delta), one of the busiest international shipping lanes, the stock only recovered after 2003. Until now, no explanation was found for these abnormal long-term trends in the shrimp stock.

The use of TBT as antifouling agent began in the 1960s, leading to exuberant TBT concentrations in the 1970s and 1980s, especially nearby recreational marinas, shipping lanes, and industrial harbours. At the end of the 1980s, the use of TBT on smaller ship (<25 m) was banned due to developmental and reproductive effects in oyster farms. A controversial ban on the use of TBT on all submerged surfaces (thus including commercial ships > 25 m) was only accepted in 2003 and finally entered-into-force in 2008. In 2004, Nishikawa et al. (2004) proved that TBT mimics vertebrate hormone signalling by activating the retinoid-X-receptor (RXR). As this receptor is strongly conserved in the animal kingdom, an identical mode of action (MOA) was generally accepted to have caused the observed reproductive and developmental defects in marine shellfish and gastropods. RXR is a nuclear receptor (NR) believed to directly modulate (i.e. by heterodimerization) the activity of many other NRs. NRs are the major targets of lipophilic hormones (e.g. steroids), and directly induce tissue specific expression of genes involved in development, reproduction, immune response, etc.

Within this PhD-thesis, three main research questions were addressed. (1) Does TBT affect the functionality of the shrimp RXR receptor?, (2) what is the temporal and spatial distribution of TBT in North Sea shrimp, and finally (3) do the TBT concentrations observed in the North Sea disrupt shrimp endocrine functioning? In chapter 1, the reader is introduced to common shrimp, endocrine disruption and TBT. In chapter 2, the open reading frame (ORF) sequences from *C. crangon* RXR (CrcRXR) and its well-known invertebrate partner protein, ecdysteroid receptor (CrcEcR), were fully retrieved through a combination of several molecular techniques. Intra- and extraspecies variant regions were identified within the cloned CrcRXR and CrcEcR isoforms. A phylogenetic analysis based on CrcRXR and CrcEcR confirmed the close relationship with Brachyuran crabs for the first time on a molecular basis. *In silico* 3D protein structures of CrcRXR and CrcEcR were reconstructed based on existing (human) RXR and (insect) EcR templates. In chapter 3, *in silico* docking of TBT within the

reconstructed ligand binding pocket (LBP) of CrcRXR showed a good fit, indicating a plausible effect on NR functioning. Through an ecdysone responsive reporter assay using a mutant *Drosophila* cell line expressing CrcRXR and CrcEcR, a strong reduction of signalling activity of the heterodimeric CrcEcR-CrcRXR complex after exposure to a subtoxic TBT concentration was shown *in vitro*. Semiquantitative RT-PCR proved that the gene expression of both receptors was severely affected after *in vivo* acute exposure of shrimp to TBT. In chapter 4, samples collected during September-November 2009 in Belgian, Dutch, German and Danish waters were analysed through gas chromatography – mass spectrometry (GC-MS) to give an extensive as well as intensive spatial overview of TBT and other OT concentrations in shrimp from the Southern North Sea. Furthermore, we focused on the environmental behaviour of OTs in the heavily polluted Westerschelde estuary, and conclude the environmental fate of OTs is similar to that of metals rather than that of organic pollutants. Concentrations of TBT and the pesticide triphenyltin (TPhT) in shrimp tail muscle ranged from 4-124 and 1-24 μg kg^{-1} DW, respectively. High levels are accumulated in estuarine areas and are clearly related with sediment concentrations. Levels in shrimp and sediment have decreased approximately 8-fold since 1999. Furthermore, common shrimp consumption is no longer considered a health risk regarding human OT intake.

In chapter 5, the effects of subtoxic TBT levels (2 ng – 2 μg l^{-1}) on shrimp gene transcription was assessed by constructing a shrimp specific cDNA microarray. 604 cDNA fragments were sex-related fragments obtained through suppression subtractive hybridization PCR (SSH-PCR) on male and female shrimp, and were appended with CrcEcR and CrcRXR isoforms and three household genes (18S rRNA, β-actin, and GADPH). The analysis revealed that the expression of 43 gene fragments was significantly affected by exposure to 2 μg l^{-1} TBTO.

Within the observed TBT induced shifts in gene expression, cytotoxic markers could be discerned related to the disruption of calcium homeostasis. The up regulation of vitellogenin and up as well as down regulation of several cuticular proteins indicate a second, potentially endocrine-disruptive effect related on the y-organ – ecdysteroidal endocrine axis, which may affect shrimp development and reproduction.

Nederlandstalige samenvatting

Met een jaarlijkse vangst van 35 000 tot 50 000 ton en een commerciële waarde van ongeveer 100 miljoen euro, is de grijze garnaal (*Crangon crangon*) één van de meest waardevolle Europese visserij- en aquacultuurproducten. Sinds eind jaren '60 daalden de Europese aanlandingen echter sterk door een grote afname in de abundantie en de vruchtbaarheid van garnaal in de Zuidelijke Noordzee (Noord-Frankrijk – Denemarken). Sinds 1991 herstelde de garnaalstock zich in de Waddenzee echter geleidelijk, tot zelfs recordvangsten in 2010. In de Zuidelijke Bocht (Noord-Frankrijk - Nederlandse Delta), één van de drukste scheepsroutes ter wereld, herstelde de garnaalstock zich pas na 2003. Tot op heden werd voor deze abnormale lange termijntrends geen oorzaak gevonden. Het gebruik van TBT als aangroeiwerend middel nam een vlucht in de jaren '60 en leidde algauw tot exuberante concentraties ervan in de jaren '70 en '80, vooral nabij jachthavens. Op het einde van de jaren '80 werd het gebruik van TBT op kleinere schepen (<25 m) verboden op basis van gerelateerde ontwikkelings- en voortplantingsstoornissen in oesterkwekerijen. Een controversieel verbod op het gebruik van TBT op alle onderwateroppervlakten (dus inclusief op de rompen van commerciële schepen >25 m) werd pas aanvaard in 2003 en trad uiteindelijk in werking in 2008. In 2004 toonden Nishikawa et al. (2004) aan dat TBT een hormoonactiviteit uitoefende op de humane retinoid-X-receptor (RXR). Doordat deze receptor sterk geconserveerd is in het dierenrijk, werd verondersteld dat een gelijkaardig werkingsmechanisme de geobserveerde stoornissen in mariene schelpdieren en slakken zou hebben veroorzaakt. RXR behoort tot de nucleaire receptor (NR) familie, en zou via heterodimerizatie rechtstreeks de activiteit van vele andere NR's moduleren. NR's zijn de fysiologische doelwitten van vetoplosbare hormonen (bvb. steroïden), en induceren rechtstreeks weefselspecifieke expressie van genen betrokken in ontwikkeling, voortplanting, immuunreactie, enzovoort.

In deze doctoraatsscriptie werd een antwoord gezocht op drie grote onderzoeksvragen: (1) beïnvloedt TBT de werking van RXR in grijze garnaal, (2) wat is de tijdelijke en ruimtelijke verspreiding van TBT in grijze garnaal in de Noordzee, en uiteindelijk (3), kunnen de geobserveerde concentraties de hormoonwerking in grijze garnaal verstoren? In hoofdstuk 1 wordt de lezer geïntroduceerd in de grijze garnaal, hormoonverstoring en TBT. In hoofdstuk 2 werden de gensequenties van de volledig open leesramen ('open reading frames') van CrcRXR en van de ecdysteroid receptor (CrcEcR), het best gekende partnereiwit van RXR in ongewervelden, via een combinatie van verschillende moleculaire technieken bekomen. Binnen de gekloneerde CrcRXR en CrcEcR isovormen werden de variante regio's tussen de verschillende isovormen en tussen verschillende soorten geïdentificeerd. Een fylogenetische

analyse gebaseerd op de CrcRXR en CrcEcR sequenties bevestigde voor de eerste maal op moleculaire basis de nauwe verwantschap van grijze garnaal met krabben. De 3D eiwitstructuren van CrcRXR en CrcEcR werden '*in silico*' gereconstrueerd op basis van bestaande (humane) RXR en (insecten)EcR 3D-structuren.

In hoofdstuk 3 werd op basis van deze reconstructies bewezen dat TBT uitstekend in de hormoonbindingsplaats van CrcRXR past. Dit toont aan dat TBT hoogstwaarschijnlijk de nucleaire receptorwerking in garnaal beïnvloedt. Via een luciferase reporter analyse met een mutante *Drosophila* cellijn, die de CrcRXR en CrcRXR sequenties in actieve eiwitten vertaalt, werd *in vitro* een sterke activiteitsdaling aangetoond van het CrcRXR-CrcEcR receptorcomplex na blootstelling aan een subtoxische concentratie van TBT. Semi-kwantitatieve 'reverse transcriptase – polymerase chain reaction' (RT-PCR) toonde aan dat de genexpressie van beide receptoren sterk aangetast werd na acute blootstelling van garnalen aan TBT. In hoofdstuk 4 werden via gaschromatografie – massa spectrometrie (GC-MS) stalen geanalyseerd die verzameld werden gedurende september-november 2009 in Belgische, Nederlandse, Duitse en Deense kustwateren, om zo een ruimtelijk overzicht te verkrijgen van de concentraties van TBT en andere organotinverbindingen (OT's) in garnaal. Daarenboven werd het milieugedrag van OT's in het zwaar vervuilde Westerschelde-estuarium meer in detail onderzocht, hetgeen aantoonde dat OTs zich in het milieu veeleer als zware metalen dan als organische polluenten gedragen. De concentraties van TBT en het pesticide trifenyltin (TPhT) varieerden respectievelijk tussen 4-124 en 1-24 µg per kg drooggewicht garnaalvlees. Hoge concentraties werden geaccumuleerd in en nabij grote riviermondingen en zijn duidelijk gerelateerd met de concentraties in het sediment. Sinds 1998 zijn de concentraties in garnaal en sediment, als gevolg van een internationaal verbod, bij benadering achtvoudig gedaald. Bovendien houdt de consumptie van garnaal niet langer een gezondheidsrisico in betreffende de inname van OT's.

In hoofdstuk 5 worden de effecten van subtoxische TBT concentraties (2 ng – 2 µg l^{-1}) op de gentranscriptie in garnaal nagegaan door een garnaalspecifieke cDNA microarray te ontwikkelen. 604 genfragmenten waren geslachtsspecifieke cDNA fragmenten die bekomen werden via 'suppression subtractive hybridisation' PCR (SSH-PCR) tussen mannelijke en vrouwelijke garnalen, waaraan de CrcRXR en CrcEcR isovormen en drie huishoudgenen (18S rRNA, β actine, GADPH) werden toegevoegd. De analyse toonde aan dat de expressie van 43 genfragmenten significant aangetast werd door blootstelling aan 2 µg l^{-1} TBTO. Binnen de geobserveerde shifts in genexpressie konden enkele cytotoxische merkers aangetoond worden

die gerelateerd zijn aan de verstoring van de celullaire calcium huishouding. De opregulatie van vitellogenine en op- en neerregulatie van meerdere cuticulaire proteines geven een tweede, mogelijk endocrien verstorend effect aan dat de ontwikkeling en voortplanting van garnaal kan aantasten.

References

Abbott O.J., and Perkins E.J. (1977). The biology of the brown shrimp *Crangon crangon* in the Solway Firth. Scientific Report Cumbria Sea Fisheries Committee 77: 1-34.

Abdu U., Davis C., Khalaila I., and Sagi A. (2002). The vitellogenin cDNA of *Cherax quadricarinatus* encodes a lipoprotein with calcium binding ability, and its expression is induced following the removal of the androgenic gland in a sexually plastic system. Gen. Comp. Endocrinol. 127: 263-272.

Abramoff M.D., Magelhaes P.J., and Ram S.J. (2004). Image Process. Image J. Biophot. Int. 11: 36–42.

Adams M.D., Celniker S.E., Holt R.A. et al. (196 co-authors) (2000). The genome sequence of *Drosophila melanogaster*. Science 287: 2185–2195.

Addison J.T., Lawler A.R., and Nicholson M.D. (2003). Adjusting for variable catchability of brown shrimps (*Crangon crangon*) in research surveys. Fish. Res. 65: 285-294.

Aguinaldo A.M., Turbeville J.M., Linford L.S., Rivera M.C., Garey J.R., Raff R.A., and Lake J.A. (1997). Evidence for a clade of nematodes, arthropods and other moulting animals. Nature 387: 489-493.

Aldridge W.N. (1958). The biochemistry of organotin compounds: trialkyltins and oxidative phosphorylation. Biochem. J. 69: 367–376.

Alzieu C., Heral M., Thibaud Y., Dardignac M., and Feuillet M. (1982). Influence des peintures antisalissures a base d'organostanniques sur la calcification de la coquille de l'huître *Crassostrea gigas*, Revue Trav. Inst. Pêches Marit. 45: 101–116.

Amara R., and Paul C. (2003). Seasonal patterns in the fish and epibenthic crustaceans community of an intertidal zone with particular reference to the population dynamics of plaice and brown shrimp. Est. Coast. Shelf Sci. 56: 807-818.

Ankley G.T., Cook P.M., Carlson A.R., Call D.J., Swenson J.A., and Corcora H.F. (1992). Bioaccumulation of PCBs from sediments by oligochaetes and fishes: comparison of laboratory and field studies. Can. J. Fish. Aquat. Sci. 49: 2080–2085.

Ankley G.T., Leonard E.N., Mattson V.R. (1994). Prediction of bioaccumulation of metals from contaminated sediments by the oligochaete *Lubriculus variegatus*. Water Res. 28: 1071–1076.

Antunes A., Siby P., Da Fonseca R.R., Armanda Reis-Henriques M., Vasconcelos V., Castro L.F.C., and Santons M.M. (2010). The modulation of retinoic acid signalling pathways by environmental pollutants in marine metazoans. Rapp. Comm. int. Mer Médit. 39:213.

Arnold C.G., Weidenhaupt A., David M.M., Müller S.R., Haderlein S.B., Schwarzenbach R.P. (1997). Aqueous speciation and 1-octanol–water partitioning of tributyl- and triphenyltin: effect of pH and ion composition. Environ. Sci. Technol. 31: 2596–2602.

Asazuma H., Nagata S., Kono M., and Nagasawa H.(2007). Molecular cloning and expression analysis of ecdysone receptor and retinoid X receptor from the kuruma prawn, *Marsupenaeus japonicus*. Comp. Biochem. Physiol. 148B: 139–150.

Avia D., Diamantis C., Neudecker T., Berkenhagen J., and Müller M. (2011). The North Sea brown shrimp fisheries. Study requested by the European Parliament (IP/B/PECH/IC/2010_102), 108 pp.

Baer K.N., and Owens K.D. (1999). Evaluation of selected endocrine disrupting compounds on sex determination in *Daphnia magna* using reduced photoperiod and different feeding rates. Bull. Environ. Contam. Toxicol. 62: 214–221.

Bamber R.N., and Henderson P.A. (1994). Seasonality of caridean decapod and mysid distribution and movements within the Severn Estuary and Bristol Channel. Biol. J. Linn. Soc. 51: 83–91.

Bauer R.T.(2004). Remarkable Shrimps: Adaptations and natural History of the Carideans. Animal Natural History Series 7, University of Oklahoma Press, 296 pp.

Becker G.A., Dick S., and Dippner J.W. (1992). Hydrography of the German Bight. Mar. Ecol. Progr. Ser. 9: 9–18.

Benjamini Y., and Hochbert Y. (1995). Controlling the false discovery rate: A practical and powerful approach to multiple testing. Journal of the Royal Statistical Society 57: 289-300.

Bennett-Lovsey R.M., Hebert A.D., Stemberg M.J.E., and Kelley L.A. (2008). Exploring the extremes of sequence/structure space with ensemble fold recognition in the program Phyre. Proteins: Struct. Funct. Bioinform. 70: 611–625.

Berghahn R. (1983). Untersuchungen an Plattfischen und Nordseegarnelen (*Crangon crangon*) im Eulitoral des Wattenmeeres nach dem Ubergang zum Bodenleben. Helgolander Meeresun. 36: 163-181.

Bertrand S., Brunet F.G., Escriva H., Parmentier G., Laudet V., and Robinson-Rechavi M. (2004). Evolutionary genomics of nuclear receptors: from twenty-five ancestral genes to derived endocrine systems. Mol. Biol. Evol. 21: 1923-1937.

Bettin C., Oehlmann J. and Stroben E. (1996). TBT-induced imposex in marine neogastropods is mediated by an increasing androgen level. Helgol. Meeres. 50: 299–317.

Beukema J.J. (1992). Dynamics of juvenile shrimp *Crangon crangon* in a tidal flat-nursery of the Wadden Sea after mild and cold winters. Mar. Ecol-Prog. Ser. 83:157-165.

Beyst B., Hostens K., and Mees J. (2001). Factors influencing fish and macrocrustacean communities in the surf zone of sandy beaches in Belgium: temporal variation. J. Sea Res. 46: 281-294.

Billas I.M.L., Browning C., Lawrence M.C., Graham L.D., Moras D., and Hill R.J. (2009)., The structure and function of ecdysone receptors. In: Smagghe G. (Ed.). Ecdysteroids, structures and functions. Springer, Berlin, 335-375 pp.

Billas I.M.L., Iwema T., Garnier J.M., Mitschler A., Rochel N., and Moras D. (2003). Structural adaptability in the ligand-binding pocket of the ecdysone hormone receptor. Nature 426: 91–96.

Boddeke R. (1962). Resultaten van drie jaar garnalenonderzoek. Visserij 15:66–70.

Boddeke R. (1982). The occurrence of winter and summer eggs in the brown shrimp (*Crangon crangon*) and the pattern of recruitment. Neth. J. Sea Res. 16:151-162.

Boddeke R., Driessen G., Doesburg W., and Ramaekers G. (1986). Food availability and predator presence in a costal nursery area of the brown Shrimp (*Crangon crangon*). Ophelia 26: 77-90.

Boddeke R. (1976). The seasonal migration of the brown shrimp *Crangon crangon.* Neth. J. Sea Res. 10: 103-130.

Boddeke R. (1989). Management of the brown shrimp (*Crangon crangon*) stock in the Dutch Coastal waters. In Marine Invertebrate Fisheries: Their Assessment and Management, Caddy J.F. (ed.), New York: 35-62.

Bryan G. W., Gibbss P. E., Hummerstone L. G., and Bunt G. R. (1986). The decline of the gastropod *Nucella lapillus* around south west England: evidence for the effect of tributyltin from antifouling paints. J. Mar. Biol. Assoc. U. K. 66: 611-640.

Budd G.E., and Telford M.J., (2009). The origin and evolution of arthropods. Nature 457: 812–817.

Burkenroad M.D. (1963). The evolution of the Eucarida (Crustacea, Eumalacostraca), in relation to the fossil record. Tulane stud. Geol. 2: 1-17.

Burkhard L., (2009). Estimation of Biota Sediment Accumulation Factor (BSAF) from paired observations of chemical concentrations in biota and sediment, US Environmental Protection Agency, Ecological Risk Assessment Support Center: Cincinnati, OH, EPA/600/R-06/047.

Calabrese E.J. (2004).Paradigm lost, paradigm found: The re-emergence of hormesis as a fundamental dose response model in the toxicological sciences. Environ. Pollut. 138: 378–411.

Calman W.T. (1904). On the classification of the *Crustacea malacostraca*. Ann. Nat. Hist. 13: 144-158.

Campos J., and Van der Veer H.W. (2008). Autecology of *Crangon crangon* (L.) with an emphasis on latitudinal trends. Oceanogr. Mar Biol. Ann. Rev. 46: 65-104.

Cantelmo A., Lazell R., and Mantel L. (1981). The effects of benzene on molting and limb regeneration in juvenile *Callinectes sapidus*. Mar. Biol. Lett. 2: 333–343.

Cantelmo A., Mantel L., Lazell R., Hospod F., Flynn E., Goldberg S., and Katz M. (1982). The effects of benzene and dimethylnaphthalene on physiological processes in juveniles of

the blue crab, *Callinectes sapidus*. In: Vernberg W., Calabrese A., Thurburg F.P., Vernberg F.J. (Eds.), Physiological Mechanisms of Marine Pollutant Toxicity. Academic Press, New York: 349-390.

Cao S., Wang J. D., Chen H. S., et al. (2011). Progress of marine biofouling and antifouling echnologies. Chinese Sci. Bull. 56: 598–612.

Carmichael J.A., Lawrence, M.C., Graham L.D., Pilling P.A., Epa V.C., Noyce L., Lovrecz G., Winkler D.A., Pawlak-Skrzecz A., Eaton R.E., Hannan G.N., and Hill R.J. (2005). The X-ray structure of a hemipteran ecdysone receptor ligand-binding domain – comparison with a Lepidopteran ecdysone receptor ligand-binding domain and implications for insecticide design. J. Biol. Chem. 280: 22258–22269.

Carpenter J., Hutter S., Baines J.F., Roller J., Saminadin-Peter S.S., Parsch J., and Jiggins F.M. (2009). The Transcriptional Response of ***Drosophila melanogaster*** to Infection with the Sigma Virus (Rhabdoviridae). PLoS ONE 4: e6838.

Carson R. (1962).Silent Spring. Houghton Mifflin, Boston, 368 pp.

Cattrijsse A., Dankwa H.R., and Mees J. (1997). Nursery function of an estuarine tidal marsh for the brown shrimp *Crangon crangon*. J. Sea Res. 38: 109-121.

Caudri L.W.D. (1937). Einfluss der Temperatur und des Salzgehalts auf die Sterblichkeit von Garnelen (*Crangon crangon L.*). Arch. Néerl. Zool 3: 179-196.

Cavener D.R. (1987). Comparison of the consensus sequence flanking translational start sites in Drosophila and vertebrates. Nucleic Acids Res. 15: 1353–1361.

Champ M.A. (2000). A review of organotin regulatory strategies, pending actions, related costs and benefits. Sci. Total Environ. 258: 21-71.

Champ M.A. (1986). Organotin symposium: introduction and review. In: Maton G.L. (Ed.). Proceedings of the Oceans 86 Conference, vol. 4. September 23-25, Washington: 1093-1100.

Chandra V., Huang P., Hamuro Y., Raghuram S., Wang Y., Burris T.P., and Rastinejad F.(2008). Structural organization of the intact PPAR-c-RXR-a nuclear receptor complex on DNA. Nature 456: 350–356.

Chang E. S., and Mykles D. L. (2011). Regulation of crustacean molting: A review and our perspectives. Gen. Comp. Endocrinol. 172: 323-330.

Charles G.D. (2004). In vitro models in endocrine disruptor screening. Ilar J. 45: 494-501.

Cheek A.O. (2006). Subtle sabotage: endocrine disruption in wild populations. Rev. Biol. Trop. 54 (Suppl. 1): 1-19.

Cherbas L., and Cherbas P. (1997). ‘‘Parahomologous’’ gene targeting in Drosophila cells: an efficient, homology-dependent pathway of illegitimate recombination near a target site. Genetics 145: 349–358.

Chomczynski P., and Sacchi N. (1987). Single-step method of RNA isolation by acid guanidinium thiocyanate-phenol-chloroform extraction. Anal. Biochem. 162: 156–159.

Chow S.C., and Orrenius S. (1994). Rapid cytoskeleton modification in thymocytes induced by the immunotoxicant tributyltin. Toxicol. Appl. Pharmacol. 127:19-26.

Chung A.-C.K., Durica D.S., and Hopkins P.M. (1998). Tissue-specific patterns and steady state concentrations of ecdysteroid receptor and retinoid-X-receptor mRNA during the moult cycle of the fiddler crab, *Uca pugilator*, Gen. Comp. Endocrinol. 109: 375–389.

Chung A.-C.K., Durica D.S., Clifton S.W., Roe B.A., and Hopkins P.M. (1998). Cloning of crustacean EcR and RXR gene homologs and elevation of RXR mRNA by retinoic acid. Mol. Cell. Endocrinol. 139: 209–227.

Cieluch U., Charmantier G., Grousset E., Charmantier-Daures M., and Anger K. (2005). Osmoregulation, immunolocalization of Na^+/K^+-ATPase, and ultrastructure of branchial epithelia in the developing brown shrimp, *Crangon crangon* (Decapoda, Caridea). Physiological and Biochemical Zoology 78:1017-1025.

Cima F., and Ballarin L. (2000). Tributyltin induces cytoskeletal alterations in the colonial ascidian *Botryllus schlosseri* phagocytes via interaction with calmodulin. Aquati. Toxicol. 48: 419-429.

Clare A.S., Rittschof D., and Costlow J.D. (1992). Effects of the nonsteroidal ecdysone mimic RH 5849 on larval crustaceans. J. Exp. Zool. 262: 436–440.

Claydon K., and Owens L. (2008). Attempts at immortalization of crustacean primary cell cultures using human cancer genes. In Vitro Cell. Dev. Biol.-Anim. 44: 451–457.

Colborn T., Soto A., and von Saal F. (1993). Developmental effects of endocrine-disrupting chemicals in wildlife and humans. Environmental Health Persp. 101(5):378–384.

Conolly R.B., and Lutz W.K. (2004). Nonmonotonic dose-response relationships: Mechanistic basis, kinetic modeling, and implications for risk assessment. Toxicol. Sci. 77:151–157.

Cory A.H., Owen T.C., Barltrop J.A., and Cory J.G. (1991). Use of an aqueous soluble tetrazolium/formazan assay for cell growth assays in culture, Cancer Commun. 3: 207–212.

Cui J., Shen X., Yan Z., Zhao H., and Nagahama Y. (2009). Homology-modelled ligand binding domains of medaka oestrogen receptors and androgen receptors: A model system for the study of reproduction. Biochem. Biophys. Res. Commun. 380: 115–121.

Dalle-Donne I., Rossi R., Milzani A., Di Simplicio P., and Colombo R. (2001). The actin cytoskeleton response to oxidants: from small heat schock protein phosphorylation to changes in the redox state of actin itself. Free Radic. Biol. Med. 31: 1624-1632.

Damstra T., Barlow S., Bergmann A., Kavlock R., and Van Der Kraak G. (2002). Global Assessment of the State-of-the-Science of endocrine disruptors. International Programme on

Chemical Safety (IPCS). WHO/PCS/EDC/02.2. World Health Organization, Geneva, Switzerland, 180 pp.

Dana J.D. (1852). Conspectus of the Crustacea of the Exploring Expedition under Capt. Wilkes, U.S.N., including the Paguridea, continued, the Megalopidea, and the Macroura. Paguridea, continued, and subtribe Megalopidea.. P. Acad. Nat. Sci. Phila. 6: 6-28.

Devarakonda S., Harp J.M., Kim Y., Ozyhar A., and Rastinejad F. (2003). Structure of the heterodimeric ecdysone receptor DNA-binding complex. EMBO J. 22: 5827-5840.

Dhadialla T.S., Carlson G.R., and Le D.P. (1998). New insecticides with ecdysteroidal and juvenile hormone activity. Ann. Rev. Entomol. 43: 545–569.

Diatchenko L., Lau Y.-F.C., Campbell A.P., Chenchik A., Mogadam F., Huang B., Lukyanov S., Lukyanov K., Gurskaya N., Sverdlov E.D., and Siebert P. D. (1996). Suppression Subtractive Hybridization: A method for generating differentially regulated or tissue-specific cDNA probes and libraries. P. Natl. Acad. Sci. USA, 93: 6025-6030.

Diatchenko L., Lukyanov S., Lau Y.-F.C., and Siebert P.D. (1999). Suppression subtractive hybridization: a versatile method for identifying differentially expressed genes. Method Enzym. 303: 349-380.

Dornheim H. (1969). Beitrage zur Biologie der Garnele *Crangon crangon* (L.) in der Kieler Bucht. Ber. Dt. Wiss. Kom. fur Meeresforsch. 20: 179-215.

Drach P. (1939). Mue et cycle d'intermue chez les crustacés decapodes. Ann. Ins. Oceanogr., Vol. 19: 103-391.

Duft M., Schulte-Oehlmann U., Tillmann M., Markert B. and Oehlmann J. (2003). Toxicity of triphenyltin and tributyltin to the freshwater mudsnail *Potamopyrgus antipodarum* in a new sediment biotest. Environ. Toxicol. Chem. 22(1): 145-152.

Durica D.S., Wu X., Anilkumar G., Hopkins P.M., and Chung A.-C.K. (2002). Characterization of crab EcR and RXR homologs and expression during limb regeneration and oocyte maturation. Mol. Cell. Endocrinol. 189: 59–76.

Dyrynda E.A. (1998). Shell diseases in the common shrimp *Crangon crangon*: variations within an enclosed estuarine system. Mar. Biol. 132: 445–452.

ECHA (European Chemicals Agency) (2008). Member state committee support document for identification of bis(tributyltin)oxide as a substance of very high concern. 26pp.

Efron B. (1979). Bootstrap methods: Another look at the jackknife. Ann. Statist. 7: 1– 26.

Ehrenbaum E. (1890). Zur Naturgeschichte von *Crangon vulgaris* Fabr. Dtsch. Seefisch.-Verein, Mittl.Sekt.Küsten-u.Hochseefisch., Sonderbeilage, 9–124.

Elsby R., Maggs J.L., Ashby J., Paton D., Sumpter J.P., and Park B.K. (2001). Assessment of the effects of metabolism on the estrogenic activity of xenoestrogens: A two stage approach

coupling human liver microsomes and a yeast estrogenicity assay. Pharmacology and Experimental Therapeutics, 296(2):329-337.

Engel D.W., Brouwer M., and McKenna S. (1993). **Hemocyanin concentrations** in **marine crustaceans** as a function of environmental conditions.MEPS 93:235-244.

Eunice H. Pinn, and Alan D. Ansell (1993). The Effect of particle size on the burying ability of the brown shrimp *Crangon crangon*. Journal of the Marine Biological Association of the United Kingdom, 73: 365-377.

Evans C.J., and Smith P.J. (1975). Organotin-based antifouling systems. J. Oil Colour Chem. Assoc. 58: 160–168.

Evans R.M. (1988). The steroid and thyroid hormone receptor superfamily. Science 240: 889–895.

Evans S. (1984). Energy budgets and predation impact of dominant epibenthic carnivores on a shallow soft bottom community at the Swedish west coast. Est. Coast. Shelf Sci. 18: 651-672.

Fabricius J.C. (1795). Fabricii Entomologia Systematica, emendata et aucta, MDCCXCII. Impensis J. Nicholson, London, 122 pp.

Fang F., Xu Y., Jones D., and Jones G. (2005). Interactions of ultraspiracle with ecdysone receptor in the transduction of ecdysone- and juvenile hormone-signalling. FEBS J. 272: 1577–1589.

FAO (Food and Agriculture Organisation) (2012). FishStat Plus v.2.3. Global dataset on capture production 1950-2010. FAO (Food and Agriculture Organisation) (2012). Species Fact sheet on *Crangon crangon* (Linnaeus, 1758). http://www.fao.org/fishery/species/3435/. Retrieved March 19, 2012.

Felgenhauer B.E. (1992). Internal anatomy of the Decapoda: An overview. In: Harrison F.W (Ed.). Microscopic Anatomy of Invertebrates, Decapod Crustacea, Vol. 10. Wiley-Liss, New York: 45-75.

Fent K. (1996). Ecotoxicology of organotin compounds. Crit. Rev. Toxicol. 26: 1-117.

Féral C., and Le Gall S. (1983). The influence of a pollutant factor (tributyltin) on the neuroendocrine mechanism responsible for the occurrence of a penis in the females of *Ocenebra erinacea*. In: Lever J., and Boer H.H. (Eds.). Molluscan neuroendocrinology, North Holland Publ. co, Amsterdam: 173-175.

Fingerman S.W., and Fingerman M. (1977). Effects of a polychlorinated biphenyl and a polychlorinated dibenzofuran on molting of the fiddler crab, *Uca pugilator*. Bull. Environ. Contam. Toxicol. 18: 138–142.

Gelin A., Crivelli A.J., Rosecchi E., and Kerambrun P. (2001). Can salinity changes affect reproductive success in the brown shrimp *Crangon crangon*. J. Crustacean Biol. 21: 905-911.

Gentleman R.C., Carey V.J., Bates D.M., Bolstad B., Dettling M., Dudoit S., Ellis B., Gautier L., Ge Y., Gentry J., Hornik K., Hothorn T., Huber W., Iacus S., Irizarry R., Leisch F., Li C., Maechler M., Rossini A.J., Sawitzki G., Smith C., Smyth G., Tierney L., Yang J.Y., and Zhang J. (2004). Bioconductor: open software development for computational biology and bioinformatics. Genome biology 5: R80.

Gibbs P.E., Bryan G.W., Pascoe P.L., and Burt G.R. (1987). The use of the dogwhelk, *Nucella lapillus*, as an indicator of tributyltin (TBT) contamination. J. Mar. Biol. Assoc. UK 67:507–523.

Gilson M.K., and Honing B.H. (1987). Calculation of electrostatic potential in an enzyme active site, Nature 330: 84–86.

Gohar M., and Souty-Grosset C. (1984). Action temporelle d'ecdysteroides sur la synthese proteique ovarienne *in vitro* chez le crustacé isopode terrestrial *Porecllio dilatatus*. Reprod. Nutr. Dev. 24: 137-145.

Gómez-Mendikute A., Etxeberria A., Olabarrieta I., and Cajaraville M.P. (2002). Oxygen radicals production and actin filament disruption in bivalve haemocytes treated with benzo(*a*)pyrene. Mar. Envir. Res. 54:431-436.

Goss-Custard J.D., Day D.G., and Blindell R.M. (1977). The density of migratory and overwintering redshank *Tringa totanus* (L.) and curlew, *Numenius arquata* (L.), in relation to the density of their prey in south-east England. Estuar. coast. Mar. Sci. 5: 497–510.

Göthel S.F., and Marahiel M.A. (1999). Peptidyl-prolyl cis-trans isomerases, a superfamily of ubiquitous folding catalysts. Cell. Mol. Life Sci. 55: 423-436.

Grobben K. (1908). Die systematische Einteilung des Tierreichs. Verhandlungen der Kaiserlich-Königlichen Zoologisch-Botanischen Gesellschaft in Wien 58: 491–511.

Gunamalai V., Kirubagaran R., and Subramoniam T. (2004). Hormonal coordination of moulting and female reproduction by ecdysteroids in the mole crab *Emerita asiatica* (Milne Edwards). Gen. Comp. Endocrinol. 138: 128-138.

Gunnarsson B., Ásgeirsson Þór H. and Ingólfsson A. (2007). The rapid colonization by *Crangon crangon* (Linnaeus, 1758) (Eucarida, Caridea, Crangonidae) of Icelandic coastal waters. Crustaceana 80(6): 747-753.

Haefner Jr. P.A. (1971). Avoidance of anoxic conditions by the sand shrimp, *Crangon septemspinosa* Say. Chesapeake Science 12: 50-51.

Hagerman L. (1970). The oxygen consumption of *Crangon vulgaris* (Fabricius) (Crustacea, Natantia) in relation to salinity. Ophelia 7:283-292.

Hagerman L., and Vismann B. (1995). Anaerobic metabolism in the shrimp *Crangon crangon* exposed to hypoxia, anoxia and hydrogen sulphide. Mar. Biol. 123: 235-240.

Hall Jr. L.W., Bushong S.J., Hall W.S., and Johnson W.E. (1988). Acute chronic effects of tributyltin on a Chesapeake bay copepod, Environ. Toxicol. Chem. 7: 41–46.

Haworth A.H. (1825). A new binary arrangement of the macrurous Crustacea. Phil. Mag. Jour. 65: 183–184.

Hannas B.R., Wang Y.H., Thomson S., Kwon G., Li H., and LeBlanc G.A. (2010).. Regulation and dysregulation of vitellogenin mRNA accumulation in daphnids (*Daphnia magna*). Aquat. Toxicol.101:351-357.

Harmon M.A., Boehm M.F., Heyman R.A., and Mangelsdorf D.J. (1995). Activation of mammalian retinoid X receptors by the insect growth regulator methoprene. Proc. Natl. Acad. Sci. USA 92:6157–6160.

Hayward D.C., Bastiani M.J., Trueman J.W.H., Truman J.W., Riddiford L.M., Ball, E.E. (1999). The sequence of Locusta RXR, homologous to *Drosophila* ultraspiracle, and its evolutionary implications. Dev. Genes Evol. 209: 564–571.

Hayward D.C., Dhadialla T.S., Zong S.T., Kuiper M.J., Ball E.E., Wyatt G.R., and Walker V.K. (2003). Ligand specificity and developmental expression of RXR and ecdysone receptor in the migratory locust. J. Insect Physiol. 49: 1135–1144.

Henderson P.A., and Holmes R.H.A. (1987). On the population biology of the common shrimp *Crangon crangon* (L.) (Crustacea: Caridea) in the Severn Estuary and Bristol Channel. J. Mar. Biol. Assoc. U.K. 67:825-847.

Herrick F.H. (1911). Natural history of the American lobster. Bull. U.S. Bur. Fish. 29: 149–408.

Hiddink J.G., Marijnissen S.A.E., Troost K., and Wolff W.J. (2002). Predation on O-group and older year classes of the bivalve *Macoma balthica*: interaction of size selection and intertidal distribution of epibenthic predators. J. Exp. Mar. Biol. Ecol. 269: 223–248.

Hirano M., Ishibashi H., Yamauchi R., Kim J.-W., and Arizono K. (2008). Expression analysis of ecdysone receptor and Ultraspiracle through molting period in mysid crustacean, *Americamysis bahia.* In: Murakami Y., Nakayama K., Kitamura S.-I., Iwata H., and Tanabe S. (Eds.). Interdisciplinary Studies on Environmental Chemistry – Biological Responses to Chemical Pollutants, Terraub, Tokyo: 303-310.

Hoch M. (2001): Organotin compounds in the environment—an overview. Appl. Geochem. 16: 719–743.

Holthuijzen Y.A. (1979). Het voedsel van de zwarte ruiter *Tringa erythropus* in de Dollard. Limosa 52: 22–23.

Holthuis L.B. (1993). The recent genera of the caridean and stenopodidean shrimps (Crustacea, Decapoda). Nationaal Natuurhistorisch Museum, Leiden, 328 pp.

Hopkins P.M., Durica D., and Washington T. (2008). RXR isoforms and endogenous retinoids in the fiddler crab, *Uca pugilator*, Comp. Biochem. Physiol. 151A: 602–614.

Hopkins P. M. (1983). Patterns of serum ecdysteroids during induced and uninduced proecdysis in the fiddler crab, *Uca pugilator*. Gen. Comp. Endocrinol. 52: 350–356.

Hopkins P.M. (2009). Crustacean ecdysteroids and their receptors. In: Smagghe G. (Ed.), Ecdysone: Structures and Functions. Springer Verlag, Netherlands, 583 pp.

Hormann R.E., Smagghe G., and Nakagawa Y. (2008). Multidimensional quantitative structure-activity relationships of diacylhydrazine toxicity in *Spodoptera exigua*, *Chilo suppresalis* and *Leptinotarsa decemlineata*. QSAR Combinat. Sci. 27: 1098–1112.

Hu X., Cherbas L., and Cherbas P. (2003). Transcription activation by the ecdysone receptor (EcR/USP): Identification of activation functions. Mol. Endocrinol. 17: 716–731.

Huang Y., Zhu L.Y., and Liu G.X. (2006). The effects of bis(tributyltin) oxide on the development, reproduction and sex ratio of calanoid copepod *Pseudodiaptomus marinus*, Estuar. Coast Shelf S. 69: 147–152.

Huber W., von Heydebreck A., Sültmann H., Poustka A., and Vingron M. (2002). Variance stabilization applied to microarray data calibration and to the quantification of differential expression. Bioinformatics. 18 Suppl. 1: 96-104.

ICES (International Council for the Exploitation of the Sea), 2010. Report of the Working Group on Crangon Fisheries and Life History (WGCRAN). C.M. - International Council for the Exploration of the Sea (ICES), CM 2011/SSGEF: 17. Copenhagen, 60 pp.

ICES (International Council for the Exploitation of the Sea), 1996. Report of the Working Group on Crangon Fisheries and Life History (WGCRAN). C.M. - International Council for the Exploration of the Sea (ICES), CM 1996/K:4. Copenhagen, 53 pp.

Iguchi T., and Katsu Y. (2008). Commonality in signalling of endocrine disruption from Snail to human. BioScience 58: 1061–1067.

Iwai H., Kurosawa M., Matsui H., et al. (1992). Inhibitory effects of organotin compounds on histamine release from rat serosal mast cells. Ind. Health 30(2):77-84.

Iwema T., Chaumot A., Studer R.A., Robinson-Rechavi M., Billas I.M.L., Moras D., Laudet V., and Bonneton F (2009). Structural and evolutionary innovation of the heterodimerization interface between USP and the ecdysone receptor EcR in insects. Mol. Biol. Evol. 26: 753–768.

Iwema T., Billas I.M.L., Beck Y., Bonneton F., Nierengarten H., Chaumot A., Richards G., Laudet V., and Moras D. (2007). Structural and functional characterization of a novel type of ligand-independent RXR-USP receptor, EMBO J. 26: 3770–3782.

Johansen K., and Mohlenberg F. (1987). Impairment of egg production in *Acartia tonsa* exposed to tributyltin oxide, Ophelia 27: 137–141.

Johnston D.J., Alexander C.G., and Yellowhees D. (1998). Epithelial cytology and function in the digestive gland of *Thenus orientalis* (Decapoda, Scyllaridae). J. Crust. Biol. 18: 271-278.

Kang J.J., Liu S.H., Chen I.L., Cheng Y.W., and Lin-Shiau S.Y. (1998). Comparative studies on the induction of muscle contracture in mouse diaphragm and Ca2_ release from sarcoplasmic reticulum vesicles by organotin compounds. Pharmacol. Toxicol 82: 23–27.

Kannan S., Corsolini S., Focardi S., Tanabe S., and Tatsukawa R. (1996). Accumulation pattern of butyltin compounds in dolphin, tuna and shark collected from Italian coastal waters. Arch. Environ. Contam. Toxicol. 31: 19–23.

Karim F.D., and Thummel C.S. (1992). Temporal coordination of regulatory gene expression by the steroid hormone ecdysone. EMBO J. 11:4083–4093.

Kato Y., Kobayashi K., Oda S., Tatarazako N., Watanabe H., and Iguchi T. (2007). Cloning and characterization of the ecdysone receptor and ultraspiracle protein from the water flea *Daphnia magna*. J. Endocrinol. 193: 183–194.

Kauffmann A., Gentleman R., and Huber W. (2009). ArrayQualityMetrics: a bioconductor package for quality assessment of microarray data. Bioinformatics 25: 415-416.

Kemp P. F., and Swartz R. C. (1988). Acute toxicity of interstitial and particle-bound cadmium to a marine infaunal amphipod. Mar. Environ. Res. 26: 135-153.

Kim H.W., Lee S.G., and Mykles D.L. (2005). Ecdysteroid-responsive genes, RXR and E75, in the tropical land crab, *Gecarcinus lateralis*: differential tissue expression of multiple RXR isoforms generated at three alternative splicing sites in the hinge and ligand-binding domains. Mol. Cell. Endocrinol. 242: 80–95.

Kim G.B., Lee J.S., Tanabe S., Iwata H., Tatsukawa R., and Shimazaki K. (1996). Specific accumulation and distribution of butyltin compounds in various organs and tissues of the Steller sea lion (*Eumetopias jubatus*) comparison with organochlorine accumulation pattern. Mar. Pollut. Bull. 32: 558–563.

Kjaerstad M.B., Taxvig C., Andersen H.R., and Nellemann C. (2009). Ecdysone: Structures and Functions. Springer Verlag, Netherlands, 583 pp.

Kleszcynska H., Hladyszowski S., Pruchnic H., and Przestalski S. (1997). Erythrocyte haemolysis by organic tin and leach compounds. Z.- Naturforsch C. 52: 65 -69.

Klingmüller B., and Waterman D. (2003). TBT – Zinnorganische Verbindungen – Eine wissenschaftliche Bestandsaufnahme. UBA-Texte 16/2003, Berlin.

Kneller D.G., Cohen F.E., and Langridge R. (1990). Improvements in protein secondary structure prediction by an enhanced neural network. J. Mol. Biol. 214: 171–182.

Knust R. (1990). The black-spot disease in *Crangon crangon* (L.) of the German Bight. ICES CM 1990/E32: 1-9.

Kuipers B., and Dapper R. (1984). Nursery function of the Wadden Sea tidal flats for the brown shrimp *Crangon crangon*. Mar. Ecol. Prog. Ser. 17:171-181.

Kusk K.O., and Petersen S. (1997). Acute and chronic toxicity of tributyltin and linear alkylbenzene sulfonate to the marine copepod *Acartia tonsa*. Environ. Toxicol. Chem. 16: 1629–1633.

Labat J.-P. (1977). Ecologie de *Crangon crangon* (L.) (Decapoda, Caridea) dans un etang de la cote Languedocienne I. - Croissance, reproduction, migrations mer/etang. Vie Milieu 27: 273-292.

Landrum P. F. (1989). Bioavailability and toxicokinetics of polycyclic aromatic hydrocarbons sorbed to sediments for the amphipod *Pontoporeia hoyi*. Environ. Sci. Technol. 23: 588-595.

Langston W. J., and Pope N. D. (1995). Determinants of TBT adsorption and desorption in estuarine sediments. Mar. Pollut. Bull. 31: 32-43.

Larkin M.A., Blackshields G., Brown N.P., Chenna R., McGettigan P.A., McWilliam H., Valentin F., Wallace I.M., Wilm A., Lopez R., Thompson J.D., Gibson T.J., and Higgins D.G. (2007). Clustal W and Clustal X version 2.0. Bioinformatics 23: 2947–2948.

Laskowski R.A., MacArthur M.W., Moss D.S., and Thornton J.M (1993). PROCHECK: a program to check the stereochemistry of protein structures, J. Appl. Cryst. 26: 283–291.

Latreille P. A. (1802). Histoire naturelle générale et particulière des Crustacés et des insectes. Tome 3. Paris: Imprimerie F. Dufart, 467 pp.

Latreille P. A. (1803). Histoire naturelle générale et particulière des Crustacés et des insectes. Tome 5. Paris: Imprimerie F. Dufart, 406 pp.

Laufer H., Ahl J., and Sagi A. (1993). The role of juvenile hormones in crustacean reproduction. Am. Zool. 33: 365-374.

Laufer H., Borst D., Baker F., Carrasco C., Sinkus M., Reuter C., Tsai L., and Schooley D. (1987). Identification of a juvenile hormone-like compound in a crustacean. Science 235: 202-205.

Laughlin Jr. R.B., and French W.J. (1980). Comparative study of the acute toxicity of a homologous series of trialkyltins to larval shore crabs, *Hemigrapsus nudus*, and lobster, *Homarus americanus*. Bull. Environ. Contam. Toxicol. 25: 802–809.

Laughlin R.B. Jr., French W., and Guard H.E. (1986). Accumulation of bis(tributyltin) oxide by the marine mussel *Mytilus edulis*. Environ. Sci. Technol. 20: 884-890.

le Maire A., Grimaldi M., Roecklin D., Dagnino S., Vivat-Hannah V., Balaguer P., and Bourguet W.(2009). Activation of RXR–PPAR heterodimers by organotin environmental endocrine disruptors, EMBO Rep. 10: 367–373.

Lee R.F., Valkirs A.O., and Seligman P.F. (1989). Importance of microalgae in the biodegradation of tributyltin in estuarine waters. Environ Sci. Technol. 23:1515-1518.

Lee R.F. (1996). Metabolism of tributyltin by aquatic organisms. In: Organotin: Environmental fate and effects. Champ M.A. and Seligman P.F. (Eds.), Chapman and Hall, London, pp. 369-382.

Lee I.L.E.J., Martin W.J., Christie A., Frischer M., Soin T., Smagghe G., Braid H., and Hanner R. (2011). Misidentification of OLGA-PH-J/92, believed to be the only crustacean cell line. In Vitro Cell. Dev. Biol. – anim. 47: 665-674.

Lewin R. (1984). Microbial adhesion is a sticky problem. Science vol. 224 no. 4647: 375-377.

Lill M.A., Dobler M., and Vedani A. (2005). In silico prediction of receptor-mediated environmental toxic phenomena – application to endocrine disruption. SAR QSAR Environ. Res. 16: 149–169.

Lloyd A.J., and Yonge C.M. (1947). The biology of *Crangon vulgaris* L. in the Bristol Channel and Severn estuary. J. Mar. Biol. Ass. U.K. 26: 626–661.

Luttikhuizen P.C., Campos J., Bleijswijk J., Peijnenburg K.T.C.A. and Van der Veer H.W. (2008). Phylogeography of the common shrimp, *Crangon crangon* (L.) in European waters. Mol. Phylogenet. Evol. 46: 1015–1030.

Ma H.Z., Dai S.G., and Huang G.L. (2000). Distribution of tributyltin chloride in laboratory simulated estuarine microcosms. Water Res 34:2829–2841.

Maguire R.J., Carey J.H., and Hale E.J. (1983). Degradation of the tri-n-butyltin species in water. J. Agric. Food Chem., 31: 1060–1065.

Maki A., Sawatsubashi S., Ito S., Shirode Y., Suzuki E., Zhao Y.,Yamagata K., Kouzmenko A., Takeyema K., and Kato S. (2004). Juvenile hormones antagonize ecdysone actions through co-repressor recruitment to EcR/USP heterodimers. Biochem. Biophys. Res. Commun. 320: 262–267.

Mangelsdorf D.J., Thummel C., Beato M., Herrlich P., Schutz G., Umesono K., Blumberg B., Kastner P., Mark M., Chambon P., and Evans R.M.(1995). The nuclear receptor superfamily: the second decade. Cell. 83:835–839.

Mark M., and Chambon P. (2003). Functions of RARs and RXRs in vivo: Genetic dissection of the retinoid signalling pathway. Pure Appl. Chem. 75: 1709–1732.

Martens E., and Redant F. (1986). Protandric hermaphroditism in the brown shrimp *Crangon crangon* (L.), and its effects on recruitment and reproductive potential. International Council for the exploration of the Sea Shellfish Committee: 1-15.

Martin J.W., and Davis G.E. (2001). An Updated Classification of the Recent Crustacea. Natural History Museum of Los Angeles County. 132 pp.

Mas M.T., Smith K.C., Yarmush D.L., Aisaka K., and Fine R.M. (1992). Modelling the anti-CEA antibody combining site by homology and conformational search. Proteins Struc. Func. Genet. 14: 483–498.

Matthiessen P., and Gibbs P.E. (1998). Critical appraisal of the evidence for tributyltin-mediated endocrine disruption in molluscs. Environ. Toxicol. Chem. 17:37-43.

Matthiessen P., Reynoldson T., Billinghurst Z., Brassard D.W., Cameron P., Chandler G.T., Davies I.M., Horiguchi T., Mount D.R., Oehlmann J., Pottinger T.G., Sibley P.K,. Thompson A., and Vethaak A.D. (1999). Field assessment for endocrine disruption in invertebrates. In: de Fur P.L., Ingersoll C., and Tattersfield L. (Eds.). Endocrine disruption in invertebrates: endocrinology, testing, and assessment. SETAC Press, Pensacola, Florida: 199-270.

Mazurová E., Hilscherová K., Triebskorn R., Köhler H.-R., Maršálek B., and Bláha L. (2008). Endocrine regulation of the reproduction in crustaceans: Identification of potential targets for toxicants and environmental contaminants. Biologia 63: 139-150.

McAllister B.G., and Kime D.E. (2003). Early life exposure to environmental levels of the aromatase inhibitor tributyltin causes masculinisation and irreversible sperm damage in zebrafish (*Danio rerio*). Aquat. Toxicol. 65:309–316.

McClelland J.L., and Rumelhart D.L. (1988). Explorations in Parallel Distributed Processing vol. 3. MIT Press, Cambridge MA. : 318–362.

Meiler J., and Baker D. (2003). Coupled prediction of protein secondary and tertiary structure, Proc. Natl. Acad. Sci. USA 100: 12105–12110.

Meiler J., Müller M., Zeidler A., and Schmäschke F. (2001). Generation and evaluation of dimension-reduced amino acid parameter representations by artificial neural networks. J. Mol. Model. 7: 360–369.

Meng Y., and Zou E. (2009a). Impacts of moult-inhibiting organochlorine compounds on epidermal ecdysteroid signalling in the fiddler crab, *Uca pugilator*, in vitro. Comp. Biochem. Physiol. 150C: 436–441.

Meng Y., and Zou E. (2009b). A Molecular Biomarker for Disruption of Crustacean Molting: The N-acetyl-beta-glucosaminidase mRNA in the Epidermis of the Fiddler Crab. Bull. Environ. Contam. Toxicol. 82: 554-558.

Messing J., Gronenborn B., Mueller-Hill B., and Hofschneider P.H (1977). Filamentous coliphage M13 as a cloning vehicle: insertion of a HindII fragment of the lac regulatory region in M13 replicative form in vitro. P. Natl. Acad. Sci. USA Volume 74, Issue 9: 3642-3646.

Minucci S., Leid M., Toyama R., Saint-Jeannet J.P., Peterson V.J., Horn V., Ishmael J.E., Bhattacharyya N., Dey A., Dawid I.B., and Ozato K. (1997). Retinoid X receptor (RXR) within the RXR-retinoic acid receptor heterodimer binds its ligand and enhances retinoid-dependent gene expression. Mol. Cell. Biol. 15: 6481– 6487.

Montagna M.C., and Collins P.A. (2007). Survival and growth of *Palaemonetes argentines* (Decapoda: Caridea) exposed to insecticides with chlorpyrifos and endosulfan as active element. Arch. Environ. Contam. Toxicol. 53: 371–378.

Monteyne E., Strand J., Vorkamp K., Bersuder P., Bolam T., Giltrap M., and McGovern E. (2010). Monitoring organotins in marine biota. ICES Techniques in Marine Environmental Sciences, vol. 47: 16.

Morton B. (2009). Recovery from imposex by a population of the dog whelk, *Nucella lapillus* (Gastropoda: Caenogastropoda), on the south eastern coast of England since May 2004: a 52-month study. Mar. Pollut. Bull. 58: 1530–1538.

Mouillet J.F., Delbecque J.P., Quennedey B., and Delachambre J. (1997). Cloning of two putative ecdysteroid receptor isoforms from *Tenebrio molitor* and their developmental expression in the epidermis during metamorphosis. Eur. J. Biochem. 248: 856–863.

Mu X., and LeBlanc G.A. (2004). Cross communication between signalling pathways: Juvenoid hormones modulate ecdysteroid activity in a crustacean, J. Exp. Zool. 301A: 793–801.

Mu Y.M., Yanase T., Nishi Y., Takayanagi R., Goto K., and Nawata H. (2001). Combined treatment with specific ligands for PPARγ:RXR nuclear receptor system markedly inhibits the expression of cytochrome P450 aromatase in human granulosa cancer cells. Mol. Cell. Endocrinol. 181:239–248.

Murbach R., and Corbaz R. (1963). Influence of three types of fungicide used in Switzerland against potato mildew (*Phytophthora infestans* [Mont.] de Bary) on the density of the population of doryphore (*Leptinotarsa decemlineata say.*). Phytopath. Z., 47 (2): 182-188.

Nahoum V., Perez E., Germain P., Rodriguez-Barrios F., Manzo F., Kammerer S., Lemaire G., Hirsch O., Royer C.A., Gronemeyer H., de Lera A.R., and Bourguet W. (2007). Modulators of the structural dynamics of the retinoid X receptor to reveal receptor function. Proc. Natl. Acad. Sci. USA 104: 17323–17328.

Nakagawa Y., Sakai A., Magata F., Ogura T., Miyashita M., and Miyagawa H. (2007). Molecular cloning of the ecdysone receptor and the retinoid X receptor from the scorpion *Liocheles australasiae*, FEBS J. 274: 6191–6203.

Nakagawa Y., Hormann R.E., and Smagghe G. (2009). SAR and QSAR studies for in vivo and in vitro activities of ecdysone agonists. In: Smagghe, G. (Ed.), Ecdysteroids Structures and Functions. Springer, Berlin, 583 pp.

Nicholls A., Sharp K.A., and Honig B. (2005). Protein folding and association: insights from the interfacial and thermodynamic properties of hydrocarbons, Proteins Struc. Func. Genet. 11: 281–296.

Nishikawa J., Mamiya S., Kanayama T., Nishikawa T., Shiraishi F., and Horiguchi T.(2004). Involvement of the retinoid X receptor in the development of imposex caused by organotins in gastropods, Environ. Sci. Technol. 38: 6271–6276.

Novac N., and Heinzel T. (2004). Nuclear receptors: overview and classification. Curr. Drug Targets Inflamm. Allergy. 3(4):335–346.

Oberdörster E., Rittschof D., and LeBlanc G.A. (1998). Alteration of [14C]-testosterone metabolism after chronic exposure of *Daphnia magna* to tributyltin, Arch. Environ. Contam. Toxicol. 34: 21–25.

Oberdörster E. and McClellan-Green P. (2000): The neuropeptide APGWamide induces imposex in the mud snail, *Ilyanassa obsoleta*. Peptides, 21: 1323–1330.

Oehlmann J., Bauer B., Minchin D., Schulte-Oehlmann U., Fioroni P. and Markert B. (1998). Imposex in *Nucella lapillus* and intersex in *Littorina littorea*: Interspecific comparison of two TBT-induced effects and their geographical uniformity. Hydrobiologia 378:199-213.

Ogura T., Minakuchi C., Nakagawa Y., Smagghe G., and Miyagawa H. (2005). Molecular cloning, expression analysis and functional confirmation of ecdysone receptor and Ultraspiracle from the Colorado potato beetle *Leptinotarsa decemlineata*, FEBS J. 272: 4114–4128.

Oh C.-W., Hartnoll R., and Nash R.D.M. (1999). Population dynamics of the common shrimp, *Crangon crangon* (L.), in Port Erin Bay, Isle of Man, Irish Sea. ICES J. Mar. Sci. 56:718-733.

Oh C.-W., Hartnoll R.G. and Nash R.D.M. (2001). Feeding ecology of the common shrimp *Crangon crangon* in Port Erin Bay, Isle of Man, Irish Sea. Mar. Ecol. Prog. Ser. 214: 211-223.

Ohji M., Arai T., and Miyazaki N. (2002). Effects of tributyltin exposure in the embryonic stage on sex ratio and survival rate in the caprellid amphipod *Caprella danilevskii*, Mar. Ecol. Prog. Ser. 235: 171–176.

Okumura T., Han C.H., Suzuki Y., Aida K., and Hanyu I. (1992). Changes in hemolymph vitellogenin and ecdysteroid levels during the reproductive and non-reproductive moult cycles in the freshwater prawn *Macrobrachium nipponense*. Zool. Sci. 9: 37-45.

Oliveira I.B., Richardson C.A., Sousa A.C., Takahashi S., Tanabe S., and Barroso C.M. (2009). Spatial and temporal evolution of imposex in dog whelk *Nucella lapillus* (L.) populations from North Wales, UK. J. Environ. Monit 11: 1462–1468.

Omae I. (2003). General aspects of tin-free antifouling paints. Chem Rev 103:3431–3448.

Omae I. (1989). Organotin Chemistry (J. Organomet. Chem. Library, vol. 21), Elsevier, Amsterdam, 355 pp.

Oro A.E., McKeown M., and Evans R.M. (1990). Relationship between the product of the *Drosophila* ultraspiracle locus and the vertebrate retinoid X receptor. Nature 347:298–301.

OSPAR Commission (2011). Background document on organic tin compounds. 33 pp.

Ouali M., King R.D. (2000). Cascaded multiple classifiers for secondary structure prediction. Prot. Sci. 9: 1162–1176.

Page D.S., Dassanayake T.M., and Gilfillan E.S. (1995). Tissue distribution and depuration of tributyltin for field-exposed *Mytilus edulis*. Mar. Environ. Res., 40: 409–421.

Palma P., Palma V.L., Matos C., Fernandes R.M., Bohn A., Soares A.M.V.M., and Barbosa L.R. (2009). Effects of atrazine and endosulfan sulphate on the ecdysteroid system of *Daphnia magna*. Chemosphere 74: 676–681.

Paschke K.A., Gebauer P., Buchholz F., and Anger K. (2004). Seasonal variation in starvation resistance of early larval North Sea shrimp *Crangon crangon* (Decapoda: Crangonidae). Mar. Ecol-Prog. Ser. 279:183-191.

Passano L.M. (1960). Moulting and its control. In: Waterman T.H. (Ed.). The Physiology of Crustacea Vol. 1, Academic Press, New York, 670 pp.

Pennant, T. (1777). A British Zoology, Vol. 4. Benj. White, London, 236 pp.

Penninks A.H. (1993). The evaluation of data-derived safety factors for bis(tri-n-butyltin) oxide. Food Addit. Contam. 10: 351–361.

Petersen B., Lundegaard C., and Petersen T.N. (2010). NetTurnP – neural network prediction of beta-turns by use of evolutionary information and predicted protein sequence features, PLoS ONE 5 e15079.

Pignatello J.J., and Xing B. (1996). Mechanisms of slow sorption of organic chemicals to natural particles. Environ. Sci. Technol. 30: 1–11.

Pihl L. and Rosenberg R. (1982). Production, abundance and biomass of mobile epibenthic marine fauna in shallow waters, western Sweden. J. Exp. Mar. Biol. Ecol. 57: 273-301.

Pihl L., and Rosenberg R. (1984). Food selection and consumption of the shrimp *Crangon crangon* in some shallow marine areas in western Sweden. Mar. Ecol. Prog. Ser. 18: 159–168.

Plagmann J. (1939). Ernahrungsbiologie der Garnele (*Crangon vulgaris* Fabr.). Helgolander Meeresun. 2: 113-162.

Pollastri G., McLysaght A. (2005). Porter: A new, accurate server for protein secondary structure prediction. Bioinformatics 2: 1719–1720.

Ponder J.W., Richards F.M. (1987). Tertiary templates for proteins use of packing criteria in the enumeration of allowed sequences for different structural classes. J. Mol. Biol. 193: 775–791.

Pongsomboon S., Tang S., Boonda S., Aoki T., Hirono I., Yasuike M., and Tassanakajon A. (2008). Differentially expressed genes in *Penaeus monodon* hemocytes following infection with yellow head virus. BMB Rep. 41: 670–677.

Price R.K.J., Uglow R.F. (1979). Some effects of certain metals on development and mortality within the moult cycle of *Crangon crangon* (L.). Mar. Environ. Res. 2: 287–299.

Redant F., and Polet H. (2002). De garnaalvisserij: een kustgebruikersgroep met kopzorgen. De Grote Rede 5: 13–17.

Redant F. (1978). Consumptie en productie van post-larvale *Crangon crangon* (L.) (Crustacea, Decapoda) in de Belgische kustwateren. PhD Thesis. Vrije Universiteit Brussel.

Reise K. (1977). Predator exclusion experiments in an intertidal mud flat. Helgolander Meeresun. 30: 263-271.

Risler J.L., Delorme M.O., Delacroix H., and Henaut A. (1998). Amino acid substitutions in structurally related proteins a pattern recognition approach. Determination of a new an efficient scoring matrix. J. Mol. Biol. 204: 1019–1029.

Robinson-Rechavi M., Marchand O., Escriva H., and Laudet V. (2001). An ancestral whole-genome duplication may not have been responsible for the abundance of duplicated fish genes. Curr. T. Biol. 11:R458–R459.

Rodríguez J.G., Tueros I., Borja A., Franco J., García Alonso J.I., Garmendia J.M., Muxika I., Sariego C., and Valencia V. (2009). Butyltin compounds, sterility and imposex assessment in *Nassarius reticulates* (Linneaus, 1758), prior to the 2008 European ban on TBT antifouling paints, within Basque ports and coastal areas. Cont. Shelf Res. 29: 1165–1173.

Rodríguez E.M., Medesani D.A., and Fingerman M. (2007) Endocrine disruption in crustaceans due to pollutants: a review. Comp. Biochem. Physiol. A: 661–671.

Rodríguez-Ortega M.J., Grøsvik B.E., Rodríguez-Ariza A., Goksøyr A., and López-Barea J. (2003). Changes in protein expression profiles in bivalve molluscs (*Chamaelea gallina*) exposed to four model environmental pollutants. Proteomics 3: 1535–1543.

Ronis M. J. J. and Mason A.Z. (1996). The metabolism of testosterone by the periwinkle (*Littorina littorea*) in vitro and in vivo: Effects of tributyltin. Mar. Environ. Res. 42: 161–166.

Roy B., Taneja R., and Chambon P. (1995). Synergistic activation of retinoic acid (RA)-responsive genes and induction of embryonal carcinoma cell differentiation by an RAR receptor a (RARa)-, RARb-, or RARc-selective ligand in combination with a Retinoid X receptor-specific ligand. Mol. Cell. Biol. 15: 6481–6487.

RPA (Risk & Policy Analysts Limited) (2003). Revised assessment of the risks to health and the environment associate with the use of organostannic compounds (excluding use in antifouling paints. RPA Organotin Report 12-2003, prepared for European Commission Directorate-General Enterprise and Industry, December 2003.

RPA (Risk & Policy Analysts Limited) (2005). Risk assessment studies on targeted consumer applications of certain organotin compounds. RPA Organotin Report 9-2005, prepared for European Commission Directorate-General Enterprise and Industry, September 2005.

RPA (Risk & Policy Analysts Limited) (2007). Impact Assessment of Potential Restrictions on the Marketing and Use of Certain Organotin Compounds, RPA Organotin Report 10-2007, prepared for European Commission Directorate-General Enterprise and Industry, October 16, 2007.

Saitoh M., Yanase T., Morinaga H., Tanabe M., Mu Y.M., Nishi Y., Nomura M., Okabe T., Goto K., Takayanagi R., and Nawata H. (2001). Tributyltin or triphenyltin inhibits aromatase

activity in the human granulosa-like tumour cell line KGN. Biochem. Biophys. Res. Commun. 289:198–204.

Saitou N., and Nei M. (1987). The neighbour-joining method: A new method for reconstructing phylogenetic trees. Mol. Biol. Evol. 4: 406–425.

Salazar M.H. and Salazar S.M. (1996). Mussels as bio indicators: effects of TBT on survival, bioaccumulation and growth under natural conditions. In: Champ M.A. and Seligman P.F. (Eds.). Organotin: Environmental Fate and Effects. Chapman & Hall. pp. 305-330.

Sarradin P. M., Lapaquellerie Y., Astruc A., Latouche C., and Astruc M. (1995). Long term behaviour and degradation kinetics of tributyltin in a marina sediment. Sci. Total Environ. 170: 59–70.

Schimmel S.C., Patrick Jr. J.M., Faas L.F., Oglesby J.L., and Wilson Jr. A.J. (1979). Kepone: Toxicity and bioaccumulation in blue crabs. Estuaries 2: 9–15.

Schmidt K., Steinberg C.E.W., Staaks G., and Pflugmacher S. (2005). Influence of a xenobiotic mixture (PCB and TBT) compared to single substances on swimming behaviour or reproduction of *Daphnia magna*, Acta Hydrochim. Hydrobiol. 33: 287–300.

Shimasaki Y., Kitano T., Oshima Y., Inoue S., Imada N., and Honjo T. (2003). Tributyltin causes masculinization in fish. Environ. Toxicol. Chem. 22: 141-144.

Siegel V., Damm U., and Neudecker T. (2008). Sex-ratio, seasonality and long-term variation in maturation and spawning of the brown shrimp *Crangon crangon* (L.) in the German Bight (North Sea). Helgol. Mar. Res. 62: 339-349.

Skinner D.M. (1962). The structure and metabolism of a crustacean integumentary tissue during a moult cycle. Biol. Bull. Mar. Biol. Lab., Woods Hole, 123: 635–647.

Sluder A. E., Mathews S.W., Hough D., Yin V.P., and Maina C.V. (1999). The nuclear receptor superfamily has undergone extensive proliferation and diversification in nematodes. Genome Res. 9:103–120.

Smedes F., de Jong A.S., and Davies I.M. (2000). Determination of (mono-, di- and) tributyltin in sediments. Analytical methods. J. Environ. Monit. 2: 541–549.

Smith B.S. (1981). Tributyltin compounds induce male characteristics on female mud snails *Nassarius obsoletus* = Ilyanassa obsolete, J. Appl. Toxicol. 1: 141– 144.

Smyth G. K. (2005). Limma: linear models for microarray data. In: Bioinformatics and Computational Biology Solutions using R and Bioconductor, R. Gentleman, V. Carey, S. Dudoit, R. Irizarry, W. Huber (eds.), Springer, New York, pp. 397–420.

Snyder M.J., and Mulder E.P. (2001). Environmental endocrine disruption in decapod crustacean larvae: Hormone titers, cytochrome P450, and stress protein responses to heptachlor exposure. Aquat. Toxicol. 55: 177–190.

Soin T., Swevers L., Kotzia G., Iatrou K., Janssen C.R., Rougé P., Harada T., Nakagawa Y., and Smagghe G. (2010). Comparison of activity of non-ecdysteroidal ecdysone agonists between dipteran and lepidopteran insects using cell-based EcR reporter assays, Pest Manag. Sci. 66: 1215–1229.

Soin T., Iga M., Swevers L., Rougé P., Janssen C.R., and Smagghe G. (2009). Towards Coleoptera-specific high-throughput screening systems for compounds with ecdysone activity: development of EcR reporter assays using weevil (*Anthonomus grandis*)-derived cell lines and in silico analysis of ligand binding to *A. Grandis* EcR ligand-binding pocket, Insect Biochem. Mol. Biol. 39: 523–534.

Soin T., De Geyter E., Mosallanejad H., Iga M., Martin D., Ozaki S., Kitsuda S., Harada T., Miyagawa H., Stefanou D., Kotzia G., Efrose R., Labropoulou V., Geelen D., Iatrou K., Nakagawa Y., Janssen C.R., Smagghe G., and Swevers L. (2010). Assessment of species specificity of molting accelerating compounds in lepidopteran insects: Comparison of activity between *Bombyx mori* and *Spodoptera littoralis* by in vitro reporter and in vivo toxicity assays. Pest Manag. Sci. 66: 526–535.

Sousa A., Laranjeiro F., Takahashi S., Tanabe S., and Barroso C.M. (2009). Imposex and organotin prevalence in a European post-legislative scenario: temporal trends from 2003 to 2008. Chemosphere 77: 566–573.

Steel C.G.H., and Vafopoulou X. (1998). Ecdysteroid titers in haemolymph and other tissues during molting and reproduction in the terrestrial isopod, *Oniscus ascellus* (L.). Invertebr. Reprod. Develop. 34: 187-194.

Stockdale M., Dawson A.P., and Selwyn M.J. (1970). Effects of trialkyltin and triphenyltin compounds on mitochondrial respiration. Eur. J. Biochem. 15: 342–351.

Stridh H., Fava E., Single B., et al. (1999). Tributyltin-induced apoptosis requires glycolytic adenosine triphosphate production. Chem Res Toxicol 12:874-882.

Swevers L., Cherbas L., Cherbas P., and Iatrou K. (1996). Bombyx EcR (BmEcR) and Bombyx USP (BmCF1) combine to form a functional ecdysone receptor, Insect Biochem. Mol. Biol. 26: 217–221.

Takahashi S., Tanabe S., Takeuchi I., and Miyazak N. (1999). Distribution and specific bioaccumulation of butyltin compounds in a marine ecosystem. Arch. Environ. Contam. Toxicol. 37: 50–61.

Tamura K., Dudley J., Nei M., and Kumar S. (2007). MEGA4: Molecular evolutionary genetics analysis (MEGA) software version 4.0. Mol. Biol. Evol. 24: 1596–1599.

Tanabe S. (1999). Butyltin contamination in marine mammals, a review. Mar. Pollut. Bull. 39: 62–72.

Thompson J.D., Gibson T.J., Plewniak F., Jeanmougin F., and Higgins D.G. (1997). The CLUSTAL-X windows interface. Flexible strategies for multiple sequence alignment aided by quality analysis tool. Nucleic Acids Res. 15: 4876–4882.

Tocchini-Valentini G.D., Rochel N., Escriva H., Germain P., Peluso-Iltis C., Paris M., Sanglier-Cianferani S., Van Dorsselaer A., Moras D., and Laudet V. (2009). Structural and functional insights into the ligand-binding domain of a nonduplicated Retinoid X nuclear receptor from the invertebrate chordate *Amphioxus*. *J.* Biol. Chem. 384: 1938–1948.

Urbanciková M., and Korytár P. (1999). Cu-complex counteracts the effect of paraquat on polymerized actin. Toxicol. In Vitro 13: 785-788.

Van Donk E, and De Wilde P.A.W.J. (1981). Oxygen consumption and motile activity of the brown shrimp *Crangon crangon* related to temperature and body size. Neth. J. Sea Res. 15: 54-64.

VanderKerk G.J.M., and Luijten J.G.A. (1954). Investigation on organotin compounds. III: the biocidal properties of organotin compounds. J. Appl. Chem., 4: 314–326.

Vedani A., Dobler M., and Lill M.A. (2006). The challenge of predicting drug toxicity *in silico*. Basic Clin. Pharmacol. Toxicol. 99: 195–208.

Veltman K., Huijbregts M.A.J., van den Heuvel-Greve M.J., Vethaak A.D., and Hendriks A.J. (2006). Organotin accumulation in an estuarine food chain: comparing field measurements with model estimations. Mar. Environ. Res. 61: 511–530.

Verhaegen Y., Parmentier K., Swevers L., Rougé P., Soin T., De Coen W., Cooreman K., and Smagghe G. (2010). The brown shrimp (*Crangon crangon* L.) ecdysteroid receptor complex: cloning, structural modelling of the ligand-binding domain and functional expression in an EcR-deficient Drosophila cell line, Gen. Comp. Endocrinol. 168: 415–423.

Verhaegen Y., Parmentier K., Swevers L., Renders E., Rougé P., De Coen W., Cooreman K., and Smagghe G. (2011). The heterodimeric ecdysteroid receptor complex in the brown shrimp *Crangon crangon*: EcR and RXR isoform characteristics and sensitivity towards the marine pollutant tributyltin. Gen. Comp. Endocrinol. 172: 158–169.

von Ballmoos C., Brunner J., and Dimroth P. (2004). The iono channel of F-ATP synthase is the target of toxic organotin compounds. P. Natl Acad. Sci. 101: 11239–11244.

Von Siebold K.T.E, and Stannius H.F. (1845).

Waddy S.L., Burridge L.E., Hamilton M.N., Mercer S.M., Aiken D.E., and Haya K. (2002). Emamectin benzoate induces molting in American lobster, *Homarus americanus*. Can. J. Fish Aquat. Sci. 59: 1096–1099.

Walker D.M., and Gore A.C. (2011). Transgenerational neuroendocrine disruption of reproduction. Nat Rev Endocrinol. 7:197-207.

Walter U. and Becker P.H. (1997). Occurence and consumption of seabirds scavenging on shrimp trawler discards in the Wadden Sea. ICES J. Mar. Sci. 54: 684-694.

Wang Y.H., and LeBlanc G.A. (2009). Interactions of methyl farnesoate and related compounds with a crustacean retinoid X receptor, Mol. Cell. Endocrinol. 309: 109–116.

Wang Y.H., Wang G.R., and LeBlanc G.A. (2007). Cloning and characterization of the retinoid X receptor from a primitive crustacean *Daphnia magna*, Gen. Comp. Endocrinol. 150: 209–318.

Wang Y.H., Kwon G., Li H., and LeBlanc G.A. (2011). Tributyltin synergizes with 20-hydroxyecdysone to produce endocrine toxicity. Toxicol. Sci. 123: 71-79.

Watermann B., and Dethlefsen V. (1983). Black spot disease of shrimps - an environmental problem, a disease or wounds. Fischwirtsch 30: 24–29.

Weber R.E., and Spaargaren D.H. (1970). On the influence of temperature on the osmoregulation of *Crangon crangon* and its significance under estuarine conditions. Netherlands J. Sea Res., 5: 108–120.

Weis J.S., Gottlieb J., and Kwiatkowski J. (1987). Tributyltin retards generation and produces deformities of limbs in the fiddler crab, *Uca pugilator*. Arch. Environ. Contam. Toxicol. 16: 321–326.

Weis J.S., and Mantel L.H. (1976). DDT as an accelerator of regeneration and molting in fiddler crabs. Estuar. Coast Mar. Sci. 4:461–466.

Welleman H.C., and Daan N. (2001). Is the Dutch shrimp fishery sustainable? Senckenb. Marit. 31: 321-328.

Wennhage H. (2002). Vulnerability of newly settled plaice *Pleuronectes platessa* L. to predation: effects of habitat structure and predator functional response. J. Exp. Mar. Biol. Ecol. 269: 129–145.

Wennhage H., and Gibson R.N. (1998). Influence of food supply and a potential predator (*Crangon crangon*) on settling behaviour of plaice (*Pleuronectes platessa)*. J. Sea Res. 39: 103–112.

Werle E., Schneider C., Renner M., Völker M., and Fiehn W. (1994). Convenient single-step, one tube purification of PCR products for direct sequencing, Nucleic Acids Res., 22: 4354-4355.

Wilcox J. R., and Jeffries H. P. (1974). Feeding habits of the sand shrimp *Crangon septemspinosa.* Biol. Bull. Mar. Biol. Lab., Woods Hole 146: 424-434.

Willemsen F., Wegener J.-W., Morabito R., and Pannier F. (2004). Sources, Consumer Exposure and Risks of Organotin Contamination in Seafood. Final report of the European Commission Research Project ‘‘OT-SAFE’’ (QLK1-2001-01437), 143 pp.

Wolf G. (2006). Is 9-cis-retinoic acid the endogenous ligand for the retinoic acid-X receptor? Nutr. Rev. 64: 532–538.

Wu X.H., Hopkins P.M., Palli S.R., and Durica D.S. (2004). Crustacean retinoid-X receptor isoforms: distinctive DNA binding and receptor-receptor interaction with a cognate ecdysteroid receptor, Mol. Cell. Endocrinol. 218: 21–38.

Yamada H., and Takayanagi K. (1992). Bioconcentration and elimination of bis(tributyltin)oxide (TBTO) and triphenyltin chloride (TPTC) in several marine fish. Wat. Res. 26(12): 1589-1595.

Yamada J., Inoue K., Furukawa T., and Fukuda A. (2010). Low-concentration tributyltin perturbs inhibitory synaptogenesis and induces neuronal death in immature but not mature neurons. Toxicol. Lett. 198: 282-288.

Yanagawa T., and Kikuchi Y. (2001). Statistical issues on the determination of the no-observed-adverse-effect levels in toxicology. Environmetrics, 12: 319–325.

Yao T.-P., Forman B.M., Jiang Z., Cherbas L., Chen J.-D., McKeown M., Cherbas P., and Evans R.M. (1993). Functional ecdysone receptor is the product of EcR and ultraspiracle genes. Nature 366: 476–479.

Yokota Y., Unuma T., Moriyama A., and Yamano K. (2003). Cleavage site of a major yolk protein (MYP) determined by cDNA isolation and amino acid sequencing in sea urchin, *Hemicentrotus pulcherrimus*. Comp. Biochem. Physiol. B Biochem. Mol. Biol. 135: 71–81.

Zhu Y.Y., Machleder E.M., Chenchik A., Li R., and Siebert P.D. (2001). Reverse transcriptase template switching: a SMART approach for full-length cDNA library construction. Biotechniques 30: 892-897.

Zou E., and Bonvillain R. (2005). Chitinase activity in the epidermis of the fiddler crab, *Uca pugilator*, as an in vivo screen for molt-interfering xenobiotics. Comp. Biochem. Physiol. C. Toxicol. Pharmacol. 139: 225-230.

Zou E., and Fingerman M. (1997). Synthetic estrogenic agents do not interfere with sex differentiation but do inhibit molting of a cladoceran, *Daphnia magna*. Bull. Environ. Contam. Toxicol. 58: 596–602.

Zou E., and Fingerman M. (1999). Effects of exposure to diethylphthalate, 4-tertoctylphenol, and 2,4,5-trichlorobiphenyl on activity of chitobiase in the epidermis and hepatopancreas of the fiddler crab, *Uca pugilator*. Comp. Biochem. Physiol. 122C: 115–120.

Zou E.M. (2005). Impacts of xenobiotics on crustacean molting: The invisible endocrine disruption. Integr. Comp. Biol. 45: 33–38.

Zuckerkandl E., and Pauling L. (1965). Evolutionary divergence and convergence in proteins. In: Bryson, V., Vogel, H.J. (Eds.), Evolving Genes and Proteins. Academic Press, New York, pp. 97–166.

Curriculum Vitae

PERSONAL DETAILS

Name	Yves Verhaegen
Gender	Male
Nationality	Belgian
Place of birth	Schoten, Belgium
Date of birth	November 19th 1980

EDUCATION

2000 – 2005 Master in Biology, with distinction at Ghent University
Facultative courses: molecular phylogeny and diagnostics, parasitology, histology, limnology, oceanology.
Master thesis: Characterization of cranial deformations in *Sparus aurata* (Sparidae). Promoter: Prof. Dr. Dominique Adriaens; co-promoters: Prof. Dr. Patrick Sorgeloos and Patrick Dhert (INVE Technologies)

WORK EXPERIENCE

2007-2011 Research associate at the Flemish Institute for Agriculture and Fisheries Research (ILVO).
2006-2007 Professor's assistant at Faculty of Biotechnology, Biochemistry and Zoophysiology, Ghent University.
2001 -2007 Free-lance guide in Antwerp Zoo
1999-2000 Student jobs as zookeeper in Antwerp Zoo

SCIENTIFIC CONTRIBUTIONS

A1 peer reviewed publications

Y. Verhaegen, D. Adriaens, T. De Wolf, P. Dhert, and P. Sorgeloos, 2007. Deformities in larval gilthead sea bream (*Sparus aurata*): A qualitative and quantitative analysis using geometric morphometrics. Aquaculture 268, 156-168.

T. Geerinckx, Y. Verhaegen and D. Adriaens, 2008. Ontogenetic allometries and shape changes in the suckermouth armoured catfish *Ancistrus cf. triradiatus* Eigenmann (Loricariidae, Siluriformes), related to suckermouth attachment and yolk-sac size. Journal of Fish Biology 72, 803-14.

Y. Verhaegen, K. Parmentier, L. Swevers, P. Rougé, T. Soin, W. De Coen, K. Cooreman and G. Smagghe, 2010. The brown shrimp (*Crangon crangon* L.) ecdysone receptor complex: cloning and functional expression in an EcR-deficient Drosophila cell line. General and Comparative Endocrinology, 168, 415-423.

Y. Verhaegen, K. Parmentier, L. Swevers, E. Renders, P. Rougé, W. De Coen, K. Cooreman and G. Smagghe, 2011. The heterodimeric ecdysteroid receptor complex in the brown shrimp *Crangon crangon*: EcR and RXR isoform characteristics and sensitivity towards the marine pollutant tributyltin. General and Comparative Endocrinology, 172, 158-169.

Y. Verhaegen, E. Monteyne, T. Neudecker, I. Tulp, G. Smagghe, K. Cooreman, P. Roose and K. Parmentier, 2012. Organotins in North Sea brown shrimp (*Crangon crangon* L.) after implementation of the TBT ban. Chemosphere, 86, 979-984.

Oral presentations

LARVI 2005 symposium 5-8 September 2005, Ghent, Belgium: Deformities in larval gilthead seabream (*Sparus aurata*): a qualitative and quantitative analysis using geometric morphometrics. Y. Verhaegen, D. Adriaens, T. De Wolf, P. Dhert and P. Sorgeloos.

12th Benelux Congress of Zoology 26-28 October 2005, Wageningen, The Netherlands: Geometric morphometrics as a useful tool for visualising and analysing deformities in gilthead seabream (*Sparus aurata*). Y. Verhaegen, D. Adriaens, T. De Wolf, P. Dhert and P. Sorgeloos.

XVIII International Ecdysone Workshop 19-23 July 2010, Ceske Budejovice, Czech Republic: The brown shrimp (*Crangon crangon* L.) ecdysone receptor complex: cloning, structural modelling of the ligand-binding domain and functional expression in an EcR-deficient *Drosophila* cell line. Y. Verhaegen, K. Parmentier, L. Swevers, P. Rougé, T. Soin, W. De Coen, K. Cooreman and G. Smagghe.

27nd Annual Conference of the European Society for Comparative Physiology and Biochemistry (ESCPB) 5-9 September 2010, Alessandria, Italy: TBT effects on nuclear hormone signalling in brown shrimp (*C. crangon* L.). Y. Verhaegen, E. Renders, T. Soin, L. Swevers, P. Rougé, K. Parmentier, J. Robbens, W. de Coen and G. Smagghe.

1st ILVO Fisheries Scientific symposium, 11 February 2011, Oostende, Belgium. Biological Effects of Pollution: a case study of TBT in shrimp. Y. Verhaegen, K. Parmentier, K. Cooreman, W. De Coen and G. Smagghe.

VLIZ Young Marine Scientist's day, 24 February 2012, Brugge, Belgium. Did the use of TBT-based antifouling paints cause severe damage to the common shrimp (*Crangon crangon*) population of the Southern Bight? Y. Verhaegen, K. Parmentier, K. Cooreman, W. De Coen and G. Smagghe.

Poster presentations

12th Benelux Congress of Zoology 26-28 October 2005, Wageningen, The Netherlands: A preliminary study on the use of geometric morphometrics as a possible early detection method for deformities in gilthead seabream (*Sparus aurata*) aquaculture. Y. Verhaegen, D. Adriaens, T. De Wolf, P. Dhert and P. Sorgeloos.

XVII International Ecdysone Workshop 20-24 July 2008, Ülm, Germany: Linking Endocrine disrupting chemicals with the decline in the North Sea brown shrimp (*Crangon crangon*) stock: a key role for the ecdysteroid receptor? Y. Verhaegen, K. Parmentier, K. Cooreman, W. De Coen and G. Smagghe.

Annual VLIZ young scientists' day 6 March 2009, Brugge, Belgium: Molecular markers for chronic toxicity of marine pollutants in North Sea brown shrimp (*Crangon crangon L.).* Y. Verhaegen, G. Smagghe, W. De Coen, K. Cooreman and K. Parmentier.

27nd Annual Conference of the European Society for Comparative Physiology and Biochemistry (ESCPB) 5-9 September 2010, Alessandria, Italy: Expression profiling of endocrine-disrupting compounds using a shrimp (*Crangon crangon* L.) cDNA microarray developed through suppression subtractive hybridization PCR. Y. Verhaegen, K. Parmentier, J. Robbens, K. Cooreman, G. Smagghe and W. De Coen.

i-SUP 2010 18-21 April 2010, Brugge, Belgium: Use of a transformed insect cell line to identify crustacean endocrine disrupters *in vitro*. Y. Verhaegen, K. Parmentier, T. Soin, L. Swevers, K. Cooreman, W. De Coen, J. Robbens and G. Smagghe.

XVIII International Ecdysone Workshop 19-23 July 2010, Ceske Budejovice, Czech Republic: The RXR receptor: a target of endocrine disruption in the brown shrimp (*Crangon crangon* L.) ? Y. Verhaegen, E. Renders, K. Parmentier, L. Swevers, P. Rougé, W. De Coen, K. Cooreman and G. Smagghe.

XVIII International Ecdysone Workshop 19-23 July 2010, Ceske Budejovice, Czech Republic: The brown shrimp (*Crangon crangon* L.) ecdysteroid receptor complex: functional expression in an EcR-deficient *Drosophila* cell line. Y. Verhaegen, K. Parmentier, L. Swevers, P. Rougé, T. Soin, W. De Coen, K. Cooreman and G. Smagghe.

ISBN 978-90-5989-535-5